

2015

Beyond alkyl transfer: synthesis of main group metal (Mg, Ca, Zn) silyl and tris(oxazoliny)borato complexes and their stoichiometric and catalytic reactions with borane Lewis acids and carbonyls

Nicole Lynn Lampland
Iowa State University

Follow this and additional works at: <https://lib.dr.iastate.edu/etd>

 Part of the [Chemistry Commons](#)

Recommended Citation

Lampland, Nicole Lynn, "Beyond alkyl transfer: synthesis of main group metal (Mg, Ca, Zn) silyl and tris(oxazoliny)borato complexes and their stoichiometric and catalytic reactions with borane Lewis acids and carbonyls" (2015). *Graduate Theses and Dissertations*. 14384.

<https://lib.dr.iastate.edu/etd/14384>

This Dissertation is brought to you for free and open access by the Iowa State University Capstones, Theses and Dissertations at Iowa State University Digital Repository. It has been accepted for inclusion in Graduate Theses and Dissertations by an authorized administrator of Iowa State University Digital Repository. For more information, please contact digirep@iastate.edu.

Beyond alkyl transfer: Synthesis of main group metal (Mg, Ca, Zn) silyl and tris(oxazolinyl)borato complexes and their stoichiometric and catalytic reactions with borane Lewis acids and carbonyls

by

Nicole Lynn Lampland

A dissertation submitted to the graduate faculty
in partial fulfillment of the requirements for the degree of

DOCTOR OF PHILOSOPHY

Major: Inorganic Chemistry

Program of Study Committee:
Aaron Sadow, Major Professor
Igor Slowing
Gordon Miller
Levi Stanley
Arthur Winter

Iowa State University

Ames, Iowa

2015

Copyright © Nicole Lynn Lampland, 2015. All rights reserved.

To Nancy Wiitanen and Conrad Thompson for inspiring me to become a chemist.

TABLE OF CONTENTS

	Page
ACKNOWLEDGEMENTS	vi
ABSTRACT	vii
CHAPTER 1 – INTRODUCTION	
General Introduction	1
Thesis Organization	4
References	6
CHAPTER 2 – LEWIS ACID-MEDIATED β-HYDROGEN ABSTRACTION IN GROUP 2 COMPLEXES	
Abstract	7
Introduction	7
Results and Discussion	9
Conclusion	27
Experimental	27
References	36
CHAPTER 3 – β-SiH RICH ZINC SILYL COMPOUNDS AND β-SiH ABSTRACTION	
Abstract	42
Introduction	42
Results and Discussion	44
Conclusion	52
Experimental	53

References	59
------------	----

CHAPTER 4 – DIVERGENT REACTION PATHWAYS OF TRIS(OXAZOLINYL)-BORATOZINC AND MAGNESIUM COMPOUNDS

Abstract	63
Introduction	64
Results and Discussion	65
Conclusion	79
Experimental	80
References	94

CHAPTER 5 – 1,4-HYDROSILYLATION OF α,β -UNSATURATED ESTERS CATALYZED BY A MAGNESIUM HYDRIDOBORATE

Abstract	99
Introduction	99
Results and Discussion	101
Conclusion	112
Experimental	113
References	125

CHAPTER 6 – MAGNESIUM-CATALYZED MILD REDUCTION OF TERTIARY AND SECONDARY AMIDES TO AMINES

Abstract	130
Introduction	131
Results and Discussion	133
Conclusion	145

Experimental	146
References	158

CHAPTER 7 – CONCLUSION

General Conclusions	163
---------------------	-----

ACKNOWLEDGEMENTS

I began grad school thinking it was the logical next step in the progression of high school, college, graduate school, career, and retirement. However, grad school was more than job training to me. It was the time to grow and test my faith against adversity. My first thank you is to the graduate school experience. I discovered many strengths and reflected deeply.

I would like to thank my Ph.D. advisor Dr. Aaron D. Sadow for molding me into a scientist and equipping me with skills that will give me a lifetime of success. In addition, I thank all who have served as my POS committee members—Dr. Igor Slowing, Dr. Gordon Miller, Dr. Levi Stanley, Dr. Arthur Winter, Dr. Javier Vela, and Dr. Andreja Bakac—for great guidance, suggestions, and discussion.

I am grateful to all past and present members of the Sadow research group. Each person taught me pieces of the puzzle I put together in order to earn this Ph.D. To the intern and undergraduate students I guided – Shealyn, Kelly, Jason, and Kelsie –I enjoyed the chance to mentor you, and even though I was in the position of teacher, I learned just as much as you did.

Dara, my greatest friend, you earn my sincerest thanks. Our mostly weekly talks on the phone kept me going and ensured that I met my quota of 2 hours of laughing for the week.

To my family, I am so lucky. Thank you for all of the love, support, and reasons to enjoy life. (And I told you I wouldn't become a professional student.)

Lastly, Chris, you are the love of my life and I am most thankful for our last five wonderful years together. This time in our lives has been filled with fun and laughter, but when it brought stress and shadows, but you made me feel light. When it brought unforeseen obstacles, nothing scared you. When it brought events out of our control, you were my rock. We earned this together. Now onward.

ABSTRACT

Recently, the fundamental knowledge of main group metal chemistry has grown. This progress is crucial for the further development of main group metal compounds in silicon chemistry and catalysis and for advancing their applications as green alternatives to many rare earth and transition metal compounds. This thesis focuses on reactivity beyond the well-documented alkyl-transfer applications for main group metals, and it highlights examples of reactions with Lewis acids and the reduction of carbonyls.

A series of magnesium, calcium, and zinc organometallic compounds are synthesized, and their characterization, stoichiometric reactions, and catalytic activity are described. A novel silyl ligand, $-\text{Si}(\text{SiHMe}_2)_3$, and the ancillary ligand To^{M} (tris(4,4-dimethyl-2-oxazoliny)phenylborate) are employed in the synthesis of these homoleptic and heteroleptic species. The silyl anion, $\text{KSi}(\text{SiHMe}_2)_3$, is prepared from the reaction of KO^tBu and $\text{Si}(\text{SiHMe}_2)_4$. A single crystal X-ray diffraction study shows that the structure is made up of a chain of alternating potassium cations and $\text{Si}(\text{SiHMe}_2)_3$ anions with K coordinated to the central Si atoms and the three Si-H moieties oriented toward the next K atom.

This unique silyl ligand incorporating β -SiH functionality undergoes salt metathesis reactions with main group metal halides (MgBr_2 , CaCl_2 , ZnCl_2) to afford disilyl compounds. While the disilylmagnesium and calcium compounds are THF adducts, the disilylzinc compound is free of coordinating solvent. All three compounds undergo coordination by *N*-donor ligands, and zinc is also stabilized by the *N*-heterocyclic carbene 1,3-di-*t*-butylimidazol-2-ylidene (Im^tBu). Interestingly, spectroscopic characterization and X-ray analysis reveal that all of the main group metal silyl compounds contain classic 2-center-2-electron bonding, and the β -SiH

groups do not show evidence of nonclassical interactions. Yet they undergo β -hydrogen abstraction with the Lewis acids $\text{PhB}(\text{C}_6\text{F}_5)_2$ or $\text{B}(\text{C}_6\text{F}_5)_3$.

The monomeric magnesium and zinc silyl complexes containing an ancillary ligand are also synthesized via salt metathesis with $\text{To}^{\text{M}}\text{MgBr}$ or $\text{To}^{\text{M}}\text{ZnCl}$, and similarly give classical interactions between the metal center and the silyl ligand. However, $\text{To}^{\text{M}}\text{Mg-Si}(\text{SiHMe}_2)_3$ and $\text{To}^{\text{M}}\text{Zn-Si}(\text{SiHMe}_2)_3$ react with the Lewis acids $\text{B}(\text{C}_6\text{F}_5)_3$ and CO_2 via contrasting pathways and yield different products. The reactivity of $\text{To}^{\text{M}}\text{Zn-Si}(\text{SiHMe}_2)_3$ was also compared to the analogous compounds $\text{To}^{\text{M}}\text{Zn-CH}(\text{SiHMe}_2)_2$ and $\text{To}^{\text{M}}\text{Zn-N}(\text{SiHMe}_2)_2$ in order to explore some of the similarities and differences in reactivity among Zn-element bonds.

The cationic complex $\text{To}^{\text{M}}\text{MgHB}(\text{C}_6\text{F}_5)_3$, which is accessible from the reaction noted above between $\text{To}^{\text{M}}\text{Mg-Si}(\text{SiHMe}_2)_3$ and $\text{B}(\text{C}_6\text{F}_5)_3$ or from the reaction of $\text{To}^{\text{M}}\text{MgMe}$, PhSiH_3 , and $\text{B}(\text{C}_6\text{F}_5)_3$, is an effective precatalyst for the 1,4-hydrosilylation of α,β -unsaturated esters. Silyl ketene acetals are isolated in high yield from a range of α,β -unsaturated esters and hydrosilanes. However, an α -alkyl group in the ester is essential. In the presence of an α -proton, rapid polymerization is observed as a competing pathway with 1,4-hydrosilylation.

The precursor to $\text{To}^{\text{M}}\text{MgHB}(\text{C}_6\text{F}_5)_3$, $\text{To}^{\text{M}}\text{MgMe}$, is also an efficient precatalyst for the reduction of carbonyls. Under catalytic conditions, tertiary and secondary amides are reduced to amines using pinacolborane (HBpin) as a reductant. The optimized reaction conditions reveal that excess HBpin gives reduction at room temperature in excellent yield. Interestingly, this system is the first example of a hydroboration of amides to amines and the first magnesium-catalyzed amide reduction.

CHAPTER 1: INTRODUCTION

General Introduction

The main group metals magnesium, calcium, and zinc have long been employed as alkyl group transfer reagents. Their stoichiometric carbanion reactivity has been utilized in inorganic synthesis, such as in metalation, and in organic and materials chemistry, such as in addition and metathesis reactions and polymerization initiation.

There are several advantages that make these metals highly effective and commonly used. First, they are economical due to their natural abundances. For example, calcium is the 5th most abundant element in the earth's crust followed closely by magnesium (Ca: 4.15×10^4 mg/kg; Mg: 2.33×10^4 mg/kg; Zn: 7.0×10^1 mg/kg).¹ In addition, they are easily isolated from their naturally occurring sources and reduced. Second, they are less biologically and environmentally toxic in comparison to some heavy transition metals. In fact, magnesium, calcium, and zinc are all found in the human body and required for proper function of the muscles, bones, and immune system. Third, these redox inactive metals have significant Lewis-acidity (essential for binding and activating substrates), ligand-basicity, sensitivity to sterics around the metal center, and sigma bond metathesis reactivity.² These advantages also make magnesium, calcium, and zinc viable reagents for silicon chemistry and catalysis. However, despite the rich history of transfer reactivity, less is known about the ability of main group metals to transfer silyl groups compared to alkyl groups, and main group metals are less developed in many catalytic reactions compared to rare-earth and transition metals.

Among the handful of reported magnesium, calcium, and zinc disilyl compounds, the most well-defined examples are limited to the hypersilyl ligand $-\text{Si}(\text{SiMe}_3)_3$ (Fig. 1).³

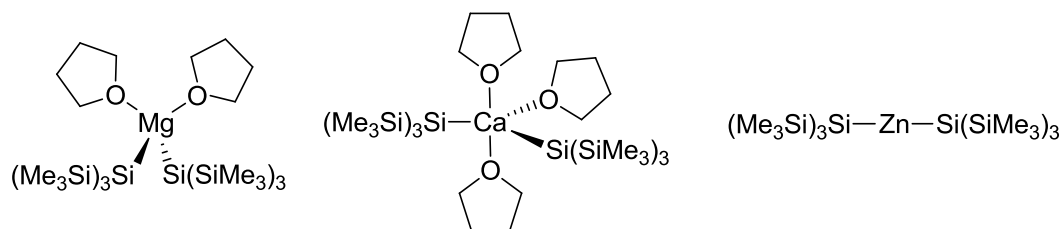
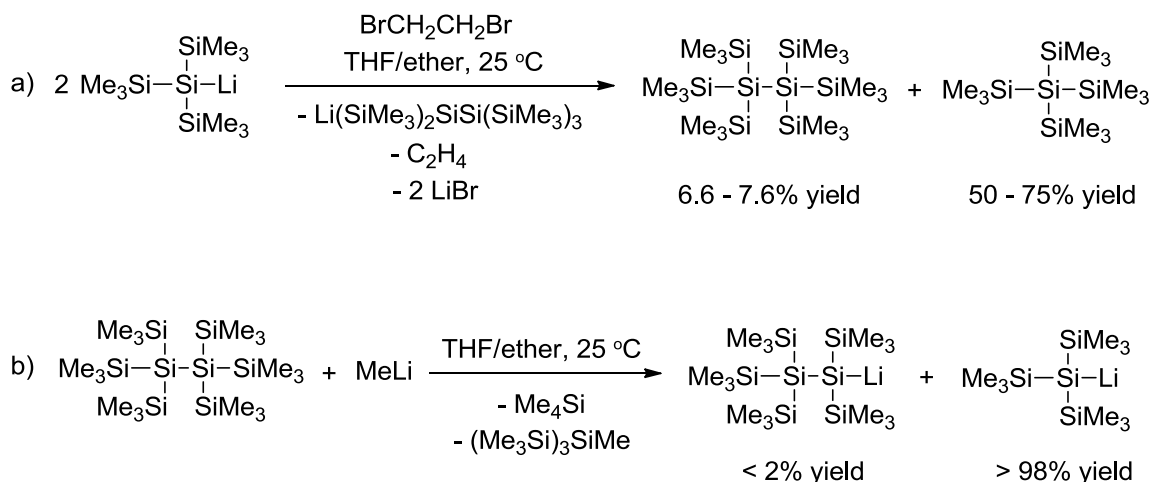


Fig. 1 Homoleptic disilylmagnesium, calcium, and zinc compounds containing $-\text{Si}(\text{SiMe}_3)_3$.

More studies and available silyl ligands are needed to further realize the potential and applications of these main group metal silyl compounds. In addition, little is yet known about the bonding between main group metals and silicon or the reactivity of this bond. However, routes to other silanes and silyl ligands through traditional methyllithium compounds and Wurtz couplings (Scheme 1), have often produced low yielding mixtures, side products, and undesired selectivity.⁴

Scheme 1. a) Reaction of tris(trimethylsilyl)silyllithium and 1,2-dibromoethane to afford a low yielding mixture of silanes. b) Undesired selectivity of MeLi in the presence of “inner” Si-Si bonds.

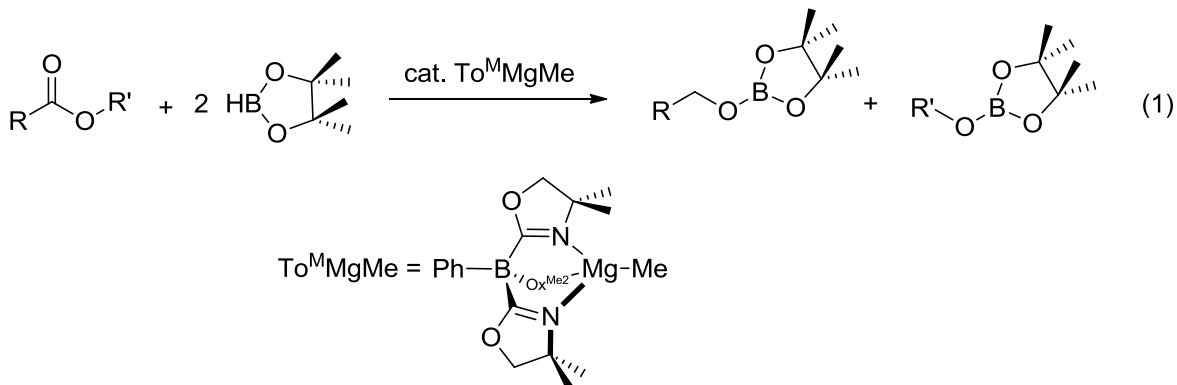


Recently, this area has made significant progress with the discovery of polysilylanylpotassium chemistry.⁵ For example, potassium *tert*-butoxide selectively cleaves terminal $-\text{SiR}_3$ groups to give silyl anions in high yield that are sometimes more soluble in nonpolar solvents than their lithium analogues. In addition, working with solid potassium alkoxides can be synthetically preferable to alkyl lithium solutions.

This thesis contributes to the diversification and availability of potassium silyl ligands through the development of the novel ligand $\text{KSi}(\text{SiHMe}_2)_3$. While ligands containing $\beta\text{-CH}$ have been reported, this ligand is the first to contain $\beta\text{-SiH}$. In addition, the nucleophilicity of the Si-H bond versus the M-Si bond is investigated through abstraction reactions with Lewis acids. It is valuable to explore this Lewis acid assisted β -hydrogen elimination as a possible pathway for main group metal compounds due to the importance of β -hydrogen elimination in rare earth and transition metal reactions. Furthermore, developments with silicon and main group metals could be used to better understand organometallic processes.

The development of main group metal catalysts can also elucidate rare earth and transition metal processes in addition to developing alternative catalysts and reactivity for these transformations. However, main group metals have traditionally been studied for stoichiometric reactions. For example, Grignard reagents are one of the most routinely employed carbanions for stoichiometric additions to carbonyls, and the mechanism has been extensively studied. Thus, it is well known that formation of the Mg-O bond (ca. 80 kcal/mol) necessitates a stoichiometric reaction and acidic work up.⁶ From a catalytic perspective, the oxophilicity of magnesium may present a challenge in reactions with carbonyls. However, some examples of the magnesium-catalyzed reduction of carbonyls do exist, driven by the formation of B-O bonds (ca. 190 kcal/mol).⁷ For example, the hydroboration of aldehydes and ketones has been observed using

pinacolborane (HBpin) as a reductant and the magnesium alkyl complex $[\text{CH}\{\text{C}(\text{Me})\text{NAr}\}_2\text{Mg}^n\text{Bu}]$ ($\text{Ar} = 2,6\text{-}i\text{Pr}_2\text{C}_6\text{H}_3$) as a pre-catalyst in as low as 0.05 mol%.⁸ In the presence of esters, main group metals often cleave substrates to give boryl ether products, which was observed in the reaction of HBpin and esters in the presence of the pre-catalyst $\text{To}^{\text{M}}\text{MgMe}$ ($\text{To}^{\text{M}} = \text{tris}(4,4\text{-dimethyl-2-oxazoliny})\text{phenylborate}$) (eq. 1).⁹



In addition, cationic magnesium complexes provide active catalysts, and CO_2 was reduced to methanol in the presence of HBpin and catalytic amounts of $\{\text{Nacnac}\}\text{Mg}[\text{HB}(\text{C}_6\text{F}_5)_3]$ ($\text{Nacnac} = ((2,6\text{-}i\text{Pr}_2\text{C}_6\text{H}_3)\text{NCMe})_2\text{CH}$).¹⁰ This thesis contributes to the development of main group metal catalysts by providing a rare example of magnesium-catalyzed hydrosilylation and the first example of a magnesium-catalyzed reduction of amides to amines.

Thesis Organization

This thesis contains seven chapters composed of published journal papers and manuscripts in preparation for publication. Chapter one gives a general introduction to the motivation behind the development of main group metal complexes in silicon chemistry and catalysis. Chapters two through five are journal articles of which chapters three and four contain published material. Each chapter is modified to some degree from the published version or the manuscript in progress to provide a more complete and coherent research description, and

relevant literature is reviewed in the introduction of each chapter to provide a deeper understanding and context for the research discussed.

Chapter two describes the synthesis of the new ligand $\text{KSi}(\text{SiHMe}_2)_3$ and a series of homoleptic disilyl magnesium and calcium compounds that contain β -SiH functionality. The potassium silyl ligand was first synthesized and characterized by X-ray diffraction by Kaking Yan, and the optimized, scaled-up synthesis was developed by the combined efforts of Nicole Lampland and Aradhana Pindwal. Chapter three continues with the synthesis of homoleptic disilylzinc compounds while chapter four describes the synthesis of heteroleptic magnesium and zinc silyl compounds. In addition, the structural analysis and reactivity of the heteroleptic compounds is extended to analogous zinc silazide and alkyl compounds for comparison. The chemistry in chapter four was developed by a close collaboration between Nicole Lampland and Debabrata Mukherjee. His contribution to the results and the contributions of other lab members are noted in detail in chapter four. The remaining work was performed by Nicole Lampland.

Chapters five and six focus on magnesium-catalyzed reduction of carbonyls, specifically the hydrosilylation of α,β -unsaturated esters and the hydroboration of amides to amines, respectively. The precatalyst in chapter five, $\text{To}^{\text{M}}\text{MgHB}(\text{C}_6\text{F}_5)_3$, was first synthesized in an NMR reaction by Steven Neal, and Debabrata Mukherjee obtained the crystal structure of $\text{To}^{\text{M}}\text{ZnHB}(\text{C}_6\text{F}_5)_3$. Furthermore, Steven Neal performed some of the preliminary catalytic hydrosilylation reactions by generating $\text{To}^{\text{M}}\text{MgHB}(\text{C}_6\text{F}_5)_3$ in situ. In chapter six, the NMR reaction between HBpin and *N,N*-dimethylformamide to give trimethylamine in the presence of catalytic amounts of $\text{To}^{\text{M}}\text{MgMe}$ was first observed by Debabrata Mukherjee. In addition, the results discussed in chapter six were obtained by Nicole Lampland and Megan Hovey. Iowa

State University's crystallographer, Dr. Arkady Ellern, is credited with collecting data and solving all of the X-ray structures presented in this thesis.

References

- (1) Haynes, W. M. *Handbook of Chemistry and Physics*, 94th ed. Taylor and Francis Group: Boca Raton, 2013.
- (2) Harder, S. *Chem. Rev.* **2010**, *110*, 3852-3876.
- (3) (a) Farwell, J. D.; Lappert, M. F.; Marschner C.; Strissel, C.; Tilley, T.D. *J. Organomet. Chem.* **2000**, *603*,185-188. (b) Teng, W.; Ruhlandt-Senge, K. *Organometallics* **2004**, *23*, 2694-2700. (c) Arnold, J.; Tilley, T. D.; Rheingold, A. L.; Geib, S. *Inorg. Chem.* **1987**, *26*, 2106-2109.
- (4) (a) Gilman, H.; Harrell, R. L., Jr. *J. Organomet. Chem.* **1967**, *9*,67-76. (b) Gilman, H.; Holmes, J. M.; Smith, C. L. *Chem. Ind. (London)*, **1965**, 848. (c) Gutekunst, G.; Brook, A. G. *J. Organomet. Chem.* **1982**, *225*, 1. (d) Apeloig, Y.; Yuzefovich, M.; Bendikov, M.; Bravo-Zhivotovskii, D.; Klinkhammer, K. *Organometallics* **1997**, *16*, 1265.
- (5) Marschner, C. *Eur. J. Inorg. Chem.* **1998**, 221-226
- (6) DeKock, R. L. *Chemical Structure and Bonding* University Science Books: Sausalito, 1989.
- (7) DeKock, R. L. *Chemical Structure and Bonding* University Science Books: Sausalito, 1989.
- (8) Arrowsmith, M.; Hadlington, T. J.; Hill, M. S.; Kociok-Köhn, G. *Chem. Commun.* **2012**, *48*, 4567-4569.
- (9) Mukherjee, D.; Ellern, A.; Sadow, A. D. *Chem. Sci.* **2014**, *5*, 959-964.
- (10) Anker, M. D.; Arrowsmith, M.; Bellham, P.; Hill, M. S.; Kociok-Kohn, G.; Liptrot, D. J.; Mahon, M. F.; Weetman, C. *Chem. Sci.* **2014**, *5*, 2826.

CHAPTER 2: LEWIS ACID-MEDIATED β -HYDROGEN ABSTRACTION IN GROUP 2 COMPLEXES

Modified from a paper to be submitted to *Organometallics*

Nicole L. Lampland, Aradhana Pindwal, Kaking Yan, Arkady Ellern, Aaron D. Sadow*

Abstract

The potassium silyl compound $\text{KSi}(\text{SiHMe}_2)_3$, which contains three β -SiH groups, is synthesized by the reaction of $\text{Si}(\text{SiHMe}_2)_4$ and KO^tBu . This potassium silyl anion reacts with group 2 metal halide salts in THF to form the homoleptic silyl compounds $\text{Mg}\{\text{Si}(\text{SiHMe}_2)_3\}_2\text{THF}_2$ (**1**·**THF**₂) and $\text{Ca}\{\text{Si}(\text{SiHMe}_2)_3\}_2\text{THF}_3$ (**2**·**THF**₃). N-donor pyridine (py) ligands readily displace THF to give tetrahedral magnesium and octahedral calcium silyl compounds. Crystallographic characterization of $\text{Ca}\{\text{Si}(\text{SiHMe}_2)_3\}_2\text{py}_4$ (**2**·**py**₄) reveals the *trans* silyl groups with Ca–Si bond distances of 3.146(2) and 3.126(2) Å. The one-bond silicon-hydrogen coupling constants ($^1J_{\text{SiH}}$) and the infrared stretching frequencies (ν_{SiH}) of these compounds, along with the solid-state structure of **2**·**py**₄ indicate classical 2-center-2-electron bonding between the metal center and the silyl ligand and only classical two-center Si-H bonds. The magnesium and calcium compounds readily react with the Lewis acid $\text{PhB}(\text{C}_6\text{F}_5)_2$ to give the corresponding hydridoborate compounds. Disilene trapping experiments provide evidence that the cationic compounds form through Lewis acid assisted β -hydrogen abstraction.

Introduction

The chemistry of early metal silyl compounds of the main group is unexplored in comparison to silicon chemistry of the transition metals¹ and organometallic chemistry of the main group metals,² both of which are important in catalysis and synthesis.³ Such compounds

may have untapped potential in catalytic and new materials applications. Of the few alkaline earth metal silyl compounds reported in the literature, reactivity is mainly limited to transmetalation.⁴ Recent and exciting discoveries in alkaline earth metal-catalyzed processes, such as in calcium-catalyzed hydrosilylations and hydroaminations, show promise for main group organometallic compounds in catalysis.⁵

Alkali metal silyls are also postulated intermediates in the Wurtz-coupling type reductive polymerization of chlorosilanes that provides polysilanes, and SiH-containing silyl anions could lead to other postulated intermediates including disilenes and silicon-centered radicals.⁶ Alkaline earth metal alkyls react with silanes to give Si–C bonds,⁷ and a related reaction of SiH-containing poly(silyl) anions could give new routes to catenated silicon compounds. In this context, we note that early, d^0 transition-metal silyl compounds that contain SiH groups, including β -SiHs through the intermediate species M–SiHR–SiHR-polymer, are also likely intermediates in silane polymerizations, in this case through catalytic silane dehydrocoupling reactions that are proposed to proceed through σ -bond metathesis.⁸ Despite the significant mechanistic differences between σ -bond metathesis and Wurtz coupling, d^0 metal silyls are common intermediates, and the study of well-defined main group metal silyl species could offer new accessible pathways and new insights into both processes.

Few homoleptic magnesium⁹ and calcium¹⁰ disilyl complexes have been isolated and structurally characterized, but these examples primarily contain bulky $-\text{Si}(\text{SiMe}_3)_3$ or $-\text{SiPh}_3$ ligands. Since no magnesium or calcium silyl complexes containing a β -SiH are known to date, this is an excellent starting place for new chemistry. Examples of β -hydrogen elimination of main group metal alkyls are scarce.¹¹ However, the calcium dialkyl compounds $\text{Ca}\{\text{C}(\text{SiHMe}_2)_3\}_2\text{L}_2$ ($\text{L}_2 = \text{TMEDA}, \text{THF}_2$) (TMEDA = tetramethylethylenediamine) contain

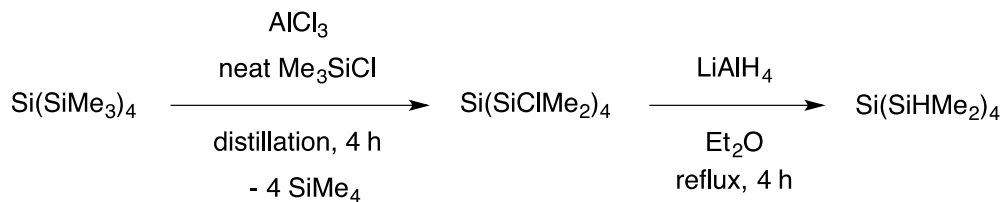
short Ca–Si distances associated with a multicenter Ca–H–Si structure. While these do not appear to undergo β -H elimination processes, the Lewis acid $B(C_6F_5)_3$ reacts with β -H containing bulky tris(dimethylsilyl)methyl through a β -hydrogen abstraction reaction and gives 1,3-disilacyclobutane.¹² A related process of a silyl compound of the type $M-Si(SiHMe_2)_3$ might provide new Si–Si bonds. We were interested in the corresponding magnesium and calcium silyl compounds that contain β -SiH: their structures for comparison to the alkyl analogues and their reactivity with Lewis acids.

Results and Discussion

Synthesis and characterization of main group metal silyl compounds containing β -SiH groups

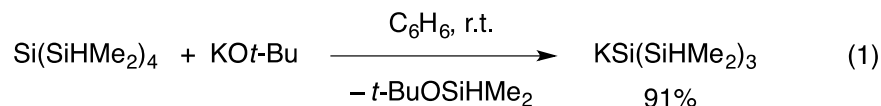
The new potassium silyl species $KSi(SiHMe_2)_3$ is a precursor for main group metal silyl compounds containing β -SiH. Its synthesis was previously reported in a communication, and a full discussion is given here.¹³ The general synthetic scheme involves Si–Si bond cleavage of $Si(SiHMe_2)_4$ by treatment with KO^tBu , and this procedure is based on Marschner's synthesis of $KSi(SiMe_3)_3$ from $Si(SiMe_3)_4$.¹⁴ The required precursor $Si(SiHMe_2)_4$ is prepared through a multistep sequence involving conversion of $Si(SiMe_3)_4$ ¹⁵ to $Si(SiClMe_2)_4$ followed by reduction with $LiAlH_4$ (Scheme 1).¹⁶

Scheme 1. Multistep synthesis of $Si(SiHMe_2)_4$.



Although $\text{Si}(\text{SiMe}_3)_4$, AlCl_3 and Me_3SiCl react readily, a mixture of chlorosilanes is obtained under reflux conditions. Full conversion to $\text{Si}(\text{SiClMe}_2)_4$ is achieved by removing the SiMe_4 byproduct through careful distillation as it is formed.¹⁷ In addition, the purity of the AlCl_3 is critical for complete conversion to $\text{Si}(\text{SiClMe}_2)_4$, and newly purchased anhydrous AlCl_3 also facilitates quantitative conversion. The chlorosilane and LiAlH_4 react over 4 h in refluxing diethyl ether to yield $\text{Si}(\text{SiHMe}_2)_4$.¹⁸

A saturated benzene solution of $\text{Si}(\text{SiHMe}_2)_4$ reacts with KO^tBu to form $\text{KSi}(\text{SiHMe}_2)_3$ (eq. 1). The product immediately precipitates from the concentrated reaction mixture and is readily isolated in good yield after recrystallization from toluene at $-30\text{ }^\circ\text{C}$.



The ^1H NMR spectrum of $\text{KSi}(\text{SiHMe}_2)_3$ dissolved in benzene- d_6 contained a doublet at 0.60 ppm assigned to the SiMe_2 and a septet at 4.22 ppm assigned to the SiH . The ^{29}Si NMR spectrum contained a doublet at -23.8 ppm ($^1J_{\text{SiH}} = 152$ Hz) and a singlet at -202.3 ppm for the SiHMe_2 and the internal Si, respectively. These data, as well as the single IR band at 2020 cm^{-1} assigned to the Si-H stretching mode, are consistent with terminal, non-bridging SiH groups. This band appeared at lower energy than the ν_{SiH} in $\text{HSi}(\text{SiHMe}_2)_3$ (2094 cm^{-1}) and $\text{Si}(\text{SiHMe}_2)_4$ (2093 cm^{-1}). Lower energy ν_{SiH} bands in $\text{KSi}(\text{SiHMe}_2)_3$ were not detected. In contrast, the IR spectrum of $\text{KC}(\text{SiHMe}_2)_3$ contained two ν_{SiH} bands at 2108 and 1973 cm^{-1} whereas the ν_{SiH} of $\text{HC}(\text{SiHMe}_2)_3$ appeared at 2111 cm^{-1} ; the high energy signal is consistent with a non-classical interaction of the Si-H with the K center.¹⁹

A single-crystal X-ray diffraction study confirmed the identity of $\text{KSi}(\text{SiHMe}_2)_3$. In the solid-state, $\text{KSi}(\text{SiHMe}_2)_3$ forms a chain of alternating potassium cations and $\text{Si}(\text{SiHMe}_2)_3$ anions (Figure 1), with the central Si pointed toward potassium with a long K1-Si1 distance of 3.309(5) Å. $\text{KSi}(\text{SiHMe}_2)_3$ crystallizes in the hexagonal space group $P6_3$, and the K1 and central Si1 are located on a crystallographically imposed three-fold rotation axis. The adjacent $\text{Si}(\text{SiHMe}_2)_3$ anion is oriented with the SiHs of the three SiHMe_2 groups pointing at the K center, and the $\text{K}\cdots\text{Si}$ distance in these K-H-Si structures is 3.876(5) Å. Although the hydrogen atoms on silicon were not located in the Fourier difference map, the tetrahedral Si center and methyl and silicon substituents provide likely positions between Si and K. The central silicon atom of one $\text{Si}(\text{SiHMe}_2)_3$ group is coordinated by the potassium center of the next $\text{KSi}(\text{SiHMe}_2)_3$ monomer to build up the $\text{K}[\text{Si}(\text{SiHMe}_2)_3\text{-K}]_n\text{-Si}(\text{SiHMe}_2)_3$ chains. In addition, there are three sets of close contacts of silicon methyl groups and the potassium center. These three methyl groups, from three neighboring $\text{Si}(\text{SiHMe}_2)_3$ anions, form a trigonal plane around the potassium cation. The sum of the Si2-Si1-Si2 angles is $100.79(15)^\circ$, while the K1-Si1-Si2 angle is $117.17(12)^\circ$. Thus, the Si1 center is distorted from tetrahedral symmetry along the C_3 axis. The fact that the bulkier SiHMe_2 groups are closer together than the K atom is to the SiHMe_2 groups suggests that steric factors around Si1 are not responsible for the distortion. One possibility is that the bridging K1-H2s-Si2 structure pulls the SiHMe_2 groups to sharper angles; however the high energy ν_{SiH} suggests that this interaction is not dominant. Alternatively, the K-Me close contacts may affect the overall steric profile of the K1 group (i.e. interchain packing forces). However, the distortion may also be attributed to Bent's rule,²⁰ in which the central Si is bonded to two electropositive elements Si and K. The polarity of the K1-Si1 interaction favors increased s-character in that bond, leaving the Si-Si bonds with greater p-character and smaller Si2-Si1-Si2 angles. A

comparison to the structure of the corresponding potassium alkyl $\text{KC}(\text{SiHMe}_2)_3$ might provide some insight into this change. The solid state structure of the potassium alkyl $[(\text{TMEDA})\text{KC}(\text{SiHMe}_2)_3]_2$ is known as a dimeric TMEDA adduct.²¹ In contrast to the tetrahedral Si1 in $\text{KSi}(\text{SiHMe}_2)_3$, this compound contained a nearly planar carbon center ($\sum\text{Si-C-Si} = 359^\circ$). In addition, two types of non-classical K–H–Si structures are present in the dimeric structure: one side-on and two linear bridges.²² The K–Si distance of the side-on K–H–Si group in that compound is 3.45 Å, whereas the K \cdots Si distances in the end-on K–H–Si groups are 3.983 and 4.096 Å, which is slightly longer than in $\text{KSi}(\text{SiHMe}_2)_3$.

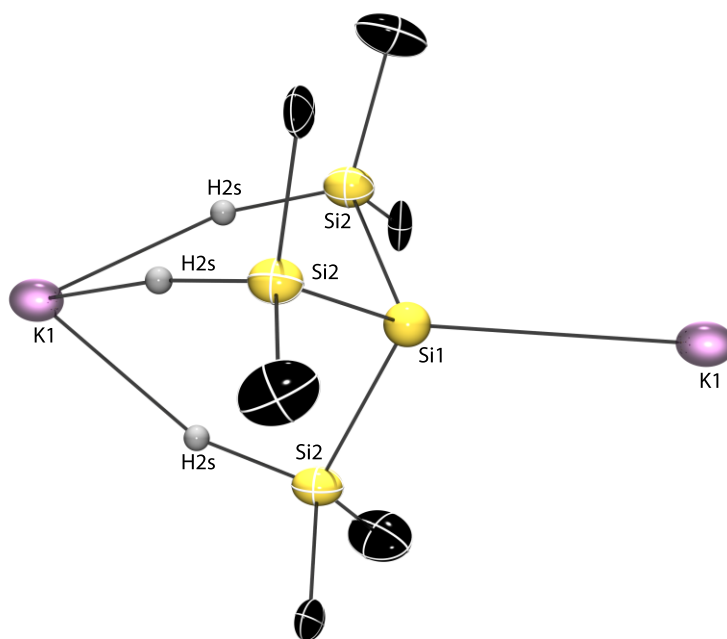


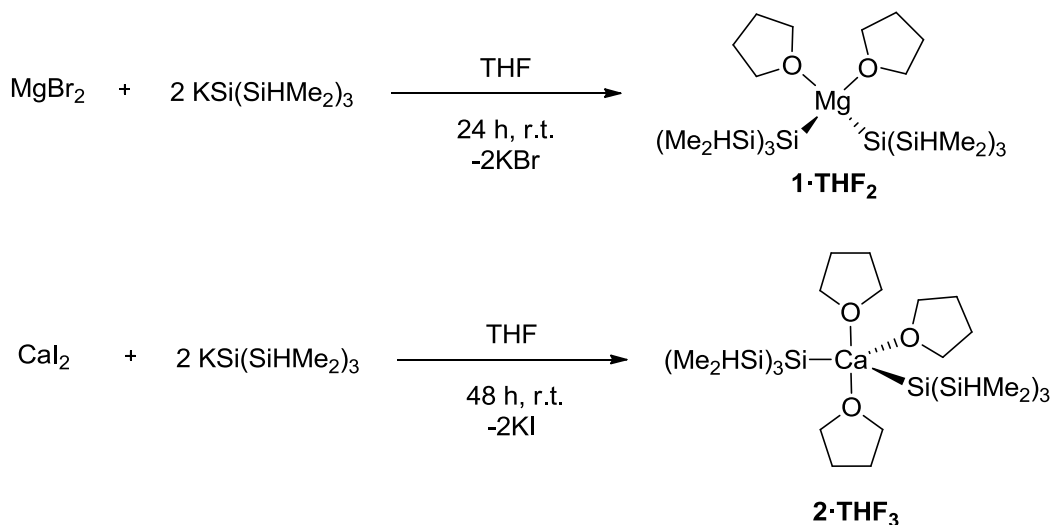
Figure 1. Rendered ellipsoid plot of $\text{KSi}(\text{SiHMe}_2)_3$. Selected interatomic distances (Å): K1–Si1, 3.309(5); K1–Si2, 3.876(5); Si1–Si2, 2.293(3). Selected interatomic angles (deg): Si2–Si1–Si2, 100.8(2); K1–Si1–Si2, 117.2(1); Si2–K1–Si2, 54.24(9); Si1–K1–Si2, 148.24(5).

There are a number of crystallographically characterized potassium silyl compounds. Most of these contain neutral ligands coordinated to the potassium center, such as 18-crown-6, THF, TMEDA, or an aromatic ring. A few potassium silyl compounds, such as ligand-free

$[\text{KSi}(\text{SiMe}_3)_2]^{23}$ and related $[(18\text{-crown-}6)\text{KSi}(\text{SiMe}_3)_3]^{24}$ and $[\text{K}(\eta^6\text{-C}_6\text{H}_6)_3\text{Si}(\text{SiMe}_3)_3]^{25}$ have been crystallographically characterized. These three compounds contain Si–Si–Si angles of ca. $101.6 \pm 0.5^\circ$, suggesting that the distorted structure in $\text{KSi}(\text{SiHMe}_2)_3$ is not a result of packing or the bridging K–H–Si motifs.

Reactions of MgBr_2 or CaI_2 and 2 equiv. of $\text{KSi}(\text{SiHMe}_2)_3$ over 24–48 h give $\text{Mg}\{\text{Si}(\text{SiHMe}_2)_3\}_2\text{THF}_2$ (**1**·**THF**₂) or $\text{Ca}\{\text{Si}(\text{SiHMe}_2)_3\}_2\text{THF}_3$ (**2**·**THF**₃) as white pyrophoric solids. Attempts to synthesize low coordinate Mg and Ca compounds were performed by reacting 2 equiv. $\text{KSi}(\text{SiHMe}_2)_3$ and MgBr_2 or CaI_2 in benzene rather than in THF, but only $\text{KSi}(\text{SiHMe}_2)_3$ was detected in solution by ¹H NMR spectroscopy even after vigorous stirring and heating to 60 °C.

Scheme 2. Salt metathesis reactions to provide **1**·**THF**₂ and **2**·**THF**₃.



Spectral data for all of the neutral compounds described in this paper are listed in Table 1 and Table 2. The ¹H NMR spectrum of the magnesium compound **1**·**THF**₂ contained a doublet at 0.56 ppm assigned to the SiMe₂ and a septet at 4.58 ppm assigned to the SiH. The ¹H NMR

spectral features of the silyl ligand in the calcium derivative **2·THF₃** were similar to that of **1·THF₂**. The ²⁹Si NMR spectrum of **1·THF₂** contained a doublet at -27.5 ppm (¹J_{SiH} = 169 Hz) and singlet at -182.3 ppm, while **2·THF₃** gave a doublet at -24.6 ppm (¹J_{SiH} = 162 Hz) and a singlet at -194.6 ppm. These signals are upfield with respect to those of the bulky silyl analogues, the values of which are also provided in Table 1.²⁶

Table 1. NMR spectral data for main group metal silyl compounds and related silanes

Compound	¹ H (C ₆ D ₆) δ		²⁹ Si (C ₆ D ₆) δ		¹ J _{SiH} (Hz)
	SiRMe ₂ , SiH	SiH	SiRMe ₂ , Si(SiRMe ₂) ₃	Si(SiRMe ₂) ₃	
KSi(SiHMe ₂) ₃ ²⁷	0.56	4.22	-23.8	-202.3	152
HSi(SiHMe ₂) ₃ (3)	0.27	4.29	-21.5	-126.8	158, 181
Si(SiHMe ₂) ₄	0.31	4.36	-33.5	-139.9	180
Mg{Si(SiHMe ₂) ₃ } ₂ THF ₂ (1·THF₂)	0.56	4.58	-27.5	-182.3	169
Mg{Si(SiMe ₃) ₃ } ₂ THF ₂ ²⁸	0.46	n.a.	-6.4	-171.9	n.a.
Mg{Si(SiHMe ₂) ₃ } ₂ py ₂ (1·py₂)	0.51	4.66	-26.3	-182.2	169
Mg{Si(SiHMe ₂) ₃ } ₂ DMAP ₂ (1·DMAP₂)	0.67	4.84	-26.8	-184.3	167
Ca{Si(SiHMe ₂) ₃ } ₂ THF ₃ (2·THF₃)	0.57	4.56	-24.6	-194.6	162
Ca{Si(SiMe ₃) ₃ } ₂ THF ₃ ²⁹	0.50	n.a.	-6.75	-172.32	n.a.
Ca{Si(SiHMe ₂) ₃ } ₂ py ₄ (2·py₄)	0.43	4.59	-23.3	-199.3	160
Ca{Si(SiHMe ₂) ₃ } ₂ DMAP ₄ (2·DMAP₄)	0.69	4.94	-22.5	-201.5	161

Table 2. IR spectroscopic data for main group metal silyl compounds and related silanes

Compound	IR (KBr, cm^{-1}) ν_{SiH}
$\text{KSi}(\text{SiHMe}_2)_3$ ³⁰	2020
$\text{HSi}(\text{SiHMe}_2)_3$ (3)	2094 (broad)
$\text{Si}(\text{SiHMe}_2)_4$	2093
$\text{Mg}\{\text{Si}(\text{SiHMe}_2)_3\}_2\text{THF}_2$ (1 · THF ₂)	2064
$\text{Mg}\{\text{Si}(\text{SiHMe}_2)_3\}_2\text{py}_2$ (1 · py ₂)	2067
$\text{Mg}\{\text{Si}(\text{SiHMe}_2)_3\}_2\text{DMAP}_2$ (1 · DMAP ₂)	2083
$\text{Ca}\{\text{Si}(\text{SiHMe}_2)_3\}_2\text{THF}_3$ (2 · THF ₃)	2045
$\text{Ca}\{\text{Si}(\text{SiHMe}_2)_3\}_2\text{py}_4$ (2 · py ₄)	2100
$\text{Ca}\{\text{Si}(\text{SiHMe}_2)_3\}_2\text{DMAP}_4$ (2 · DMAP ₄)	2036

The magnesium compounds have higher coupling constants than the calcium silyls, following expectations based on Bent's Rule.³¹ The spectroscopic data suggest that the SiH groups are not interacting with the magnesium or calcium centers in a β -agostic-like fashion. In contrast to $\text{Ca}\{\text{C}(\text{SiHMe}_2)_3\}_2\text{THF}_2$,³² the chemical shifts and coupling constants in ¹H NMR spectra of **2**·**THF**₃ acquired in toluene from 180 K to 298 K were essentially invariant, indicating that rotation processes are fast on the ¹H NMR timescale. The ν_{SiH} in the vibrational spectra appeared as single, high energy bands at 2064 cm^{-1} for **1**·**THF**₂ and 2045 cm^{-1} for **2**·**THF**₃ (2045 cm^{-1}).

The number of coordinated THF is determined from integration of the ¹H NMR spectra; however, elemental composition analysis of these highly air sensitive compounds are more consistent with $\text{Mg}\{\text{Si}(\text{SiHMe}_2)_3\}_2\text{THF}$ and $\text{Ca}\{\text{Si}(\text{SiHMe}_2)_3\}\text{THF}_2$ rather than the higher coordination observed in solution. Despite the apparent lability of THF, attempts to isolate lower coordinate compounds by allowing the solids to stand under vacuum provided intractable,

unidentified materials. The geometries of known bulky silyl analogues $\text{Mg}\{\text{Si}(\text{SiMe}_3)_3\}_2\text{THF}_2$ ³³ and $\text{Ca}\{\text{Si}(\text{SiMe}_3)_3\}_2\text{THF}_3$ ³⁴ are tetrahedral and trigonal bipyramidal, respectively, as determined by X-ray crystallographic analysis, and the structures of $\mathbf{1}\cdot\text{THF}_2$ and $\mathbf{2}\cdot\text{THF}_3$ are likely similar (see below).

Both compounds are highly air, moisture, and temperature sensitive, apparently to a greater degree than the alkyl $\text{C}(\text{SiHMe}_2)_3$ and bulky silyl $\text{Si}(\text{SiMe}_3)_3$ analogues. In addition, the persistence of $\mathbf{1}\cdot\text{THF}_2$ ($t_{1/2} = 48$ h) in benzene- d_6 was noticeably greater than $\mathbf{2}\cdot\text{THF}_3$ ($t_{1/2} = 12$ h) at room temperature. Thermolysis of $\mathbf{2}\cdot\text{THF}_3$ at 60 °C in benzene- d_6 affords $\text{Si}(\text{SiHMe}_2)_4$ after 12 h as the only observed species in the ^1H NMR spectrum, while thermolysis of $\mathbf{1}\cdot\text{THF}_2$ at 80 °C for 72 h is required for full conversion to $\text{Si}(\text{SiHMe}_2)_4$. No precipitate was observed in these reactions, and the identity of the metal-containing byproducts has not been assigned. For comparison, $\text{Ca}\{\text{Si}(\text{SiMe}_3)_3\}_2\text{THF}_3$ undergoes rapid SiMe_3 redistribution to give $\text{Si}(\text{SiMe}_3)_4$ when dissolved in THF,³⁵ and $\text{Ca}\{\text{C}(\text{SiHMe}_2)_3\}_2\text{THF}_2$ forms $\text{HC}(\text{SiHMe}_2)_3$ after 120 h at 120 °C.³⁶ A solution of $\mathbf{1}\cdot\text{THF}_2$ or $\mathbf{2}\cdot\text{THF}_3$ in benzene- d_6 exposed to air results in essentially instantaneous hydrolysis to $\text{HSi}(\text{SiHMe}_2)_3$ (**3**).

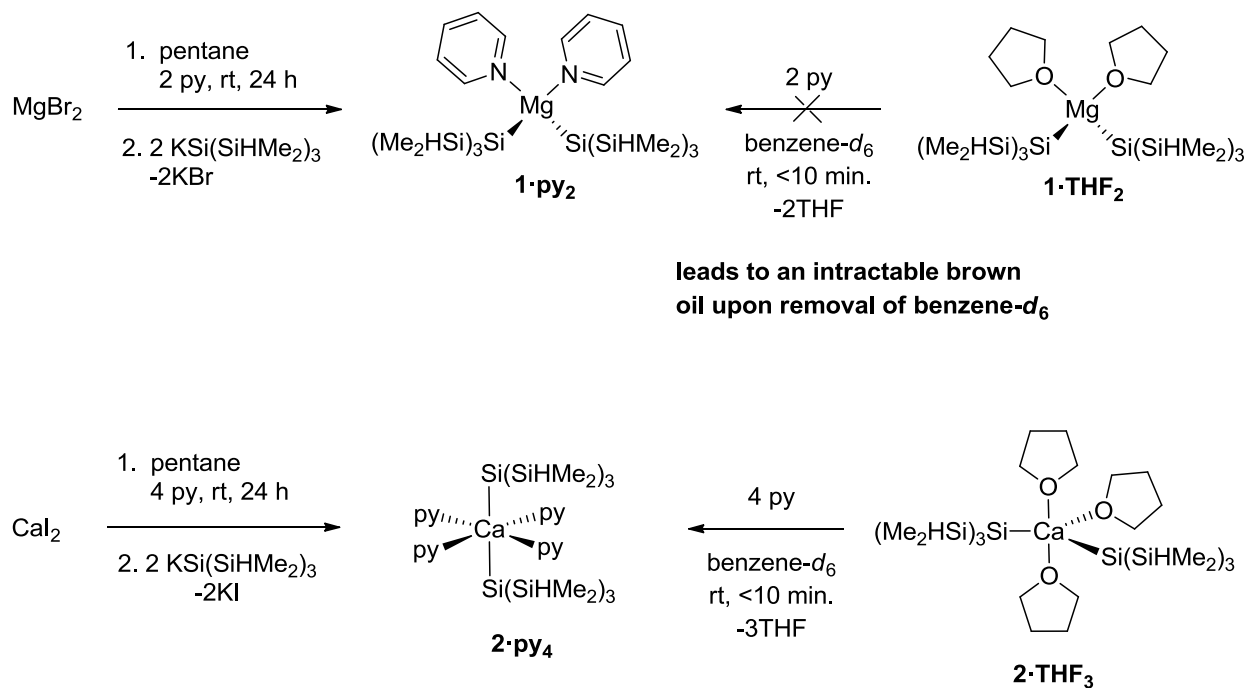
Substitution reactions with N-donor ligands

We hypothesized that replacing THF with *N*-donor ligands might improve crystallinity and the compounds' lifetime under ambient conditions. In benzene- d_6 , 2 and 4 equiv. of pyridine (py) react instantaneously with $\mathbf{1}\cdot\text{THF}_2$ and $\mathbf{2}\cdot\text{THF}_3$ to yield $\text{Mg}\{\text{Si}(\text{SiHMe}_2)_3\}_2\text{py}_2$ ($\mathbf{1}\cdot\text{py}_2$) and $\text{Ca}\{\text{Si}(\text{SiHMe}_2)_3\}_2\text{py}_4$ ($\mathbf{2}\cdot\text{py}_4$). THF is displaced from the magnesium and calcium coordination spheres, as determined by ^1H NMR spectra that contained resonances corresponding to THF dissolved in benzene- d_6 . However, an intractable brown oil was obtained upon evaporation of

benzene- d_6 from the magnesium reaction mixture. Fortunately, a 1:2 mixture of MgBr_2 and pyridine, stirred for 24 h in pentane, gives a suspension that reacts with 2 equiv. of $\text{KSi}(\text{SiHMe}_2)_3$ at $-30\text{ }^\circ\text{C}$. Careful filtration followed by crystallization at $-30\text{ }^\circ\text{C}$ provides $\text{Mg}\{\text{Si}(\text{SiHMe}_2)_3\}_2\text{py}_2$ in 66% yield (Scheme 3).

Pre-coordination of py to CaI_2 followed by salt metathesis or the reaction of $2\cdot\text{THF}_3$ and 4 equiv. of pyridine produces $\text{Ca}\{\text{Si}(\text{SiHMe}_2)_3\}_2\text{py}_4$ ($2\cdot\text{py}_4$) in 59% yield. Both main group metal silyl pyridine complexes are yellow, highly pyrophoric solids. The ^1H NMR spectra of $1\cdot\text{py}_2$ and $2\cdot\text{py}_4$ contained the expected SiMe_2 and SiH resonances. The SiMe_2 signals for $1\cdot\text{py}_2$ and $2\cdot\text{py}_4$ are shifted upfield relative to the chemical shifts of the THF analogues, whereas the SiH resonances are shifted downfield. The resonances in the ^{29}Si NMR spectrum are comparable

Scheme 3. Synthetic routes for the isolation of $1\cdot\text{py}_2$ and $2\cdot\text{py}_4$.



for **1**·THF₂ and **1**·py₂ with a small shift of ca. 1 ppm in each silicon value. Similarly, the SiHMe₂ resonances in **2**·THF₃ and **2**·py₄ are nearly equivalent, however, the internal silicon resonance in **2**·py₄ shifted ca. 5 ppm upfield compared to the internal silicon resonance in **2**·THF₃. A resonance in the ¹⁵N NMR spectrum appeared at –80 ppm for **2**·py₄, however, a resonance was not detected for **1**·py₂. For comparison, a resonance in the ¹⁵N NMR spectrum was observed at –68 ppm for an authentic pyridine sample. Additionally, the IR spectra for **1**·py₂ and **2**·py₄ contained bands at 2067 and 2100 cm⁻¹, respectively, assigned to ν_{SiH} that are shifted higher in energy compared to **1**·THF₂ and **2**·THF₃.

Crystallization from pentane at –30 °C gives X-ray quality yellow, needle-like crystals of the bis(silyl)calcium pyridine adduct. The **2**·py₄ molecule (Figure 2) has a pseudo-octahedral geometry with the silyl ligands disposed *trans* (∠Si1–Ca1–Si5, 177.86(7)°) in axial sites and the four pyridine ligands occupying the equatorial sites.

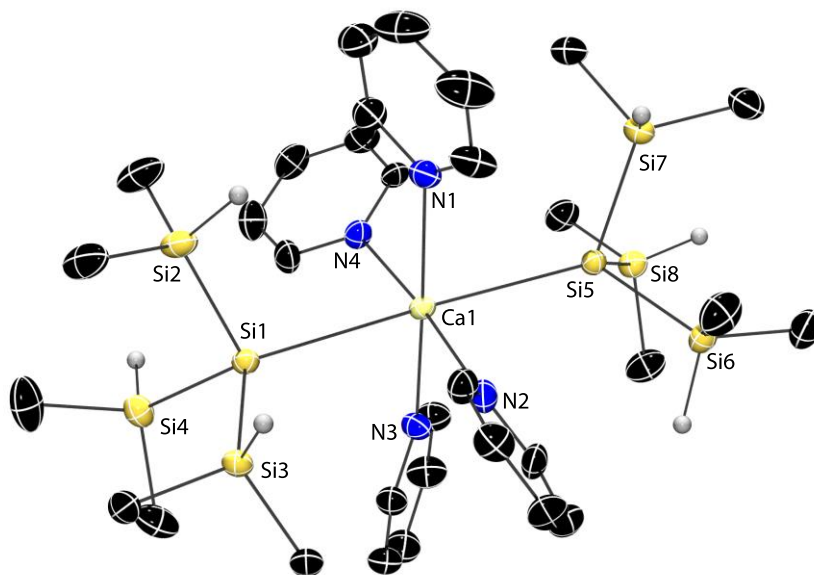
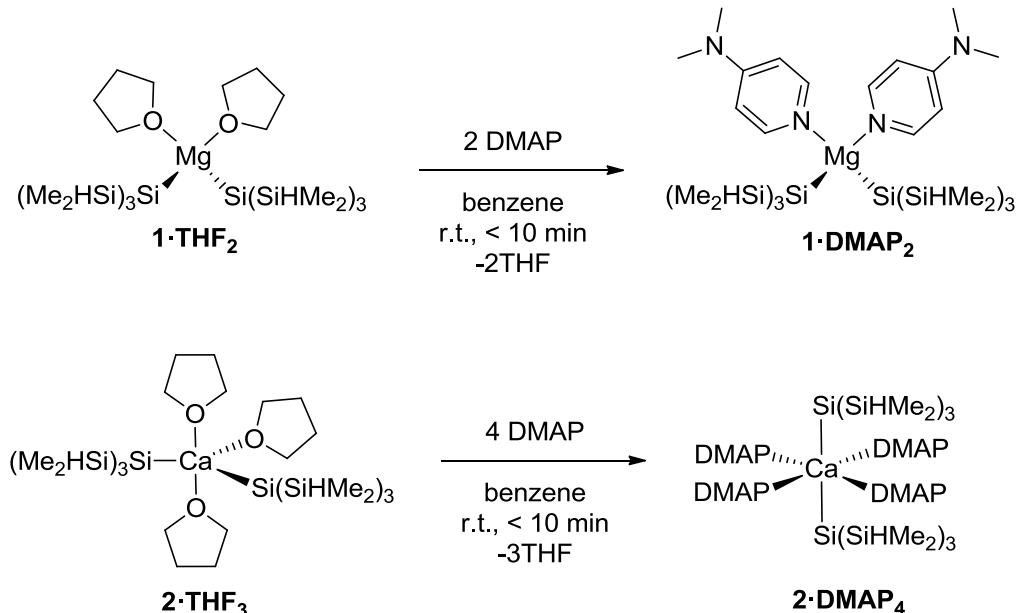


Figure 2. Rendered thermal ellipsoid plot of Ca(Si(SiHMe₂)₃)₂(py)₄ (**2**·py₄). Selected interatomic distances (Å): Ca1–Si1, 3.146(2); Ca1–Si5, 3.126(2); Ca1–N1, 2.529(6); Ca1–N2, 2.523(6); Ca1–N3, 2.516(6); Ca1–N4, 2.516(6). Selected interatomic angles (deg): Si1–Ca1–Si5, 177.86(7); N1–Ca1–N3, 174.9(2); N2–Ca1–N4, 175.6(2); Si1–Ca1–N1–C5, 104.8(7); Si1–Ca1–N2–C6, 120.7(6); Si1–Ca1–N3–C11, 133.1(6); Si1–Ca1–N4–C16, 154.6(5).

The Ca–Si distances of 3.126(2) and 3.146(2) Å are inequivalent; however, the Ca1–N distances (mean Ca–N distance, 2.521 ± 0.005 Å) are equivalent within 3σ error. The Ca–Si interatomic distances are slightly longer than the corresponding distances in the five-coordinate $\text{Ca}\{\text{Si}(\text{SiMe}_3)_3\}_2\text{THF}_3$ (3.0421(9) and 3.0861(9) Å),³⁷ which is likely related to the Ca center's increased coordination number, and slightly shorter than the corresponding distances in the six-coordinate $\text{Ca}\{\text{SiPh}_3\}_2\text{THF}_4$ (3.1503(8) Å).³⁸ The H atoms belonging to the β -Si atoms were found objectively on a difference Fourier map and refined isotropically. The Si–H moieties point away from the calcium center, and together with the IR and NMR spectroscopic data rules out any non-classical interactions in the solid-state. In addition, the equatorial pyridine rings form a pinwheel-like structure with systematically increasing torsion angles over the four ligands defined with respect to one of the silyl ligands, giving overall C_1 symmetry in the solid state. Note that **2**·**py**₄ crystallizes in the P-1 space group with $Z = 2$. The chiral molecule resulting from the pin-wheel rotated pyridine groups is related to the enantiomorphic structure through a crystallographically imposed inversion center.

DMAP reacts with **1**·**THF**₂ or **2**·**THF**₃ in toluene or benzene to give $\text{Mg}\{\text{Si}(\text{SiHMe}_2)_3\}_2\text{DMAP}_2$ (**1**·**DMAP**₂) and $\text{Ca}\{\text{Si}(\text{SiHMe}_2)_3\}_2\text{DMAP}_4$ (**2**·**DMAP**₄) in 27% and 67% yield (Scheme 4). The ¹H NMR resonances assigned to the SiHMe₂ groups in the DMAP adducts **1**·**DMAP**₂ and **2**·**DMAP**₄ are shifted downfield compared to the THF and py adducts. The IR band assigned to ν_{SiH} for **1**·**DMAP**₂ (2083 cm⁻¹) is the highest energy band of the magnesium compounds while ν_{SiH} for **2**·**DMAP**₄ (2036 cm⁻¹) is the lowest energy band of the calcium compounds. The solution to a single crystal X-ray diffraction study of **2**·**DMAP**₄ supports the same octahedral geometry and *trans* orientation of silyl ligands as in **2**·**py**₄, but the quality of the crystal limits any additional analysis.

Scheme 4. Substitution reactions with DMAP to afford **1·DMAP₂** and **2·DMAP₄**.

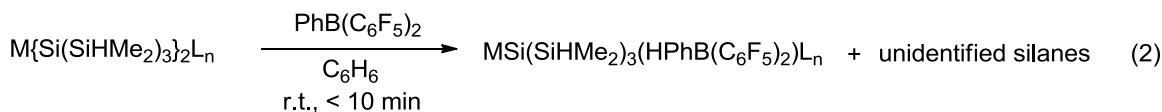
While the presence of twinning was reduced in the crystals of the pyridine and DMAP coordinated compounds in comparison to the THF adducts, the robustness under thermal conditions was also reduced, though most notably for the pyridine adducts. Compounds **1·py₂** and **2·py₄** undergo decomposition to intractable brown oils in the solid state at room temperature within 12 h, and thermolysis of **1·py₂** or **2·py₄** at 60 °C in benzene-*d*₆ afforded Si(SiHMe₂)₄ as the only observed species in the ¹H NMR spectrum after 1 h. The DMAP adducts showed similar but slightly decreased stability compared to **1·THF₂** and **2·THF₃**. The bidentate pyridine donor ligand, 2,2'-bipyridine (bipy), further decreased the robustness of the disilyl magnesium and calcium compounds. For example, the reaction of 2 equiv. bipy and 1 equiv. of **1·THF₂** or **2·THF₃** in THF-*d*₈ resulted in instantaneous formation of a deep red solution that showed resonances assigned to Si(SiHMe₂)₄ and uncoordinated THF in the ¹H NMR spectrum in addition to one broad resonance in the aryl region. No precipitate was observed in these reactions, and the identity of the metal-containing byproducts has not been yet assigned.

However, upon lowering the temperature to 230 K, the broad aryl resonance resolved into 4 broad peaks, which we attribute to $\text{Ca}(\text{bipy})_n$ or $\text{Mg}(\text{bipy})_n$ species.

Reactivity of main group metal silyl compounds with Lewis acids

The contrasting reactivity of $\text{Ca}\{\text{C}(\text{SiHMe}_2)_3\}_2\text{THF}_2$ and $\text{Ca}\{\text{Si}(\text{SiHMe}_2)_3\}_2\text{THF}_3$ is of fundamental interest. The alkyl compound contains non-classical Ca–H–Si interactions and reacts with Lewis acids such as $\text{B}(\text{C}_6\text{F}_5)_3$ and BPh_3 via hydrogen abstraction to give $\text{CaC}(\text{SiHMe}_2)_3(\text{HB}(\text{C}_6\text{R}_5)_3)\text{THF}$ compounds. Though the ligand count is higher in $\text{Ca}\{\text{Si}(\text{SiHMe}_2)_3\}_2\text{THF}_3$ than in the alkyl analogue, the non-classical interactions in the latter, combined with steric effects, may protect the Ca–C bond from strong electrophiles. The longer Ca–Si bonds and 2-center-2-electron classical Ca–Si bonding in the silyl compounds might reflect lower β -SiH nucleophilicity.

To test this, the magnesium and calcium compounds were allowed to react with the Lewis acid $\text{BPh}(\text{C}_6\text{F}_5)_2$. The reaction of $\mathbf{1}\cdot\text{THF}_2$ and $\text{BPh}(\text{C}_6\text{F}_5)_2$ gives $\text{MgSi}(\text{SiHMe}_2)_3(\text{HBPh}(\text{C}_6\text{F}_5)_2)\text{THF}_2$ ($\mathbf{4}\{\text{HBPh}(\text{C}_6\text{F}_5)_2\}\text{THF}_2$) in 60% yield. The corresponding reaction of $\mathbf{2}\cdot\text{THF}_3$ and the Lewis acid provides $\text{CaSi}(\text{SiHMe}_2)_3(\text{HBPh}(\text{C}_6\text{F}_5)_2)\text{THF}_2$ ($\mathbf{5}\{\text{HBPh}(\text{C}_6\text{F}_5)_2\}\text{THF}_2$) in 81% yield (eq. 2). The byproduct of the reaction is proposed to be disilene and evidence for this is provided by trapping experiments below; however, $^1\text{H NMR}$



$\mathbf{1}\cdot\text{THF}_2$ M = Mg, L = THF, n = 2
 $\mathbf{2}\cdot\text{THF}_3$ M = Ca, L = THF, n = 3
 $\mathbf{2}\cdot\text{py}_4$ M = Ca, L = py, n = 4

$\mathbf{4}\{\text{HBPh}(\text{C}_6\text{F}_5)_2\}\text{THF}_2$ M = Mg, L = THF, n = 2
 $\mathbf{5}\{\text{HBPh}(\text{C}_6\text{F}_5)_2\}\text{THF}_2$ M = Ca, L = THF, n = 2
 $\mathbf{5}\{\text{HBPh}(\text{C}_6\text{F}_5)_2\}\text{py}_4$ M = Ca, L = py, n = 4

spectra of the reaction mixtures of $\text{PhB}(\text{C}_6\text{F}_5)_2$ and $\mathbf{1}\cdot\text{THF}_2$ or $\mathbf{2}\cdot\text{THF}_3$ showed only a complicated mixture of silane products. Spectral data for all of the cationic silyl compounds described in this paper are listed in Table 3 and Table 4.

In the ^1H NMR spectrum of $\mathbf{4}\{\text{HBPh}(\text{C}_6\text{F}_5)_2\}\text{THF}_2$ in benzene- d_6 a doublet at 0.47 ppm was assigned to the SiMe_2 and a septet at 4.38 ppm was assigned to the SiH . These chemical shifts are upfield compared to the parent compound $\mathbf{1}\cdot\text{THF}_2$. Integration of the silyl and THF resonances indicated only one $-\text{Si}(\text{SiHMe}_2)_3$ group was present in the compound. In addition, the ^{11}B NMR spectrum showed a doublet at -18.6 ppm ($^1J_{\text{BH}} = 69$ Hz), indicative of the $\text{HBPh}(\text{C}_6\text{F}_5)_2$ moiety as a result of β -H abstraction. The ^{29}Si NMR spectrum contained a doublet at -28.5 ppm ($^1J_{\text{SiH}} = 165$ Hz) and a singlet at -109.1 ppm. Notably, the internal silicon resonance is significantly shifted from the parent compound ($\mathbf{1}\cdot\text{THF}_2$: $\delta -182.3$). The ν_{SiH} IR band to $\mathbf{4}\{\text{HBPh}(\text{C}_6\text{F}_5)_2\}\text{THF}_2$ at 2089 cm^{-1} indicated terminal SiH consistent with $\mathbf{1}\cdot\text{THF}_2$, and a band assigned to ν_{BH} at 2329 cm^{-1} characterized the $\text{HBPh}(\text{C}_6\text{F}_5)_2$ moiety.

Table 3. NMR spectral data for main group metal silyl hydridoborate compounds

Compound	^1H δ (C_6D_6)		^{29}Si δ (C_6D_6)		$^1J_{\text{SiH}}$ (Hz)	^{11}B δ (C_6D_6)	$^1J_{\text{BH}}$ (Hz)
	SiMe_2 , SiH		SiHMe_2 , Si				
$\text{MgSi}(\text{SiHMe}_2)_3(\text{HBPh}(\text{C}_6\text{F}_5)_2)\text{THF}_2$ $\mathbf{4}\{\text{HBPh}(\text{C}_6\text{F}_5)_2\}\text{THF}_2$	0.47	4.38	-28.5	-109.1	165	-18.6	69
$\text{MgSi}(\text{SiHMe}_2)_3(\text{HBPh}(\text{C}_6\text{F}_5)_2)\text{DMAP}_n$ $\mathbf{4}\{\text{HBPh}(\text{C}_6\text{F}_5)_2\}\text{DMAP}_n$	0.59	4.81	-25.4	-183.8	168	-19.3	63
$\text{CaSi}(\text{SiHMe}_2)_3(\text{HBPh}(\text{C}_6\text{F}_5)_2)\text{THF}_2^a$ $\mathbf{5}\{\text{HBPh}(\text{C}_6\text{F}_5)_2\}\text{THF}_2$	-0.03	3.77	-22.1	-117.3	170	-19.6	93
$\text{CaSi}(\text{SiHMe}_2)_3(\text{HBPh}(\text{C}_6\text{F}_5)_2)\text{py}_4$ $\mathbf{5}\{\text{HBPh}(\text{C}_6\text{F}_5)_2\}\text{py}_4$	0.42	4.52	-22.9	-195.8	170	-18.7	111
$\text{CaSi}(\text{SiHMe}_2)_3(\text{HBPh}(\text{C}_6\text{F}_5)_2)\text{DMAP}_n$ $\mathbf{5}\{\text{HBPh}(\text{C}_6\text{F}_5)_2\}\text{DMAP}_n$	0.43	4.32	-21.3	-195.7	170	-18.8	92

^a Solvent is THF- d_8 .

Table 4. IR spectral data for main group metal silyl hydridoborate compounds

Compound	IR (KBr, cm ⁻¹)	
	ν_{BH}	ν_{SiH}
MgSi(SiHMe ₂) ₃ (HBPh(C ₆ F ₅) ₂)THF ₂ 4{HBPh(C₆F₅)₂}THF₂	2329	2089
MgSi(SiHMe ₂) ₃ (HBPh(C ₆ F ₅) ₂)DMAP _n 4{HBPh(C₆F₅)₂}DMAP_n	2341	2097
CaSi(SiHMe ₂) ₃ (HBPh(C ₆ F ₅) ₂)THF ₂ 5{HBPh(C₆F₅)₂}THF₂	2330	2074
CaSi(SiHMe ₂) ₃ (HBPh(C ₆ F ₅) ₂)py ₄ 5{HBPh(C₆F₅)₂}py₄	2381	2091
CaSi(SiHMe ₂) ₃ (HBPh(C ₆ F ₅) ₂)DMAP _n 5{HBPh(C₆F₅)₂}DMAP_n	2388	2089

Compound **5{HBPh(C₆F₅)₂}THF₂** followed the spectroscopic trends of **4{HBPh(C₆F₅)₂}THF₂**. However, unlike the magnesium cation, the calcium cation was insoluble in benzene and characterized in THF-*d*₈. The ¹H NMR spectrum contained a doublet at -0.03 ppm assigned to SiMe₂ and a septet at 3.77 ppm assigned to the SiH. The ¹¹B NMR spectrum for **5{HBPh(C₆F₅)₂}THF₂** contained a doublet at -19.6 ppm (¹J_{BH} = 93 Hz), which is comparable to CaC(SiHMe₂)₃(HB(C₆F₅)₃)(THF)₂.³⁹ The ²⁹Si NMR spectrum contained a doublet at -22.1 ppm (¹J_{SiH} = 170 Hz) and a singlet at -117.3 ppm. Similar to **4{HBPh(C₆F₅)₂}THF₂**, the internal silicon resonance in **5{HBPh(C₆F₅)₂}THF₂** is shifted downfield almost 80 ppm compared to the internal silicon resonance in **2·THF₃**. In the IR spectrum, a band assigned to ν_{BH} appeared at 2330 cm⁻¹, and the single ν_{SiH} IR band appeared at 2074 cm⁻¹. Contrastingly, CaC(SiHMe₂)₃(HB(C₆F₅)₃)THF₂ contained β -agostic SiH. Thermolysis of **4{HBPh(C₆F₅)₂}THF₂** and **5{HBPh(C₆F₅)₂}THF₂** in sealed NMR tubes gives Si(SiHMe₂)₄ after 72 h at 120 °C in toluene-*d*₈ and 12 h at 80 °C in benzene-*d*₆, respectively.

β -H abstraction reactions were also investigated with the N-donor silyl complexes. Compound **1**·**py**₂ reacts immediately with BPh(C₆F₅)₂ in benzene-*d*₆ at room temperature to give a complicated mixture of several unidentified silyl containing species. Repeated attempts to cool a solution of **1**·**py**₂ in toluene to -30 °C or remove solvent gave a benzene insoluble brown, sticky solid. Compound **2**·**py**₄ reacts with 1 equiv. BPh(C₆F₅)₂ to give CaSi(SiHMe₂)₃(HBPh(C₆F₅)₂)py₄ (**5**{HBPh(C₆F₅)₂}py₄) in 63% yield. The ¹H NMR spectrum contained a doublet at 0.42 ppm for the SiMe₂ group and a septet at 4.52 ppm for the SiH, which is shifted slightly upfield compared to its precursor. The ¹¹B NMR spectrum contained a doublet at -18.7 ppm (¹J_{BH} = 111 Hz), and the ²⁹Si NMR spectrum showed a doublet at -22.9 ppm and a singlet at -195.8 ppm. Unlike the THF adducts, the internal silicon resonance of the pyridine adduct is nearly equivalent to the parent compound **2**·**py**₄, but the ¹J_{SiH} coupling constant (170 Hz) increased in the cationic compound. The Si-H stretching frequency in the IR spectrum of **5**{HBPh(C₆F₅)₂}py₄ observed at 2091 cm⁻¹ was also comparable to the high energy IR band in **2**·**py**₄ (2100 cm⁻¹), and the stretching frequency assigned to ν_{BH} (2381) was in the expected energy range. Thermolysis of **5**{HBPh(C₆F₅)₂}py₄ also gives Si(SiHMe₂)₄ after 10 h at room temperature in benzene-*d*₆.

1·**DMAP**₂ or **2**·**DMAP**₄ partially react with 1 equiv. of BPh(C₆F₅)₂ to give a mixture of β -H abstraction, formation of a DMAP-borane adduct, and some decomposition. The complicated ¹H NMR spectrum in benzene-*d*₆ showed resonances assigned to several species including starting material, DMAP-BPh(C₆F₅)₂ (**6**), and the decomposition products HSi(SiHMe₂)₃ and Si(SiHMe₂)₄. However, the target products MSi(SiHMe₂)₃(HBPh(C₆F₅)₂)DMAP_n (M = Mg **4**{HBPh(C₆F₅)₂}DMAP_n; M = Ca **5**{HBPh(C₆F₅)₂}DMAP_n) could also be identified. The ¹¹B NMR spectrum contained a singlet

at -1.9 ppm assigned to DMAP-BPh(C₆F₅)₂ (**6**) and a doublet at -19.3 ppm ($^1J_{\text{BH}} = 63$ Hz) for **4**{HBPh(C₆F₅)₂}DMAP_n or -18.8 ppm ($^1J_{\text{BH}} = 92$ Hz) for **5**{HBPh(C₆F₅)₂}DMAP_n. Attempts to isolate and purify these cationic silyl compounds were unsuccessful; therefore, only the NMR spectral properties are reported and used for comparison.

While the above ¹H NMR experiments showed the byproducts of β-H abstraction to be a complicated mixture of unidentified silanes, experiments to provide evidence for the β-H abstraction pathway and transient disilene formation were attempted. In the related β-H abstraction of Ca{C(SiHMe₂)₃}₂THF₂ by B(C₆F₅)₃, the organometallic product is CaC(SiHMe₂)₃(HB(C₆F₅)₃)THF₂, and the organic by-product is proposed to be the silene, Me₂Si=C(SiHMe₂)₂, which is not directly detected, but instead its head-to-tail dimer 1,3-dimethyl-2,4-bis(dimethylsilyl)-1,3-disilacyclobutane is isolated.⁴⁰ Though we do not observe a head to tail dimer of disilene, we wondered if other alkenes and alkynes would react in a similar 2+2-addition pathway.

In the absence of a trapping substrate, 1equiv. B(C₆F₅)₃ reacts with **1**·THF₂ or **2**·THF₃ to give β-H abstraction from both silyl ligands yielding M{HB(C₆F₅)₃}₂THF₂ (M = Mg, Ca⁴¹) a complex mixture of silanes, and ring opened THF as the products. Similarly, 2 equiv. of B(C₆F₅)₃ reacts with **1**·THF₂ and **2**·THF₃ to afford M{HB(C₆F₅)₃}₂THF₂ (M = Mg, Ca). For comparison, the Brønsted acid HCl reacts with M(Si(SiHMe₂)₃)₂L_n to give HSi(SiHMe₂)₃ (**3**), and the Lewis acid B(C₆F₅)₃ reacts with the alkyl compound Ca{C(SiHMe₂)₃}₂THF₂ to give CaC(SiHMe₂)₃(HB(C₆F₅)₃)THF₂.⁴²

When reacting **2**·THF₃ with 2 equiv. of B(C₆F₅)₃ in the presence of anthracene, ketones, alkenes or acetylenes, complex NMR spectra containing several unidentified silanes were observed. However, the reaction of **2**·THF₃ and 2 equiv. of B(C₆F₅)₃ in the presence of

bis(trimethylsilyl)acetylene resulted in formation of $\text{Ca}\{\text{HB}(\text{C}_6\text{F}_5)_3\}_2\text{THF}_3$ and a sharp set of new resonances corresponding to a distinct silyl-containing species in the ^1H NMR spectrum in addition to multiple broad resonances corresponding to unidentified silanes. Compound **2**· THF_3 was dissolved in benzene followed by dropwise addition of a benzene solution containing 2 equiv. bis(trimethylsilyl)acetylene and 2 equiv. $\text{B}(\text{C}_6\text{F}_5)_3$ (eq. 3). After 10 min. the reaction mixture was passed through a neutral alumina plug, and the solvent and excess bis(trimethylsilyl)acetylene was removed under reduced pressure. The ^1H NMR spectrum of the resultant yellow oil contained a mixture of silanes with the major species identified by a septet at 3.99 ppm and a doublet at 0.24 ppm assigned to SiHMe_2 groups. Two additional singlets appeared at 0.41 ppm assigned to SiMe_2 and 0.16 ppm assigned to SiMe_3 . These peaks were determined to be within the same species rather than from different silanes based on NOESY NMR correlations. We observe a $\text{C}=\text{C}$ resonance in the ^{13}C NMR spectrum at 100.86 ppm. The ^{29}Si NMR spectrum contained a singlet at -19.6 ppm for SiMe_3 and a doublet at -26.2 ppm ($^1J_{\text{SiH}} = 164$ Hz) for SiHMe_2 . The internal Si peaks were assigned at -135.0 ppm for $\text{Si}(\text{SiHMe}_2)_2$ and -146.6 ppm for SiMe_2 . The IR spectrum showed one stretching frequency at 2091 cm^{-1} assigned to ν_{SiH} , and a peak was observed in the mass spectrum corresponding to $\text{M}^+ - \text{CH}_3$ (calcd. 359.14; found: 359.24), however, the parent ion was not observed. For comparison, the $\text{C}=\text{C}$ resonance was observed at 115.1 ppm (CDCl_3) in the ^{13}C NMR spectrum for 1,1,2,2-tetrakis(mesityl)-3,4-bis(trimethylsilyl)-1,2-disilacyclobutene.⁴³ Therefore, we tentatively assign this species as the disilacyclobutene resulting from the trapping of disilene with bis(trimethylsilyl)acetylene.

Conclusion

The incorporation of β -SiH functionality into the hypersilyl ligand motif ($\text{KSi}(\text{SiMe}_3)_3$) results in highly air, moisture sensitive bisilyl magnesium and calcium compounds, which show increased sensitivity toward thermolysis than their hypersilyl analogues. In contrast to related bisalkyl magnesium and calcium compounds containing $\text{C}(\text{SiHMe}_2)_3$ moieties, the silyl compounds give classical 2-center-2-electron bonding between the metal center and the silyl ligand based on the one-bond silicon-hydrogen ($^1J_{\text{SiH}}$) coupling constants and the single infrared stretching frequencies (ν_{SiH}). However, similar to the alkyl analogues, the silyl compounds undergo selective β -H abstraction rather than silyl group abstraction or a mixture of abstraction products with Lewis acids, providing cationic hydridoborate species, albeit with a greater sensitivity to the Lewis acid strength. For example, 1 equiv. of $\text{PhB}(\text{C}_6\text{F}_5)_3$ with $2 \cdot \text{THF}_3$ affords clean conversion to the corresponding cation whereas 1 equiv. of $\text{B}(\text{C}_6\text{F}_5)_3$ with $2 \cdot \text{THF}_3$ yields the dication. Interestingly, modification of the 2-electron donor ligand present in the silyl compounds allows access to highly reactive yet isolable octahedral calcium silyl compounds. We are currently studying the group transfer chemistry of these group 2 silyl compounds and their reactivity with ancillary ligands.

Experimental

General Procedures. All reactions were performed under a dry argon atmosphere using standard Schlenk techniques or under a nitrogen atmosphere in a glovebox, unless otherwise indicated. Benzene, toluene, pentane, diethyl ether, and tetrahydrofuran were dried and deoxygenated using an IT PureSolv system. Benzene- d_6 was heated to reflux over Na/K alloy

and vacuum-transferred. $\text{PhB}(\text{C}_6\text{F}_5)_2$ ⁴⁴ and $\text{B}(\text{C}_6\text{F}_5)_3$ ⁴⁵ were synthesized according to literature procedures. KO^tBu was purchased from Sigma Aldrich and sublimed prior to use. Anhydrous AlCl_3 was purchased from Sigma Aldrich and used as received. ^1H , $^{13}\text{C}\{^1\text{H}\}$, ^{29}Si and ^{11}B NMR spectra were collected on a Bruker AVII 600 spectrometer. ^{15}N chemical shifts were determined by ^1H - ^{15}N HMBC experiments on a Bruker AVII 600 spectrometer. ^{15}N chemical shifts were originally referenced to an external liquid NH_3 standard and recalculated to the CH_3NO_2 chemical shift scale by adding -381.9 ppm. Elemental analyses were performed using a Perkin-Elmer 2400 Series II CHN/S by the Iowa State Chemical Instrumentation Facility. X-ray diffraction data was collected on a Bruker APEX II diffractometer.

$\text{KSi}(\text{SiHMe}_2)_3$.⁴⁶ $\text{Si}(\text{SiHMe}_2)_4$ (6.00 g, 0.027 mol) and KO^tBu (3.95 g, 0.027 mol) were dissolved in minimal benzene (ca. 10 mL). The yellow homogenous solution was allowed to sit for 30 min, and the product precipitated as a white solid during this time. Aliquots of pentane were added to the benzene and decanted to wash the solid three times. Because of the high solubility of $\text{KSi}(\text{SiHMe}_2)_3$ in benzene, the decanted solutions were concentrated to recover a second crop of product. Recrystallization from toluene at -30 °C gave a white crystalline solid (5.99 g, 0.024 mol, 90.7%). ^1H NMR (benzene- d_6 , 600 MHz): δ 4.22 (sept, 3 H, $^3J_{\text{HH}} = 4.5$ Hz), 0.56 (d, 18 H, $^3J_{\text{HH}} = 4.5$ Hz, SiHMe_2). $^{13}\text{C}\{^1\text{H}\}$ NMR (benzene- d_6 , 150 MHz): δ 2.47 (SiHMe_2). ^{29}Si (benzene- d_6 , 119.3 MHz) δ -23.8 (d, $^1J_{\text{SiH}} = 152$ Hz, SiHMe_2 , SiHMe_2), -202.3 (s, $\text{Si}(\text{SiHMe}_2)_3$). IR (KBr, cm^{-1}): 2959 (s), 2894 (s), 2020 (s, ν_{SiH}), 1419 (m), 1242 (s), 1041 (s), 872 (s), 766 (m), 685 (m), 645 (m). Anal. Calcd. for $\text{C}_6\text{H}_{21}\text{KSi}_4$: C, 29.45; H, 8.65. Found C, 29.20; H, 8.51. Mp: 123-125 °C.

$\text{Mg}\{\text{Si}(\text{SiHMe}_2)_3\}_2\text{THF}_2$ ($1 \cdot \text{THF}_2$). Magnesium bromide (0.038 g, 0.20 mmol) and $\text{KSi}(\text{SiHMe}_2)_3$ (0.100 g, 0.41 mmol) were stirred in THF (10 mL) for 24 h, and then the solution

was filtered. Evaporation of the solvent provided a yellow oil, which was dissolved in pentane and cooled to $-30\text{ }^{\circ}\text{C}$ to give a white solid (0.065 g, 0.11 mmol, 55.1%). ^1H NMR (benzene- d_6 , 600 MHz): δ 4.58 (sept, 6 H, $^3J_{\text{HH}} = 4.2\text{ Hz}$, SiHMe_2), 3.70 (br, 8 H, α -THF), 1.32 (br, 8 H, β -THF), 0.56 (d, 36 H, $^3J = 4.2\text{ Hz}$, SiHMe_2). $^{13}\text{C}\{^1\text{H}\}$ NMR (benzene- d_6 , 150 MHz): δ 70.43 (α -THF), 25.52 (β -THF), 0.89 (SiHMe_2). ^{29}Si (benzene- d_6 , 119.3 MHz) δ -27.5 (d, $^1J_{\text{SiH}} = 169\text{ Hz}$, SiHMe_2), -182.3 (s, $\text{Si}(\text{SiHMe}_2)_3$). IR (KBr, cm^{-1}): ν 2953 (s), 2896 (s), 2064 (s, ν_{SiH}), 1460 (w), 1424 (w), 1244 (s), 1023 (s), 862 (s), 745 (m), 687 (s), 646 (s), 445 (w). Anal. Calcd. for $\text{C}_{16}\text{H}_{50}\text{MgOSi}_8$ (corresponding to the loss of 1 THF during analysis): C, 37.86; H, 9.93. Found C, 37.68; H, 9.62. Mp: 60-63 $^{\circ}\text{C}$.

$\text{Mg}\{\text{Si}(\text{SiHMe}_2)_3\}_2\text{py}_2$ ($\mathbf{1}\cdot\text{py}_2$). Solid MgBr_2 (0.031 g, 0.17 mmol) was suspended in pentane (10 mL) and pyridine (27.2 μL , 0.34 mmol) and allowed to stir for 24 h at room temperature. $\text{KSi}(\text{SiHMe}_2)_3$ (0.082 g, 0.34 mmol) was added at $-30\text{ }^{\circ}\text{C}$, and the solution was stirred for 3 h and then filtered at $-30\text{ }^{\circ}\text{C}$. Further cooling of the pentane solution at $-30\text{ }^{\circ}\text{C}$ gave a yellow solid which was isolated by filtration (0.066 g, 0.11 mmol, 65.9%). ^1H NMR (benzene- d_6 , 600 MHz): δ 8.62 (br, 4 H, *ortho*- $\text{C}_5\text{H}_5\text{N}$), 6.79 (br, 2 H, *para*- $\text{C}_5\text{H}_5\text{N}$), 6.59 (br, 4 H, *meta*- $\text{C}_5\text{H}_5\text{N}$), 4.66 (sept, 6 H, $^3J_{\text{HH}} = 4.2\text{ Hz}$, SiHMe_2), 0.51 (d, 36 H, $^3J = 4.2\text{ Hz}$, SiHMe_2). $^{13}\text{C}\{^1\text{H}\}$ NMR (benzene- d_6 , 150 MHz): δ 149.63 (*ortho*- $\text{C}_5\text{H}_5\text{N}$), 139.77 (*para*- $\text{C}_5\text{H}_5\text{N}$), 125.45 (*meta*- $\text{C}_5\text{H}_5\text{N}$), 0.73 (SiHMe_2). ^{29}Si (benzene- d_6 , 119.3 MHz) δ -26.3 (d, $^1J_{\text{SiH}} = 169\text{ Hz}$, SiHMe_2), -182.2 (s, $\text{Si}(\text{SiHMe}_2)_3$). IR (KBr, cm^{-1}): ν 2957 (s), 2900 (m), 2067 (s, ν_{SiH}), 1595 (w), 1414 (m), 1250 (s), 1022 (s), 887 (s), 858 (s), 834 (s), 797 (m), 752 (w), 699 (m), 677 (m), 650 (s), 623 (m). Anal. Calcd. for $\text{C}_{17}\text{H}_{47}\text{MgNSi}_8$ (corresponding to the loss of 1 py during analysis): C, 39.68; H, 9.21; N, 2.72. Found C, 40.02; H, 9.65; N, 2.28. Mp: 47-49 $^{\circ}\text{C}$ (dec).

Mg{Si(SiHMe₂)₃}₂DMAP₂ (1·DMAP₂). Mg{Si(SiHMe₂)₃}₂THF₂ (0.024 g, 0.041 mmol) and DMAP (0.010 g, 0.082 mmol) were dissolved in benzene (10 mL). The resulting solution was allowed to stir for 1 h, and then solvent was removed under reduced pressure. The residue was recrystallized from pentane at -30 °C to give a white solid (0.015 g, 0.022 mmol, 26.6%). ¹H NMR (benzene-*d*₆, 600 MHz): δ 8.47 (d, 8 H, ³J_{HH} = 5.4 Hz, DMAP), 6.07 (d, 8 H, ³J_{HH} = 4.2 Hz, DMAP), 4.84 (sept, 6 H, ³J_{HH} = 4.2 Hz, SiHMe₂), 2.09 (s, 24 H, DMAP), 0.67 (d, 36 H, ³J_{HH} = 4.2 Hz, SiHMe₂). ¹³C{¹H} NMR (benzene-*d*₆, 150 MHz): δ 155.03 (*ipso*-DMAP), 150.02 (*ortho*-DMAP), 107.19 (*meta*-DMAP), 38.54 (DMAP), 1.05 (SiHMe₂). ¹⁵N{¹H} NMR (benzene-*d*₆, 60.6 MHz): δ -327.3 (DMAP). ²⁹Si (benzene-*d*₆, 119.3 MHz) δ -26.8 (d, ¹J_{SiH} = 167 Hz, SiHMe₂), -184.3 (s, Si(SiHMe₂)₃). IR (KBr, cm⁻¹): ν 2945 (s), 2083 (s, ν_{SiH}), 1616 (s), 1536 (s), 1445 (m), 1389 (m), 1231 (s), 1114 (w), 1063 (w), 1003 (s), 951 (w), 881 (m), 854 (m), 810 (s), 760 (w), 675 (w), 637 (m). Anal. Calcd. for C₁₉H₅₂MgN₂Si₈ (corresponding to the loss of 1 DMAP during analysis): C, 40.92; H, 9.40; N, 5.02. Found C, 41.18; H, 9.36; N, 4.62. Mp: 92-94 °C (dec).

Ca{Si(SiHMe₂)₃}₂THF₃ (2·THF₃). Calcium iodide (0.150 g, 0.51 mmol) and KSi(SiHMe₂)₃ (0.250 g, 1.02 mmol) were dissolved in THF (15 mL). The resulting solution was allowed to stir for 48 h, and then solvent was removed under reduced pressure leaving a cream colored solid. The product was extracted with pentane, and recrystallization from a concentrated pentane solution at -30 °C gave a white solid (0.187 g, 0.28 mmol, 63.7%). ¹H NMR (benzene-*d*₆, 400 MHz): δ 4.56 (sept, 6 H, ³J_{HH} = 4.0 Hz, Si(SiHMe₂), 3.84 (br, 12 H, α-THF), 1.48 (br, 12 H, β-THF), 0.57 (d, 36 H, ³J = 4.0 Hz, SiHMe₂). ¹³C{¹H} NMR (benzene-*d*₆, 100 MHz): δ 69.76 (α-THF), 25.62 (β-THF), 1.74 (SiHMe₂). ²⁹Si (benzene-*d*₆, 119.3 MHz) δ -24.6 (d, ¹J_{SiH} = 162 Hz, SiHMe₂), -194.6 (s, Si(SiHMe₂)₃). IR (KBr, cm⁻¹): ν 2958 (s), 2894 (s), 2045 (s, ν_{SiH}), 1421 (w),

1620 (s), 1032 (s), 859 (s), 681 (w). Anal. Calcd. for $C_{20}H_{58}CaO_2Si_8$ (corresponding to the loss of 1 THF during analysis): C, 40.34; H, 9.82. Found C, 40.28; H, 9.53. Mp: 104-106 °C.

Ca{Si(SiHMe₂)₃}₂py₄ (2•py₄). CaI₂ (0.050 g, 0.17 mmol) was added to pentane (10 mL) and pyridine (55.0 μL, 0.68 mmol). The resulting solution was allowed to stir for 24 h, and then KSi(SiHMe₂)₃ (0.083 g, 0.34 mmol) was added to the solution. The mixture was stirred for 3 h at room temperature followed by filtration. Crystallization from the resultant pentane solution at -30 °C gave a yellow solid (0.076 g, 0.099 mmol, 58.7%). ¹H NMR (benzene-*d*₆, 400 MHz): δ 8.92 (d, 8 H, ³J_{HH} = 4.2 Hz, *ortho*-C₅H₅N), 6.87 (t, 4 H, ³J_{HH} = 7.2 Hz, *para*-C₅H₅N), 6.75 (t, 8 H, ³J_{HH} = 6.0 Hz, *meta*-C₅H₅N), 4.59 (sept, 6 H, ³J_{HH} = 4.1 Hz, SiHMe₂), 0.43 (d, 36 H, ³J = 4.1 Hz, Si(SiHMe₂)₃). ¹³C{¹H} NMR (benzene-*d*₆, 150 MHz): δ 150.60 (*ortho*-C₅H₅N), 138.52 (*para*-C₅H₅N), 124.85 (*meta*-C₅H₅N), 1.32 (SiHMe₂). ¹⁵N{¹H} NMR (benzene-*d*₆, 60.6 MHz): δ -79.6. ²⁹Si (benzene-*d*₆, 119.3 MHz) δ -23.3 (d, ¹J_{SiH} = 160 Hz, SiHMe₂), -199.3 (s, Si(SiHMe₂)₃). IR (KBr, cm⁻¹): ν 2963 (s), 2853 (m), 2100 (s, ν_{SiH}), 1878 (w), 1598 (m), 1440 (s), 1342 (w), 1248 (s), 1216 (w), 1150 (w), 1008 (s), 889 (s), 861 (s), 840 (s), 825 (m), 806 (m), 786 (m), 734 (m). Anal. Calcd. for C₂₇H₅₇CaN₃Si₈ (corresponding to the loss of 1 THF during analysis): C, 47.10; H, 8.34; N, 6.10. Found C, 46.84; H, 8.07; N, 6.09. Mp: 83-85 °C (dec).

Ca{Si(SiHMe₂)₃}₂DMAP₄ (2•DMAP₄). Ca{Si(SiHMe₂)₃}₂THF₃ (0.200 g, 0.30 mmol) and DMAP (0.146 g, 1.20 mmol) were dissolved in toluene (10 mL). The resulting solution was allowed to stir for 1 hour, and then the solution was placed in the freezer and crystallization from the toluene solution at -30 °C gave a pale yellow solid (0.189 g, 0.20 mmol, 67.2%). ¹H NMR (benzene-*d*₆, 600 MHz): δ 8.88 (br, 8 H, DMAP), 6.27 (br, 8 H, DMAP), 4.94 (sept, 6 H, ³J_{HH} = 4.2 Hz, SiHMe₂), 2.05 (s, 24 H, DMAP), 0.69 (d, 36 H, ³J_{HH} = 4.2 Hz, SiHMe₂). ¹³C{¹H} NMR (benzene-*d*₆, 150 MHz): δ 155.14 (*ipso*-DMAP), 150.99 (*ortho*-DMAP), 106.91 (*meta*-DMAP),

38.43 (DMAP), 1.81 (SiHMe₂). ¹⁵N{¹H} NMR (benzene-*d*₆, 60.6 MHz): δ -321.6 (DMAP). ²⁹Si (benzene-*d*₆, 119.3 MHz) δ -22.5 (d, ¹J_{SiH} = 161 Hz, SiHMe₂), -201.5 (Si(SiHMe₂)₃). IR (KBr, cm⁻¹): ν 2926 (s), 2036 (s, ν_{SiH}), 1614 (s), 1532 (s), 1444 (m), 1384 (m), 1230 (s), 1110 (w), 1065 (w), 1001 (s), 949 (w), 887 (m), 859 (s), 826 (m), 804 (s), 754 (w), 678 (w), 640 (w). Anal. Calcd. for C₃₃H₇₂CaN₆Si₈ (corresponding to the loss of 1 DMAP during analysis): C, 48.47; H, 8.87; N, 10.28. Found C, 48.41; H, 8.24; N, 10.46. Mp: 104-106 °C.

HSi(SiHMe₂)₃ (3)⁴⁷. KSi(SiHMe₂)₃ (0.113 g, 0.46 mmol) and Et₃NHCl (0.200 g, 1.45 mmol) was dissolved in THF (10 mL) and stirred for 12 h followed removal of solvent under reduced pressure. The residue was dissolved in benzene, filtered, and solvent was removed under reduced pressure to give to give a colorless oil that was a 1: 1.5 mixture of Si(SiHMe₂)₄: HSi(SiHMe₂)₃ (0.169 g) and the compound could not be cleanly isolated. ¹H NMR (benzene-*d*₆, 600 MHz): δ 4.29 (sept, 3 H, ³J_{HH} = 4.8 Hz, SiHMe₂), 2.7 (br mult, 1H, HSi(SiHMe₂)₃), 0.27 (d, 18 H, ³J = 4.8 Hz, SiHMe₂). ¹³C{¹H} NMR (benzene-*d*₆, 150 MHz): δ 0.32 (SiHMe₂). ²⁹Si (benzene-*d*₆, 119.3 MHz) δ -21.5 (d, ¹J_{SiH} = 181 Hz, SiHMe₂), -126.8 (d, ¹J_{SiH} = 158 Hz HSi(SiHMe₂)₃). IR (KBr, cm⁻¹): ν 2956 (s), 2899 (s), 2094 (br s, ν_{SiH}), 1479 (w), 1418 (s), 1247 (s), 1037 (w), 858 (s).

MgSi(SiHMe₂)₃(HBPh(C₆F₅)₂)THF₂ (4{HBPh(C₆F₅)₂}THF₂). Mg{Si(SiHMe₂)₃}₂THF₂ (0.050 g, 0.086 mmol) and BPh(C₆F₅)₂ (0.036 g, 0.086 mmol) were dissolved in benzene (10 mL). The resulting solution was allowed to stir for 30 min, and then solvent was removed under reduced pressure. The product was washed with pentane (3 × 5 mL) to give a white solid (0.041 g, 0.051 mmol, 59.6 %). ¹H NMR (benzene-*d*₆, 600 MHz): δ 7.60 (d, ³J_{HH} = 7.2 Hz, 2 H, *ortho*-C₆H₅), 7.06 (m, ³J_{HH} = 7.6 Hz, 2 H, *meta*-C₆H₅), 6.88 (m, ³J_{HH} = 7.2 Hz, 1 H, *para*-C₆H₅), 4.38 (sept, 3 H, ³J_{HH} = 4.2 Hz, SiHMe₂), 3.29 (br, 8 H, α-THF), 3.03 (br, 1 H, HB), 1.20 (br, 8 H, β-THF), 0.47 (d, 18 H, ³J_{HH} = 4.2 Hz, SiHMe₂). ¹³C{¹H} NMR (benzene-*d*₆, 150 MHz): δ 149.7 (br,

C_6F_5), 148.2 (br, C_6F_5), 140.6 (br, C_6F_5), 138.8 (br, C_6F_5), 137.2 (br, C_6F_5), 134.2 (br, C_6F_5), 132.2 (br, *ipso*- C_6H_5), overlaps with C_6D_6 (*ortho*- C_6H_5), overlaps with C_6D_6 (*meta*- C_6H_5), 126.61 (*para*- C_6H_5), 71.21 (α -THF), 25.30 (β -THF), 0.25 ($SiHMe_2$). ^{11}B NMR (benzene- d_6 , 192 MHz): δ -18.6 (d, $^1J_{HB} = 69$ Hz, $HBPh(C_6F_5)_2$). ^{19}F NMR (benzene- d_6 , 376 MHz): δ -126.3 (*ortho*- C_6F_5), -164.1 (*para*- C_6F_5), -166.3 (*meta*- C_6F_5). ^{29}Si (benzene- d_6 , 119.3 MHz) δ -28.5 (d, $^1J_{SiH} = 165$ Hz, $SiHMe_2$), -109.1 ($Si(SiHMe_2)_3$). IR (KBr, cm^{-1}): ν 3066 (w), 2959 (m), 2901 (m), 2329 (br m, ν_{BH}), 2089 (s, ν_{SiH}), 1642 (w), 1512 (s), 1462 (s), 1373 (w), 1247 (m), 1083 (s), 1012 (m), 968 (s), 860 (s), 739 (w), 679 (w), 649 (w). Anal. Calcd. for $C_{28}H_{35}BF_{10}MgOSi_4$ (corresponding to the loss of 1 THF during analysis): C, 46.38; H, 4.87. Found C, 46.86; H, 4.56. Mp: 59-61 °C.

$MgSi(SiHMe_2)_3(HBPh(C_6F_5)_2)DMAP_n$ ($4\{HBPh(C_6F_5)_2\}DMAP_n$). $Mg\{Si(SiHMe_2)_3\}_2DMAP_2$ (0.010 g, 0.015 mmol) and $BPh(C_6F_5)_2$ (0.006 g, 0.015 mmol) reacted in benzene- d_6 at room temperature. The compound could not be isolated; therefore, only solution characterization is given. 1H NMR (benzene- d_6 , 600 MHz): δ 7.55 (d, 2 H, $^3J_{HH} = 7.2$ Hz, *ortho*- C_6H_5), 7.25 (br, n H, DMAP), 7.03 (t, 2 H, $^3J_{HH} = 7.8$ Hz, *meta*- C_6H_5), 6.95 (t, 1 H, $^3J_{HH} = 7.8$ Hz, *para*- C_6H_5), 5.65 (br, n H, DMAP), 4.81 (sept, 3 H, $^3J_{HH} = 4.2$ Hz, $SiHMe_2$), 4.15 (br, 1 H, *HB*), 1.91 (s, n H, DMAP), 0.59 (d, 18 H, $^3J_{HH} = 4.2$ Hz, $SiHMe_2$). ^{11}B NMR (benzene- d_6 , 192 MHz): δ -19.3 (d, $^1J_{HB} = 63$ Hz, $HBPh(C_6F_5)_2$). ^{19}F NMR (benzene- d_6 , 376 MHz): δ -130.1 (*ortho*- C_6F_5), -166.7 (*para*- C_6F_5), -169.1 (*meta*- C_6F_5). ^{29}Si (benzene- d_6 , 119.3 MHz) δ -25.37 (d, $^1J_{SiH} = 168$ Hz, $SiHMe_2$), -183.82 ($Si(SiHMe_2)_3$). IR (benzene- d_6 solution, cm^{-1}): ν 2958 (s), 2341 (br w, ν_{BH}), 2097 (s, ν_{SiH}), 1622 (s), 1539 (s), 1514 (s), 1460 (s), 1394 (m), 1232 (s), 1157 (w), 1094 (s), 1012 (s), 970 (s), 887 (s), 861 (s), 811 (s), 761 (w).

$CaSi(SiHMe_2)_3(HBPh(C_6F_5)_2)THF_2$ ($5\{HBPh(C_6F_5)_2\}THF_2$). $Ca\{Si(SiHMe_2)_3\}_2THF_3$ (0.100 g, 0.15 mmol) and $BPh(C_6F_5)_2$ (0.063 g, 0.15 mmol) were dissolved in benzene (10 mL). The

resulting solution was allowed to stir for 30 min, and then solvent was removed under reduced pressure. The product was washed with pentane (3×5 mL) and then benzene (3×5 mL) to give a white solid (0.098 g, 0.12 mmol, 80.8%). ^1H NMR (THF- d_8 , 600 MHz): δ 7.20 (d, $^3J_{\text{HH}} = 7.2$ Hz, 2 H, *ortho*- C_6H_5), 6.90 (m, $^3J_{\text{HH}} = 7.6$ Hz, 2 H, *meta*- C_6H_5), 6.79 (m, $^3J_{\text{HH}} = 7.2$ Hz, 1 H, *para*- C_6H_5), 3.77 (sept, 3 H, $^3J_{\text{HH}} = 4.8$ Hz, SiHMe₂), 3.71 (br, 1 H, HB), 3.62 (br, 8 H, α -THF), 1.78 (br, 8 H, β -THF), -0.03 (d, 18 H, $^3J_{\text{HH}} = 4.8$ Hz, SiHMe₂). $^{13}\text{C}\{^1\text{H}\}$ NMR (THF- d_8 , 150 MHz): δ 149.7 (br, C_6F_5), 148.2 (br, C_6F_5), 139.0 (br, C_6F_5), 138.3 (br, C_6F_5), 137.4 (br, C_6F_5), 136.7 (br, C_6F_5), 134.4 (br, *ipso*- C_6H_5), 129.16 (*ortho*- C_6H_5), 126.54 (*meta*- C_6H_5), 123.40 (*para*- C_6H_5), 68.38 (α -THF), 26.52 (β -THF), -1.81 (SiHMe₂). ^{11}B NMR (THF- d_8 , 192 MHz): δ -19.6 (d, $^1J_{\text{HB}} = 93$ Hz, HBPh(C_6F_5)₂). ^{19}F NMR (THF- d_8 , 376 MHz): δ -126.0 (*ortho*- C_6F_5), -167.3 (*para*- C_6F_5), -168.8 (*meta*- C_6F_5). ^{29}Si (THF- d_8 , 119.3 MHz) δ -22.1 (d, $^1J_{\text{SiH}} = 170$ Hz, SiHMe₂), -117.3 (Si(SiHMe₂)₃). IR (KBr, cm^{-1}): ν 3062 (w), 3039 (w), 2961 (s), 2896 (s), 2330 (br m, ν_{BH}), 2074 (s, ν_{SiH}), 1886 (w), 1638 (m), 1588 (m), 1510 (s), 1450 (s), 1267 (s), 1243 (s), 1176 (m), 1083 (s), 1018 (s), 971 (s), 886 (s), 863 (s), 750 (w), 683 (w), 650 (m). Anal. Calcd. for $\text{C}_{24}\text{H}_{27}\text{BCaF}_{10}\text{Si}_4$ (corresponding to the loss of 2 THF during analysis): C, 43.11; H, 4.07. Found C, 42.85; H, 3.99. Mp: 139-141 °C.

CaSi(SiHMe₂)₃(HBPh(C₆F₅)₂)py₄ (5{HBPh(C₆F₅)₂}py₄). Ca{Si(SiHMe₂)₃}₂py₄ (0.255 g, 0.33 mmol) and BPh(C₆F₅)₂ (0.140 g, 0.33 mmol) were dissolved in benzene (10 mL). The resulting solution was allowed to stir for 10 min, and then solvent was removed under reduced pressure. The product was washed with pentane (3×5 mL) to give a yellow solid (0.173 g, 0.21 mmol, 63.1%). ^1H NMR (benzene- d_6 , 600 MHz): δ 8.43 (d, 8 H, $^3J_{\text{HH}} = 4.2$ Hz, *ortho*- $\text{C}_5\text{H}_5\text{N}$), 7.46 (d, $^3J_{\text{HH}} = 7.2$ Hz, 2 H, *ortho*- C_6H_5), 7.30 (t, $^3J_{\text{HH}} = 7.2$ Hz, 2 H, *meta*- C_6H_5), 6.87 (t, 4 H, $^3J_{\text{HH}} = 7.2$ Hz, *para*- $\text{C}_5\text{H}_5\text{N}$), 6.75 (t, 8 H, $^3J_{\text{HH}} = 6.0$ Hz, *meta*- $\text{C}_5\text{H}_5\text{N}$), 6.56 (t, $^3J_{\text{HH}} = 7.2$ Hz, 1 H, *para*-

C_6H_5), 4.52 (sept, 3 H, $^3J_{HH} = 3.6$ Hz, $SiHMe_2$), 2.95 (br, 1 H, HB), 0.42 (d, 18 H, $^3J_{HH} = 3.6$ Hz, $SiHMe_2$). $^{13}C\{^1H\}$ NMR (benzene- d_6 , 150 MHz): δ 150.37 (*ortho*- C_5H_5N), 150.3 (br, C_6F_5), 150.1 (br, C_6F_5), 149.2 (br, C_6F_5), 147.0 (br, C_6F_5), 141.3 (*para*- C_5H_5N), 133.7 (br, *ipso*- C_6H_5), 128.47 (*ortho*- C_6H_5), 127.29 (*meta*- C_6H_5), 125.32 (*para*- C_6H_5), 124.65 (*meta*- C_5H_5N), -2.26 ($SiHMe_2$). ^{11}B NMR (benzene- d_6 , 192 MHz): δ -18.7 (d, $^1J_{HB} = 111$ Hz, $HBPh(C_6F_5)_2$). ^{19}F NMR (benzene- d_6 , 376 MHz): δ -126.0 (*ortho*- C_6F_5), -164.2 (*para*- C_6F_5), -166.2 (*meta*- C_6F_5). ^{29}Si (benzene- d_6 , 119.3 MHz) δ -22.9 (d, $^1J_{SiH} = 170$ Hz, $SiHMe_2$), -195.8 (s, $Si(SiHMe_2)_3$). IR (KBr, cm^{-1}): ν 3071 (w), 2959 (s), 2381 (br w, ν_{BH}), 2091 (s, ν_{SiH}), 1642 (w), 1598 (w), 1515 (s), 1461 (s), 1251 (m), 1155 (m), 1089 (w), 1036 (s), 1004 (w), 971 (s), 887 (s), 859 (s), 836 (s), 752 (m), 703 (s), 675 (m), 620 (w). Anal. Calcd. for $C_{39}H_{42}BCaF_{10}N_3Si_4$ (corresponding to the loss of 1 py during analysis): C, 51.70; H, 4.67; N, 4.64. Found C, 52.16; H, 4.84; N, 4.87. Mp: 68-70 °C (dec).

CaSi(SiHMe₂)₃(HBPh(C₆F₅)₂)DMAP_n (5{HBPh(C₆F₅)₂}DMAP_n). Ca{Si(SiHMe₂)₃}₂DMAP₄ (0.010 g, 0.011 mmol) and BPh(C₆F₅)₂ (0.005 g, 0.011 mmol) reacted in benzene- d_6 at room temperature. The compound could not be isolated; therefore, only solution characterization is given. 1H NMR (benzene- d_6 , 600 MHz): δ 8.25 (br, n H, DMAP), 7.77 (d, $^3J_{HH} = 7.2$ Hz, 2 H, *ortho*- C_6H_5), 7.19 (t, $^3J_{HH} = 7.2$ Hz, 2 H, *meta*- C_6H_5), 7.05 (t, $^3J_{HH} = 7.2$ Hz, 1 H, *para*- C_6H_5), 6.09 (br, n H, DMAP), 4.32 (sept, 3 H, $^3J_{HH} = 4.2$ Hz, $SiHMe_2$), 4.54 (br, 1 H, HB), 2.06 (s, n H, DMAP), 0.43 (d, 18 H, $^3J_{HH} = 4.2$ Hz, $SiHMe_2$). ^{11}B NMR (benzene- d_6 , 192 MHz): δ -18.8 (d, $^1J_{HB} = 92$ Hz, $HBPh(C_6F_5)_2$). ^{19}F NMR (benzene- d_6 , 376 MHz): δ -129.7 (*ortho*- C_6F_5), -165.2 (*para*- C_6F_5), -167.1 (*meta*- C_6F_5). ^{29}Si (benzene- d_6 , 119.3 MHz) δ -21.3 (d, $^1J_{SiH} = 170$ Hz, $SiHMe_2$), -195.7 (s, $Si(SiHMe_2)_3$). IR (benzene- d_6 solution, cm^{-1}): ν 2955 (s), 2896 (w), 2388 (br

w, ν_{BH} , 2089 (s, ν_{SiH}), 1642 (s), 1553(s), 1515 (s), 1394 (m), 1281 (w), 1231 (m), 1132 (s), 1092 (s), 1013 (m), 974 (s), 887 (s), 863 (s), 764 (w).

DMAP-BPh(C₆F₅)₂ (6). BPh(C₆F₅)₂ (0.050 g, 0.12 mmol) was dissolved in benzene (5 mL) and added dropwise to a benzene solution of DMAP (0.015 g, 0.12 mmol). The resulting solution was allowed to stir for 10 min, and then solvent was removed under reduced pressure. The product was washed with pentane to give a white solid (0.058 g, 0.11 mmol, 90.0%). ¹H NMR (benzene-*d*₆, 600 MHz): δ 7.99 (d, 2 H, ³*J*_{HH} = 7.2 Hz, DMAP), 7.69 (d, 2H, ³*J*_{HH} = 7.2 Hz, *ortho*-C₆H₅), 7.38 (t, 2H, ³*J*_{HH} = 7.2 Hz, *meta*-C₆H₅), 7.23 (t, 1H, ³*J*_{HH} = 7.2 Hz, *para*-C₆H₅), 5.35 (d, 2 H, ³*J*_{HH} = 7.2 Hz, DMAP), 1.86 (s, DMAP). ¹³C{¹H} NMR (benzene-*d*₆, 150 MHz): δ 149.5 (br, C₆F₅), 147.8 (br, C₆F₅), 145.03 (DMAP), 138.8 (br, C₆F₅), 138.7 (br, *ipso*-C₆H₅), 138.00 (DMAP), 137.0 (br, C₆F₅), 133.03 (*ortho*-C₆H₅), 127.62 (*meta*-C₆H₅), 126.07 (*para*-C₆H₅), 105.54 (DMAP), 38.49 (DMAP). ¹¹B NMR (benzene-*d*₆, 192 MHz): δ -1.89. ¹⁹F NMR (benzene-*d*₆, 376 MHz): δ -130.9 (*ortho*-C₆F₅), -158.7 (*para*-C₆F₅), -163.9 (*meta*-C₆F₅). ¹⁵N{¹H} NMR (benzene-*d*₆, 60.6 MHz): δ -314.1 (DMAP). IR (KBr, cm⁻¹): ν 2962 (m), 2931 (m), 2874 (w), 1650 (s), 1560 (s), 1518 (s), 1465 (w), 1399 (m), 1371 (m), 1284 (m), 1232 (m), 1095 (s), 1038 (m), 974 (s). Anal. Calcd. for C₂₅H₁₅BF₁₀N₂: C, 55.18; H, 2.78; N, 5.15. Found C, 54.66; H, 2.30; N, 4.64. Mp: 94-96 °C.

References

- (1) (a) Rochow, E.G. *J. Am. Chem. Soc.* **1945**, *67*, 963-965. (b) Rösch, L.; John, P.; Reitmeier, R. "Organic Silicon Compounds" *Ullmann's Encyclopedia of Industrial Chemistry*; John Wiley and Sons: San Francisco, 2003.

- (2) (a) Enthaler, S. *ACS Catal.* **2013**, *3*, 150-158. (b) Wakefield, B. J. "Compounds of the Alkali and Alkaline Earth Metals in Organic Synthesis." Vol. 7 in *Comprehensive Organometallic Chemistry*; Wilkinson, G.; Stone, F. G. A.; Abel E. W., Ed.; Elsevier Science Ltd. 1982; pp 1-110.
- (3) (a) Chalk, A. J.; Harrod, J. F. *J. Am Chem. Soc.* **1965**, *87*, 16-21. (b) Liu, X.; Wu, Z.; Cai, H.; Yang, Y.; Chen, T.; Vallet, C. E.; Zuhr, R. A.; Beach, D. B.; Peng, Z.-H.; Wu, Y.-D.; Concolino, T. E.; Rheingold, A. L.; Xue, Z. *J. Am. Chem. Soc.* **2001**, *123*, 8011-8021. (c) No, J.-T.; O, J.-H.; Lee, C.-M. *Mater. Chem. Phys.* **2000**, *63*, 44. (d) Park, J.; Sohn, D. K.; Lee, B. H.; Bae, J.; Byun, J. S.; Park, J. W. *J. Electrochem. Soc.* **1999**, *146*, 1579-1582.
- (4) (a) Leich, V.; Spaniol, T. P.; Maron, L.; Okuda, J. *Chem. Commun.* **2014**, *50*, 2311-2314. (b) Teng, W.; Ruhlandt-Senge, K. *Organometallics* **2004**, *23*, 2694-2700. (c) Farwell, J. D.; Lappert, M. F.; Marschner, C.; Strissel, C.; Tilley, T. D. *J. Organomet. Chem.* **2000**, *603*, 185-188. (d) Gaderbauer, W.; Zirngast, M.; Baumgartner, J.; Marschner, C.; Tilley, T. D. *Organometallics* **2006**, *25*, 2599-2606.
- (5) (a) Leich, V.; Spaniol, T. P.; Maron, L.; Okuda, J. *Chem. Commun.* **2014**, *50*, 2311-2314. (b) Harder, S. *Chem. Rev.* **2010**, *110*, 3852-3876. (c) Buch, F.; Brettar, J.; Harder, S. *Angew. Chem. Int. Ed.* **2006**, *45*, 2741-2745. (d) Crimmin, M. R.; Arrowsmith, M.; Barrett, A. G. M.; Casely, I. J.; Hill, M. S.; Procopiou, P. A. *J. Am. Chem. Soc.* **2009**, *131*, 9670-9685. (e) Arrowsmith, M.; Hadlington, T. J.; Hill, M.; Kociok-Kohn, G. *Chem. Commun.* **2012**, *48*, 4567-4569. (f) Mukherjee, D.; Ellern, A.; Sadow, A. D. *Chem. Sci.* **2014**, *5*, 959-964. (g) Liu, B.; Roisnel, T.; Carpentier, J.-F.; Sarazin, Y. *Chem. Eur. J.* **2013**, *19*, 2784-2802.
- (6) Miller, R. D.; Michl, J. *Chem. Rev.* **1989**, *89*, 1359-1410.

- (7) (a) Arrowsmith, M.; Maitland, B.; Kociok-Köhn, G.; Stasch, A.; Jones, C.; Hill, M. S. *Inorg. Chem.* **2014**, *53*, 10543-10552. (b) Harder, S.; Spielmann, J.; Intemann, J. *Dalton Trans.* **2014**, *43*, 14284. (c) Jochmann, P.; Davin, J. P.; Spaniol, T. P.; Maron, L.; Okuda, J. *Angew. Chem. Int. Ed.* **2012**, *51*, 1-5. (d) Harder, S.; Brettar, J. *Angew. Chem. Int. Ed.* **2006**, *45*, 3474-3478.
- (8) (a) Tilley, T. D. *Acc. Chem. Res.* **1993**, *26*, 22-29. (b) Dioumaev, V. K.; Harrod, J. F. *Organometallics* **1994**, *13*, 1548-1550.
- (9) (a) Farwell, J. D.; Lappert, M. F.; Marschner, C.; Strissel, C.; Tilley, T. D. *J. Organomet. Chem.* **2000**, *603*, 185-188. (b) Gaderbauer, W.; Zirngast, M.; Baumgartner, J.; Marschner, C. *Organometallics* **2006**, *25*, 2599-2606.
- (10) (a) Teng, W.; Ruhlandt-Senge, K. *Organometallics* **2004**, *23*, 2694-2700. (b) Leich, V.; Spaniol, T. P.; Maron, L.; Okuda, J. *Chem. Commun.* **2014**, *50*, 2311-2314.
- (11) (a) Spielmann, J.; Piesik, D. F.-J.; Harder, S. *Chem. Eur. J.* **2010**, *16*, 8307-8318. (b) Linney, R. E.; Russell, D. K.; *J. Mater. Chem.* **1993**, *3*, 587-590; (c) Kim, Y.S.; Won, Y. S.; Hagelin-Weaver, H.; Omenetto, N.; Anderson, T. *J. Phys. Chem. A*, **2008**, *112*, 4246-4253. (d) Lennartson, A.; Hakansson, M.; Jagner, S. *Angew. Chem., Int. Ed.* **2007**, *46*, 6678-6680.
- (12) Yan, K.; Upton, B. M.; Ellern, A.; Sadow, A. D. *J. Am. Chem. Soc.* **2009**, *131*, 15110-15111.
- (13) Mukherjee, D.; Lampland, N. L.; Yan, K.; Dunne, J. F.; Ellern, A.; Sadow, A. D. *Chem. Commun.* **2013**, *49*, 4334-4336.
- (14) Marschner, C., *Eur. J. Inorg. Chem.* **1998**, *1998*, 221-226.
- (15) Gilman, H.; Smith, C. L., *J. Am. Chem. Soc.* **1964**, *86*, 1454-1454.
- (16) Lambert, J. B.; Pflug, J. L.; Denari, J. M., *Organometallics* **1996**, *15*, 615-625.

- (17) Ishikawa, M.; Kumada, M.; Sakurai, H., *J. Organomet. Chem.* **1970**, *23*, 63-69.
- (18) Kulpinski, P.; Lickiss, P. D.; Stanczyk, W., *Bull. Polish Acad. Sci.-Chem.* **1992**, *40*, 21-24.
- (19) Yan, K.; Schoendorff, G.; Upton, B. M.; Ellern, A.; Windus, T. L.; Sadow, A. D.,
Organometallics **2013**, *32*, 1300-1316.
- (20) Bent, H. A. *Chem. Rev.* **1961**, *61*, 275-311.
- (21) Yan, K.; Schoendorff, G.; Upton, B. M.; Ellern, A.; Windus, T. L.; Sadow, A. D.
Organometallics **2013**, *32*, 1300-1316.
- (22) Yan, K.; Schoendorff, G.; Upton, B. M.; Ellern, A.; Windus, T. L.; Sadow, A. D.
Organometallics **2013**, *32*, 1300-1316.
- (23) Klinkhammer, K. W. *Chem. Eur. J.* **1997**, *3*, 1418-1431.
- (24) Jenkins, D. M.; Teng, W.; English, U.; Stone, D.; Ruhlandt-Senge, K. *Organometallics*
2001, *20*, 4600-4606.
- (25) Klinkhammer, K. W. *Chem. Eur. J.* **1997**, *3*, 1418-1431.
- (26) Teng, W.; Ruhlandt-Senge, K. *Organometallics* **2004**, *23*, 2694-2700.
- (27) Mukherjee, D.; Lampland, N. L.; Yan, K.; Dunne, J. F.; Ellern, A.; Sadow, A. D. *Chem. Commun.* **2013**, *49*, 4334-4336.
- (28) Farwell, J. D.; Lappert, M. F.; Marschner, C.; Strissel, C.; Tilley, T. D. *J. Organomet. Chem.* **2000**, *603*, 185-188.
- (29) Teng, W.; Ruhlandt-Senge, K. *Organometallics* **2004**, *23*, 2694-2700.
- (30) Mukherjee, D.; Lampland, N. L.; Yan, K.; Dunne, J. F.; Ellern, A.; Sadow, A. D. *Chem. Commun.* **2013**, *49*, 4334-4336.
- (31) Bent, H. A. *Chem. Rev.* **1961**, *61*, 275-311.

- (32) Yan, K.; Upton, B. M.; Ellern, A.; Sadow, A. D. *J. Am. Chem. Soc.* **2009**, *131*, 15110-15111.
- (33) Farwell, J. D.; Lappert, M. F.; Marschner, C.; Strissel, C.; Tilley, T. D. *J. Organomet. Chem.* **2000**, *603*, 185-188.
- (34) Teng, W.; Ruhlandt-Senge, K. *Organometallics* **2004**, *23*, 2694-2700.
- (35) Teng, W.; Ruhlandt-Senge, K. *Organometallics* **2004**, *23*, 2694-2700.
- (36) Yan, K.; Upton, B. M.; Ellern, A.; Sadow, A. D. *J. Am. Chem. Soc.* **2009**, *131*, 15110-15111.
- (37) Teng, W.; Ruhlandt-Senge, K. *Organometallics* **2004**, *23*, 2694-2700.
- (38) Leich, V.; Spaniol, T. P.; Maron, L.; Okuda, J. *Chem. Commun.* **2014**, *50*, 2311-2314.
- (39) Yan, K.; Upton, B. M.; Ellern, A.; Sadow, A. D. *J. Am. Chem. Soc.* **2009**, *131*, 15110-15111.
- (40) Yan, K.; Upton, B. M.; Ellern, A.; Sadow, A. D. *J. Am. Chem. Soc.* **2009**, *131*, 15110-15111.
- (41) Yan, K.; Upton, B. M.; Ellern, A.; Sadow, A. D. *J. Am. Chem. Soc.* **2009**, *131*, 15110-15111.
- (42) Yan, K.; Upton, B.; Ellern, A.; Sadow, A. D. *J. Am. Chem. Soc.* **2009**, *131*, 15110-15111.
- (43) Ishikawa, M.; Matsuzawa, S.; Sugisawa, H.; Yano, F.; Kamitori, S.; Higuchi, T. *J. Am. Chem. Soc.* **1985**, *107*, 7706-7710.
- (44) Sundararaman, A.; Jakle, F. *J. Organomet. Chem.* **2003**, *681*, 134-142.
- (45) Wang, C.; Erker, G.; Kehr, G.; Wedeking, K.; Fröhlich, R. *Organometallics* **2005**, *24*, 4760-4773.

- (46) Mukherjee, D.; Lampland, N. L.; Yan, K.; Dunne, J. F.; Ellern, A.; Sadow, A. D. *Chem. Commun.* **2013**, 4334-4336.
- (47) Herzog, U.; Roewer, G. *J. Organomet. Chem.* **1997**, 544, 217-223.

CHAPTER 3: β -SiH RICH ZINC SILYL COMPOUNDS AND β -SiH ABSTRACTION

Modified from a paper published in *Inorganica Chimica Acta*

Nicole L. Lampland, Arkady Ellern, Aaron D. Sadow*

Department of Chemistry, U.S. DOE Ames Laboratory, Iowa State University, Ames, IA

50011-3111

Abstract

The two-coordinate compound $\text{Zn}\{\text{Si}(\text{SiHMe}_2)_3\}_2$ is generated by the reaction of ZnCl_2 and 2 equiv. of $\text{KSi}(\text{SiHMe}_2)_3$, but this species degrades to $\text{Si}(\text{SiHMe}_2)_4$ as the only NMR observed species over 48 h at room temperature. The transient disilylzinc compound is stabilized by a neutral NHC 1,3-di-*t*-butylimidazol-2-ylidene (Im^tBu) or the chelating *N*-donor ligands 1,2-dipyrrolidinoethane (dpe) or 2,2'-bipyridine (bipy). The one-bond silicon-hydrogen ($^1J_{\text{SiH}}$) coupling constants and the infrared stretching frequencies (ν_{SiH}) of these disilyl zinc compounds indicate that the zinc center and silyl ligand interact through a classic 2-center-2-electron bond, and the β -SiH groups do not show evidence of nonclassical interactions with the zinc center. Still, the β -SiH groups undergo β -SiH abstraction, rather than silyl group abstraction, upon reaction with the Lewis acid $\text{B}(\text{C}_6\text{F}_5)_3$ to give the corresponding silylzinc hydridoborate compounds.

Introduction

Zinc silyl compounds could have synthetic utility as silyl group transfer agents to access new metal silyl compounds and as nucleophilic silylating agents in organic chemistry.¹ These species are potentially useful as materials precursors, and homoleptic zinc silyls $\text{Zn}(\text{SiR}_3)_2$ may

serve as precursors for new zinc complexes where an ancillary ligand is used to modulate the reactivity of the Zn–Si bond. In addition, zinc compounds catalyze important transformations of silanes, such as dehydrogenative coupling of alcohols and hydrosilanes as well as hydrosilylation of carbonyls including CO₂.²

There are a few notable patterns associating the chemical properties of homoleptic zinc silyls and the silyl ligand's steric and structural properties. Relatively small silyl ligands can form zincate structures such as [K·(THF)₄][Zn{SiMe(SiMe₃)₂]₃],³ while bulkier silyl ligands yield isolable neutral zinc species. For example, the homoleptic disilyl zinc compound Zn{Si(SiMe₃)₃]₂⁴ is isolable and persistent at room temperature, as are bulky cyclic polysilylzinc compounds.⁵ For some silyl ligands, reduction of Zn(II) is observed. Thus, Zn(SiPh₃)₂ disproportionates at 105 °C to yield SiPh₄ and polymeric phenyl silanes with concurrent reduction of zinc,⁶ although hexaphenyldisilane was not detected. Alternatively, the β-CH containing Zn(SiMe₃)₂ readily undergoes reductive elimination at room temperature.⁷ The β-CHs in this compound do not play an obvious role in the reductive elimination. Additionally, β-H elimination is not a common pathway for zinc. For this reason, a sterically hindered silyl ligand containing β-SiH groups, -Si(SiHMe₂)₃, was chosen for study because the β-functionality might allow access to new reaction pathways; moreover, the zinc silyls [Zn]Si(SiHMe₂)₃ could provide a mild synthetic route to β-SiH-containing transition-metal compounds.

Notably, in a heteroleptic zinc compound, the -Si(SiHMe₂)₃ group is surprisingly robust, contrasting the aforementioned decomposition of homoleptic silyls. Thus, To^MZnSi(SiHMe₂)₃ (To^M = tris(4,4-dimethyl-2-oxazolinyl)phenylborate) is unchanged at 170 °C for at least 24 h and is inert to O₂ (100 psi, 120 °C or photolysis with a 450 W medium pressure Hg lamp), methanol and methanol/water to 60 °C. It reacts with CO₂ only under forcing conditions (60 psi, 120 °C) to

give $\text{To}^{\text{M}}\text{ZnOCHO}$.⁸ The β -SiH-free analogue $\text{To}^{\text{M}}\text{ZnSi}(\text{SiMe}_3)_3$ is unreactive toward CO_2 , O_2 , thermolysis and photolysis under these conditions.

On the basis of these precedents, the target of the present study, $\text{Zn}\{\text{Si}(\text{SiHMe}_2)_3\}_2$, might be isolable and long-lived like the bulkier zinc silyls or heteroleptic analogue, form zincates following the smaller silyl ligands, or undergo reductive elimination. In addition, we were interested in the reactivity of the Zn–Si bond in comparison to the β -SiH bond. The latter position has been the reactive site in a zinc tetramethyldisilazido compound,⁹ zirconium tetramethyldisilazido compounds,¹⁰ and in calcium and ytterbium tris(dimethylsilyl)methyl compounds.¹¹

Results and Discussion

Synthesis and characterization of disilylzinc compounds

Salt metathesis reactions of zinc chloride and $\text{KSi}(\text{SiHMe}_2)_3$ provide zinc silyl compounds containing β -SiH moieties. As shown in eq. 1, ZnCl_2 and 2 equiv. of $\text{KSi}(\text{SiHMe}_2)_3$ react in benzene- d_6 to generate $\text{Zn}\{\text{Si}(\text{SiHMe}_2)_3\}_2$ (**1**). As noted above, a number of two-coordinate disilylzinc compounds have been reported including β -hydrogen containing $\text{Zn}(\text{SiMe}_3)_2$,¹² but to the best of our knowledge, **1** is the first that contains β -SiH functionality. The SiMe_2 and SiH ^1H NMR resonances appeared at 0.38 and 4.49 ppm. The ^{29}Si NMR spectrum contained a doublet at -31.4 ppm ($^1J_{\text{SiH}} = 181$ Hz) and a singlet at -134.2 ppm. Spectral data for all of the neutral compounds described in this paper are listed in Table 1.

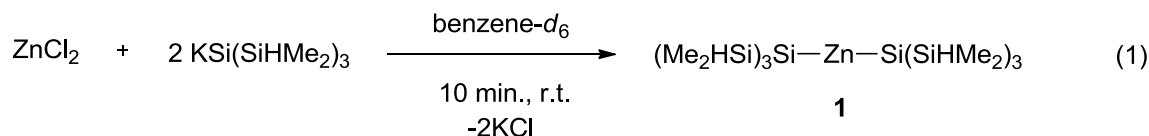


Table 1. Spectral data for zinc silyl compounds and related silanes

Compound	²⁹ Si NMR δ (C ₆ D ₆)		¹ J _{SiH} (Hz)	ν _{SiH} (cm ⁻¹)
	Si(SiRMe ₂) ₃	Si(SiRMe ₂) ₃		
KS _i (SiHMe ₂) ₃ ¹³	-23.8	-202.3	152	2020
Si(SiHMe ₂) ₄ ¹⁴	-33.5	-139.9	180	2093
Zn{Si(SiHMe ₂) ₃ } ₂ (1)	-31.4	-134.2	181	2078
Zn{Si(SiMe ₃) ₃ } ₂ ¹⁵	-7.2	-123.9	n.a.	n.a.
(Im ^t Bu)Zn{Si(SiHMe ₂) ₃ } ₂ (1 ·Im ^t Bu)	-28.2	-163.9	171	2070
(dpe)Zn{Si(SiHMe ₂) ₃ }Cl (2 ·dpe)	-28.4	-166.9	171	2069
(dpe)Zn{Si(SiHMe ₂) ₃ } ₂ (1 ·dpe)	-27.5	-169.2	171	2069
(bipy)Zn{Si(SiHMe ₂) ₃ } ₂ (1 ·bipy)	-28.9	-161.7	171	2063
(dpe)Zn{Si(SiHMe ₂) ₃ }HB(C ₆ F ₅) ₃ ([3]·dpe) ^a	-27.0	-140.9	182	2096
(bipy)Zn{Si(SiHMe ₂) ₃ }HB(C ₆ F ₅) ₃ ([3]·bipy)	-30.1	-133.8	180	2091

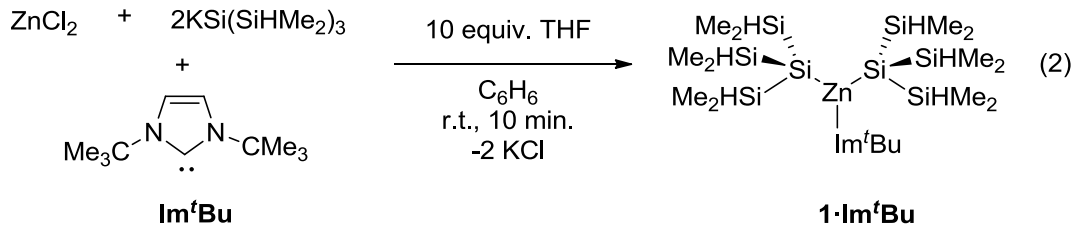
^a Spectra were acquired in bromobenzene-*d*₅.

Compound **1** does not persist in solution, and after 48 h at room temperature, a precipitate is observed and the only species detected in the ¹H NMR spectrum is Si(SiHMe₂)₄,¹⁶ which contained a doublet at 0.31 ppm assigned to SiMe₂ and a septet at 4.36 ppm assigned to SiH. The ²⁹Si NMR spectrum showed a doublet at -33.5 ppm (¹J_{SiH} = 180 Hz) and a singlet at -139.9 ppm. Similarly, Si(SiMe₃)₄ was identified in the decomposition of M{Si(SiMe₃)₃}₂ (M = Ca, Sr, Ba) in the presence of THF.¹⁷ The precipitate was characterized as containing zinc metal by powder X-ray diffraction; the diffraction pattern of the precipitate also revealed the presence of KCl and ZnO that had formed in an adventitious oxidation upon sample preparation in air.

Although a number of approaches were pursued to isolate the desired intermediate **1**, its transient nature hindered its isolation. For example, immediate workup by evaporation of the solvent from the reaction mixture provides Si(SiHMe₂)₄, zinc, and other unidentified products.

Attempts to crystallize **1** in toluene at $-30\text{ }^{\circ}\text{C}$ also provide the rearrangement products. Addition of 1 equiv. $\text{KSi}(\text{SiHMe}_2)_3$ to **1** shows signals of the starting materials rather than a potassium zincate in the ^1H NMR spectrum, and over time silane is still observed. The decomposition of **1** offers a straightforward synthetic route to a SiH-rich silane,¹⁸ but in fact, $\text{Si}(\text{SiHMe}_2)_4$ is most easily isolated by the reaction of $\text{KSi}(\text{SiHMe}_2)_3$ and bipy. Thus, compound **1** follows reactivity reported for other s-block metal silyl complexes rather than the reductive elimination reactivity reported for $\text{Zn}(\text{SiMe}_3)_2$ or the persistence of $\text{Zn}\{\text{Si}(\text{SiMe}_3)_3\}$, which is stable indefinitely in the solid-state under nitrogen and for at least 3 days in benzene- d_6 .¹⁹ Of course, dialkylzinc ZnR_2 ($\text{R} = \text{Me}, \text{Et}, i\text{-C}_3\text{H}_7, \text{CMe}_3, \text{C}(\text{SiHMe}_2)_3,$ ²⁰ $\text{C}(\text{SiMe}_3)_3$)²¹ are isolable and do not readily undergo degradation. Alternatively, ZnH_2 reacts over 1 to 2 days at room temperature to give Zn and H_2 .²² However, recently $[(\text{ImMes})\text{ZnH}_2]_2$ ($\text{ImMes} = 1,3\text{-dimesitylimidazole}$) was isolated, characterized, and shown to be a persistent substance.²³ In addition, Arduengo reported carbene adducts of dialkyl zinc compounds in early studies of N-heterocyclic carbenes,²⁴ and other NHC adducts of zinc have been described.²⁵

Following the stabilization method for ZnH_2 , we applied a ligand coordination strategy to facilitate the isolation of $\text{LZn}\{\text{Si}(\text{SiHMe}_2)_3\}_2$ or $\text{L}_2\text{Zn}\{\text{Si}(\text{SiHMe}_2)_3\}_2$ compounds and inhibit silane formation. The reaction of $\text{KSi}(\text{SiHMe}_2)_3$ and 1,3-di-*t*-butylimidazol-2-ylidene (**Im^tBu**) gives an adduct that does not react with ZnCl_2 at room temperature in benzene- d_6 over 1 d. However, addition of a small amount of THF facilitates the salt metathesis reaction. Thus, the reaction of ZnCl_2 , 2 equiv. $\text{KSi}(\text{SiHMe}_2)_3$, and 1 equiv. of **Im^tBu** in the presence of 10 equiv. of THF instantaneously gives $(\text{Im}^t\text{Bu})\text{Zn}\{\text{Si}(\text{SiHMe}_2)_3\}_2$ (**1·Im^tBu**) (eq. 2), which is stabilized against $\text{Si}(\text{SiHMe}_2)_4$ formation at room temperature. However, **1·Im^tBu** converts to unidentified silicon-containing products over 4 d.



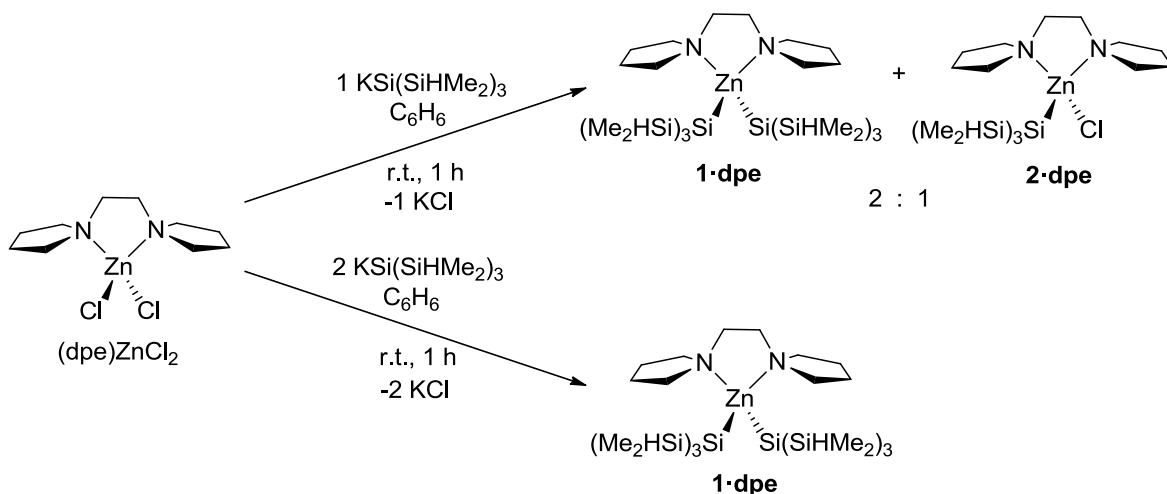
Following an immediate workup, **1·Im^tBu** was isolated as a viscous, colorless oil in 94% yield. The ¹H NMR spectrum contained a doublet at 0.48 ppm assigned to SiMe₂ and a septet at 4.54 ppm assigned to SiH and singlets at 6.40 and 1.37 ppm assigned to the *N*-heterocyclic carbene. The ²⁹Si NMR spectrum showed a doublet at -28.2 ppm (¹J_{SiH} = 171 Hz) and a singlet resonance at -163.9 ppm that was shifted significantly upfield with respect to the value observed for **1**. The coupling constant for the SiH and single IR stretching frequency assigned to the ν_{SiH} (2070 cm⁻¹) are consistent with terminal Si-H.

Other monodentate donors, including THF, pyridine, and 4-dimethylaminopyridine, are not effective at stabilizing **1**, either under conditions with 2 equivalents or with large excesses of the donor. However, adducts of **1** with the bidentate nitrogen-based donors 1,2-dipyrrolidinoethane (dpe) or 2,2'-bipyridine (bipy) are isolable under appropriate conditions. The compounds L₂Zn{Si(SiHMe₂)₃}₂ may be prepared either by addition of ZnCl₂ and the ligand followed by reaction with 2 equiv. of KSi(SiHMe₂)₃ or through in situ generation of **1** followed by coordination of the donor ligand. The first route is preferable for dpe, whereas the second route is required for bipy.

In the first route, ZnCl₂ is stirred with dpe in benzene for 24 h at room temperature to form a benzene-soluble, isolable complex (dpe)ZnCl₂. The reaction of (dpe)ZnCl₂ and 1 equiv. of KSi(SiHMe₂)₃ provides a mixture of (dpe)Zn{Si(SiHMe₂)₃}₂ (**1·dpe**) and (dpe)Zn{Si(SiHMe₂)₃}Cl (**2·dpe**) products in a 2:1 ratio (Scheme 1), along with unreacted

(dpe)ZnCl₂. The monosilyl compound **2·dpe** is easily isolated by selective crystallization from pentane at -30 °C.

Scheme 1. Synthesis of 1,2-dipyrrolidinoethane-coordinated zinc silyl compounds.



The zinc center in **2·dpe** is coordinated in the expected pseudo-tetrahedral geometry, as determined by a single crystal X-ray diffraction study (Figure 1). The Zn–Si bond length of 2.4000(9) Å is slightly longer than the corresponding distances in [(Me₃Si)₃SiZnCl]₂·(THF)₂ (2.3537(9) Å)²⁶ and in (Me₃Si)₃SiZnCl·TMEDA (2.3671(13) Å).²⁷ The distance in To^MZnSi(SiHMe₂)₃ of 2.4028(5) Å,²⁸ however, is nearly identical. The H atoms belonging to the β-Si atoms were objectively located on a difference Fourier map, refined isotropically, and show that the Si–H moieties point away from the zinc center.

The target disilyl zinc compound **1·dpe** is readily synthesized by the reaction of 2 equiv. of KSi(SiHMe₂)₃ and (dpe)ZnCl₂ in 85% yield. The ¹H NMR spectrum of **1·dpe** contained a doublet at 0.56 ppm assigned to the SiMe₂ and a septet at 4.55 ppm assigned to the SiH group. The ²⁹Si NMR spectrum showed a doublet at -27.5 ppm (¹J_{SiH} = 171 Hz) and a singlet at -169.2 ppm, and this upfield chemical shift is similar to that of **1·Im^tBu**. As expected, the IR spectra of

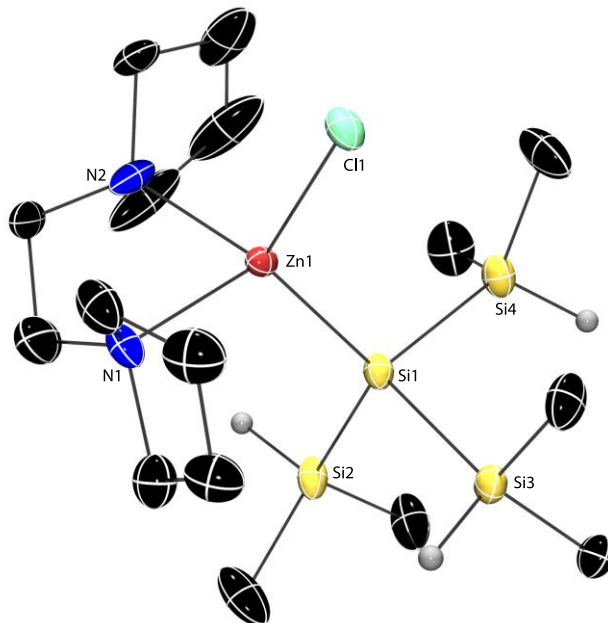
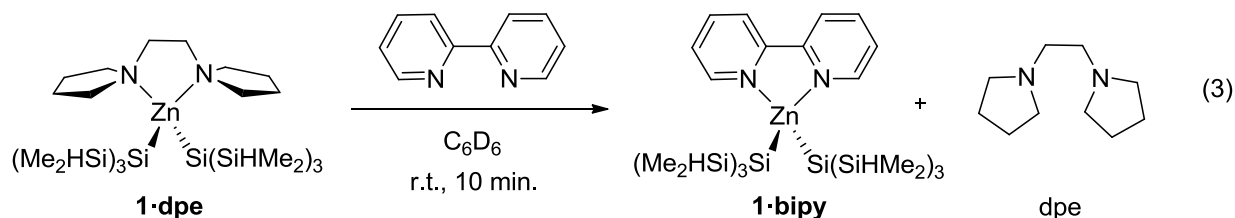


Figure 1. Rendered thermal ellipsoid plot of **2·dpe**. Selected interatomic distances (Å): Zn1–N1, 2.155(3); Zn1–N2, 2.148(3); Zn1–Cl1, 2.2722(8); Zn1–Si1, 2.4000(9). Selected interatomic angles (°): N2–Zn1–N1, 84.0(1); Cl1–Zn1–Si1, 117.04(3); Zn1–Si1–Si2, 121.92(4); Zn1–Si1–Si3, 108.53(4); Zn1–Si1–Si4, 113.8(2).

1·dpe and **2·dpe** indicate that the SiH moieties are involved in 2-center-2-electron bonding on the basis of single stretching frequencies assigned to ν_{SiH} (**1·dpe**: 2069 cm^{-1} , **2·dpe**: 2069 cm^{-1}).

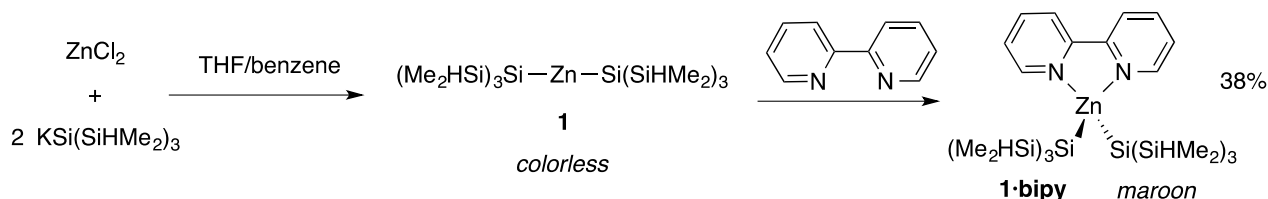
1·dpe persists in solution at room temperature, however, $\text{Si}(\text{SiHMe}_2)_4$ is the only species observed in the ^1H NMR spectrum after 10 h at 60 °C.

In contrast to the $(\text{dpe})\text{ZnCl}_2$ adduct, the $(\text{bipy})\text{ZnCl}_2^{29}$ adduct reacts with $\text{KSi}(\text{SiHMe}_2)_3$ to give the silane $\text{Si}(\text{SiHMe}_2)_4$. Therefore, to access a bipy-stabilized zinc silyl compound, we used **1·dpe** as a starting material. **1·dpe** and 1 equiv. of bipy react instantaneously to give free dpe and $(\text{bipy})\text{Zn}\{\text{Si}(\text{SiHMe}_2)_3\}_2$ (**1·bipy**) (eq. 3). Further addition of bipy shows only



resonances assigned to **1·bipy** and free bipy in the ^1H NMR spectrum. This synthesis employs dpe as a sacrificial ligand, and a direct route to **1·bipy** would be preferred. An improved preparation of **1·bipy** is accomplished by the sequence shown in Scheme 2. The challenges of bipy-induced decomposition of $\text{KSi}(\text{SiHMe}_2)_3$ and decomposition of **1** are avoided by close monitoring the color of the reaction mixture. Thus, ZnCl_2 and $\text{KSi}(\text{SiHMe}_2)_3$ are allowed to react in a benzene/THF mixture. A color change from yellow to colorless indicates that all the $\text{KSi}(\text{SiHMe}_2)_3$ is consumed and **1** is formed, and bipy is immediately added and followed by workup. **1·bipy** is extracted with pentane and isolated as a viscous maroon oil in 38% yield, and its NMR and IR spectroscopy follow the patterns established for **1**, **1·Im^tBu**, and **1·dpe**.

Scheme 2. Stepwise synthesis of **1·bipy** monitored by color change.

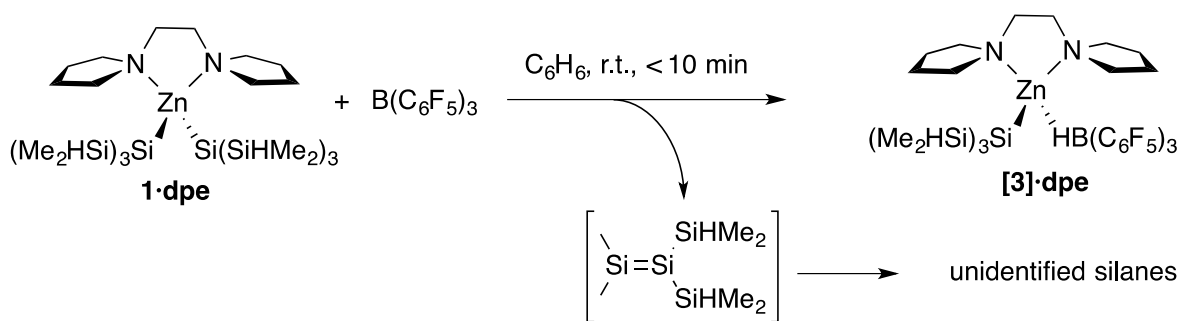


Reactivity of N-donor silyl complexes with borane Lewis acids

The reaction of 1 equiv. of $\text{B}(\text{C}_6\text{F}_5)_3$ and **1·dpe** occurs within 10 min. to give $(\text{dpe})\text{Zn}\{\text{Si}(\text{SiHMe}_2)_3\}\text{HB}(\text{C}_6\text{F}_5)_3$ (**[3]·dpe**) as shown in Scheme 3. **[3]·dpe** forms an immiscible oil in benzene, therefore, NMR characterization was obtained in bromobenzene- d_5 . The ^1H NMR spectrum of **[3]·dpe** contained a doublet at 0.27 ppm assigned to the SiMe_2 and a septet at 3.99 ppm assigned to SiH . A ^1H - ^{11}B HMQC experiment revealed a correlation between a broad singlet at 4.05 ppm in the ^1H dimension and a doublet in the ^{11}B NMR spectrum at -24.4 ($^1J_{\text{HB}} = 69$ Hz). Thus, **[3]·dpe** contains a $\text{HB}(\text{C}_6\text{F}_5)_3$ group from β - SiH abstraction rather than a

(Me₂HSi)₃Si–B(C₆F₅)₃ moiety from silyl group abstraction. Further support for BH bond formation is obtained from the infrared spectrum, which contained a band at 2331 cm⁻¹ assigned to a BH stretch. Interestingly, the ν_{SiH} (2096 cm⁻¹) appears at higher energy than in **1·dpe** and **2·dpe** (2069 cm⁻¹ for both compounds). In addition, the chemical shift of the central silicon atom in the ²⁹Si NMR spectrum of **[3]·dpe** appeared at -140.9 ppm, ca. 30 ppm downfield of **1·dpe**, and it is worth noting, similar in chemical shift to the silane Si(SiHMe₂)₄.

Scheme 3. Abstraction of a β-hydrogen from **1·dpe**.



Similarly, 1 equiv. of B(C₆F₅)₃ and **1·bipy** also react within 10 min. at room temperature to give a pale yellow solid in 71% yield that is characterized as (bipy)Zn{Si(SiHMe₂)₃}HB(C₆F₅)₃ (**[3]·bipy**). The characteristic spectroscopic features associated with HB(C₆F₅)₃ were observed. Notably, the ²⁹Si NMR signal assigned to the central silicon is shifted downfield, consistent with **[3]·dpe**.

A number of related β-H abstractions have been observed in related early main group and rare earth tris(silyl)alkyl compounds, such as Ca{C(SiHMe₂)₃}₂(THF)₂.³⁰ In those reactions, the organometallic product is M{C(SiHMe₂)₃}HB(C₆F₅)₃(THF)₂, and the organic by-product is proposed to be the silene, Me₂Si=C(SiHMe₂)₂, which is not directly detected, but instead its head-to-tail dimer 1,3-dimethyl-2,4-bis(dimethylsilyl)-1,3-disilacyclobutane is

isolated. Unfortunately, in the current case, we were unable to identify any of the silicon-containing byproducts, and the presumed disilene compound does not react in a selective manner to give a characterizable product.

For comparison to **[3]·dpe** and **[3]·bipy**, reaction of the tris(silyl)alkyl compound $\text{Zn}\{\text{C}(\text{SiHMe}_2)_3\}_2$ and $\text{B}(\text{C}_6\text{F}_5)_3$ show only resonances assigned to starting materials in the ^1H NMR spectra over 6 h at room temperature,³¹ while **1·dpe** or **1·bipy** react with $\text{B}(\text{C}_6\text{F}_5)_3$ instantaneously to give the hydridoborate silicon-containing species. A similar but less Lewis acidic compound was also investigated for silyl group vs. β -hydrogen abstraction. However, $\text{BPh}(\text{C}_6\text{F}_5)_2$ and **1·dpe** mixed in benzene- d_6 show only resonances assigned to the starting materials in the ^1H NMR spectra.

Conclusion

Comparisons between $\text{Zn}\{\text{Si}(\text{SiHMe}_2)_3\}_2$ (**1**) and the previously reported zinc silyls, particularly $\text{Zn}\{\text{Si}(\text{SiMe}_3)_3\}_2$, $\text{Zn}\{\text{SiMe}(\text{SiMe}_3)_2\}_2$ and $\text{Zn}(\text{SiMe}_3)_2$, show a surprising dissimilarity; while the previously reported zinc silyls are thermally robust or prone to zincate formation or reductive elimination, **1** shows a spontaneous SiHMe_2 migration pathway similar to $\text{M}\{\text{Si}(\text{SiMe}_3)_3\}_2$ ($\text{M} = \text{Ca}, \text{Sr}, \text{Ba}$). We have seen that the zinc disilyl compound, like zinc dihydride, is made kinetically resistant to silane formation by a *N*-heterocyclic carbene ligand, as well as chelating *N*-donor ligands. Since the syntheses are performed in a non-coordinating solvent, the stoichiometry and complete consumption of suspended ZnCl_2 are crucial for isolating clean compounds and avoiding decomposition via reactions between ligand and $\text{KSi}(\text{SiHMe}_2)_3$. While coordination of these ligands to **1** reveals that the zinc center is Lewis acidic, it is insufficiently strong to abstract a β -hydrogen, as it undergoes SiHMe_2 migration

instead. However, addition of the strong Lewis acid, $B(C_6F_5)_3$, exclusively mediates β -hydrogen abstraction over silyl group abstraction. The ^{29}Si NMR chemical shift trends for neutral compounds are similar to those observed by Marschner and co-workers for "Si-H-free" zinc silyls and their Lewis base adducts.³² In addition, spectroscopy trends show the central silicon in the cationic complexes are shifted downfield compared to the neutral compounds, which is accompanied by larger $^1J_{SiH}$ coupling constants and higher energy ν_{SiH} . Interestingly, these values for the cationic complexes shift close to those of $Si(SiHMe_2)_4$. We are currently exploring the group transfer chemistry of $Zn\{Si(SiHMe_2)_3\}_2$ as well as synthesizing other divalent metal disilyl compounds of the type $M\{Si(SiHMe_2)_3\}_2$.

Experimental

General Procedures. All reactions were performed under a dry argon atmosphere using standard Schlenk techniques or under a nitrogen atmosphere in a glovebox, unless otherwise indicated. Benzene, toluene, pentane, diethyl ether, and tetrahydrofuran were dried and deoxygenated using an IT PureSolv system. Benzene- d_6 was heated to reflux over Na/K alloy and vacuum-transferred. $KSi(SiHMe_2)_3$ ³³ and 1,2-dipyrrolidinoethane (dpe)³⁴ were synthesized according to literature procedures. 1H , $^{13}C\{^1H\}$, and ^{11}B NMR spectra were collected on a Bruker AVII 600 spectrometer or a Bruker DRX-400 spectrometer. ^{15}N chemical shifts were determined by 1H - ^{15}N HMBC experiments on a Bruker AVII 600 spectrometer. ^{15}N chemical shifts were originally referenced to an external liquid NH_3 standard and recalculated to the CH_3NO_2 chemical shift scale by adding -381.9 ppm. Elemental analyses were performed using a Perkin-Elmer 2400 Series II CHN/S by the Iowa State Chemical Instrumentation Facility. X-ray diffraction data was collected on a Bruker APEX II diffractometer.

Zn{Si(SiHMe₂)₃}₂ (1). ZnCl₂ (0.0050 g, 0.037 mmol) and KSi(SiHMe₂)₃ (0.018 g, 0.074 mmol) were dissolved in benzene-*d*₆ at room temperature and mixed on a vortex stirrer. After several minutes, the solution changed from pale yellow to colorless, and KCl was observed as a gray precipitate. Because Si(SiHMe₂)₄, zinc metal, and unidentified products were obtained after standing at low temperature or evaporation of the volatile materials, the data provided was obtained from an *in situ* generated species. ¹H NMR (benzene-*d*₆, 600 MHz): δ 4.49 (sept, 6 H, ³J_{HH} = 4.2 Hz, SiHMe₂), 0.38 (d, 36 H, ³J_{HH} = 4.2 Hz, SiHMe₂). ¹³C{¹H} NMR (benzene-*d*₆, 150 MHz): δ -0.65 (SiHMe₂). ²⁹Si (benzene-*d*₆, 119.3 MHz) δ -31.4 (d, ¹J_{SiH} = 181 Hz, SiHMe₂), -134.2 (Si(SiHMe₂)₃). IR (benzene-*d*₆ solution, cm⁻¹): ν 2975 (s), 2078 (s, ν_{SiH}), 1364 (w), 1244 (s), 1032 (s), 911 (m), 887 (s), 859 (s), 751 (w).

Si(SiHMe₂)₄.³⁵ KSi(SiHMe₂)₃ (0.061 g, 0.250 mmol) and 2,2'-bipyridine (0.039 g, 0.250 mmol) were allowed to react in benzene (10 mL) for 30 min. The reaction mixture was filtered, and the volatile materials were evaporated under reduced pressure to give a colorless oil (0.088 g, 0.213 mmol, 85.6%). ¹H NMR (benzene-*d*₆, 600 MHz): δ 4.36 (sept, 6 H, ³J_{HH} = 4.3 Hz, SiHMe₂), 0.31 (d, 36 H, ³J_{HH} = 4.3 Hz, SiHMe₂). ¹³C{¹H} NMR (benzene-*d*₆, 150 MHz): δ -2.27 (SiHMe₂). ²⁹Si (benzene-*d*₆, 119.3 MHz) δ -33.5 (d, ¹J_{SiH} = 180 Hz, SiHMe₂), -139.9 (Si(SiHMe₂)₃). IR (KBr, cm⁻¹): ν 2958 (s), 2093 (s, ν_{SiH}), 1643 (m), 1514 (s), 1466 (s), 1250 (s), 1089 (s), 971 (s), 886 (s), 859 (s), 835 (s), 681 (m).

(Im^tBu)Zn{Si(SiHMe₂)₃}₂ (1·Im^tBu). ZnCl₂ (0.010 g, 0.074 mmol) was suspended in a small amount of THF. KSi(SiHMe₂)₃ (0.035 g, 0.147 mmol) and 1,3-di-*t*-butylimidazol-2-ylidene (0.013 g, 0.074 mmol) were dissolved in benzene (10 mL) and added to the ZnCl₂. The reaction was stirred for 30 min., and then the solvent was evaporated under reduced pressure. The residue was extracted with pentane, filtered, and dried under reduced pressure to give a viscous,

colorless oil (0.044 g, 0.072 mmol, 93.6%). ^1H NMR (benzene- d_6 , 600 MHz): δ 6.40 (s, 2 H, $\text{C}_3\text{H}_2\text{N}_2(t\text{-Bu})_2$), 4.54 (sept, 6 H, $^3J_{\text{HH}} = 4.2$ Hz, SiHMe_2), 1.37 (s, 18 H, CMe_3), 0.48 (d, 36 H, $^3J_{\text{HH}} = 4.2$ Hz, SiHMe_2). $^{13}\text{C}\{^1\text{H}\}$ NMR (benzene- d_6 , 150 MHz): δ 179.56 (2C- $\text{C}_3\text{H}_2\text{N}_2(t\text{-Bu})_2$), 119.51 (4, 5C- $\text{C}_3\text{H}_2\text{N}_2(t\text{-Bu})_2$), 58.70 (CMe_3), 30.45 (CMe_3), -0.07 (SiHMe_2). $^{15}\text{N}\{^1\text{H}\}$ NMR (benzene- d_6 , 60.6 MHz): δ -176.8 . ^{29}Si (benzene- d_6 , 119.3 MHz) δ -28.2 (d, $^1J_{\text{SiH}} = 171$ Hz, SiHMe_2), -163.9 ($\text{Si}(\text{SiHMe}_2)_3$). IR (KBr, cm^{-1}): ν 2951 (s), 2895 (m), 2070 (s, ν_{SiH}), 1465 (w), 1400 (m), 1305 (w), 1235 (s), 1209 (w), 1145 (w), 1118 (w), 1033 (w), 887 (s), 859 (s), 830 (s), 730 (m), 689 (m), 647 (m). Anal. Calcd. for $\text{C}_{23}\text{H}_{62}\text{N}_2\text{Si}_8\text{Zn}$: C, 42.06; H, 9.51; N, 4.27. Found C, 41.62; H, 9.83; N, 4.27.

(dpe)ZnCl₂. ZnCl₂ (0.144 g, 1.06 mmol) and 1,2-dipyrrolidinoethane (0.178 g, 1.06 mmol) were dissolved in benzene (10 mL) and stirred for 24 h. The solvent was evaporated under reduced pressure, and the residue was washed with pentane (3×5 mL) to give the white solid product (0.290 g, 0.952 mmol, 90.2%). ^1H NMR (benzene- d_6 , 600 MHz): δ 3.38 (t, 4 H, $^3J_{\text{HH}} = 6.0$ Hz, $\text{NCH}_2(\text{CH}_2)_2\text{CH}_2$), 1.99 (br d, 4 H, $^3J_{\text{HH}} = 6.0$ Hz, $\text{NCH}_2(\text{CH}_2)_2\text{CH}_2$), 1.83 (s, 4 H, NCH_2), 1.48 (q, 4 H, $^3J_{\text{HH}} = 6.0$ Hz, $\text{NCH}_2(\text{CH}_2)_2\text{CH}_2$), 1.31 (t, 4 H, $^3J_{\text{HH}} = 6.0$ Hz, $\text{NCH}_2(\text{CH}_2)_2\text{CH}_2$). $^{13}\text{C}\{^1\text{H}\}$ NMR (benzene- d_6 , 150 MHz): δ 56.33 ($\text{NCH}_2(\text{CH}_2)_2\text{CH}_2$), 54.87 (NCH_2), 23.17 ($\text{NCH}_2(\text{CH}_2)_2\text{CH}_2$). $^{15}\text{N}\{^1\text{H}\}$ NMR (benzene- d_6 , 60.6 MHz): δ -329.5 . IR (KBr, cm^{-1}): ν 2983 (s), 2871 (s), 1462 (s), 1346 (m), 1333 (m), 1262 (m), 1194 (w), 1107 (s), 1065 (s), 979 (m), 948 (s), 868 (m). Anal. Calcd. for $\text{C}_{10}\text{H}_{20}\text{Cl}_2\text{N}_2\text{Zn}$: C, 39.44; H, 6.62; N, 9.20. Found C, 39.25; H, 6.27; N, 8.89. Mp: 215-218 °C.

(dpe)Zn{Si(SiHMe₂)₃}₂(1·dpe). (dpe)ZnCl₂ (0.040 g, 0.131 mmol) and KSi(SiHMe₂)₃ (0.064 g, 0.262 mmol) were dissolved in benzene (10 mL) and stirred for 1 h followed by filtration to remove KCl. The solvent was evaporated under reduced pressure, and the residue was

recrystallized from pentane at $-30\text{ }^{\circ}\text{C}$ to give a white solid (0.072 g, 0.116 mmol, 84.6%). ^1H NMR (benzene- d_6 , 600 MHz): δ 4.55 (sept, 6 H, $^3J_{\text{HH}} = 4.2\text{ Hz}$, SiHMe_2), 2.68 (br, 8 H, $\text{NCH}_2(\text{CH}_2)_2\text{CH}_2$), 2.08 (s, 4 H, NCH_2), 1.56 (br, 8 H, $\text{NCH}_2(\text{CH}_2)_2\text{CH}_2$), 0.56 (d, 36 H, $^3J_{\text{HH}} = 4.2\text{ Hz}$, SiHMe_2). $^{13}\text{C}\{^1\text{H}\}$ NMR (benzene- d_6 , 150 MHz): δ 58.27 ($\text{NCH}_2(\text{CH}_2)_2\text{CH}_2$), 56.58 (NCH_2), 23.90 ($\text{NCH}_2(\text{CH}_2)_2\text{CH}_2$), 0.64 (SiHMe_2). $^{15}\text{N}\{^1\text{H}\}$ NMR (benzene- d_6 , 60.6 MHz): δ -327.9 . ^{29}Si (benzene- d_6 , 119.3 MHz) δ -27.5 (d, $^1J_{\text{SiH}} = 171\text{ Hz}$, SiHMe_2), -169.2 ($\text{Si}(\text{SiHMe}_2)_3$). IR (KBr, cm^{-1}): ν 2951(s), 2894 (s), 2069 (s, ν_{SiH}), 1458 (w), 1422 (w), 1236 (m), 1046 (w), 966 (w), 886 (s), 858 (s), 827 (s), 742 (w), 686 (m), 646 (m). Anal. Calcd. for $\text{C}_{22}\text{H}_{62}\text{N}_2\text{Si}_8\text{Zn}$: C, 40.98; H, 9.69; N, 4.34. Found C, 40.49; H, 9.56; N, 4.48. Mp: $133\text{-}135\text{ }^{\circ}\text{C}$.

(dpe)Zn{Si(SiHMe₂)₃}Cl (2·dpe). (dpe)ZnCl₂ (0.040 g, 0.131 mmol) and KSi(SiHMe₂)₃ (0.064 g, 0.131 mmol) were dissolved in benzene (10 mL) and stirred for 1 h to give a 1:2 mixture of mono and di(silyl) products as indicated by ^1H NMR. The solution was filtered and then the solvent was evaporated under reduced pressure. The residue was recrystallized from pentane at $-30\text{ }^{\circ}\text{C}$, and (dpe)Zn{Si(SiHMe₂)₃}Cl selectively crystallized as a white solid (0.018 g, 0.038 mmol, 28.6%). ^1H NMR (benzene- d_6 , 600 MHz): δ 4.52 (sept, 3 H, $^3J_{\text{HH}} = 4.2\text{ Hz}$, SiHMe_2), 3.76 (t, 2 H, $^3J_{\text{HH}} = 4.2\text{ Hz}$, dpe), 3.10 (t, 2 H, $^3J_{\text{HH}} = 4.2\text{ Hz}$, dpe), 1.93 (m, 8 H, dpe), 1.72 (q, 2 H, $^3J_{\text{HH}} = 4.2\text{ Hz}$, dpe), 1.64 (q, 2 H, $^3J_{\text{HH}} = 4.2\text{ Hz}$, dpe), 1.38 (m, 4 H, dpe), 0.58 (d, 36 H, $^3J_{\text{HH}} = 4.2\text{ Hz}$, SiHMe_2). $^{13}\text{C}\{^1\text{H}\}$ NMR (benzene- d_6 , 150 MHz): δ 56.98 (NCH_2), 55.81 ($\text{NCH}_2(\text{CH}_2)_2\text{CH}_2$), 23.60 ($\text{NCH}_2(\text{CH}_2)_2\text{CH}_2$), -0.10 (SiHMe_2). $^{15}\text{N}\{^1\text{H}\}$ NMR (benzene- d_6 , 60.6 MHz): δ -327.4 . ^{29}Si (benzene- d_6 , 119.3 MHz) δ -28.4 (d, $^1J_{\text{SiH}} = 171\text{ Hz}$, SiHMe_2), -166.9 ($\text{Si}(\text{SiHMe}_2)_3$). IR (KBr, cm^{-1}): ν 2962 (s), 2890 (s), 2069 (s, ν_{SiH}), 1459 (w), 1420 (w), 1350 (w), 1255 (m), 1190 (w), 1043 (w), 972 (m), 950 (m), 857 (m), 831 (s), 739 (w), 680 (m). Anal.

Calcd. for $C_{16}H_{41}ClN_2Si_4Zn$: C, 40.48; H, 8.71; N, 5.90. Found C, 40.49; H, 8.67; N, 5.93. Mp: 137-140 °C.

(bipy)Zn{Si(SiHMe₂)₃}₂ (1•bipy). ZnCl₂ (0.017 g, 0.126 mmol) was suspended in THF, and KSi(SiHMe₂)₃₂ (0.060 g, 0.245 mmol) was dissolved in benzene. The yellow benzene solution was added to the ZnCl₂ suspension and the resulting mixture was stirred for several seconds until the yellow color faded to colorless, indicating that the KSi(SiHMe₂)₃ was consumed. A benzene solution of 2,2'-bipyridine (bipy) (0.019 g, 0.123 mmol) was immediately added, and the solution turned deep red. The solvent was evaporated under reduced pressure, and the residue was extracted with pentane and filtered to give a dark purple solution. The pentane was evaporated under reduced pressure to give a viscous maroon oil (0.029 g, 0.046 mmol, 37.6 %). ¹H NMR (benzene-*d*₆, 600 MHz): δ 8.77 (d, 2 H, ³J_{HH} = 7.8 Hz, bipy), 7.07 (d, 2 H, ³J_{HH} = 12.0 Hz, bipy), 6.90 (t, 2 H, ³J_{HH} = 12.0 Hz, bipy), 6.54 (t, 2 H, ³J_{HH} = 10.2 Hz, bipy), 4.43 (sept, 6 H, ³J_{HH} = 4.2 Hz, SiHMe₂), 0.37 (d, 36 H, ³J_{HH} = 4.2 Hz, SiHMe₂). ¹³C{¹H} NMR (benzene-*d*₆, 150 MHz): δ 150.33 (bipy), 149.52 (bipy), 138.79 (bipy), 121.74 (bipy), -0.14 (SiHMe₂). ²⁹Si (benzene-*d*₆, 119.3 MHz) δ -28.9 (d, ¹J_{SiH} = 171 Hz, SiHMe₂), -161.7 (Si(SiHMe₂)₃). IR (benzene-*d*₆ solution, cm⁻¹): ν 2952 (s), 2895 (m), 2063 (s, ν_{SiH}), 1599 (m), 1541 (m), 1507 (w), 1441 (m), 1239 (s), 884 (s), 857 (s), 830 (s), 758 (m), 677 (m), 648 (m). Anal. Calcd. for C₂₂H₅₀N₂Si₈Zn: C, 41.76; H, 7.97; N, 4.43. Found C, 41.40; H, 7.48; N, 4.35.

(dpe)Zn{Si(SiHMe₂)₃}HB(C₆F₅)₃ ([3]•dpe). (dpe)Zn{Si(SiHMe₂)₃}₂ (0.057 g, 0.088 mmol) and B(C₆F₅)₃ (0.045 g, 0.088 mmol) were allowed to stir in benzene (10 mL) for 30 min., and then the solvent was evaporated under reduced pressure. The residue was washed with pentane (3 × 5 mL) to give a white solid (0.075 g, 0.079 mmol, 87.6 %). ¹H NMR (bromobenzene-*d*₅, 600 MHz): δ 4.05 (br, HB), 3.99 (sept, 3 H, ³J_{HH} = 4.0 Hz, SiHMe₂), 2.83 (br m, 8 H,

$\text{NCH}_2(\text{CH}_2)_2\text{CH}_2$), 2.43 (s, 4 H, NCH_2), 1.63 (br m, 8 H, $\text{NCH}_2(\text{CH}_2)_2\text{CH}_2$), 0.27 (d, 18 H, $^3J_{\text{HH}} = 4.0$ Hz, SiHMe_2). $^{13}\text{C}\{^1\text{H}\}$ NMR (bromobenzene- d_5 , 150 MHz): δ 148.80 (br, C_6F_5), 146.21 (br, C_6F_5), 141.27 (br, C_6F_5), 138.13 (br, C_6F_5), 135.73 (br, C_6F_5), 134.27 (br, C_6F_5), 54.98 (NCH_2), 54.15 ($\text{NCH}_2(\text{CH}_2)_2\text{CH}_2$), 21.49 ($\text{NCH}_2(\text{CH}_2)_2\text{CH}_2$), -0.30 (SiHMe_2). ^{11}B NMR (bromobenzene- d_5 , 192 MHz): δ -24.4 (d, $^1J_{\text{HB}} = 69$ Hz, $\text{HB}(\text{C}_6\text{F}_5)_3$). ^{19}F NMR (bromobenzene- d_5 , 376 MHz): δ -132.7 (*ortho*- C_6F_5), -162.6 (*para*- C_6F_5), -165.9 (*meta*- C_6F_5). $^{15}\text{N}\{^1\text{H}\}$ NMR (bromobenzene- d_5 , 60.6 MHz): δ -333.2 . ^{29}Si (bromobenzene- d_5 , 119.3 MHz) δ -27.0 (d, $^1J_{\text{SiH}} = 182$ Hz, SiHMe_2), -140.9 ($\text{Si}(\text{SiHMe}_2)_3$). IR (KBr, cm^{-1}): ν 2957 (m), 2925 (s), 2855 (m), 2331 (br m, ν_{BH}), 2096 (s, ν_{SiH}), 1734 (w), 1559 (w), 1541 (w), 1507 (s), 1458 (s), 1375 (m), 1275 (m), 1096 (s), 969 (s), 906 (w). Anal. Calcd. for $\text{C}_{34}\text{H}_{42}\text{BF}_{15}\text{N}_2\text{Si}_4\text{Zn}$: C, 42.89; H, 4.45; N, 2.94. Found C, 43.03; H, 4.93; N, 2.49. Mp: 61-63 °C.

(bipy)Zn{Si(SiHMe₂)₃}₂HB(C₆F₅)₃ ([3]•bipy). (Bipy)Zn{Si(SiHMe₂)₃}₂ (0.040 g, 0.063 mmol) and $\text{B}(\text{C}_6\text{F}_5)_3$ (0.032 g, 0.063 mmol) were allowed to react for 30 min., and then the reaction was worked-up analogously to [3]•dpe, giving [3]•bipy as a pale yellow solid (0.042 g, 0.045 mmol, 71.4 %). ^1H NMR (benzene- d_6 , 600 MHz): δ 8.31 (d, 2 H, $^3J_{\text{HH}} = 6.0$ Hz, bipy), 7.35 (d, 2 H, $^3J_{\text{HH}} = 8.4$ Hz, bipy), 7.08 (t, 2 H, $^3J_{\text{HH}} = 8.4$ Hz, bipy), 6.48 (t, 2 H, $^3J_{\text{HH}} = 6.0$ Hz, bipy), 4.13 (sept, 3 H, $^3J_{\text{HH}} = 4.2$ Hz, SiHMe_2), 3.80 (br, *HB*), 0.17 (d, 18 H, $^3J_{\text{HH}} = 4.2$ Hz, SiHMe_2). $^{13}\text{C}\{^1\text{H}\}$ NMR (benzene- d_6 , 150 MHz): δ 149.50 (br, C_6F_5), 148.88 (bipy), 148.25 (bipy), 148.05 (br, C_6F_5), 142.70 (bipy), 138.21 (br, C_6F_5), 136.61 (br, C_6F_5), 127.46 (bipy), 122.77 (bipy), -1.83 (SiHMe_2). ^{11}B NMR (benzene- d_6 , 192 MHz): δ -22.0 (d, $^1J_{\text{HB}} = 54$ Hz, $\text{HB}(\text{C}_6\text{F}_5)_3$). ^{19}F NMR (benzene- d_6 , 376 MHz): δ -132.5 (*ortho*- C_6F_5), -161.6 (*para*- C_6F_5), -165.4 (*meta*- C_6F_5). ^{29}Si (benzene- d_6 , 119.3 MHz) δ -30.1 (d, $^1J_{\text{SiH}} = 180$ Hz, SiHMe_2), -133.8 ($\text{Si}(\text{SiHMe}_2)_3$). IR (KBr, cm^{-1}): ν 2958 (m), 2929 (m), 2899 (w), 2855 (w), 2387 (br m, ν_{BH}), 2091 (s, ν_{SiH}), 1642

(w), 1601 (w), 1510 (s), 1465 (s), 1375 (w), 1319 (m), 1250 (m), 1098 (s), 1027 (s), 969 (s), 886 (m), 858 (m), 833 (m), 792 (m), 766 (m), 682 (w), 652 (w). Anal. Calcd. for $C_{34}H_{30}BF_{15}N_2Si_4Zn$: C, 43.44; H, 3.22; N, 2.98. Found C, 43.53; H, 2.74; N, 2.71. Mp: 63-65 °C.

References

- (1) (a) Nakamura, S.; Uchiyama, M. *J. Am. Chem. Soc.* **2007**, *129*, 28. (b) Nakamura, S.; Uchiyama, M.; Ohwada, T. *J. Am. Chem. Soc.* **2005**, *127*, 13116. (c) Auer, G.; Oestreich, M. *Chem. Commun.* **2006**, 311. (d) Nakamura, S.; Uchiyama, M.; Ohwada, T. *J. Am. Chem. Soc.* **2004**, *126*, 11146. (e) Oestreich, M.; Auer, G. *Adv. Syn. Catal.* **2005**, *347*, 637. (f) Fleming, I.; Ramarao, C. *Chem. Commun.* **2000**, 2185.
- (2) (a) H. Mimoun, J. Y. de Saint Laumer, L. Giannini, R. Scopelliti and C. Floriani, *J. Am. Chem. Soc.* **1999**, *121*, 6158-6166. (b) H. Mimoun, *J. Org. Chem.* **1999**, *64*, 2582-2589. (c) V. Bette, A. Mortreux, F. Ferioli, G. Martelli, D. Savoia and J.-F. Carpentier, *Eur. J. Org. Chem.* **2004**, *2004*, 3040-3045. (d) Bette, V.; Mortreux, A.; Savoia, D.; Carpentier, J.-F. *Tetrahedron*, **2004**, *60*, 2837-2842. (e) Bette, V.; Mortreux, A.; Savoia, D.; Carpentier, J.-F. *Adv. Syn. Catal.* **2005**, *347*, 289-302. (f) Enthaler, S.; Eckhardt, B.; Inoue, S.; Irran, E.; Driess, M. *Chem. Asian J.* **2010**, *5*, 2027. (g) Marinos, N. A.; Enthaler, S.; Driess, M. *ChemCatChem*, **2010**, *2*, 846. (h) Enthaler, S. *Catal. Sci. Technol.* **2011**, *1*, 104. (i) Mukherjee, D.; Thompson, R. R.; Ellern, A.; Sadow, A. D. *ACS Catal.* **2011**, *1*, 698. (j) Enthaler, S. *ACS Catal.* **2013**, *3*, 150. (k) Boone, C.; Korobkov, I.; Nikonov, G. I. *ACS Catal.* **2013**, *3*, 2336.
- (3) Gaderbauer, W.; Balatoni, I.; Wagner, H.; Baumgartner, J.; Marschner, C. *Dalton Trans.* **2010**, *39*, 1598-1603.

- (4) Arnold, J.; Tilley, T. D.; Rheingold, A. L.; Geib, S. J. *Inorg. Chem.* **1987**, *26*, 2106-2109.
- (5) Gaderbauer, W.; Balatoni, I.; Wagner, H.; Baumgartner, J.; Marschner, C. *Dalton Trans.* **2010**, *39*, 1598-1603.
- (6) Wiberg, E.; Stecher, O.; Andrascheck, H. J.; Kreuzbichler, L.; Staude, E. *Angew. Chem. Int. Ed. Engl.* **1963**, *2*, 507-515.
- (7) Rösch, L.; Altnau, G. *Angew. Chem. Int. Ed. Engl.* **1979**, *18*, 60-61.
- (8) Mukherjee, D.; Lampland, N. L.; Yan, K.; Dunne, J. F.; Ellern, A.; Sadow, A. D. *Chem. Commun.* **2013**, *49*, 4334-4336.
- (9) Mukherjee, D.; Ellern, A.; Sadow, A. D. *J. Am. Chem. Soc.* **2010**, *132*, 7582-7583.
- (10) Yan, K.; Duchimaza Heredia, J. J.; Ellern, A.; Gordon, M. S.; Sadow, A. D. *J. Am. Chem. Soc.* **2013**, *135*, 15225-15237.
- (11) (a) Yan, K.; Schoendorff, G.; Upton, B. M.; Ellern, A.; Windus, T. L.; Sadow, A. D. *Organometallics* **2013**, *32*, 1300-1316. (b) Yan, K.; Upton, B. M.; Ellern, A.; Sadow, A. D. *J. Am. Chem. Soc.* **2009**, *131*, 15110-15111.
- (12) Rösch, L.; Altnau, G. *Angew. Chem. Int. Ed. Engl.* **1979**, *18*, 60-61.
- (13) Mukherjee, D.; Lampland, N. L.; Yan, K.; Dunne, J. F.; Ellern, A.; Sadow, A. D. *Chem. Commun.* **2013**, *49*, 4334-4336.
- (14) Kulpinski, P.; Lickiss, P. D.; Stanczyk, W. *Bull. Polish Acad. Sci. Chem.* **1992**, *40*, 21-24.
- (15) Arnold, J.; Tilley, T. D.; Rheingold, A. L.; Geib, S. J. *Inorg. Chem.* **1987**, *26*, 2106-2109.
- (16) Kulpinski, P.; Lickiss, P. D.; Stanczyk, W. *Bull. Polish Acad. Sci. Chem.* **1992**, *40*, 21-24.
- (17) Teng, W.; Ruhlandt-Senge, K. *Organometallics* **2004**, *23*, 2694-2700.
- (18) Marschner, C. *Organometallics* **2006**, *25*, 2110-2125.
- (19) Arnold, J.; Tilley, T. D.; Rheingold, A. L.; Geib, S. J. *Inorg. Chem.* **1987**, *26*, 2106-2109.

- (20) Yan, K.; Upton, B. M.; Ellern, A.; Sadow, A. D. *J. Am. Chem. Soc.* **2009**, *131*, 15110-15111.
- (21) Eaborn, C.; Retta, N.; Smith, J. D. *J. Organomet. Chem.* **1980**, *190*, 101-106.
- (22) Barbaras, G. D.; Dillard, C.; Finholt, A. E.; Wartik, T.; Wilzbach, K. E.; Schlesinger, H. I. *J. Am. Chem. Soc.* **1951**, *73*, 4585-4590.
- (23) Rit, A.; Spaniol, T. P.; Maron, L.; Okuda, J. *Angew. Chem. Int. Ed.* **2013**, *52*, 4664-4667.
- (24) Arduengo III, A. J.; Dias, H. V. R.; Davidson, F.; Harlow, R. L. *J. Organomet. Chem.* **1993**, *462*, 13-18.
- (25) (a) Naktode, K.; Anga, S.; Kottalanka, R. K.; Nayek, H. P.; Panda, T. K. *J. Coord. Chem.* **2014**, *67*, 236-248. (b) Jensen, T. R.; Schaller, C. P.; Hillmyer, M. A.; Tolman, W. B. *J. Organomet. Chem.* **2005**, *690*, 5881-5891. (c) Wang, D.; Wurst, K.; Buchmeiser, M. R. *J. Organomet. Chem.* **2004**, *689*, 2123-2130.
- (26) Nanjo, M.; Oda, T.; Mochida, K. *J. Organomet. Chem.* **2003**, *672*, 100-108.
- (27) Gaderbauer, W.; Balatoni, I.; Wagner, H.; Baumgartner, J.; Marschner, C. *Dalton Trans.* **2010**, *39*, 1598-1603.
- (28) Mukherjee, D.; Lampland, N. L.; Yan, K.; Dunne, J. F.; Ellern, A.; Sadow, A. D. *Chem. Commun.* **2013**, *49*, 4334-4336.
- (29) Notes, J. G.; Boersma, J. *J. Organomet. Chem.* **1967**, *9*, 1-4.
- (30) Yan, K.; Upton, B. M.; Ellern, A.; Sadow, A. D. *J. Am. Chem. Soc.* **2009**, *131*, 15110-15111.
- (31) Yan, K.; Upton, B. M.; Ellern, A.; Sadow, A. D. *J. Am. Chem. Soc.* **2009**, *131*, 15110-15111.

- (32) Gaderbauer, W.; Balatoni, I.; Wagner, H.; Baumgartner, J.; Marschner, C. *Dalton Trans.* **2010**, 39, 1598-1603.
- (33) Mukherjee, D.; Lampland, N. L.; Yan, K.; Dunne, J. F.; Ellern, A.; Sadow, A. D. *Chem. Commun.* **2013**, 49, 4334-4336.
- (34) Remenar, J. F.; Lucht, B. L.; Collum, D. B. *J. Am. Chem. Soc.* **1997**, 119, 5567-5572.
- (35) Kulpinski, P.; Lickiss, P. D.; Stanczyk, W. *Bull. Polish Acad. Sci. Chem.* **1992**, 40, 21-24.

**CHAPTER 4: DIVERGENT REACTION PATHWAYS OF
TRIS(OXAZOLINYL)BORATOZINC AND MAGNESIUM COMPOUNDS**

Modified from a paper published in *Chemical Communications*

Nicole L. Lampland, Debabrata Mukherjee, Kaking Yan, James F. Dunne, Arkady Ellern and

Aaron D. Sadow*

Department of Chemistry, U.S. DOE Ames Laboratory, Iowa State University, Ames, IA

50011-3111

This work has been carried out in close collaboration with other lab members.[†]

Abstract

Synthesis and reactivity of monomeric magnesium and zinc silyl compounds $To^M M-Si(SiHMe_2)_3$ and $To^M M-Si(SiMe_3)_3$ are described ($To^M =$ tris(4,4-dimethyl-2-oxazoliny)phenylborate). The magnesium compounds react slowly with water and air, while the zinc compounds are inert. With CO_2 , $To^M Mg-Si(SiHMe_2)_3$ provides $To^M MgO_2CSi(SiHMe_2)_3$ through CO_2 insertion, whereas $To^M Zn-Si(SiHMe_2)_3$ affords $To^M ZnOCHO$. For comparison, a series of zinc complexes $To^M Zn-R$ ($R = Si(SiHMe_2)_3, CH(SiHMe_2)_2, N(SiHMe_2)_2$) was explored under thermal conditions and in reactions with $[Li(Et_2O)_n][B(C_6F_5)_4]$, $B(C_6F_5)_3$, and CO_2 . Contrasting the robustness of $To^M Zn-Si(SiHMe_2)_3$, solutions of $To^M Zn-CH(SiHMe_2)_2$ and

[†] **Debabrata Mukherjee:** Crystal structures of $To^M Zn-Si(SiHMe_2)_3$, $To^M Zn-Si(SiMe_3)_3$, $(To^M MgOMe)_2$, $To^M ZnOCHO$, and $To^M Zn-CH(SiHMe_2)_2$; reactions of $To^M Zn$ and $To^M Mg$ silyl species with O_2 , a 450 W Hg lamp, AIBN, and CO_2 ; independent synthesis and characterization of $To^M ZnOCHO$ from $To^M ZnH$ and CO_2 ; synthesis and characterization of $(To^M MgOMe)_2$.

Kaking Yan: First person in our group to synthesize the silyl ligands $KSi(SiHMe_2)_3$ and $KSi(SiMe_3)_3$. Synthesized and characterized $Li[CH(SiHMe_2)_2](THF)$.

James F. Dunne: First person in our group to synthesize the magnesium starting materials, $To^M MgBr$ and $To^M MgMe$, used in this study. Also, the first person to observe the formation of $(To^M MgOMe)_2$ species in a NMR-scale reaction between $To^M MgMe$ and $MeOH$.

$\text{To}^{\text{M}}\text{Zn-N}(\text{SiHMe}_2)_2$ give oxazoline ring-opening and O–Si bond formation upon heating. In the presence of $[\text{Li}(\text{Et}_2\text{O})_n][\text{B}(\text{C}_6\text{F}_5)_4]$ ring-opening is promoted in $\text{To}^{\text{M}}\text{Zn-N}(\text{SiHMe}_2)_2$, while the silyl and alkyl complexes show no ring-opening. With $\text{B}(\text{C}_6\text{F}_5)_3$, $\text{To}^{\text{M}}\text{Zn-N}(\text{SiHMe}_2)_2$ and $\text{To}^{\text{M}}\text{Zn-CH}(\text{SiHMe}_2)_2$ yield $\text{To}^{\text{M}}\text{ZnHB}(\text{C}_6\text{F}_5)_3$, while $\text{To}^{\text{M}}\text{Zn-Si}(\text{SiHMe}_2)_3$ yields a new C_s -symmetric species. Furthermore, like $\text{To}^{\text{M}}\text{Zn-Si}(\text{SiHMe}_2)_3$, $\text{To}^{\text{M}}\text{Zn-CH}(\text{SiHMe}_2)_2$ reacts with CO_2 to give $\text{To}^{\text{M}}\text{ZnOCHO}$, whereas $\text{To}^{\text{M}}\text{Zn-N}(\text{SiHMe}_2)_2$ gives $\text{To}^{\text{M}}\text{ZnNCO}$.

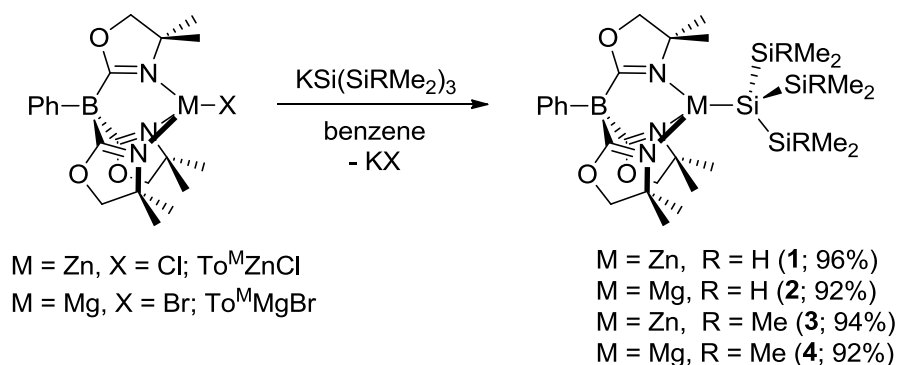
Introduction

Zinc and magnesium alkyls are among the earliest and most frequently used organometallic compounds, whereas related metal silyls have received less attention. Magnesium and zinc-catalyzed hydrosilylations¹ and dehydrogenative silylations² involve mixtures of organosilanes and these main group organometallics. However, metal silyl species are generally not postulated intermediates in most proposed catalytic cycles for such transformations, and studies of main-group metal silyl compounds have mostly focused on structural characterization and applications in transmetalation.³ Less is known about their reactivity in steps that might be involved in catalysis. Metal silyl compounds, supported by tris(oxazolonyl)borate ancillaries employed in our catalytic investigations, may provide further insight into catalysis, possible side reactions, and the fundamental reactivity of these compounds. Moreover, reactivity studies between metal silyls and analogous metal alkyls or silazides can afford understanding of the M–Si bond and its comparability to the well-studied M–C and M–N bonds.

Results and Discussion

The targeted silyl complexes $\text{To}^{\text{M}}\text{Zn-Si}(\text{SiHMe}_2)_3$ (**1**), $\text{To}^{\text{M}}\text{Mg-Si}(\text{SiHMe}_2)_3$ (**2**), $\text{To}^{\text{M}}\text{Zn-Si}(\text{SiMe}_3)_3$ (**3**) and $\text{To}^{\text{M}}\text{Mg-Si}(\text{SiMe}_3)_3$ (**4**) (To^{M} = tris(4,4-dimethyl-2-oxazolinyl)phenylborate) are efficiently prepared by salt metathesis reactions. $\text{To}^{\text{M}}\text{ZnCl}^4$ or $\text{To}^{\text{M}}\text{MgBr}$ react with the appropriate potassium silyl reagent, $\text{KSi}(\text{SiHMe}_2)_3$ or $\text{KSi}(\text{SiMe}_3)_3$,⁵ in benzene at ambient temperature (Scheme 1).

Scheme 1. Synthesis of zinc silyls and magnesium silyls.



Compounds **1**, **2** and **4** are formed quantitatively within 30 min. at ambient temperature, whereas the preparation of compound **3** requires longer time (2 h). One set of oxazoline resonances was observed in the ^1H NMR spectra of compounds **1–4** (as well as all the $\text{To}^{\text{M}}\text{MX}$ compounds reported here). This pattern is consistent with time-averaged C_{3v} -symmetry for the complexes and suggests tridentate coordination of To^{M} . Downfield SiH chemical shifts of **1** (4.64 ppm) and **2** (4.71 ppm), high silicon–hydrogen coupling constants ($^1J_{\text{SiH}} = 172.2$ and 169.7 Hz respectively), and infrared bands assigned to the ν_{SiH} of **1** (2064 cm^{-1}) and **2** (2054 cm^{-1}) are consistent with terminal, 2-center-2-electron bonded Si–H moieties. In addition, the infrared spectra provide support for tridentate To^{M} coordination by the single ν_{CN} band for each compound (**1** and **3**: 1591 cm^{-1} ; **2** and **4**: 1582 cm^{-1}).

Single crystal X-ray analyses of **1** (Fig. 1) and **3** (see experimental section) further support the spectroscopically assigned structures.⁶ Terminal β -SiH's in **1** are located in the difference Fourier map, but the $\text{Si}(\text{SiHMe}_2)_3$ is disordered. In the model, the three SiHMe_2 groups are oriented with the SiH's pointing away from the zinc center and are related by pseudo- C_3 rotations. The Zn1–Si1 interatomic distance is slightly shorter in **1** (2.4028(5) Å) than in **3** (2.427(1) Å), and these distances are on the long side compared to other zinc silyls. For example, the Zn–Si distances in $\text{Zn}(\text{Si}(\text{SiMe}_3)_3)_2$,⁷ $(\text{Me}_3\text{Si})_3\text{SiZnCl}(\text{thf})_2$, and $(\text{Ph}(\text{Me}_3\text{Si})_2\text{SiZnCl}(\text{thf}))_2$ are similar (2.35 ± 0.01 Å).⁸ Sterically hindered groups give longer Zn–Si distances; for example, the distances in $\text{Zn}(\text{Si}(\text{SiMe}_3)_2\text{Si}(\text{SiMe}_3)_3)_2$ are $\sim 2.405 \pm 0.002$ Å.⁹

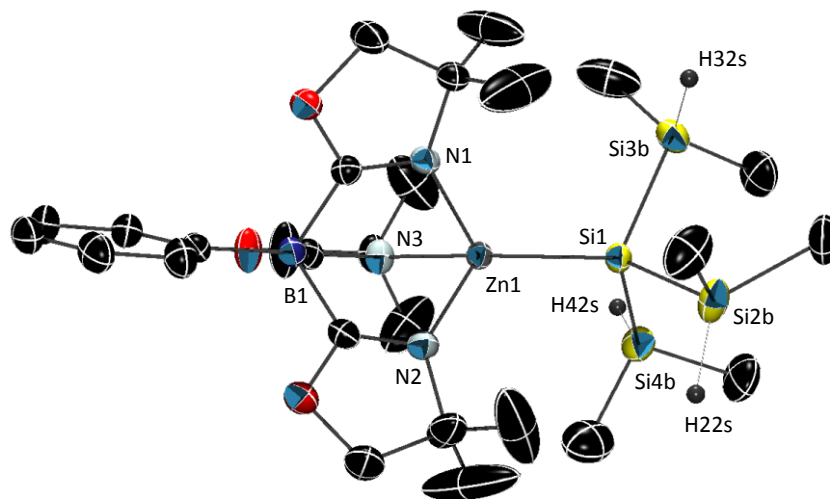


Fig. 1 Rendered thermal ellipsoid plot of $\text{To}^{\text{M}}\text{Zn}-\text{Si}(\text{SiHMe}_2)_3$ (**1**). One of the $\text{Si}(\text{SiHMe}_2)_3$ positions and the hydrogen atoms on the To^{M} and Me groups are not illustrated for clarity.

Metal silyls **1–4** are thermally resilient, and starting materials are recovered after heating toluene- d_8 solutions in sealed NMR tubes at 170 °C for 24 h. Furthermore, the zinc compounds **1** and **3** are inert to reaction with O_2 at pressures up to 100 psi and temperatures up to 120 °C for 24 h, under a 450 W Hg lamp at ambient temperature, or in the presence of AIBN at 60 °C. For

comparison, $To^M ZnH$ and $To^M ZnMe$ also are inert to O_2 , whereas $To^M ZnR$ compounds react with O_2 following the trend ($R = Et < n-C_3H_7 < i-C_3H_7 < t-Bu$) to form isolable alkylperoxyzinc species.¹⁰ These data suggest that, despite their steric bulk, the resistance of **1** and **3** to oxidation may result from electronic effects associated with the To^M ligand. For comparison, $Zn(Si(SiMe_3)_3)_2$ and $Zn(Si(SiMe_3)_3)_2 TMEDA$ are air sensitive (the TMEDA adduct reacts slowly in air).¹¹

Magnesium silyls **2** and **4** react with 1 atm of O_2 at ambient temperature over 24 and 36 h forming mixtures of unidentified species. Under similar reaction conditions, $To^M MgMe$ and O_2 form $(To^M Mg(\mu-O Me))_2$ (**5**) within 5 min. Compound **5** is crystallographically characterized as a dimer containing tridentate tris-(oxazolinyl)borate and bridging methoxide ligands (Fig. 2), centered on a two-fold axis.¹² The 1H NMR spectrum is consistent with pseudo- C_{3v} symmetry.

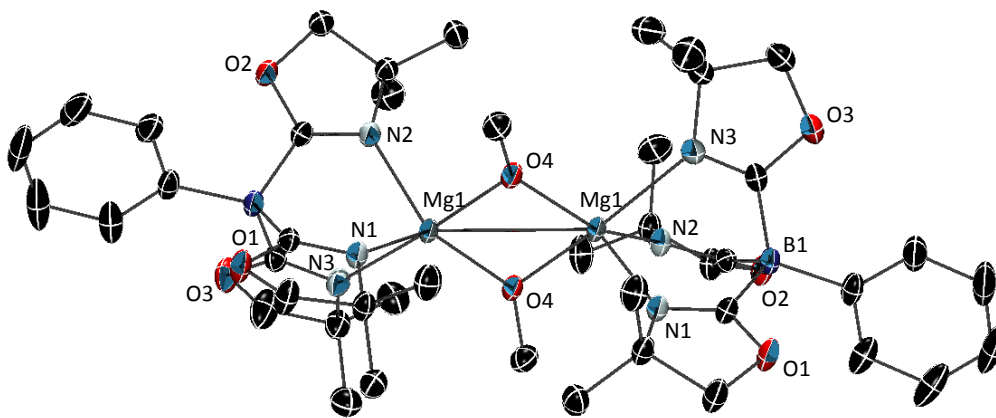
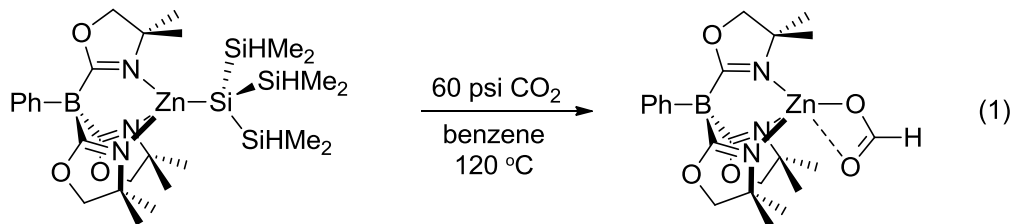


Fig. 2 Rendered thermal ellipsoid plot of $(To^M Mg(\mu-O Me))_2$ (**5**) with ellipsoids plotted at 35% probability. Hydrogen atoms and two benzene molecules are not plotted for clarity.

Surprisingly, zinc silyls **1** and **3** are also inert to water and methanol. Only starting materials are detected after attempted thermolysis of **1** or **3** in benzene- d_6 with excess water at 80 °C for 12 h. Compounds **1** and **3** are insoluble in pure water, and the 1H NMR spectra of the

solids recovered from water and redissolved in benzene- d_6 contain only signals assigned to the zinc silyls. Similarly, **1** and **3** are insoluble in methanol at room temperature. A suspension of **1** partly dissolves in methanol- d_4 after heating at 60 °C for 4 h. The ^1H NMR spectrum of the resulting solution contained silyl and oxazoline resonances for **1** that are distinct from $\text{HSi}(\text{SiHMe}_2)_3$ and $\text{To}^{\text{M}}\text{ZnOMe}$. Additionally, the ^1H NMR spectrum (acquired in benzene- d_6) of the solid recovered from methanol contained only signals assigned to **1**. This inert nature contrasts the reactions of $\text{To}^{\text{M}}\text{ZnR}$ ($\text{R} = \text{H}$, alkyl, phenyl) and H_2O that provide a trimeric hydroxide $(\text{To}^{\text{M}}\text{ZnOH})_3$.¹³ Addition of 12 M HCl to a benzene- d_6 solution of **1**, however, produces $\text{HSi}(\text{SiHMe}_2)_3$. The magnesium silyls **2** and **4** are hydrolytically sensitive, forming hydrosilanes $\text{HSi}(\text{SiHMe}_2)_3$ and $\text{HSi}(\text{SiMe}_3)_3$ upon treatment with water. Compounds **2** and **4** slowly react with methanol (**2**: 4 h, r.t.; **4**: 5 h, r.t.) to provide **5**. Note that $\text{To}^{\text{M}}\text{MgMe}$ and methanol provide **5** quantitatively after 5 min. in benzene.

Interestingly, **1** and CO_2 (60 psi) react at 120 °C to form the zinc formate $\text{To}^{\text{M}}\text{ZnOCHO}$ (**6**) ($t_{1/2} = 18$ h, eq. 1). The ^1H NMR spectrum of **6** contained a downfield singlet resonance attributed to the ZnOCHO (8.76 ppm); a similar signal was reported for $\text{Tp}^{\text{tBu}}\text{ZnOCHO}$ ($\text{Tp}^{\text{tBu}} = \text{tris}(3\text{-tert-butyl-pyrazolyl})\text{borate}$) (8.91 ppm).¹⁴ A peak at 169 ppm in the $^{13}\text{C}\{^1\text{H}\}$ NMR spectrum of **6** was assigned to the formate carbon.



The identity of compound **6** is further supported by its independent preparation from $\text{To}^{\text{M}}\text{ZnH}$ and CO_2 (1 atm) in benzene at ambient temperature. Two new bands in the solid-state infrared spectrum of **6** at 1629 and 1307 cm^{-1} are assigned to the $\nu_{\text{CO}(\text{asym})}$ and $\nu_{\text{CO}(\text{sym})}$ of the

[Zn]OCHO moiety; the $\Delta\nu_{\text{CO}}$ of 322 cm^{-1} suggests monodentate formate coordination.¹⁵ For comparison, the assigned bands for $\text{Tp}^{\text{tBu}}\text{ZnOCHO}$ are 1655 and 1290 cm^{-1} ($\Delta\nu_{\text{CO}} = 365\text{ cm}^{-1}$), and the bands for TptmZnOCHO are 1621 and 1317 cm^{-1} ($\Delta\nu_{\text{CO}} = 304\text{ cm}^{-1}$, $\text{Tptm} = \text{tris}(2\text{-pyridylthio})\text{methane}$).¹⁶

An X-ray structure determination provides additional characterization of **6** (Fig. 3).¹⁷ The zinc–oxygen distances associated with the formate moiety are inequivalent (Zn1-O4 , $1.909(1)$; Zn1-O5 , 2.792 \AA). The first distance is equal to the sum of covalent radii of Zn–O (1.9 \AA),¹⁸ and the latter distance is slightly shorter than the sum of van der Waal radii (2.91 \AA). For comparison, the Zn–O distance in monomeric $\text{To}^{\text{M}}\text{ZnO}^{\text{tBu}}$ is $1.835(1)\text{ \AA}$,¹⁹ whereas the distance in TptmZnOCHO is $2.036(1)\text{ \AA}$.²⁰

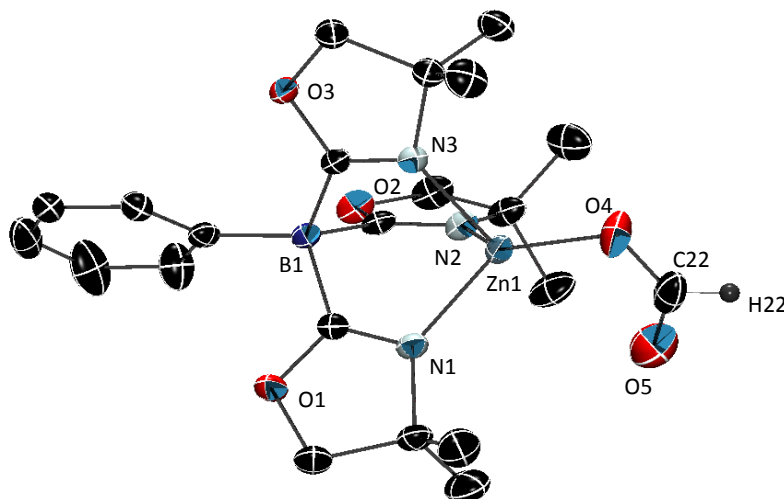
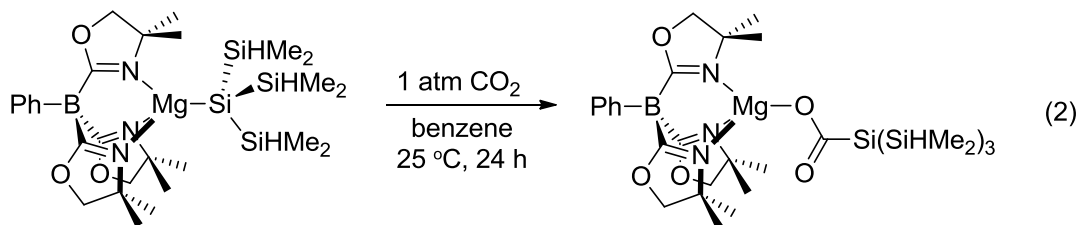


Fig. 3 Rendered thermal ellipsoid plot of $\text{To}^{\text{M}}\text{ZnOCHO}$ (**6**), with ellipsoids plotted at 35% probability. Only the formate hydrogen atom is illustrated.

Interestingly, reactions of CO_2 with isostructural **1** and **2** provide dissimilar products. CO_2 (1 atm) reacts with **2** at ambient temperature in benzene to give $\text{To}^{\text{M}}\text{MgO}_2\text{CSi}(\text{SiHMe}_2)_3$ (**7**) quantitatively over 24 h (eq. 2). Higher temperature and greater CO_2 pressure increase the



reaction rate. For example, complete conversion of **2** to **7** is achieved in 45 min at 100 °C with 70 psi of CO₂. A ¹³C{¹H} NMR resonance at 202.61 ppm is assigned to the silanecarboxylate MgOC(O)Si(SiHMe₂)₃. This value is similar to those of other metal silanecarboxylates, such as monomeric Mo(=NAr)(=CHCMe₂Ph){O₂CSi(SiMe₃)₃}₂ (211.4 ppm, Aryl = 2,6-C₆(*i*-C₃H₇)₂H₃)²¹ and (Cp₂Sc{μ-O₂CSi(SiMe₃)₃}₂) (200.81 ppm).²² Unfortunately, early attempts at X-ray diffraction experiments on **7** were unsuccessful, and the IR bands associated with the silanecarboxylate were not assigned. Compound **7** was characterized as a monomeric species by DOSY experiments that reveal similar diffusion constants of monomeric **2** ($6.95 \times 10^{-10} \text{ m}^2 \text{ s}^{-1}$) and **7** ($6.85 \times 10^{-10} \text{ m}^2 \text{ s}^{-1}$) (see experimental section). To further support this conclusion, X-ray quality crystals of **7** were eventually obtained from a concentrated toluene solution, which showed a monomeric structure (Fig. 4).²³ Terminal β-SiH's in **7** are located in the difference

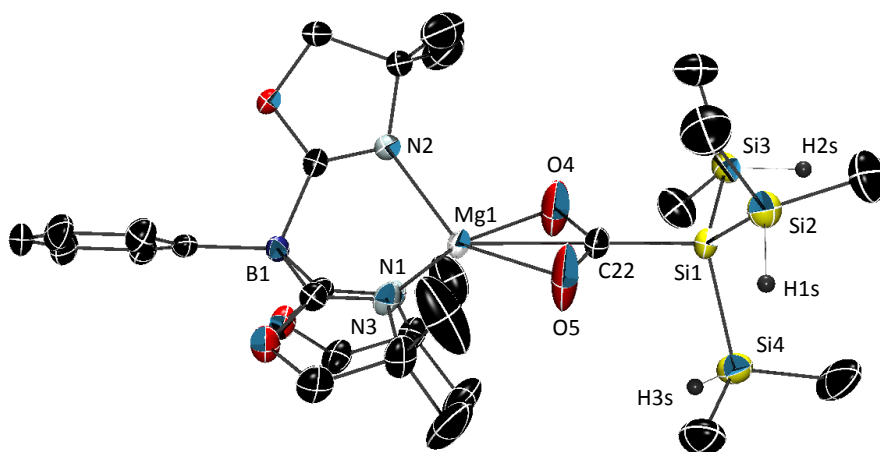


Fig. 4 Rendered thermal ellipsoid plot of To^MMgO₂CSi(SiHMe₂)₃ (**7**), with ellipsoids plotted at 35% probability. Hydrogen atoms on the To^M and Me groups are not illustrated for clarity.

Fourier map. The monomer contains tridentate tris-(oxazolinyl)borate and a bidentate silanecarboxylate moiety. The magnesium–oxygen distances associated with the carboxylate are nearly equivalent (Mg1–O4, 2.067(2); Mg1–O5, 2.041(2) Å).

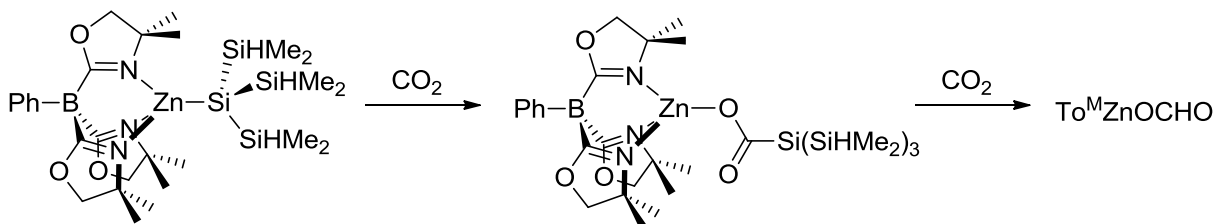
Compound **7** is thermally robust, and the starting material is unchanged after a benzene-*d*₆ solution is heated at 120 °C for 12 h. During the conversion of **2** to **7**, signals assigned to those two compounds are the only ones observed in the ¹H NMR spectra of reaction mixtures. In contrast, Cp₂Zr(η²-SiMe₂N^tBu) and CO₂ react to give the decarbonylated product [Cp₂Zr(μ-*O*-κ²-*O,N*-OSiMe₂N^tBu)]₂ and CO.²⁴ The dimeric silanecarboxylate (Cp₂Sc{μ-O₂CSi(SiMe₃)₃})₂ is unchanged after 60 h at 95 °C.²⁵ However, a side-product, postulated to be Cp₂ScOSi(SiMe₃)₃, is formed during the reaction of Cp₂ScSi(SiMe₃)₃THF and CO₂. This species may form from monomeric Cp₂ScO₂CSi(SiMe₃)₃ prior to dimerization.

Additional evidence for Si–C bond formation is provided by the reaction of **7** and MeOH, which gives compound **5** and HO₂CSi(SiHMe₂)₃ (**8**). Compounds **7** and **8** are characterized by their independent preparation: **8** is synthesized by adapting a literature procedure for HO₂CSi(SiMe₃)₃.²⁶ Compound **7** is independently prepared from To^MMgMe and **8**. The identical spectroscopic properties of the two species support the assignment of **7** as a silanecarboxylate.

To^MZnO₂CSi(SiHMe₂)₃ (**9**) is a possible intermediate in the formation of **6** from **2**. Therefore, the zinc silanecarboxylate To^MZnO₂CSi(SiHMe₂)₃ was prepared from To^MZnEt and **8**. The ¹³C{¹H}NMR spectrum of **9** contained a resonance at 193.38 ppm assigned to the carboxylate. The diffusion constant 6.43 × 10⁻¹⁰ m² s⁻¹ obtained from a DOSY experiment in benzene-*d*₆ indicated that **9** is monomeric in solution. Thermolysis of **9** at 120 °C for 12 h under a N₂ atmosphere returns starting material unchanged. However, thermal treatment of **9** under 60 psi of CO₂ at 120 °C affords the formate **6** (*t*_{1/2} = 6 h). Thus, a plausible and kinetically

competent pathway for the formation of **6** is shown in Scheme 2, although **9** is not detected in the reaction mixture and our current evidence does not rule out a one-step pathway.

Scheme 2. A possible pathway for the formation of $\text{To}^{\text{M}}\text{ZnOCHO}$ from $\text{To}^{\text{M}}\text{Zn-Si}(\text{SiHMe}_2)_3$ and CO_2 .



The dichotomic reactivity of isostructural zinc and magnesium silyls and silanecarboxylates toward carbon dioxide is intriguing. In addition, the reaction of zinc silanecarboxylate (**9**) with CO_2 provides a new fundamental step that could be applied in catalytic CO_2 conversions. As a complimentary study to this system (varied metal center and consistent ligand), another series of complexes (consistent metal center and varied ligand) was chosen for study. The comparison of $\text{To}^{\text{M}}\text{Zn-Si}(\text{SiHMe}_2)_3$, $\text{To}^{\text{M}}\text{Zn-N}(\text{SiHMe}_2)_2$, and $\text{To}^{\text{M}}\text{Zn-CH}(\text{SiHMe}_2)_3$ could provide Zn–element trends and insights into the reactivity of the Zn–E bond in comparison to the β -SiH bond.

$\text{To}^{\text{M}}\text{Zn-CH}(\text{SiHMe}_2)_2$ is synthesized according to the procedure used for $\text{To}^{\text{M}}\text{Zn-Si}(\text{SiHMe}_2)_3$ (**1**) noted above and the reported procedure for $\text{To}^{\text{M}}\text{Zn-N}(\text{SiHMe}_2)_2$.²⁷ $\text{To}^{\text{M}}\text{ZnCl}$ reacts with 1 equiv. $\text{Li}[\text{CH}(\text{SiHMe}_2)_2](\text{THF})$ in benzene after 24 h at ambient temperature to form $\text{To}^{\text{M}}\text{Zn-CH}(\text{SiHMe}_2)_2$ (**10**). The characteristic features in the ^1H NMR spectrum include a singlet assigned to the α -CH resonance at -0.94 ppm and a septet assigned to the β -SiH resonance at 4.86 ppm. An X-ray structure determination provides additional characterization of

10 (Fig. 5).²⁸ In the model, the two SiHMe₂ groups are oriented with the SiH's pointing toward the zinc center. However, the coupling constant for the SiH ($^1J_{\text{SiH}} = 175$ Hz) and single IR stretching frequency assigned to the ν_{SiH} (2093 cm⁻¹) are consistent with terminal, 2-center-2-electron bonded Si–H moieties. The Zn1–C1 distance is 2.012(3) Å, which is shorter than the Zn–C distances in bipyZn{CH(SiMe₃)₂}₂ (2.034(5) and 2.035(5) Å) (bipy = 2,2'-bipyridine).²⁹

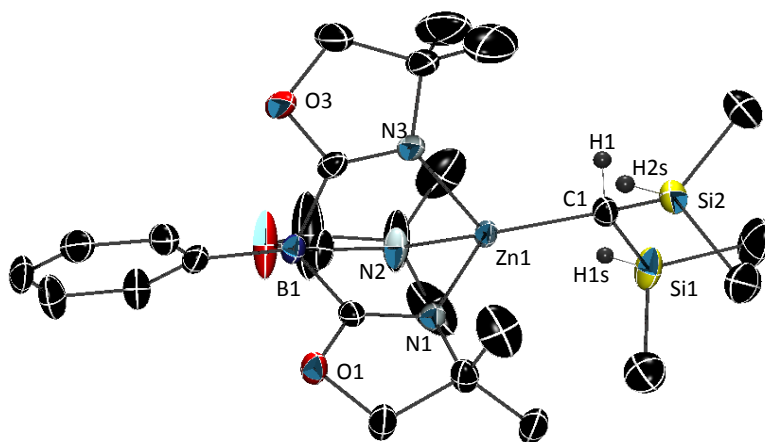
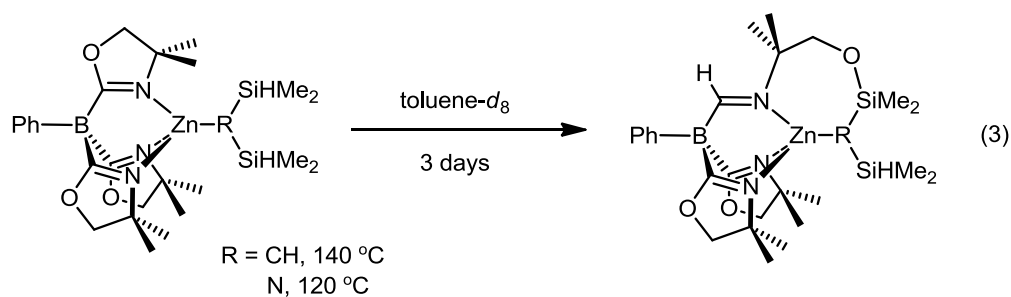


Fig. 5 Rendered thermal ellipsoid plot of To^MZn–CH(SiHMe₂)₂ (**10**), with ellipsoids plotted at 35% probability. For clarity, only the α -CH and β -SiH hydrogen atoms are illustrated.

Compound **10** undergoes oxazoline ring-opening to give O–Si bond formation and transfer of hydrogen from silicon to the imide carbon in the oxazoline moiety in toluene-*d*₈ after heating for 3 d at 140 °C in a sealed NMR tube (eq. 3). To^MZn–N(SiHMe₂)₂ undergoes the

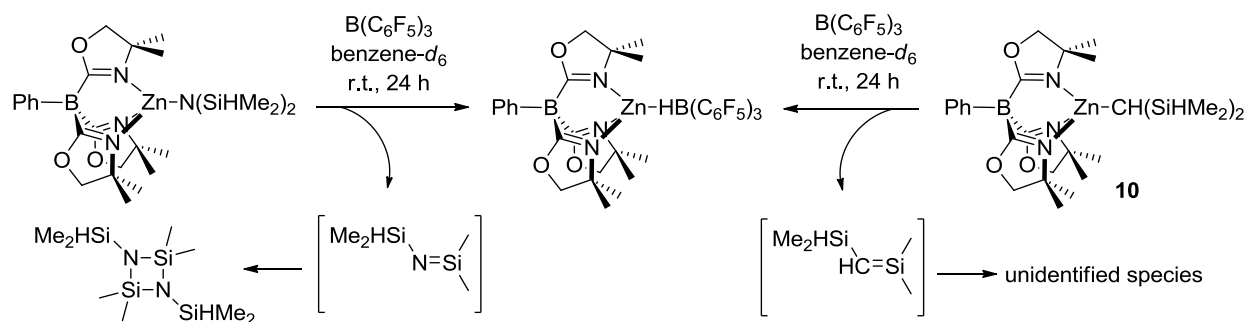


analogous ring opening reaction in toluene- d_8 after at 3 d at 120 °C.³⁰ As formerly mentioned, $To^M Zn-Si(SiHMe_2)_3$ (**1**) is thermally resilient, and starting materials are recovered after heating a toluene- d_8 solution at 170 °C for 24 h.

It was previously shown that $[Li(Et_2O)_n][B(C_6F_5)_4]$ facilitated the oxazoline ring-opening in $To^M Zn-N(SiHMe_2)_3$ under mild conditions (24 h at ambient temperature).³¹ However, **10** and **1** each show only starting materials in their respective 1H NMR spectrum in toluene- d_8 after 24 h at r.t. Upon heating, there is no change in the spectra until 120 °C, at which the $To^M Zn$ compounds decompose to several unidentified species.

Reactions with Lewis acids, such as the strong borane, $B(C_6F_5)_3$, were explored next. $To^M Zn-N(SiHMe_2)_2$ or $To^M Zn-CH(SiHMe_2)_2$ reacts with 1 equiv. $B(C_6F_5)_3$ at ambient temperature to give $To^M ZnHB(C_6F_5)_3$ after 24 h (Scheme 3). The β -SiH abstraction byproduct observed in the 1H NMR spectrum of the borane reaction with $To^M Zn-N(SiHMe_2)_2$ is the head to tail dimer of $Me_2Si=N-SiHMe_2$, 1,3-bis(dimethylsilyl)-2,2,4,4-tetramethyl-cyclodisilazane,³² while several unidentified species were observed in the 1H NMR spectrum of the borane reaction with $To^M Zn-CH(SiHMe_2)_2$.

Scheme 3. Reaction of $To^M Zn-N(SiHMe_2)_2$ or $To^M Zn-CH(SiHMe_2)_2$ with $B(C_6F_5)_3$.



The ^1H NMR spectrum of $\text{To}^{\text{M}}\text{ZnHB}(\text{C}_6\text{F}_5)_3$ in benzene- d_6 contained one set of oxazoline resonances. This spectral data is consistent with a pseudo- C_{3v} -symmetric structure and tridentate coordination of To^{M} to the zinc center. The C_6F_5 groups in the anion are equivalent on the NMR timescale at room temperature, as indicated by the three resonances observed in the ^{19}F NMR spectrum at -130.3 , -156.9 and -163.0 ppm. In the ^{11}B NMR spectrum, a singlet at -18.6 ppm was assigned to the tris(oxazoliny)borate ligand, and a broad doublet at -24.8 ppm ($^1J_{\text{HB}} = 94$ Hz) characterized the $\text{HB}(\text{C}_6\text{F}_5)_3$ anion. However, this $\text{HB}(\text{C}_6\text{F}_5)_3$ resonance has also been observed as a broad singlet at -13.2 ppm, depending on the synthetic route used. $\text{To}^{\text{M}}\text{ZnHB}(\text{C}_6\text{F}_5)_3$ is also synthesized by the reaction of $\text{To}^{\text{M}}\text{ZnH}$ and 1 equiv. $\text{B}(\text{C}_6\text{F}_5)_3$ in benzene at ambient temperature, and it is crystallographically characterized from this alternative route (see chapter 4). Additionally, B–H bond formation was evidenced by an IR absorption at 2379 cm^{-1} .

In contrast to the zinc silazide and zinc alkyl compounds, $\text{To}^{\text{M}}\text{Zn-Si}(\text{SiHMe}_2)_3$ (**1**) reacts over 5 d at r.t. in benzene- d_6 to give a new C_s -symmetric complex as the only To^{M} -containing species observed in the ^1H NMR spectrum. This change in symmetry indicates one oxazoline is uncoordinated to the zinc center and/or has participated in the reaction. In addition, several features and functional groups can be deduced from the spectroscopy of this interesting compound. A doublet at 0.29 ppm and a septet at 4.38 ppm, which integrate to 12 and 2 protons, respectively, were assigned to the SiHMe_2 groups in the ^1H NMR spectrum. The corresponding resonances in the ^{29}Si NMR spectrum were observed at -28.7 ppm (SiHMe_2) and -156.3 ppm ($\text{Si}(\text{SiHMe}_2)_2$). These values are comparable to the parent compound **1**; however, the internal silicon resonance is shifted ca. 20 ppm from the resonance in **1**, likely because the $\text{Si}(\text{SiHMe}_2)_2$ group is no longer interacting with the zinc center. A singlet in the ^{11}B NMR spectrum at -18.4

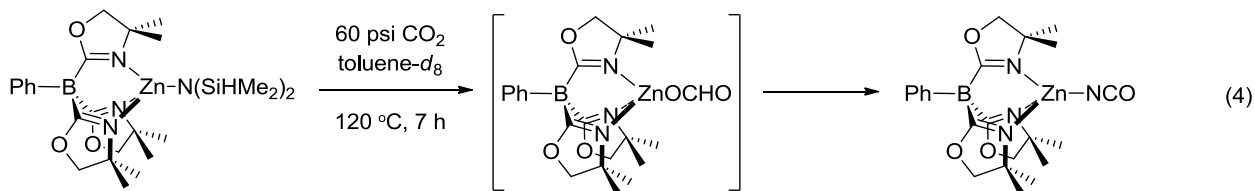
ppm characterized the tris(oxazoliny)borate ligand and a doublet at -24.6 ppm ($^1J_{\text{HB}} = 94$ Hz) characterized the $\text{HB}(\text{C}_6\text{F}_5)_3$ anion, which is nearly identical to the shift observed for the anion in $\text{To}^{\text{M}}\text{ZnHB}(\text{C}_6\text{F}_5)_3$. This provides evidence that the $\text{HB}(\text{C}_6\text{F}_5)_3$ anion interacts with the zinc center as in $\text{To}^{\text{M}}\text{ZnHB}(\text{C}_6\text{F}_5)_3$, and supports that the Zn–Si bond has been disrupted. Furthermore, IR absorptions at 2392 cm^{-1} for the B–H and 2097 cm^{-1} for the Si–H compare well with $\text{To}^{\text{M}}\text{ZnHB}(\text{C}_6\text{F}_5)_3$ and $\text{To}^{\text{M}}\text{Zn–CH}(\text{SiHMe}_2)_3$ rather than $\text{To}^{\text{M}}\text{Zn–Si}(\text{SiHMe}_2)_3$. The C_6F_5 groups are equivalent in the ^{19}F NMR spectrum, and the three resonances observed at -132.6 , -163.0 , and -166.1 ppm are slightly shifted compared to those of $\text{To}^{\text{M}}\text{ZnHB}(\text{C}_6\text{F}_5)_3$. The $^{15}\text{N}\{^1\text{H}\}$ NMR spectrum contains two resonances for the inequivalent oxazoline rings at -164.3 and -209.9 ppm, which are similar to those reported for the ring-opened product of $\text{To}^{\text{M}}\text{Zn–N}(\text{SiHMe}_2)_2$ (-166.1 and -263.6 ppm) (eq. 3).³³

Given the tendency of these $\text{To}^{\text{M}}\text{Zn–R}(\text{SiHMe}_2)_2$ ($\text{R} = \text{N}, \text{CH}$) compounds toward ring-opening and the oxophilicity of silicon, oxazoline ring-opening and O–Si bond formation concurrent with β -SiH abstraction by borane could be occurring in this reaction between $\text{To}^{\text{M}}\text{Zn–Si}(\text{SiHMe}_2)_3$ (**1**) and $\text{B}(\text{C}_6\text{F}_5)_3$. However, further characterization is needed to determine the absolute structure of the C_s -symmetric species, and unfortunately, several attempts at X-ray characterization failed. **1** reacts with the weaker Lewis acid $\text{PhB}(\text{C}_6\text{F}_5)_2$ over 5 d in benzene- d_6 to give nearly identical spectroscopy as the product from $\text{B}(\text{C}_6\text{F}_5)_3$ discussed above. In contrast, **1** reacts with 1 equiv. $[\text{CPh}_3][\text{B}(\text{C}_6\text{F}_5)_4]$ to give $[\text{To}^{\text{M}}\text{Zn}][\text{B}(\text{C}_6\text{F}_5)_4]$ after 12 h in bromobenzene- d_5 .

As proposed in scheme 2, CO_2 may also act as a Lewis acid toward silanecarboxylates. For comparison with compound **1**, the reactions of $\text{To}^{\text{M}}\text{Zn–CH}(\text{SiHMe}_2)_2$ (**10**) and $\text{To}^{\text{M}}\text{Zn–N}(\text{SiHMe}_2)_2$ with CO_2 were investigated. Similar to **1**, compound **10** and CO_2 (60 psi) react at $120\text{ }^\circ\text{C}$ to form $\text{To}^{\text{M}}\text{ZnOCHO}$ (**6**) ($t_{1/2} = 24$ h). However, unlike **1**, unknown intermediate species

in addition to starting material are observed in the ^1H NMR spectrum during the reaction, and at 48 h the only observed species is **6**. These intermediate species could be the result of CO_2 insertion to form carboxylates analogous to $\text{To}^{\text{M}}\text{ZnO}_2\text{CSi}(\text{SiHMe}_2)_3$ and $\text{To}^{\text{M}}\text{MgO}_2\text{CSi}(\text{SiHMe}_2)_3$ or other β -SiH abstracted species.

Interestingly, $\text{To}^{\text{M}}\text{Zn}-\text{N}(\text{SiHMe}_2)_2$ and CO_2 (60 psi) react at $120\text{ }^\circ\text{C}$ in toluene- d_8 to show some formation of **6** after 2 h. However, after 3 hours the starting material is consumed and a new species assigned as $\text{To}^{\text{M}}\text{ZnNCO}$ (**11**) is also present in the reaction mixture. After 7 hours **11** is the only observed species in the ^1H NMR spectrum (eq. 4).



Compound **11** was isolated as colorless crystals by concentrating the toluene- d_8 solution and cooling to $-30\text{ }^\circ\text{C}$. Though the ^1H NMR spectrum shows only features of the tris(oxazolinyl)borate ligand, a key resonance in the ^{13}C NMR spectrum at 160.08 ppm, and an IR absorption at 2234 cm^{-1} were assigned to the NCO group. To confirm these assignments, $\text{To}^{\text{M}}\text{ZnNCO}$ was independently synthesized from the reaction of $\text{To}^{\text{M}}\text{ZnCl}$ and KOCN (THF, 24 h, r.t.), and the identical spectroscopic properties of the two species support the assignment of **11** as the isocyanate. An X-ray structure determination provides additional characterization of **11**,³⁴ although the NCO moiety was highly disordered (Fig. 6). Still the structure shows pseudo- C_{3v} -symmetry and tridentate coordination of To^{M} to the zinc center, and the $\text{Zn1}-\text{N4a}$ distance of $1.913(9)\text{ \AA}$ is equal to the sum of covalent radii of $\text{Zn}-\text{N}$ (1.9 \AA).³⁵ For comparison, the $\text{Zn}-\text{N}$ distances in $\text{Zn}(\text{C}_{10}\text{H}_{10}\text{N}_4)_2(\text{NCO})_2$ ($\text{C}_{10}\text{H}_{10}\text{N}_4 = 1\text{-methyl-2-(phenyldiazenyl)-1H-imidazole}$) are $1.944(2)$ and $1.937(3)\text{ \AA}$.³⁶

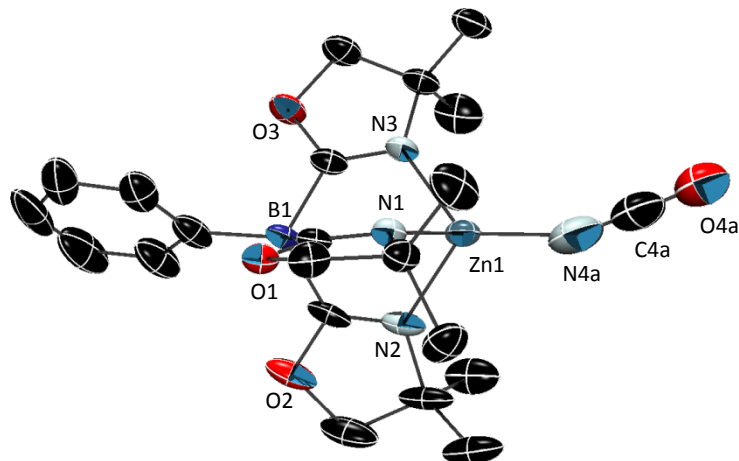


Fig. 6 Rendered thermal ellipsoid plot of $To^M ZnNCO$ (**11**), with ellipsoids plotted at 35% probability. The hydrogen atoms on the To^M group are not illustrated for clarity.

The formation of **11** could occur through a number of pathways. Therefore, we investigated the reaction of $To^M ZnOCHO$ (**6**) with silazane. Only starting materials were detected in the 1H NMR spectrum after heating **6** and 1 equiv. $HN(SiHMe_2)_2$ at $120\text{ }^\circ C$ for 24 h. Likewise, only starting materials were detected in the presence of CO_2 (60 psi) under the previous reaction conditions. From these results, we conclude that the $N(SiHMe_2)_2$ group undergoes a rearrangement to facilitate the formation of **11**. Isocyanate formation is also observed in the reactions of $[\kappa^3\text{-Tpsem}]ZnN(SiMe_3)_2$ (Tpsem = tris(2-pyridylseleno)methyl) or $[\kappa^3\text{-Tptm}]ZnN(SiMe_3)_2$ (Tptm = tris(2-pyridylthio)methyl) with CO_2 .³⁷ The proposed pathway proceeds via CO_2 insertion into the $Zn-N(SiMe_3)_2$ bond to give a carboxylate species, followed by conversion to Me_3SiNCO and $[Zn]OSiMe_3$. The $[Zn]OSiMe_3$ compound is thought to undergo another CO_2 insertion, and metathesis with Me_3SiNCO yields the isocyanate and $(Me_3SiO)_2CO$. Though $[\kappa^3\text{-Tptm}]ZnH$ reacts readily with CO_2 to give $[\kappa^4\text{-Tptm}]ZnOCHO$, the formate is not observed in the transformation of $[\kappa^3\text{-Tptm}]ZnN(SiMe_3)_2$ to $[\kappa^4\text{-Tptm}]ZnNCO$.³⁸

Therefore, β -SiH abstraction, which is not an option in the $N(\text{SiMe}_3)_2$ containing complexes, likely plays a crucial role in the multi-step conversion of **1** to **11**.

Since $\text{To}^M\text{Zn-CH}(\text{SiHMe}_2)_2$ and $\text{To}^M\text{Zn-N}(\text{SiHMe}_2)_2$ both show formation of To^MZnOCHO in the presence of CO_2 like $\text{To}^M\text{Zn-Si}(\text{SiHMe}_2)_3$, they may proceed through a CO_2 insertion pathway to give carboxylate intermediates. Several synthetic routes were attempted to independently synthesize $\text{To}^M\text{ZnO}_2\text{CCH}(\text{SiHMe}_2)_2$ based on the synthesis of $\text{To}^M\text{ZnO}_2\text{CSi}(\text{SiHMe}_2)_3$ and the known compounds $\text{HO}_2\text{CC}(\text{SiMe}_3)_3$ and $\text{HO}_2\text{CCH}(\text{SiMe}_3)_2$,³⁹ but none were successful for $\text{HO}_2\text{CCH}(\text{SiHMe}_2)_2$. Furthermore, the routes used for the carbon and silanecarboxylic acids are not viable for the $N(\text{SiHMe}_2)_2$ moiety as the N-Si bonds readily hydrolyze. The reactions of $\text{LiCH}(\text{SiHMe}_2)_2(\text{THF})$ or $\text{LiN}(\text{SiHMe}_2)_2$ and CO_2 (60 psi) yielded complicated mixtures that did not contain resonances in the ^1H or ^{13}C NMR spectra identified as CO_2 inserted into the parent lithium alkyl or lithium silazide. Therefore, the silanecarboxylic acid, $\text{HO}_2\text{CSi}(\text{SiHMe}_2)_3$, seems to be uniquely accessible, currently providing a plausible model for the reactions of CO_2 with $\text{To}^M\text{M-R}$ compounds ($M = \text{Mg, Zn}$; $R = \text{Si}(\text{SiHMe}_2)_3, \text{CH}(\text{SiHMe}_2)_2, \text{N}(\text{SiHMe}_2)_2$).

Conclusion

While CO_2 is sufficiently strong to abstract a β -SiH in $\text{To}^M\text{ZnO}_2\text{CSi}(\text{SiHMe}_2)_3$ (**9**) to yield To^MZnOCHO (**6**), it is not strong enough to abstract a β -SiH in $\text{To}^M\text{MgO}_2\text{CSi}(\text{SiHMe}_2)_3$ to afford a magnesium formate. Furthermore, our observations suggest that the Zn-Si bond is initially the preferred site of reactivity with CO_2 , but the Si-H bond is the preferred site upon Zn-O bond formation. Since **6** is observed in all three $\text{To}^M\text{Zn-R}(\text{SiHMe}_2)_2$ ($R = \text{Si}(\text{SiHMe}_2)_3, \text{CH}, \text{N}$) complexes, the same reactivity trend may apply. We are currently exploring the

spectroscopy and isolation of transient intermediates observed in the reactions of $\text{To}^{\text{M}}\text{Zn}-\text{CH}(\text{SiHMe}_2)_2$ and $\text{To}^{\text{M}}\text{Zn}-\text{N}(\text{SiHMe}_2)_2$ with CO_2 , as well as synthesizing other $\text{To}^{\text{M}}\text{Zn}$ -alkyl compounds for the independent synthesis of zinc carboxylate species and mechanistic studies.

Experimental

General Procedures. All reactions were performed under a dry argon atmosphere using standard Schlenk techniques or under a nitrogen atmosphere in a glovebox, unless otherwise indicated. Benzene, toluene, pentane, diethyl ether, and tetrahydrofuran were dried and deoxygenated using an IT PureSolv system. Benzene- d_6 was heated to reflux over Na/K alloy and vacuum-transferred. The starting materials $(\text{TMEDA})\text{MgMeBr}$,⁴⁰ $\text{H}[\text{To}^{\text{M}}]$,⁴¹ $\text{To}^{\text{M}}\text{MgMe}$,⁴² $\text{To}^{\text{M}}\text{ZnCl}$,⁴³ $\text{Si}(\text{SiHMe}_2)_4$,⁴⁴ $\text{KSi}(\text{SiMe}_3)_3$,⁴⁵ $\text{H}_2\text{C}(\text{SiHMe}_2)_2$,⁴⁶ and $\text{Li}[\text{CH}(\text{SiHMe}_2)_2](\text{THF})$ ⁴⁷ were synthesized according to literature procedures. ^1H , $^{13}\text{C}\{^1\text{H}\}$, ^{29}Si and ^{11}B NMR spectra were collected on Agilent MR-400, Bruker DRX400 or AVIII 600 spectrometers. ^{11}B NMR spectra were referenced to an external BF_3OEt_2 standard. ^{29}Si NMR spectra were acquired with INEPT sequences and referenced to an external SiMe_4 standard. ^{15}N chemical shifts were determined by ^1H - ^{15}N HMBC experiments on a Bruker AVIII 600 spectrometer. ^{15}N chemical shifts were originally referenced to an external liquid NH_3 standard and recalculated to the CH_3NO_2 chemical shift scale by adding -381.9 ppm. Elemental analyses were performed using a Perkin-Elmer 2400 Series II CHN/S by the Iowa State Chemical Instrumentation Facility. X-ray diffraction data was collected on a Bruker APEX II diffractometer.

Caution! High-pressure glass apparatuses must be handled with care. Thick-walled NMR tubes equipped with J. Young-style resealable Teflon valves (pressured to 100 psi with CO_2) were obtained from Wilmad-Labglass and attached to a high-pressure steel manifold through

commercial Swagelock fittings. The pressurized NMR tubes were handled in protective jackets.

To^MMgBr(THF)₂. H[To^M] (0.100 g, 4.25 mmol) and (TMEDA)MgMeBr (0.163 g, 4.25 mmol) were dissolved in THF and stirred for 30 min. at ambient temperature. The volatile materials were evaporated, the residue was washed with pentane (3 × 5 mL), and the resulting white solid was dried under vacuum to provide To^MMgBr(THF)₂ (0.230 g, 0.36 mmol, 85.8%). Analytically pure To^MMgBr(THF)₂ and X-ray quality single crystals were obtained from a concentrated THF solution of To^MMgBr(THF)₂ at -30 °C. Additionally, the quantity of THF in the product can vary from zero to two equivalents; the data is given for a batch isolated with two equivalents of THF. ¹H NMR (400 MHz, benzene-*d*₆): δ 1.06 (s, 18 H, CNCMe₂CH₂O), 1.42 (t, ³J_{HH} = 6.6 Hz, 8 H, β-THF), 3.36 (s, 6 H, CNCMe₂CH₂O), 3.58 (t, ³J_{HH} = 6.6 Hz, 8 H, α-THF), 7.36 (t, ³J_{HH} = 7.2 Hz, 1 H, *para*-C₆H₅), 7.53 (t, ³J_{HH} = 7.2 Hz, 2 H, *meta*-C₆H₅), 8.23 (d, ³J_{HH} = 7.2 Hz, 2 H, *ortho*-C₆H₅). ¹³C{¹H} NMR (150 MHz, benzene-*d*₆): δ 26.15 (β-THF), 28.44 (CNCMe₂CH₂O), 65.64 (CNCMe₂CH₂O), 68.17 (α-THF), 80.80 (CNCMe₂CH₂O), 126.54 (*para*-C₆H₅), 127.32 (*meta*-C₆H₅), 136.32 (*ortho*-C₆H₅), 142.8 (br, *ipso*-C₆H₅), 191.3 (br, CNCMe₂CH₂O). ¹¹B NMR (128 MHz, benzene-*d*₆): δ -18.2. ¹⁵N NMR (60.6 MHz, benzene-*d*₆): δ -160.9. IR (KBr, cm⁻¹): 3050 (m), 2972 (s), 2873 (m), 1599 (s, ν_{CN}), 1492 (w), 1462 (s), 1433 (m), 1389 (m), 1371 (s), 1354 (m), 1303 (m), 1273 (s), 1253 (m), 1197 (s), 1155 (s), 1047 (s), 995 (s), 966 (s), 939 (m), 890 (m), 843 (m), 822 (w), 777 (w), 708 (m), 695 (s), 685 (w), 666 (w), 649 (w). Anal. Calcd. for C₂₉H₄₅BBrMgN₃O₅: C, 55.23; H, 7.19; N, 6.66. Found: C, 54.75; H, 6.70; N, 6.58. Mp: 251-253 °C.

KS₂Si(SiHMe₂)₃. Si(SiHMe₂)₄ (6.00 g, 0.027 mol) and KO^tBu (3.95 g, 0.027 mol) were dissolved in benzene (25 mL). The solution was allowed to stir for 30 min., and the product precipitated as a white solid during this time. The solid was isolated by filtration, washed with pentane, and

recrystallized from toluene at $-30\text{ }^{\circ}\text{C}$ to give a white crystalline solid (5.99 g, 0.024 mol, 90.7%). ^1H NMR (600 MHz, benzene- d_6): δ 0.56 (d, 18 H, $^3J_{\text{HH}} = 4.5\text{ Hz}$, SiHMe_2), 4.22 (sept, 3 H, $^3J_{\text{HH}} = 4.5\text{ Hz}$, $^1J_{\text{SiH}} = 151.8\text{ Hz}$, SiHMe_2). $^{13}\text{C}\{^1\text{H}\}$ NMR (150 MHz, benzene- d_6): δ 2.47 (SiHMe_2). ^{29}Si (120 MHz, benzene- d_6) δ -23.8 (SiHMe_2), -202.3 ($\text{Si}(\text{SiHMe}_2)_3$). IR (KBr, cm^{-1}): 2959 (s), 2894 (s), 2020 (s, ν_{SiH}), 1419 (m), 1242 (s), 1041 (s), 872 (s), 766 (m), 685 (m), 645 (m). Anal. Calcd. for $\text{C}_6\text{H}_{21}\text{KSi}_4$: C, 29.45; H, 8.65. Found C, 29.20; H, 8.51. Mp 123-125 $^{\circ}\text{C}$.

To^MZnSi(SiHMe₂)₃ (1). To^MZnCl (0.235 g, 0.486 mmol) and KSi(SiHMe₂)₃ (0.119 g, 0.486 mmol) were dissolved in benzene, and the reaction mixture was stirred for 30 min. The reaction mixture was filtered to remove KCl, the filtrate was evaporated, and the resulting solid residue was washed with pentane and dried under vacuum to afford To^MZnSi(SiHMe₂)₃ (0.303 g, 0.464 mmol, 95.5%) as an analytically pure white solid. X-ray quality single crystals were grown by slow pentane diffusion into a concentrated toluene solution of To^MZnSi(SiHMe₂)₃ at $-30\text{ }^{\circ}\text{C}$. ^1H NMR (400 MHz, benzene- d_6): δ 0.57 (d $^3J_{\text{HH}} = 4.4\text{ Hz}$, 18 H, SiHMe_2), 1.14 (s, 18 H, $\text{CNCMe}_2\text{CH}_2\text{O}$), 3.45 (s, 6 H, $\text{CNCMe}_2\text{CH}_2\text{O}$), 4.64 (sept, $^3J_{\text{HH}} = 4.4\text{ Hz}$, 3 H, SiHMe_2), 7.35 (t, $^3J_{\text{HH}} = 7.2\text{ Hz}$, 1 H, *para*- C_6H_5), 7.53 (t, $^3J_{\text{HH}} = 7.6\text{ Hz}$, 2 H, *meta*- C_6H_5), 8.31 (d, $^3J_{\text{HH}} = 7.2\text{ Hz}$, 2 H, *ortho*- C_6H_5). $^{13}\text{C}\{^1\text{H}\}$ NMR (150 MHz, benzene- d_6): δ 0.16 (SiHMe_2), 28.76 ($\text{CNCMe}_2\text{CH}_2\text{O}$), 66.08 ($\text{CNCMe}_2\text{CH}_2\text{O}$), 81.06 ($\text{CNCMe}_2\text{CH}_2\text{O}$), 126.37 (*para*- C_6H_5), 127.30 (*meta*- C_6H_5), 136.46 (*ortho*- C_6H_5), 142.3 (br, *ipso*- C_6H_5), 190.2 (br, $\text{CNCMe}_2\text{CH}_2\text{O}$). ^{11}B NMR (192 MHz, benzene- d_6): δ -18.5 . ^{29}Si NMR (120 MHz, benzene- d_6): δ -28.3 ($^1J_{\text{SiH}} = 172.2\text{ Hz}$, $\text{Si}(\text{SiHMe}_2)_3$), -171.3 ($\text{Si}(\text{SiHMe}_2)_3$). ^{15}N NMR (60.6 MHz, benzene- d_6): δ -157.4 . IR (KBr, cm^{-1}): 3079 (w), 2967 (s), 2897 (m), 2064 (s, ν_{SiH}), 1591 (s, ν_{CN}), 1495 (w), 1462 (m), 1431 (w), 1387 (m), 1368 (m), 1276 (s), 1241 (s), 1195 (s), 1158 (s), 961 (s), 867 (s), 747 (m), 703 (s). Anal. Calcd. for $\text{C}_{27}\text{H}_{50}\text{BSi}_4\text{N}_3\text{O}_3\text{Zn}$: C, 49.64; H, 7.71; N, 6.43. Found: C, 49.21; H, 7.58; N,

6.37. Mp: 208-210 °C.

To^MMgSi(SiHMe₂)₃ (2). To^MMgBr(THF)₂ (0.706 g, 1.12 mmol) and KSi(SiHMe₂)₃ (0.275 g, 1.12 mmol) were dissolved in benzene (12 mL) and stirred for 30 min. at ambient temperature. The reaction mixture was filtered, and evaporation of the filtrate gave a white solid. The solid was washed with pentane (3 × 5 mL) and dried under vacuum providing crystalline, analytically pure To^MMgSi(SiHMe₂)₃ (0.630 g, 1.03 mmol, 91.5%). X-ray quality single crystals were obtained from a concentrated toluene solution cooled to -30 °C. ¹H NMR (600 MHz, benzene-*d*₆): δ 0.61 (d, ³J_{HH} = 4.2 Hz, 18 H, SiHMe₂), 1.13 (s, 18 H, CNCMe₂CH₂O), 3.38 (s, 6 H, CNCMe₂CH₂O), 4.71 (sept, ³J_{HH} = 4.2 Hz, 3 H, SiHMe₂), 7.36 (t, ³J_{HH} = 7.2 Hz, 1 H, *para*-C₆H₅), 7.53 (t, ³J_{HH} = 7.6 Hz, 2 H, *meta*-C₆H₅), 8.26 (d, ³J_{HH} = 7.2 Hz, 2 H, *ortho*-C₆H₅). ¹³C{¹H} NMR (150 MHz, benzene-*d*₆): δ 0.76 (SiHMe₂), 28.89 (CNCMe₂CH₂O), 65.91 (CNCMe₂CH₂O), 80.65 (CNCMe₂CH₂O), 126.42 (*para*-C₆H₅), 127.27 (*meta*-C₆H₅), 136.41 (*ortho*-C₆H₅), 142.3 (br, *ipso*-C₆H₅), 192.8 (br, CNCMe₂CH₂O). ¹¹B NMR (192 MHz, benzene-*d*₆): δ -18.2. ²⁹Si NMR (120 MHz, benzene-*d*₆): δ -27.2 (¹J_{SiH} = 169.7 Hz, Si(SiHMe₂)₃), -186.8 (Si(SiHMe₂)₃). ¹⁵N NMR (60.6 MHz, benzene-*d*₆): δ -161.9. IR (KBr, cm⁻¹): 3078 (w), 3048 (w), 2966 (s), 2054 (s, ν_{SiH}), 1582 (s, ν_{CN}), 1495 (w), 1463 (m), 1432 (w), 1387 (w), 1369 (m), 1352 (m), 1274 (s), 1246 (m), 1194 (s), 1160 (m), 963 (s), 894 (s), 861 (s), 832 (s), 747 (m), 703 (m), 689 (m), 670 (m), 650 (m), 639 (m). Anal. Calcd. for C₂₇H₅₀BN₃O₃Si₄Mg: C, 52.98; H, 8.23; N, 6.86. Found: C, 53.14; H, 8.35; N, 6.91. Mp: 201-203 °C.

To^MZnSi(SiMe₃)₃ (3). To^MZnCl (0.310 g, 0.642 mmol) and KSi(SiMe₃)₃ (0.184 g, 0.642 mmol) were dissolved in benzene (12 mL), and the reaction mixture was stirred for 2 h at ambient temperature. Filtration and evaporation of the benzene provided a white solid. The solid was washed with pentane (3 × 5 mL) and further dried under vacuum to obtain crystalline,

analytically pure $\text{To}^{\text{M}}\text{ZnSi}(\text{SiMe}_3)_3$ (0.420 g, 0.604 mmol, 94.1%). X-ray quality single crystals were grown from a concentrated toluene solution of $\text{To}^{\text{M}}\text{ZnSi}(\text{SiMe}_3)_3$ at $-30\text{ }^\circ\text{C}$. ^1H NMR (600 MHz, benzene- d_6): δ 0.53 (SiMe_3), 1.14 (s, 18 H, $\text{CNCMe}_2\text{CH}_2\text{O}$), 3.43 (s, 6 H, $\text{CNCMe}_2\text{CH}_2\text{O}$), 7.36 (t, $^3J_{\text{HH}} = 7.2$ Hz, 1 H, *para*- C_6H_5), 7.55 (t, $^3J_{\text{HH}} = 7.6$ Hz, 2 H, *meta*- C_6H_5), 8.33 (d, $^3J_{\text{HH}} = 7.2$ Hz, 2 H, *ortho*- C_6H_5). $^{13}\text{C}\{^1\text{H}\}$ NMR (150 MHz, benzene- d_6): δ 6.22 (SiHMe_2), 29.47 ($\text{CNCMe}_2\text{CH}_2\text{O}$), 66.23 ($\text{CNCMe}_2\text{CH}_2\text{O}$), 81.08 ($\text{CNCMe}_2\text{CH}_2\text{O}$), 126.28 (*para*- C_6H_5), 127.22 (*meta*- C_6H_5), 136.54 (*ortho*- C_6H_5), 140.6 (br, *ipso*- C_6H_5), 190.2 (br, $\text{CNCMe}_2\text{CH}_2\text{O}$). ^{11}B NMR (192 MHz, benzene- d_6): δ -18.7 . $^{29}\text{Si}\{^1\text{H}\}$ NMR (120 MHz, benzene- d_6): δ -8.1 (SiMe_3), -162.4 ($\text{Si}(\text{SiMe}_3)_3$). ^{15}N NMR (60.6 MHz, benzene- d_6): δ -157.4 . IR (KBr, cm^{-1}): 3078 (w), 3039 (w), 2968 (m), 2893 (m), 1591 (s, ν_{CN}), 1496 (w), 1462 (m), 1432 (w), 1386 (w), 1367 (m), 1355 (m), 1277 (s), 1241 (s), 1196 (s), 1162 (s), 1022 (s), 978 (s), 961 (s), 896 (w), 862 (m), 828 (s), 746 (m), 733 (w), 703 (s), 676 (s), 634 (m), 623 (s). Anal. Calcd. for $\text{C}_{30}\text{H}_{56}\text{BSi}_4\text{N}_3\text{O}_3\text{Zn}$: C, 51.82; H, 8.12; N, 6.04. Found: C, 51.43; H, 7.88; N, 6.01. Mp: 254-258 $^\circ\text{C}$ (dec).

$\text{To}^{\text{M}}\text{MgSi}(\text{SiMe}_3)_3$ (4). The preparation of $\text{To}^{\text{M}}\text{MgSi}(\text{SiMe}_3)_3$ follows the method used for $\text{To}^{\text{M}}\text{MgSi}(\text{SiHMe}_2)_3$ given above. $\text{To}^{\text{M}}\text{MgBr}$ (0.151 g, 0.24 mmol) and $\text{KSi}(\text{SiMe}_3)_3$ (0.068 g, 0.24 mmol) afforded $\text{To}^{\text{M}}\text{MgSi}(\text{SiMe}_3)_3$ (0.145 g, 0.22 mmol, 91.7%) as an analytically pure white solid. X-ray quality single crystals were grown from a concentrated toluene solution of $\text{To}^{\text{M}}\text{MgSi}(\text{SiMe}_3)_3$ at $-30\text{ }^\circ\text{C}$. ^1H NMR (600 MHz, benzene- d_6): δ 0.55 (SiMe_3), 1.15 (s, 18 H, $\text{CNCMe}_2\text{CH}_2\text{O}$), 3.38 (s, 6 H, $\text{CNCMe}_2\text{CH}_2\text{O}$), 7.35 (t, $^3J_{\text{HH}} = 7.2$ Hz, 1 H, *para*- C_6H_5), 7.53 (vt, $^3J_{\text{HH}} = 7.6$ Hz, 2 H, *meta*- C_6H_5), 8.26 (d, $^3J_{\text{HH}} = 7.2$ Hz, 2 H, *ortho*- C_6H_5). $^{13}\text{C}\{^1\text{H}\}$ NMR (150 MHz, benzene- d_6): δ 6.42 (SiMe_3), 29.41 ($\text{CNCMe}_2\text{CH}_2\text{O}$), 66.02 ($\text{CNCMe}_2\text{CH}_2\text{O}$), 80.67 ($\text{CNCMe}_2\text{CH}_2\text{O}$), 126.37 (*para*- C_6H_5), 127.27 (*meta*- C_6H_5), 136.48 (*ortho*- C_6H_5), 141.3 (br, *ipso*- C_6H_5), 192.6 (br, $\text{CNCMe}_2\text{CH}_2\text{O}$). ^{11}B NMR (192 MHz, benzene- d_6): δ -18.5 . ^{29}Si NMR

(120 MHz, benzene- d_6): δ -6.8 (SiMe₃), -179.7 (Si(SiMe₃)₃). ¹⁵N NMR (60.6 MHz, benzene- d_6): δ -155.8. IR (KBr, cm⁻¹): 3082 (w), 3044 (w), 2965 (s), 2894 (s), 1582 (s, ν_{CN}), 1496 (w), 1463 (m), 1433 (w), 1387 (w), 1368 (m), 1355 (m), 1369 (m), 1275 (s), 1239 (s), 1192 (s), 1162 (s), 1020 (s), 960 (s), 895 (w), 830 (s), 747 (m), 702 (s), 675 (s), 640 (s), 619 (s), 415 (s). Anal. Calcd. for C₃₀H₅₆BN₃O₃Si₄Mg: C, 61.80; H, 6.53; N, 8.01. Found: C, 61.25; H, 6.30; N, 8.01. Mp: 215-217 °C.

(To^MMgOMe)₂ (5). A benzene solution of To^MMgMe (0.300 g, 0.712 mmol) was exposed to O₂ (1 atm) for 5 minutes in a 100 mL Schlenk flask. The flask was sealed and then allowed to stand for 1 h at room temperature to form crystals. White, X-ray quality crystals were isolated by cannula filtration. The crystals were washed with pentane (3 × 5 mL) and dried under vacuum providing analytically pure (To^MMgOMe)₂ (0.225 g, 0.514 mmol, 72.2%). ¹H NMR (400 MHz, benzene- d_6): δ 1.16 (s, 18 H, CNCMe₂CH₂O), 3.54 (s, 6 H, CNCMe₂CH₂O), 3.57 (s, 3 H, OMe), 7.29 (t, ³J_{HH} = 7.2 Hz, 1 H, *para*-C₆H₅), 7.49 (t, ³J_{HH} = 7.2 Hz, 2 H, *meta*-C₆H₅), 8.20 (d, ³J_{HH} = 7.2 Hz, 2 H, *ortho*-C₆H₅). ¹³C{¹H} NMR (150 MHz, benzene- d_6): δ 28.71 (CNCMe₂CH₂O), 52.51 (OMe), 66.68 (CNCMe₂CH₂O), 79.10 (CNCMe₂CH₂O), 125.96 (*para*-C₆H₅), 127.47 (*meta*-C₆H₅), 135.29 (*ortho*-C₆H₅), 151.9 (br, *ipso*-C₆H₅), 190.0 (br, CNCMe₂CH₂O). ¹¹B NMR (128 MHz, benzene- d_6): δ -17.6. ¹⁵N NMR (60.6 MHz, benzene- d_6): δ -154.9. IR (KBr, cm⁻¹): 3047 (w), 2965 (s), 2884 (s), 1595 (s, ν_{CN}), 1496 (w), 1465 (m), 1434 (w), 1383 (w), 1365 (m), 1349 (m), 1267 (s), 1198 (s), 1153 (s), 1024 (w), 966 (s), 934 (w), 892 (w), 837 (w), 810 (w), 748 (w), 702 (s), 658 (s), 638 (s). Anal. Calcd. for C₂₂H₃₂BN₃O₄Mg: C, 60.38; H, 7.37; N, 9.60. Found: C, 59.95; H, 6.95; N, 9.77. Mp 275-280 °C (dec).

To^MZnOCHO (6). A 100 mL sealable reaction flask with a Teflon valve was charged with To^MZnH (0.450 g, 1.00 mmol) dissolved in benzene (15 mL). The solution was degassed, the

flask was cooled to $-78\text{ }^{\circ}\text{C}$, and excess, dry CO_2 was condensed into the flask. The reaction was allowed to warm to room temperature, and the resulting mixture was stirred for 30 min. The volatile materials were evaporated, and the white residue was washed with pentane ($3 \times 5\text{ mL}$) and subsequently dried under vacuum to provide analytically pure $\text{To}^{\text{M}}\text{ZnOCHO}$ as a white powder. X-ray quality single crystals were grown from a concentrated toluene solution of $\text{To}^{\text{M}}\text{ZnOCHO}$ at $-35\text{ }^{\circ}\text{C}$ (0.463 g, 0.940, 93.7%). ^1H NMR (600 MHz, benzene- d_6): δ 1.13 (s, 18 H, $\text{CNCMe}_2\text{CH}_2\text{O}$), 3.46 (s, 6 H, $\text{CNCMe}_2\text{CH}_2\text{O}$), 7.37 (m, $^3J_{\text{HH}} = 7.2\text{ Hz}$, 1 H, *para*- C_6H_5), 7.55 (m, $^3J_{\text{HH}} = 7.2\text{ Hz}$, 2 H, *meta*- C_6H_5), 8.31 (d, $^3J_{\text{HH}} = 7.2\text{ Hz}$, 2 H, *ortho*- C_6H_5), 8.76 (s, 1 H, OCHO). $^{13}\text{C}\{^1\text{H}\}$ NMR (150 MHz, benzene- d_6): δ 27.95 ($\text{CNCMe}_2\text{CH}_2\text{O}$), 65.84 ($\text{CNCMe}_2\text{CH}_2\text{O}$), 81.36 ($\text{CNCMe}_2\text{CH}_2\text{O}$), 126.54 (*para*- C_6H_5), 127.37 (*meta*- C_6H_5), 136.37 (*ortho*- C_6H_5), 140.9 (br, *ipso*- C_6H_5), 169.18 (ZnOCHO), 189.8 (br, $\text{CNCMe}_2\text{CH}_2\text{O}$). ^{11}B NMR (192 MHz, benzene- d_6): δ -18.1 . ^{15}N NMR (60.6 MHz, benzene- d_6): δ -160.3 . IR (KBr, cm^{-1}): 3072 (w), 2965 (s), 2923 (w), 1629 (s, ν_{CO}), 1595 (s, ν_{CN}), 1461 (m), 1423 (m), 1389 (m), 1370 (m), 1351 (m), 1307 (s, ν_{CO}), 1273 (s), 1197 (s), 1163 (m), 1124 (m), 1033 (w), 1019 (m), 996 (m), 957 (s), 946 (s), 893 (m), 871 (m), 844 (w), 819 (m). Anal. Calcd. For $\text{C}_{22}\text{H}_{30}\text{BZnN}_3\text{O}_5$: C, 53.63; H, 6.14; N, 8.53. Found C, 53.91; H, 6.19; N, 8.49. Mp $207\text{-}213\text{ }^{\circ}\text{C}$.

$\text{To}^{\text{M}}\text{MgO}_2\text{CSi}(\text{SiHMe}_2)_3$ (7). A 15 mL benzene solution of $\text{To}^{\text{M}}\text{MgSi}(\text{SiHMe}_2)_3$ (0.230 g, 0.376 mmol) was degassed and stirred under CO_2 (1 atm) for 24 h at ambient temperature. The volatile components were evaporated, and the white residue was washed with pentane ($3 \times 5\text{ mL}$). Vacuum drying provided analytically pure $\text{To}^{\text{M}}\text{MgO}_2\text{CSi}(\text{SiHMe}_2)_3$ (0.226 g, 0.344 mmol, 91.5%). ^1H NMR (600 MHz, benzene- d_6): δ 0.48 (d, $^3J_{\text{HH}} = 4.4\text{ Hz}$, 18 H, SiHMe_2), 1.16 (s, 18 H, $\text{CNCMe}_2\text{CH}_2\text{O}$), 3.46 (s, 6 H, $\text{CNCMe}_2\text{CH}_2\text{O}$), 4.45 (sept, $^3J_{\text{HH}} = 4.4\text{ Hz}$, 3 H, SiHMe_2) 7.37 (t, $^3J_{\text{HH}} = 7.2\text{ Hz}$, 1 H, *para*- C_6H_5), 7.55 (t, $^3J_{\text{HH}} = 7.8\text{ Hz}$, 2 H, *meta*- C_6H_5), 8.36 (d, $^3J_{\text{HH}} = 7.2$

Hz, 2 H, *ortho*-C₆H₅). ¹³C{¹H} NMR (150 MHz, benzene-*d*₆): δ -3.65 (SiHMe₂), 28.20 (CNCMe₂CH₂O), 65.87 (CNCMe₂CH₂O), 80.63 (CNCMe₂CH₂O), 126.16 (*para*-C₆H₅), 127.16 (*meta*-C₆H₅), 136.57 (*ortho*-C₆H₅), 191.7 (br, CNCMe₂CH₂O), 202.61 (MgO₂CSi). ¹¹B NMR (192 MHz, benzene-*d*₆): δ -18.1. ²⁹Si NMR (120 MHz, benzene-*d*₆): δ -35.51 (d, ¹J_{SiH} = 169.7 Hz, SiHMe₂), -86.34 (Si(SiHMe₂)₃). ¹⁵N NMR (60.6 MHz, benzene-*d*₆): d -157.4. IR (KBr, cm⁻¹): 3076 (w), 3046 (w), 2965 (s), 2928 (w), 2897 (w), 2101 (s, ν_{SiH}), 1593 (s, ν_{CN}), 1463 (s), 1389 (w), 1366 (s), 1272 (s), 1248 (s), 1195 (s), 1161 (m), 963 (s), 888 (s), 859 (s), 838 (s), 705 (m), 672 (m), 639 (w), 619 (w), 514 (m). Anal. Calcd. for C₂₈H₅₀BSi₄N₃O₅Mg: C, 51.25; H, 7.68; N, 6.40. Found: C, 51.25; H, 7.39; N, 6.46. Mp: 190-193 °C.

HO₂CSi(SiHMe₂)₃ (8). Tetrakis(dimethylsilyl)silane (2.00 g, 7.56 mmol) was dissolved in THF (20 mL). Methyllithium (7.08 mL, 11.3 mmol, 1.6 M in ether) was added. The reaction was stirred at room temperature for 3 days, and then the mixture was poured into a slurry of dry ice in ether. After excess CO₂ had evaporated, the reaction mixture was washed with 2% HCl (3 × 50 mL), and the ether layer was collected and dried over Na₂SO₄. The ether was evaporated to give a colorless oil (0.697 g, 2.78 mmol, 36.9%). ¹H NMR (600 MHz, benzene-*d*₆): δ 0.30 (br, 18 H, SiHMe₂), 4.27 (sept, 3 H, ³J_{HH} = 4.5 Hz, SiHMe₂), 11.67 (br, 1 H, HO₂CSi). ¹³C{¹H} NMR (150 MHz, benzene-*d*₆): δ 195.22 (HO₂CSi), 1.76 (SiHMe₂). ²⁹Si (120 MHz, benzene-*d*₆) δ -26.1 (d, ¹J_{SiH} = 180.6 Hz, SiHMe₂), -85.2 (Si(SiHMe₂)₃). HRMS Calcd. For C₇H₂₂O₂Si₄: (M⁺-1), 249.0619. Found: *m/z*, 249.0974 (M⁺-1).

To^MZnO₂CSi(SiHMe₂)₃ (9). To^MZnEt (0.035 g, 0.073 mmol) and HO₂CSi(SiHMe₂)₃ (0.018 g, 0.073 mmol) were dissolved in benzene and stirred for 30 min. Evaporation of the volatile components under reduced pressure provided a white solid, which was washed with pentane (3 × 5 mL) and dried under vacuum to obtain analytically pure To^MZnO₂CSi(SiHMe₂)₃ (0.047 g,

0.067 mmol, 92.3%). ^1H NMR (400 MHz, benzene- d_6): δ 0.51 (d, $^3J_{\text{HH}} = 4.3$ Hz, 18 H, SiHMe_2), 1.18 (s, 18 H, $\text{CNCMe}_2\text{CH}_2\text{O}$), 3.48 (s, 6 H, $\text{CNCMe}_2\text{CH}_2\text{O}$), 4.46 (sept, $^3J_{\text{HH}} = 4.3$ Hz, 3 H, SiHMe_2), 7.35 (t, $^3J_{\text{HH}} = 7.6$ Hz, 1 H, *para*- C_6H_5), 7.53 (vt, $^3J_{\text{HH}} = 7.4$ Hz, 2 H, *meta*- C_6H_5), 8.31 (d, $^3J_{\text{HH}} = 7.2$ Hz, 2 H, *ortho*- C_6H_5). $^{13}\text{C}\{^1\text{H}\}$ NMR (150 MHz, benzene- d_6): δ -3.75 (SiHMe_2), 28.00 ($\text{CNCMe}_2\text{CH}_2\text{O}$), 65.90 ($\text{CNCMe}_2\text{CH}_2\text{O}$), 81.30 ($\text{CNCMe}_2\text{CH}_2\text{O}$), 126.41 (*para*- C_6H_5), 127.30 (*meta*- C_6H_5), 136.42 (*ortho*- C_6H_5), 141.7 (br, *ipso*- C_6H_5), 190.2 (br, $\text{CNCMe}_2\text{CH}_2\text{O}$), 193.38 (ZnO_2CSi). ^{11}B NMR (192 MHz, benzene- d_6): δ -18.3. ^{29}Si NMR (120 MHz, benzene- d_6): δ -36.36 (d, $^1J_{\text{SiH}} = 169.7$ Hz, $\text{ZnOC}(\text{O})\text{Si}(\text{SiHMe}_2)_3$), -87.38 (s, $\text{ZnOC}(\text{O})\text{Si}(\text{SiHMe}_2)_3$). ^{15}N NMR (60.6 MHz, benzene- d_6): δ -158.0. IR (KBr, cm^{-1}): 3077 (w), 3049 (w), 2963 (s), 2928 (w), 2898 (w), 2103 (s, ν_{SiH}), 1598 (s, ν_{CN}), 1510 (m), 1464 (m), 1368 (m), 1352 (m), 1261 (s), 1196 (m), 961 (m), 907 (m), 838 (s), 813 (s), 777 (w), 704 (m), 687 (m), 639 (m), 624 (w). Anal. Calcd. for $\text{C}_{28}\text{H}_{50}\text{BSi}_4\text{N}_3\text{O}_5\text{Zn}$: C, 48.23; H, 7.23; N, 6.03. Found: C, 47.81; H, 7.38; N, 5.69. Mp: 218-220 °C.

To^MZnCH(SiHMe₂)₃ (10). To^MZnCl (0.100 g, 0.21 mmol) and LiCH(SiHMe₂)₂(THF) (0.043 g, 0.21 mmol) were dissolved in benzene (10 mL) and stirred for 24h at ambient temperature followed by filtration to remove LiCl. Removal of the volatiles under reduced pressure and further washing with pentane (3 × 5 mL) produced analytically pure To^MZnCH(SiHMe₂)₃ as a white solid (0.112 g, 0.19 mmol, 94.1%). ^1H NMR (600 MHz, benzene- d_6): δ -0.94 (s, 1 H, $\text{CH}(\text{SiHMe}_2)_2$), 0.47 (d, $^3J_{\text{HH}} = 3.6$ Hz, 6 H, SiHMe_2), 0.49 (d, $^3J_{\text{HH}} = 3.6$ Hz, 6 H, SiHMe_2), 1.13 (s, 18 H, $\text{CNCMe}_2\text{CH}_2\text{O}$), 3.43 (s, 6 H, $\text{CNCMe}_2\text{CH}_2\text{O}$), 4.86 (sept, $^3J_{\text{HH}} = 3.6$ Hz, 3 H, SiHMe_2), 7.37 (m, $^3J_{\text{HH}} = 7.2$ Hz, 1 H, *para*- C_6H_5), 7.56 (m, $^3J_{\text{HH}} = 7.2$ Hz, 2 H, *meta*- C_6H_5), 8.32 (d, $^3J_{\text{HH}} = 7.2$ Hz, 2 H, *ortho*- C_6H_5). $^{13}\text{C}\{^1\text{H}\}$ NMR (150 MHz, benzene- d_6): δ -10.73 ($\text{CH}(\text{SiHMe}_2)_2$), 1.56 ($\text{CH}(\text{SiHMe}_2)_2$), 3.60 ($\text{CH}(\text{SiHMe}_2)_2$), 28.43 ($\text{CNCMe}_2\text{CH}_2\text{O}$), 66.43

(CNCMe₂CH₂O), 81.04 (CNCMe₂CH₂O), 126.24 (*para*-C₆H₅), 127.22 (*meta*-C₆H₅), 136.53 (*ortho*-C₆H₅), 143 (br, *ipso*-C₆H₅), 191 (br, CNCMe₂CH₂O). ¹¹B NMR (192 MHz, benzene-*d*₆): δ -18.5. ¹⁵N{¹H} NMR (60.6 MHz, benzene-*d*₆): δ -158.3. ²⁹Si (120 MHz, benzene-*d*₆) δ -14.7 (d, ¹J_{SiH} = 175.2 Hz, SiHMe₂). IR (KBr, cm⁻¹): ν 3046 (w), 2965 (s), 2929 (s), 2897 (m), 2851 (m), 2093 (m), 1591 (s), 1463 (m), 1433 (w), 1387 (w), 1367 (m), 1253 (s), 1196 (s), 1159 (m), 1109 (w), 1031(m), 1000 (m), 962 (s), 925 (w), 894 (m), 907 (s), 835 (m), 736 (m), 704 (m), 638 (w). Anal. Calcd. for C₂₆H₄₄BN₃O₃Si₂Zn: C, 53.93; H, 7.66; N, 7.26. Found: C, 53.90; H, 7.81; N, 7.07. Mp: 123-125 °C.

To^MZnHB(C₆F₅)₃. To^MZnH (0.100 g, 0.22 mmol) and B(C₆F₅)₃ (0.114 g, 0.22 mmol) were dissolved in benzene (10 mL) and stirred for 10 min at ambient temperature. Evaporation of the solvent under reduced pressure and pentane washes (3 × 5 mL) produced analytically pure To^MZnHB(C₆F₅)₃ as a white solid (0.197 g, 0.20 mmol, 90.0%). X-ray quality single crystals were grown from a concentrated toluene solution of To^MZnHB(C₆F₅)₃ at -30°C. ¹H NMR (600 MHz, benzene-*d*₆): δ 0.68 (s, 18 H, CNCMe₂CH₂O), 2.73 (br, 1 H, ZnHB(C₆F₅)₃), 3.24 (s, 6 H, CNCMe₂CH₂O), 7.36 (m, ³J_{HH} = 7.2 Hz, 1 H, *para*-C₆H₅), 7.52 (m, ³J_{HH} = 7.2 Hz, 2 H, *meta*-C₆H₅), 8.16 (d, ³J_{HH} = 7.2 Hz, 2 H, *ortho*-C₆H₅). ¹³C{¹H} NMR (150 MHz, benzene-*d*₆): δ 26.32 (CNCMe₂CH₂O), 66.43 (CNCMe₂CH₂O), 81.12 (CNCMe₂CH₂O), 126.98 (*para*-C₆H₅), 127.52 (*meta*-C₆H₅), 136.15 (*ortho*-C₆H₅), 137.27 (C₆F₅), 138.94 (C₆F₅), 139 (br, *ipso*-C₆H₅), 139.92 (C₆F₅), 141.62 (C₆F₅), 147.98 (C₆F₅), 149.55 (C₆F₅), 192 (br, CNCMe₂CH₂O). ¹¹B NMR (192 MHz, benzene-*d*₆): δ -13.2 (br, ZnHB(C₆F₅)₃), -18.6 (To^M). ¹⁹F NMR (544 MHz, benzene-*d*₆): δ -130.3 (*ortho*-C₆F₅), -156.9 (*para*-C₆F₅), -163.0 (*meta*-C₆F₅). ¹⁵N NMR (60 MHz, benzene-*d*₆): δ -163.8. IR (KBr, cm⁻¹): ν 3082 (w), 3054 (w), 2978 (s), 2938 (m), 2906 (w), 2379 (w br), 1645 (m), 1567 (s), 1516 (s), 1467 (s), 1373 (m), 1281 (s), 1166 (s), 1102 (s), 968 (s), 896 (w), 844

(w), 790 (w), 763 (w), 733 (m), 705 (m), 662 (m), 648 (m), 554 (w). Anal. Calcd. for $C_{39}H_{30}B_2N_3O_3F_{15}Zn$: C, 48.76; H, 3.15; N, 4.37. Found: C, 48.77; H, 2.80; N, 4.08. Mp: 164-165 °C.

***C_s*-symmetric [Zn]HB(C₆F₅)₃.** To^MZnSi(SiHMe₂)₃ (0.114 g, 0.17 mmol) and B(C₆F₅)₃ (0.089 g, 0.17 mmol) were dissolved in toluene (10 mL) and stirred for 5 days. The solution was concentrated under reduced pressure and washed with pentane to give a sticky white solid (0.121 g, 0.10 mmol, 59.8%). ¹H NMR (600 MHz, benzene-*d*₆): δ 0.29 (d, 12 H, ³*J* = 4.2 Hz, SiHMe₂), 0.632 (s, 6 H, CNCMe₂CH₂O), 1.09 (s, 6 H, CNCMe₂CH₂O), 1.16 (s, 6 H, CNCMe₂CH₂O), 3.49 (s, 2 H, CNCMe₂CH₂O), 3.65 (d, 2 H, ²*J*_{HH} = 8.40 Hz, CNCMe₂CH₂O), 3.71 (d, 2 H, ²*J*_{HH} = 8.40 Hz, CNCMe₂CH₂O), 4.38 (sept, 2 H, ³*J*_{HH} = 4.2 Hz, SiHMe₂), 7.20 (m, 5 H, C₆H₅). ¹³C{¹H} NMR (150 MHz, benzene-*d*₆): δ -0.78 (SiHMe₂), 25.42 (CNCMe₂CH₂O), 27.58 (CNCMe₂CH₂O), 29.07 (CNCMe₂CH₂O), 62.46 (CNCMe₂CH₂O), 67.01 (CNCMe₂CH₂O), 80.75 (CNCMe₂CH₂O), 83.15 (CNCMe₂CH₂O), 126.24 (*para*-C₆H₅), 129.59 (*meta*-C₆H₅), 132.21 (*ortho*-C₆H₅), 136.78 (br, C₆F₅), 138.47 (br, C₆F₅), 139.78 (br, C₆F₅), 142.6 (br, *ipso*-C₆H₅), 148.57 (br, C₆F₅), 150.19 (br, C₆F₅), 187.9 (br, CNCMe₂CH₂O), 194.9 (br, CNCMe₂CH₂O). ¹¹B NMR (192 MHz, benzene-*d*₆): δ -18.4 (B of To^M), -24.6 (d, ¹*J*_{HB} = 94 Hz, ZnHB(C₆F₅)₃). ¹⁹F NMR (544 MHz, benzene-*d*₆): δ -132.6 (m, 6 F, *ortho*-C₆F₅), -163.0 (m, 3 F, *para*-C₆F₅), -166.1 (m, 6 F, *meta*-C₆F₅). ¹⁵N{¹H} NMR (60.6 MHz, benzene-*d*₆): δ -164.3, -209.9. ²⁹Si (120 MHz, benzene-*d*₆) δ -28.7 (d, ¹*J*_{SiH} = 183.6 Hz, SiHMe₂), -156.3 (s, Si(SiHMe₂)₃). IR (KBr, cm⁻¹): ν 2968 (m), 2392 (br, w), 2097 (m), 1643 (m), 1585 (s), 1511 (s), 1464 (s), 1373 (m), 1277 (m), 1203(w), 1176 (w), 1095 (s), 968 (s), 892 (w), 858 (m), 831 (m), 734 (w), 649 (w). Mp: 60-62.

To^MZnNCO (11). A high pressure NMR tube containing To^MZnN(SiHMe₂)₂ (0.030 g, 0.047 mmol) and C₆D₆ was charged with 60 psi of CO₂. After heating at 120 °C for 7 h, the solution was concentrated under reduced pressure. Recrystallization from toluene at -30 °C gave a white solid (0.023 g, 0.046 mmol, 92.1%). ¹H NMR (600 MHz, benzene-*d*₆): δ 0.954 (s, 18 H, CNCMe₂CH₂O), 3.38 (s, 6 H, CNCMe₂CH₂O), 7.34 (t, 1H, ³J_{HH} = 7.2 Hz, *para*-C₆H₅), 7.51 (t, 2H, ³J_{HH} = 7.6 Hz, *meta*-C₆H₅), 8.20 (d, 2 H, ³J_{HH} = 7.2 Hz, *ortho*-C₆H₅). ¹³C{¹H} NMR (150 MHz, benzene-*d*₆): δ 28.05 (CNCMe₂CH₂O), 65.43 (CNCMe₂CH₂O), 81.19 (CNCMe₂CH₂O), 126.65 (*para*-C₆H₅), 127.41 (*meta*-C₆H₅), 136.18 (*ortho*-C₆H₅), 141.9 (br, *ipso*-C₆H₅), 160.08 (Zn-NCO), 190.7 (br, CNCMe₂CH₂O). ¹¹B NMR (192 MHz, benzene-*d*₆): δ -18.2. ¹⁵N{¹H} NMR (60.6 MHz, benzene-*d*₆): δ -161.37. IR (KBr, cm⁻¹): ν 2961 (s), 2897 (s), 2820 (m), 2234 (s), 1639 (m), 1589 (s), 1451 (m), 1369 (m), 1267 (m), 1177 (m), 968 (m), 830 (w), 741 (m), 705 (s). Anal. Calcd. for C₂₂H₂₉BN₄O₄Zn: C, 53.96; H, 5.97; N, 11.44. Found C, 54.28; H, 5.84; N, 11.35. Mp: 206-208.

Procedures for DOSY (Diffusion-Ordered Spectroscopy) experiment. All the measurements were performed on a Bruker DRX400 spectrometer using a DOSY stimulated spin-echo pulse program with bipolar gradients.⁴⁸ Accurately known concentrations of the species in question, To^MMgSi(SiHMe₂)₃ (**2**) and To^MMgO₂CSi(SiHMe₂)₃ (**7**), and To^MZnO₂CSi(SiHMe₂)₃ (**9**) were determined by integration of resonances corresponding to species of interest and integration of a tetrakis(trimethylsilyl)silane standard of accurately known concentration. The temperature in the NMR probe was preset to 296 K, and the probe was maintained at a constant temperature for each experiment. The delay time in between pulses was set to 5 s in order to ensure the spins are fully relaxed to their ground states. During the experiments, a series of 1D ¹H NMR spectra were acquired at increasing gradient strength. The signal intensity decay was fit by non-linear least

squares regression analysis to eq. 1 to obtain the diffusion coefficient D (Figure S-1, S-2, and S-3).⁴⁹

$$\ln\left(\frac{I}{I_0}\right) = -(\gamma\delta)^2 G^2 \left(\Delta - \frac{\delta}{3}\right) D \quad (1)$$

where I is the observed intensity, D is the diffusion coefficient, γ is the gyromagnetic ratio of the nucleus, δ is the length of the gradient pulse, and Δ is the diffusion time. These experiments were performed on $\text{To}^{\text{M}}\text{MgSi}(\text{SiHMe}_2)_3$ ($6.945 \times 10^{-10} \text{ m}^2/\text{s}$), $\text{To}^{\text{M}}\text{MgO}_2\text{CSi}(\text{SiHMe}_2)_3$ ($6.849 \times 10^{-10} \text{ m}^2/\text{s}$), $\text{To}^{\text{M}}\text{ZnO}_2\text{CSi}(\text{SiHMe}_2)_3$ ($6.429 \times 10^{-10} \text{ m}^2/\text{s}$), and $\text{To}^{\text{M}}_2\text{Mg}$ ($6.00 \times 10^{-10} \text{ m}^2/\text{s}$). From this trend, we conclude that the silane carboxylate compounds are monomeric, as we would expect diffusion constants $< 6 \times 10^{-10} \text{ m}^2/\text{s}$ for dimeric compounds.

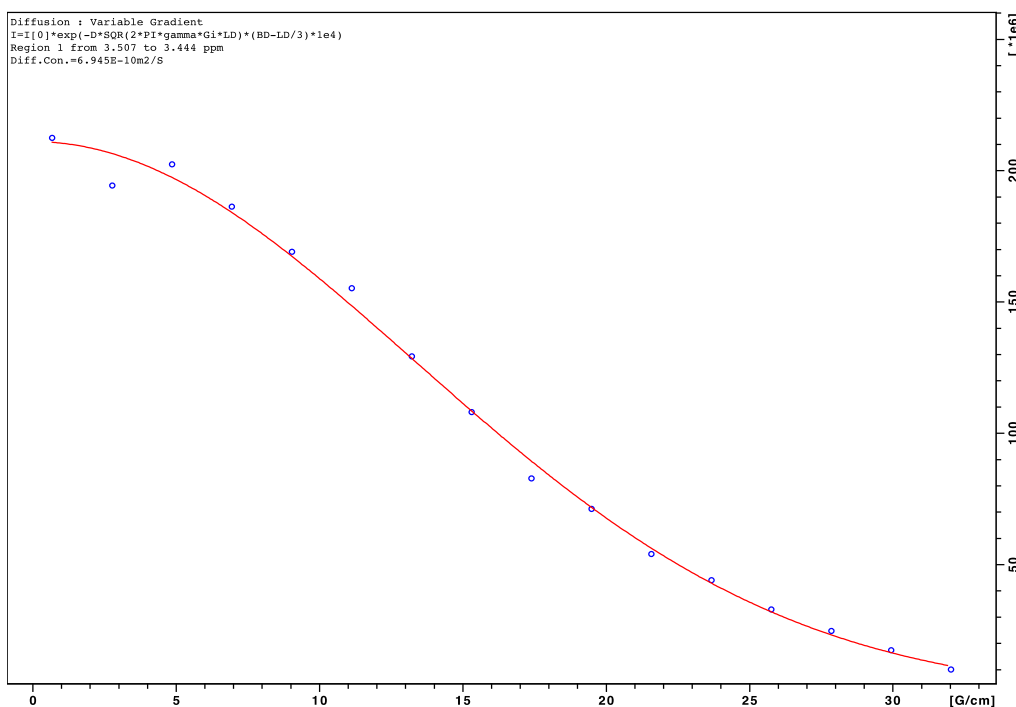


Figure S-1. Plot of intensity versus gradient strength that was used to determine the diffusion coefficient ($6.945 \times 10^{-10} \text{ m}^2/\text{s}$) for $\text{To}^{\text{M}}\text{MgSi}(\text{SiHMe}_2)_3$ (2).

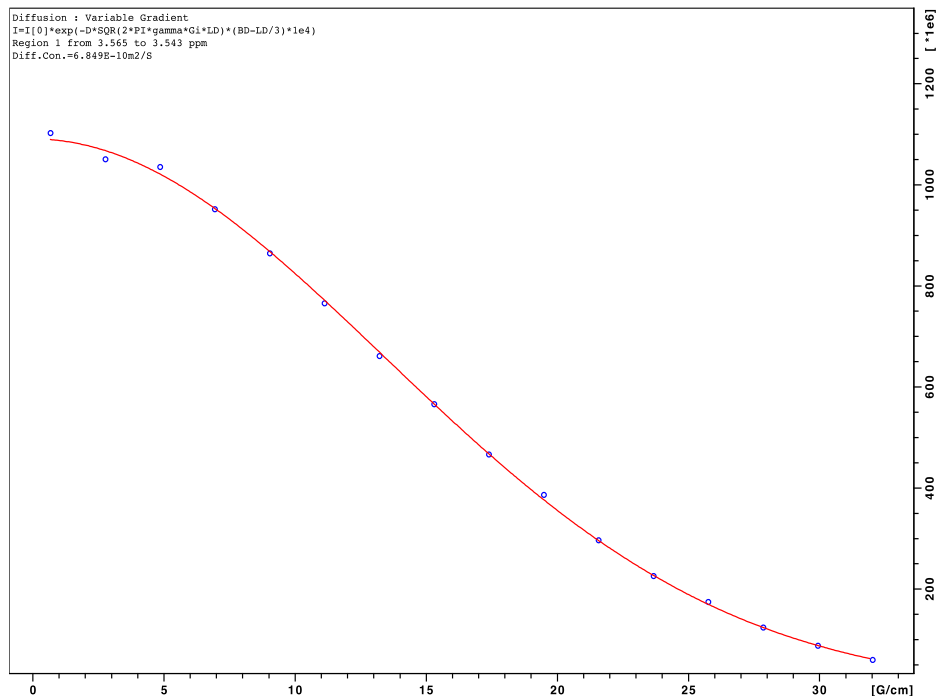


Figure S-2. Plot of intensity versus gradient strength that was used to determine the diffusion coefficient ($6.849 \times 10^{-10} \text{ m}^2/\text{s}$) for $\text{To}^{\text{M}}\text{MgO}_2\text{CSi}(\text{SiHMe}_2)_3$ (**7**).

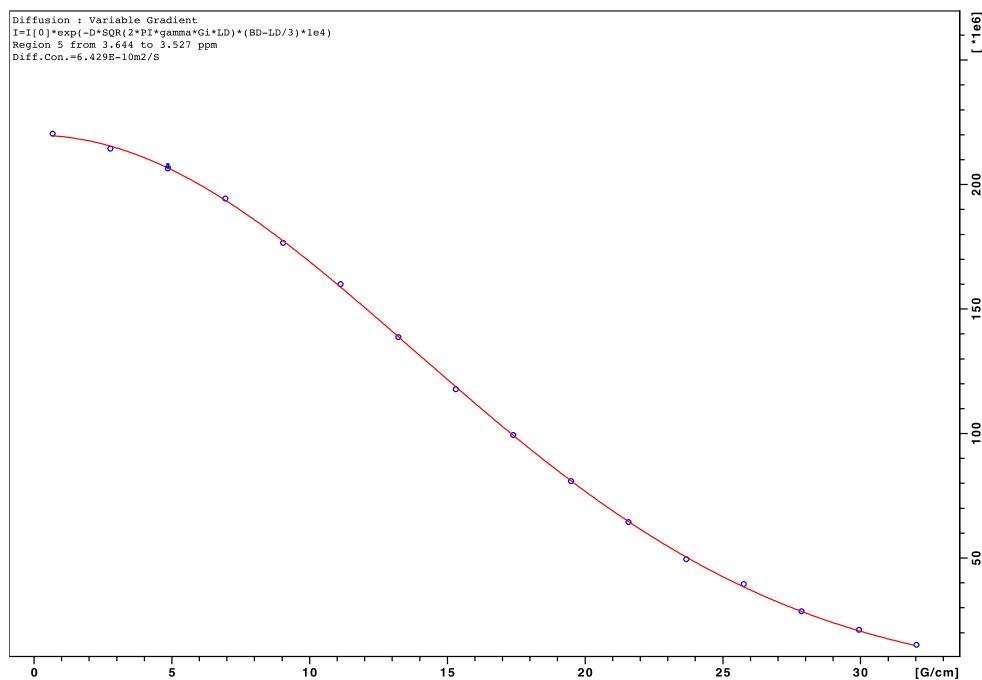


Figure S-3. Plot of intensity versus gradient strength that was used to determine the diffusion coefficient ($6.429 \times 10^{-10} \text{ m}^2/\text{s}$) for $\text{To}^{\text{M}}\text{ZnO}_2\text{CSi}(\text{SiHMe}_2)_3$ (**9**).

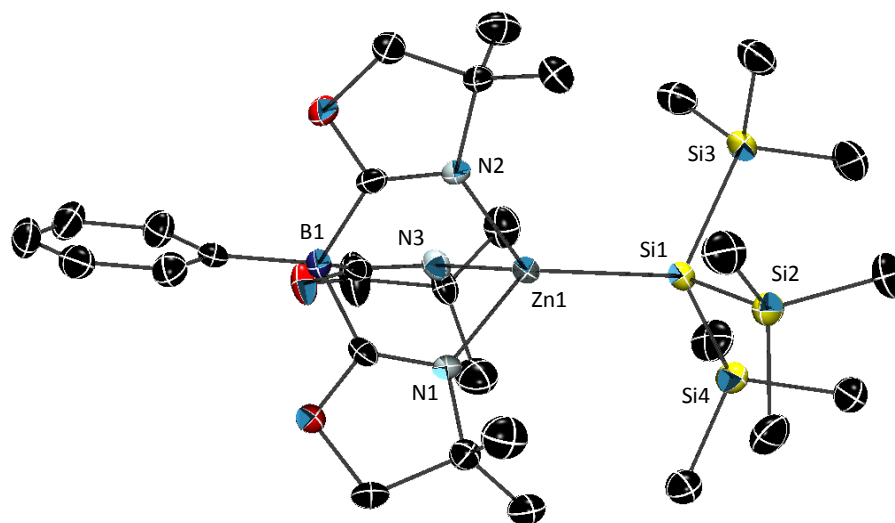


Figure S-4. Rendered thermal ellipsoid plot of $\text{To}^{\text{M}}\text{ZnSi}(\text{SiMe}_3)_3$ with ellipsoids plotted at 35% probability. Hydrogen atoms on the To^{M} and Me groups are not illustrated for clarity.

References

- (1) (a) Marciniak, B. *Hydrosilylation: A comprehensive Review on Recent Advances*, Springer, Berlin, 2009. (b) Mimoun, H.; de Saint Laumer, J. Y.; Giannini, L.; Scopelliti, R.; Floriani, C. *J. Am. Chem. Soc.* **1999**, *121*, 6158–6166. (c) Mastranzo, V. M.; Quintero, L.; Anaya de Parrodi, C.; Juaristi, E.; Walsh, P. J. *Tetrahedron*, **2004**, *60*, 1781–1789. (d) Bette, V.; Mortreux, A.; Savoia, D.; Carpentier, J.-F. *Adv. Synth. Catal.* **2005**, *347*, 289–302. (e) Gerard, S.; Pressel, Y.; Riant, O. *Tetrahedron: Asymmetry*, **2005**, *16*, 1889–1891.
- (2) (a) Mimoun, H. *J. Org. Chem.* **1999**, *64*, 2582–2589. (b) Mukherjee, D.; Thompson, R. R.; Ellern, A.; Sadow, A. D. *ACS Catal.* **2011**, 698–702. (c) Dunne, J. F.; Neal, S. R.; Engelkemier, J.; Ellern, A.; Sadow, A. D. *J. Am. Chem. Soc.* **2011**, *133*, 16782–16785.
- (3) (a) Marschner, C. *Organometallics* **2006**, *25*, 2110–2125. (b) Arnold, J.; Tilley, T. D.; Rheingold, A. L.; Geib, S. J. *Inorg. Chem.* **1987**, *26*, 2106–2109.
- (4) Mukherjee, D.; Ellern, A.; Sadow, A. D. *J. Am. Chem. Soc.* **2010**, *132*, 7582–7583.

- (5) Marschner, C. *Eur. J. Inorg. Chem.* **1998**, 221–226.
- (6) (a) Crystal data for $C_{27}H_{47}BN_3O_3Si_4Zn$ ($To^M Zn-Si(SiHMe_2)_3$) (**1**), $M = 650.22$, monoclinic, $P2_1/c$, $a = 9.449(1) \text{ \AA}$, $b = 27.824(4) \text{ \AA}$, $c = 13.611(2) \text{ \AA}$, $\beta = 93.087(2)^\circ$, $V = 3573.2(8) \text{ \AA}^3$, $T = 173(2) \text{ K}$, $Z = 4$, reflections: 38908 collected, 9895 independent ($R_{int} = 0.0609$), $R_1 = 0.0471$, $wR_2 = 0.1285$ ($I > 2\sigma(I)$). (b) Crystal data for $C_{30}H_{56}BN_3O_3Si_4Zn$ ($To^M Zn-Si(SiMe_3)_3$) (**3**), $M = 695.32$, triclinic, $P-1$, $a = 10.242(4) \text{ \AA}$, $b = 11.576(4) \text{ \AA}$, $c = 17.786 \text{ \AA}$, $\alpha = 92.073(6)^\circ$, $\beta = 106.240(6)^\circ$, $\gamma = 103.685(6)^\circ$, $V = 1955(1) \text{ \AA}^3$, $T = 173(2) \text{ K}$, $Z = 2$, reflections: 15694 collected, 6954 independent ($R_{int} = 0.0690$), $R_1 = 0.0468$, $wR_2 = 0.0783$ ($I > 2\sigma(I)$).
- (7) Arnold, J.; Tilley, T. D.; Rheingold, A. L.; Geib, S. J. *Inorg. Chem.* **1987**, 26, 2106–2109.
- (8) Nanjo, M.; Oda, T.; Mochida, K. *J. Organomet. Chem.* **2003**, 672, 100–108.
- (9) Gaderbauer, W.; Balatoni, I.; Wagner, H.; Baumgartner, J.; Marschner, C. *Dalton Trans.* **2010**, 39, 1598–1603.
- (10) Mukherjee, D.; Ellern, A.; Sadow, A. D. *J. Am. Chem. Soc.* **2012**, 134, 13018–13026.
- (11) Arnold, J.; Tilley, T. D.; Rheingold, A. L.; Geib, S. J. *Inorg. Chem.* **1987**, 26, 2106–2109.
- (12) Crystal data for $C_{56}H_{76}B_2Mg_2N_6O_8$ ($(To^M MgOMe)_2$) (**5**), $M = 1031.47$, monoclinic, $C2/c$, $a = 9.500(2) \text{ \AA}$, $b = 26.648(6) \text{ \AA}$, $c = 22.844(5) \text{ \AA}$, $\beta = 97.235(3)^\circ$, $V = 5753(2) \text{ \AA}^3$, $T = 173(2) \text{ K}$, $Z = 4$, reflections: 29698 collected, 7356 independent ($R_{int} = 0.0326$), $R_1 = 0.0403$, $wR_2 = 0.1001$ ($I > 2\sigma(I)$).
- (13) Mukherjee, D.; Ellern, A.; Sadow, A. D. *J. Am. Chem. Soc.* **2012**, 134, 13018–13026.
- (14) Looney, A.; Han, R.; Gorrell, I. B.; Cornebise, M.; Yoon, K.; Parkin, G.; Rheingold, A. L. *Organometallics* **1995**, 14, 274–288.

- (15) Deacon, G. B.; Phillips, R. J. *Coord. Chem. Rev.* **1980**, *33*, 227–250.
- (16) Sattler, W.; Parkin, G. *J. Am. Chem. Soc.* **2011**, *133*, 9708–9711.
- (17) Crystal data for $C_{22}H_{30}BN_3O_5Zn$ ($To^M ZnOCHO$) (**6**), $M = 492.67$, monoclinic, $P2_1/c$, $a = 11.1030(5)$ Å, $b = 13.3614(5)$ Å, $c = 16.2115(7)$ Å, $\beta = 95.795(1)^\circ$, $V = 2392.7(2)$ Å³, $T = 173(2)$ K, $Z = 4$, reflections: 24027 collected, 5942 independent ($R_{int} = 0.0369$), $R_1 = 0.0307$, $wR_2 = 0.0699$ ($I > 2\sigma(I)$).
- (18) Cordero, B.; Gomez, V.; Platero-Prats, A. E.; Reves, M.; Echeverria, J.; Cremades, E.; Barragan, F.; Alvarez, S. *Dalton Trans.* **2008**, 2832–2838.
- (19) Mukherjee, D.; Ellern, A.; Sadow, A. D. *J. Am. Chem. Soc.* **2010**, *132*, 7582–7583.
- (20) Sattler, W.; Parkin, G. *J. Am. Chem. Soc.* **2011**, *133*, 9708–9711.
- (21) Schrock, R. R.; Tonzetich, Z. J.; Lichtscheidl, A. G.; Müller, P.; Schattenmann, F. J. *Organometallics* **2008**, *27*, 3986–3995.
- (22) Champion, B. K.; Heyn, R. H.; Tilley, T. D. *Inorg. Chem.* **1990**, *29*, 4355–4356.
- (23) Crystal data for $C_{28}H_{50}BSi_4N_3O_5Mg$ ($To^M MgO_2CSi(SiHMe_2)_3$) (**7**), $M = 656.19$, triclinic, $P-1$, $a = 9.0369(13)$ Å, $b = 12.0247(17)$ Å, $c = 18.907(3)$ Å, $\alpha = 80.763(2)^\circ$, $\beta = 78.770(2)^\circ$, $\gamma = 74.162(2)^\circ$, $V = 1926.1(5)$ Å³, $T = 173(2)$ K, $Z = 2$, reflections: 15662 collected, 6779 independent ($R_{int} = 0.0386$), $R_1 = 0.0485$, $wR_2 = 0.1094$ ($I > 2\sigma(I)$).
- (24) Procopio, L. J.; Carroll, P. J.; Berry, D. H. *Organometallics* **1993**, *12*, 3087–3093.
- (25) Champion, B. K.; Heyn, R. H.; Tilley, T. D. *Inorg. Chem.* **1990**, *29*, 4355–4356.
- (26) Brook, A. G.; Yau, L. *J. Organomet. Chem.* **1984**, *271*, 9–14.
- (27) Mukherjee, D.; Ellern, A.; Sadow, A. D. *J. Am. Chem. Soc.* **2010**, *132*, 7582–7583.
- (28) Crystal data for $C_{26}H_{44}BN_3O_3Si_2Zn$ ($To^M Zn-CH(SiHMe_2)_2$) (**10**), $M = 579.00$, triclinic, $P-1$, $a = 10.0581(14)$ Å, $b = 11.0165(16)$ Å, $c = 15.228(2)$ Å, $\alpha = 72.407(2)^\circ$, $\beta = 72.954(2)^\circ$, $\gamma =$

81.770(2)°, $V = 1535.0(4) \text{ \AA}^3$, $T = 173(2) \text{ K}$, $Z = 2$, reflections: 14567 collected, 5756 independent ($R_{\text{int}} = 0.0298$), $R_1 = 0.0388$, $wR_2 = 0.0892$ ($I > 2\sigma(I)$).

- (29) Westerhausen, M.; Rademacher, B.; Schwarz, W. *J. Organomet. Chem.* **1992**, 427, 275-287.
- (30) Mukherjee, D.; Ellern, A.; Sadow, A. D. *J. Am. Chem. Soc.* **2010**, 132, 7582-7583.
- (31) Mukherjee, D.; Ellern, A.; Sadow, A. D. *J. Am. Chem. Soc.* **2010**, 132, 7582-7583.
- (32) Xiao, Y.; Son, D. Y. *Organometallics* **2004**, 23, 4438-4443.
- (33) Mukherjee, D.; Ellern, A.; Sadow, A. D. *J. Am. Chem. Soc.* **2010**, 132, 7582-7583.
- (34) Crystal data for $\text{C}_{22}\text{H}_{29}\text{BN}_4\text{O}_4\text{Zn}$ ($\text{To}^{\text{M}}\text{ZnNCO}$) (**11**), $M = 489.67$, monoclinic, $P2_1/c$, $a = 11.233(3) \text{ \AA}$, $b = 13.350(4) \text{ \AA}$, $c = 16.337(5) \text{ \AA}$, $\beta = 95.027(5)^\circ$, $V = 2440.5(12) \text{ \AA}^3$, $T = 173(2) \text{ K}$, $Z = 4$, reflections: 19498 collected, 4305 independent ($R_{\text{int}} = 0.0419$), $R_1 = 0.0767$, $wR_2 = 0.2274$ ($I > 2\sigma(I)$).
- (35) Cordero, B.; Gomez, V.; Platero-Prats, A. E.; Reves, M.; Echeverria, J.; Cremades, E.; Barragan, F.; Alvarez, S. *Dalton Trans.* **2008**, 2832-2838.
- (36) Ray, U.; Banerjee, D.; Chand, B. G.; Cheng, J.; Lu, T.-H.; Sinha, C. *J. Coord. Chem.* **2005**, 58, 1105-1113.
- (37) (a) Rong, Y.; Parkin, G. *Aust. J. Chem.* **2013**, 66, 1306-1310. (b) Sattler, W.; Parkin, G. *J. Am. Chem. Soc.* **2011**, 133, 9708-9711.
- (38) Sattler, W.; Parkin, G. *J. Am. Chem. Soc.* **2011**, 133, 9708-9711.
- (39) Steward, O. W.; Johnson, J. *J. Organomet. Chem.* **1972**, 46, 97-100.
- (40) Yousef, R. I.; Walfort, B.; Ruffer, T.; Wagner, C.; Schmidt, H.; Herzog, R.; Steinborn, D. *J. Organomet. Chem.* **2005**, 690, 1178-1191.
- (41) Dunne, J. F.; Su, J.; Ellern, A.; Sadow, A. D. *Organometallics* **2008**, 27, 2399-2401.

- (42) Dunne, J. F.; Fulton, D. B.; Ellern, A.; Sadow, A. D. *J. Am. Chem. Soc.* **2010**, *132*, 17680-17683.
- (43) Mukherjee, D.; Ellern, A.; Sadow, A. D. *J. Am. Chem. Soc.* **2010**, *132*, 7582-7583.
- (44) (a) Lambert, J. B.; Pflug, J. L.; Denari, J. M. *Organometallics* **1996**, *15*, 615-625. (b) Kulpinski, P.; Lickiss, P. D.; Stanczyk, W. *Bull. Polish Acad. Sci. Chem.* **1992**, *40*, 21-24.
- (45) Marschner, C. *Eur. J. Inorg. Chem.* **1998**, *1998*, 221-226.
- (46) Bacque, E.; Pillot, J.-P.; Birot, M.; Dunogues, J. *J. Organomet. Chem.* **1998**, *346*, 147-160.
- (47) Prepared according to the procedure reported in Kaking Yan's doctoral thesis, "Synthesis of main group, rare-earth, and d0 metal complexes containing beta-hydrogen."
- (48) (a) Pregosin, P. S.; Martinez-Viviente, E.; Kumar, P. G. A. *Dalton Trans.* **2003**, 4007-4014. (b) Valentini, M.; Pregosin, P. S.; Ruegger, H. *Organometallics* **2000**, *19*, 2551-2555.
- (49) (a) Pregosin, P. S.; Martinez-Viviente, E.; Kumar, P. G. A. *Dalton Trans.* **2003**, 4007-4014. (b) Valentini, M.; Pregosin, P. S.; Ruegger, H. *Organometallics* **2000**, *19*, 2551-2555.

CHAPTER 5: 1,4-HYDROSILYLATION OF α,β -UNSATURATED ESTERS CATALYZED BY A MAGNESIUM HYDRIDOBORATE

Modified from a paper prepared for journal submission

Nicole L. Lampland, Steven R. Neal, Debabrata Mukherjee, Shealyn Schlauderaff, Arkady Ellern, and

Aaron D. Sadow*

Abstract

To^MMgHB(C₆F₅)₃ (**1**, To^M = tris(4,4-dimethyl-2-oxazolinyl)phenylborate) catalyzes the 1,4-hydrosilylation of α,β -unsaturated esters. This magnesium hydridoborate compound is synthesized by the reaction of To^MMgMe, PhSiH₃, and B(C₆F₅)₃, and it persists in solution and in the solid state. Crystallographic characterization revealed tripodal coordination of the HB(C₆F₅)₃ moiety to the six-coordinate magnesium center with a \angle Mg–H–B of 141(3)°. In contrast, the zinc analogue is four-coordinate with a monopodal, nearly linear Zn–H–B structure. The pathway for formation of **1** is proposed to involve the reaction of To^MMgMe and a PhSiH₃/B(C₆F₅)₃ adduct because the other possible intermediates, To^MMgH and To^MMgMeB(C₆F₅)₃, react to give an intractable black solid and To^MMgC₆F₅, respectively. Under catalytic conditions, silyl ketene acetals are isolated in high yield from the addition of hydrosilanes to α,β -unsaturated esters.

Introduction

Catalytic addition reactions, such as hydrosilylation¹ and hydroboration² are important synthetic tools for the reduction of unsaturated moieties. These reactions also provide access to carbon-element, oxygen-element, and nitrogen-element (element (E) = Si, B, H) bonds that allow further elaboration of organic and inorganic substances through cross-coupling³ or oxidation.⁴

Although hydroboranes directly react with some unsaturated substrates, catalyst-controlled

processes can provide highly selective additions. However, transition-metal, main-group metal, and rare earth metal complexes catalyze hydrosilylation and hydroboration through a range of pathways including 2-electron metal-centered redox chemistry, single-electron processes, σ -bond metathesis, or hydride abstraction reactions involving Lewis acid sites. Even a single compound, such as the strong Lewis acid $B(C_6F_5)_3$, can be involved in catalytic additions through a number of pathways. For example, $B(C_6F_5)_3$ catalyzes hydrosilylation of alkenes and carbonyls by action upon silanes,⁵ through Frustrated Lewis Pairs in the presence of a bulky base,⁶ or through its combination with a metal center.⁷

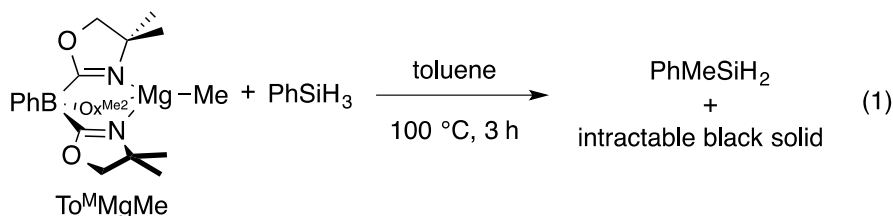
The availability of many pathways creates a challenge to control the selective conversion of carbonyl or olefin functional groups in substrates that contain both moieties. α,β -Unsaturated carbonyls are a particular challenge for reduction as they may be susceptible to 1,2- or 1,4-additions, α - or β -adducts, polymerization, cleavage of the ester, or deoxygenation of the carbonyl. Systems that selectively yield 1,4-addition products have developed many uses in organic chemistry with the resulting silyl ketene acetals being versatile nucleophiles in Mukaiyama aldol and Michael reactions, alkylations, arylations, and haloketone or ketol formations. Since Wilkinson's and Karstedt's catalysts were shown to give selective 1,4-addition of R_3SiH to α,β -unsaturated ketones,⁸ mainly heavy transition metals have been studied for the 1,4-hydrosilylation of α,β -unsaturated esters. Examples using more earth-abundant metals, such as main group or first row transition-metals, are less common and largely limited to Cu systems.⁹ While a few examples of the hydrosilylation of alkenes exist for heavy group 2 metals (Ca, Sr, Ba),¹⁰ $[(DIPP-nacnac)CaH\cdot thf]_2$ ($DIPP-nacnac = ((2,6-iPr_2C_6H_3)NCMe)_2CH$) provides a rare example of a 1,2-hydrosilylation of ketones.¹¹ In the stoichiometric dearomatisation of pyridine and quinoline derivatives utilizing $[(DIPP-nacnac)Mg^nBu]$ and $PhSiH_3$, it was found that $PhSiH_3$

was insufficiently reactive to provides catalytic turnover.¹² To the best of our knowledge, no hydrosilylation systems have been reported with a homogeneous magnesium catalyst.

More often, esters are cleaved under hydrosilylation or hydroboration conditions with 3d transition-metal or main group catalysts.¹³ For example, in a magnesium catalyzed hydroboration of esters, the α,β -unsaturated ester reacts through C–O bond cleavage while the C=C bond is unaffected.¹⁴ Moreover, an important postulated intermediate, $\text{To}^{\text{M}}\text{Mg}\{\text{RO}(\text{H})\text{Bpin}\}$ (To^{M} = tris(4,4-dimethyl-2-oxazoliny)phenylborate); Bpin = boron pinacol ester), apparently does not contain a classical 2-center-2-electron magnesium-hydrogen bond. The $[\text{M}]\{\text{HB}(\text{OR})\text{pin}\}$ motif contains features often associated with $[\text{M}]\{\text{HB}(\text{C}_6\text{F}_5)_3\}$ complexes,¹⁵ and recently, a $\{\text{Nacnac}\}\text{Mg}[\text{HB}(\text{C}_6\text{F}_5)_3]$ complex (Nacnac = $((2,6\text{-}i\text{Pr}_2\text{C}_6\text{H}_3)\text{NCMe})_2\text{CH}$) was reported to catalyze the hydroboration of carbon dioxide.¹⁶ Interestingly, the tris(oxazoliny)borato magnesium catalyst precursors studied do not mediate hydrosilylation of esters under the conditions tested, further suggesting that the boron center provides a key feature for magnesium-catalyzed conversions of oxygenates. Following this idea in the present study, we have incorporated the $[\text{M}]\{\text{HB}(\text{C}_6\text{F}_5)_3\}$ motif into the complex $\text{To}^{\text{M}}\text{MgHB}(\text{C}_6\text{F}_5)_3$ and report the first magnesium-catalyzed hydrosilylation, providing 1,4-hydrosilylation of α,β -unsaturated esters.

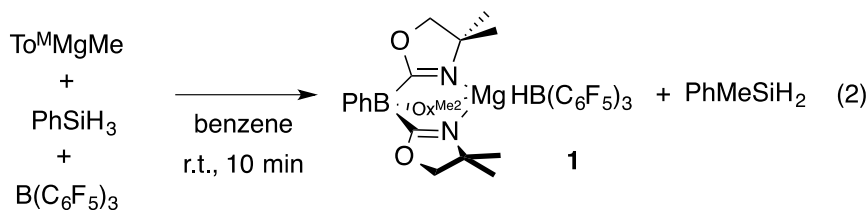
Results and Discussion

The monomeric magnesium methyl $\text{To}^{\text{M}}\text{MgMe}$ reacts slowly with organosilanes to provide Me–Si bond-containing compounds. For example, $\text{To}^{\text{M}}\text{MgMe}$ and PhSiH_3 react in toluene- d_8 to form PhMeSiH_2 over 3 h at 100 °C (eq. 1).



The presumed magnesium-containing product, $\text{To}^{\text{M}}\text{MgH}$, is rapidly converted into an intractable black solid at elevated temperature. This black material is also formed as a byproduct in room temperature reactions of $\text{To}^{\text{M}}\text{MgNHR}$ and hydrosilanes that provide Si–N bond-containing products¹⁷ and in 1:1 reactions of $\text{To}^{\text{M}}\text{MgMe}$ and HBpin that afford Me-Bpin.¹⁸ As a result, the identity of $\text{To}^{\text{M}}\text{MgH}$ is assumed based on reaction stoichiometry and its apparent reactivity as a catalytic intermediate.¹⁹ In order to obtain more evidence for $\text{To}^{\text{M}}\text{MgH}$, we attempted to trap it as a Lewis acid adduct with $\text{B}(\text{C}_6\text{F}_5)_3$.

A mixture of $\text{To}^{\text{M}}\text{MgMe}$, PhSiH_3 , and $\text{B}(\text{C}_6\text{F}_5)_3$ gives PhMeSiH_2 and $\text{To}^{\text{M}}\text{MgHB}(\text{C}_6\text{F}_5)_3$ (**1**, eq. 2). Notably, this reaction occurs at room temperature over 10 min., whereas the direct interaction of $\text{To}^{\text{M}}\text{MgMe}$ and PhSiH_3 requires the forcing conditions noted above. The optimized preparation of **1** involves dropwise addition of $\text{To}^{\text{M}}\text{MgMe}$ to a mixture of PhSiH_3 and $\text{B}(\text{C}_6\text{F}_5)_3$ dissolved in benzene.



The ^1H NMR spectrum of **1** (benzene- d_6 , r.t.) contained one set of oxazoline resonances. This spectral data is consistent with a pseudo- C_{3v} -symmetric structure and tridentate coordination of To^{M} to the magnesium center. In the ^{11}B NMR spectrum, a singlet at -18.2 ppm was assigned to the tris(oxazolinyl)borate ligand, and a doublet at -21.1 ppm ($^1J_{\text{HB}} = 69$ Hz) characterized the $\text{HB}(\text{C}_6\text{F}_5)_3$ anion. The C_6F_5 groups in the anion are equivalent on the NMR

timescale at room temperature, as indicated by the three resonances observed in the ^{19}F NMR spectrum at -134.2 , -156.5 and -161.4 ppm. Based on the single-crystal X-ray diffraction study (see below), ^{19}F NMR spectra were acquired from 298 to 180 K, and these signals did not vary over that temperature range. A single infrared band assigned to the oxazoline ν_{CN} at 1579 cm^{-1} also supported the assignment of tridentate To^{M} -coordination. In addition, B–H bond formation was evidenced by an IR absorption at 2372 cm^{-1} .

A single crystal X-ray diffraction study further supports the identity of compound **1** as $\text{To}^{\text{M}}\text{MgHB}(\text{C}_6\text{F}_5)_3$ and the tridentate coordination mode of the To^{M} ligand (Figure 1). Interestingly, the $\text{Mg}-\text{HB}(\text{C}_6\text{F}_5)_3$ interaction is also tripodal making the magnesium center six-coordinate.

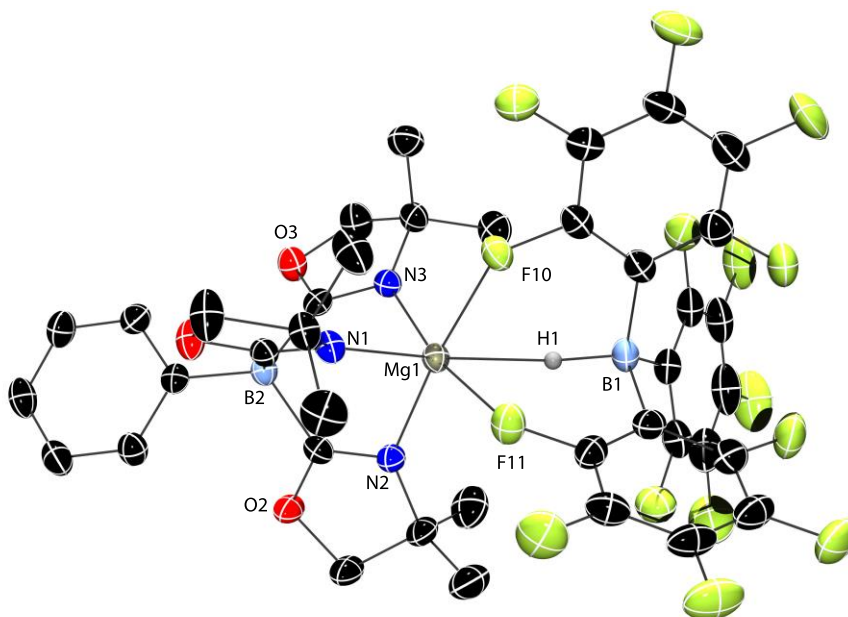


Figure 1. Rendered thermal ellipsoid diagram of $\text{To}^{\text{M}}\text{MgHB}(\text{C}_6\text{F}_5)_3$ (**1**) plotted at 50% probability. Two molecules of toluene and H atoms on To^{M} are not included in the depiction for clarity.

The Mg1–H1 and B1–H1 interatomic distances are 2.06(3) Å and 1.24(3) Å, respectively. The distances are longer than the sum of recently tabulated covalent radii for Mg–H (1.72 Å) and B–H (1.15 Å),²⁰ but the B1–H1 distance is between the bridging (1.33(2) Å) and terminal (1.19(3) Å) B–H distances in diborane²¹ and much longer than in the terminal B–H (1.06(6) Å) of Cp*₂ZrH{HB(C₆F₅)₃}.²² The B–H distance in **1** is also similar to that of the recently reported {Nacnac}CaHB(C₆F₅)₃ (1.16(2) Å).²³ The nonlinear ∠Mg1–H1–B1 (141(3)°) angle is probably strongly influenced by the magnesium-fluorine interactions rather than from a Mg-(η²-H–B) interaction because the Mg1–B1 distance is long (3.15 Å). The Mg1–F10 (2.154(2) Å) and Mg1–F11 (2.188(2) Å) interatomic distances are also slightly longer than the sum of Mg–F covalent radii (Σ(Mg–F) = 1.98 Å). The ∠Mg1–F10–C28 (137.9(2)°) and ∠Mg1–F11–C34 (137.7(2)°) angles are nearly equivalent. Similar to To^MMg{κ³-HB(C₆F₅)₃}, Cp*₂Sm{κ³-HB(C₆F₅)₃} (Cp* = C₅Me₅) contains two Sm–F interactions from the aryl rings and a possible interaction between Sm and the hydride.²⁴ We have also observed tridentate interactions in MC(SiHMe₂)₃{κ³-HB(C₆F₅)₃}THF₂ (M = Ca, Yb),²⁵ and this motif is observed in {Nacnac}Ca{κ³-HB(C₆F₅)₃}.²⁶ Despite the size difference and the bulky tridentate oxazolinylborate ligand, Mg²⁺ still forms an analogous structure to these larger 2⁺ metal cations. In contrast, Cp*₂Sc{HB(C₆F₅)₃}²⁷ and Cp*₂ZrH{HB(C₆F₅)₃}²⁸ are bidentate through two M–F interactions.

Because we had previously synthesized To^MZnH from a variety of routes including reaction of To^MZnOR and hydrosilanes,²⁹ and because zinc and magnesium often provide complementary chemistry toward oxygenates, we attempted the reaction of To^MZnH and B(C₆F₅)₃ and analyzed the resulting single-crystal diffraction data (Figure 2). In contrast to **1**, the zinc analogue To^MZnHB(C₆F₅)₃ contains a tetrahedral zinc center bonded to the hydridoborate

through a nearly linear monodentate $\angle\text{Zn1-H1-B2}$ bridge ($172(2)^\circ$). The Zn1-H1 interaction ($1.73(2)$ Å) is longer than in $\text{To}^{\text{M}}\text{ZnH}$ ($1.52(2)$ Å).³⁰ The B2-H1 distance in $\text{To}^{\text{M}}\text{ZnHB}(\text{C}_6\text{F}_5)_3$ is $1.29(2)$ Å, which is longer than in **1**.

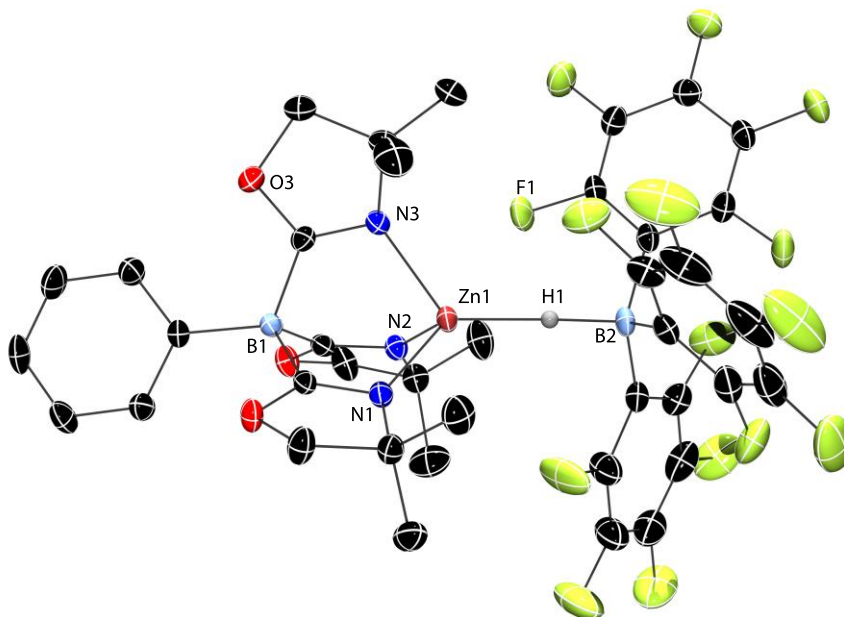
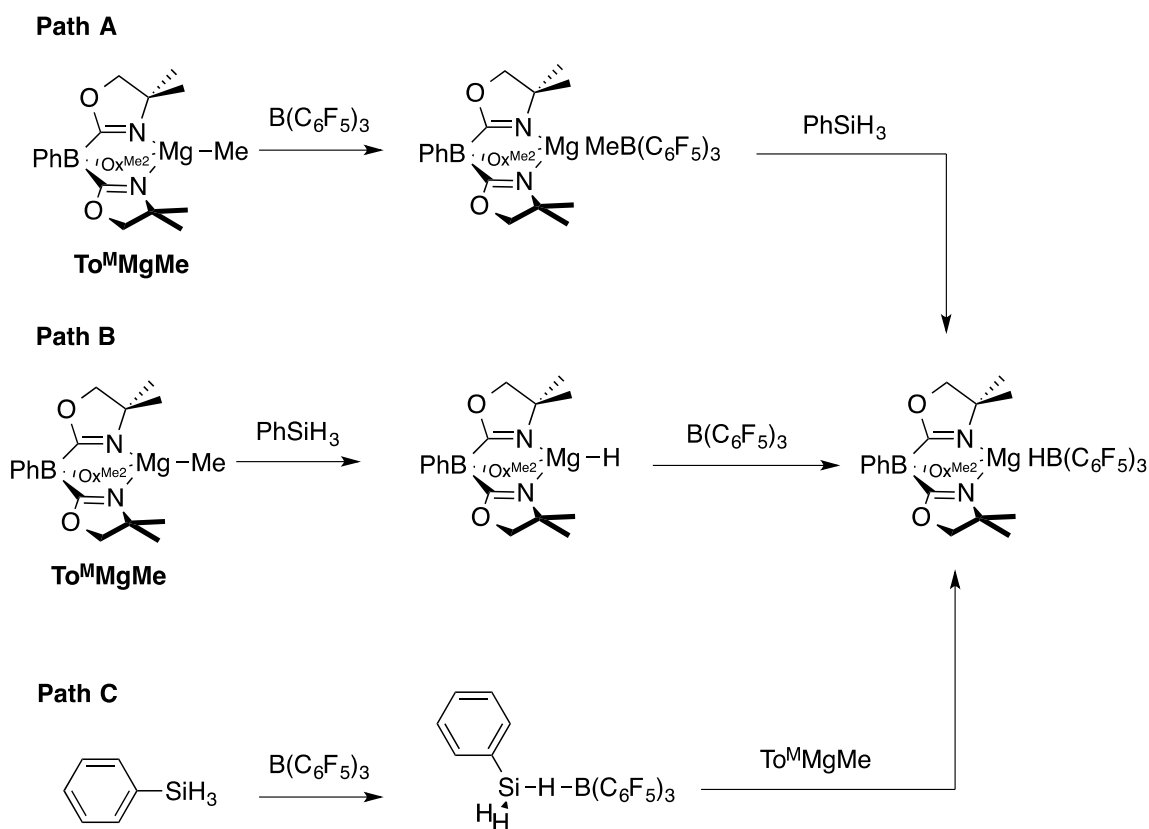


Figure 2. Rendered thermal ellipsoid diagram of $\text{To}^{\text{M}}\text{ZnHB}(\text{C}_6\text{F}_5)_3$ plotted at 50% probability.

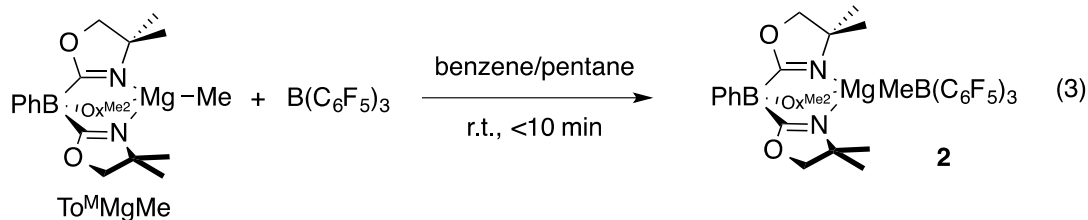
Three plausible pathways were considered for the formation of $\text{To}^{\text{M}}\text{MgHB}(\text{C}_6\text{F}_5)_3$ (Scheme 1). The first one involves the reaction of $\text{To}^{\text{M}}\text{MgMe}$ and $\text{B}(\text{C}_6\text{F}_5)_3$ to give $\text{To}^{\text{M}}\text{MgMeB}(\text{C}_6\text{F}_5)_3$ (**2**), followed by reaction of this species with PhSiH_3 to give PhMeSiH_2 and **1** (Path A). In path B, the reaction of $\text{To}^{\text{M}}\text{MgMe}$ and PhSiH_3 forms $\text{To}^{\text{M}}\text{MgH}$, which is trapped by $\text{B}(\text{C}_6\text{F}_5)_3$ to give **1**. This latter step is suggested by the example of $\text{To}^{\text{M}}\text{ZnH}$ and $\text{B}(\text{C}_6\text{F}_5)_3$. Alternatively, PhSiH_3 and $\text{B}(\text{C}_6\text{F}_5)_3$ could interact to give a transient adduct $[\text{PhH}_2\text{SiHB}(\text{C}_6\text{F}_5)_3]$, and this intermediate reacts with $\text{To}^{\text{M}}\text{MgMe}$ to give the products (Path C). Related adducts have been proposed in $\text{B}(\text{C}_6\text{F}_5)_3$ -catalyzed hydrosilylations with tertiary silanes³¹ and recently a tris(pentafluorophenyl)-boraindene and triethylsilane adduct was spectroscopically

characterized.³² The intermediate $To^M MgMeB(C_6F_5)_3$ in the first pathway is well preceded by $B(C_6F_5)_3$ abstractions of methide anion.³³ Furthermore, $Cp^*_2ZrMe\{\mu-MeB(C_6F_5)_3\}$ is reported to undergo hydrogenation with H_2 to give $Cp^*_2ZrH\{HB(C_6F_5)_3\}$,³⁴ and $(C_5R_5)_2MMe\{\mu-MeB(C_6F_5)_3\}$ ($M = Zr, Hf$; $C_5R_5 = C_5H_5, C_5H_4Me, C_5Me_5$) and silanes react to give $(C_5R_5)_2MH\{HB(C_6F_5)_3\}$.³⁵

Scheme 1. Possible Pathways to $To^M MgHB(C_6F_5)_3$ (**1**).

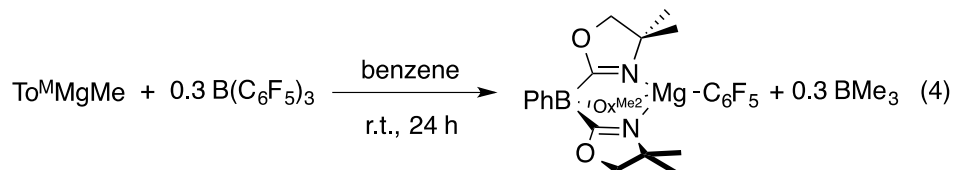


Path **B** is immediately ruled out by the apparent reaction kinetics, which requires forcing conditions for a slower reaction that gives $To^M MgH$. To test the feasibility of Path **A**, the proposed intermediate, $To^M MgMeB(C_6F_5)_3$, is independently synthesized by addition of $B(C_6F_5)_3$ dissolved in pentane to a benzene solution containing $To^M MgMe$ (eq. 3).



The product immediately precipitates giving analytically pure **2**. Reactions in benzene- d_6 or methylene chloride- d_2 provide $\text{To}^{\text{M}}\text{MgMeB}(\text{C}_6\text{F}_5)_3$ as a partially soluble species that may be quickly characterized by solution-phase spectroscopy. However, once solvent is removed and $\text{To}^{\text{M}}\text{MgMeB}(\text{C}_6\text{F}_5)_3$ is isolated, it becomes insoluble in benzene and methylene chloride and only partially redissolves in THF. As in **1**, equivalent oxazoline groups were observed in the ^1H NMR spectrum of in situ generated **2**. The resonance assigned to the $\text{MeB}(\text{C}_6\text{F}_5)_3$ was observed at 1.27 ppm, and this peak correlated in an ^1H - ^{11}B HMBC experiment with a singlet in the ^{11}B NMR spectrum at -15.5 ppm. However as **2** stands in benzene- d_6 , the signals for $\text{To}^{\text{M}}\text{MgMeB}(\text{C}_6\text{F}_5)_3$ decrease as the new species $\text{To}^{\text{M}}\text{MgC}_6\text{F}_5$ forms along with BMe_3 . After 7 h, $\text{To}^{\text{M}}\text{MgMeB}(\text{C}_6\text{F}_5)_3$ is still the major component, but it is completely consumed over 20 h. This transformation occurs more rapidly in methylene chloride- d_2 ($t_{1/2} = 1$ h).

$\text{To}^{\text{M}}\text{MgC}_6\text{F}_5$ is most conveniently prepared and isolated by the reaction of 1 equiv. of $\text{To}^{\text{M}}\text{MgMe}$ and 0.3 equiv. of $\text{B}(\text{C}_6\text{F}_5)_3$ in benzene- d_6 over 24 h (eq. 4).

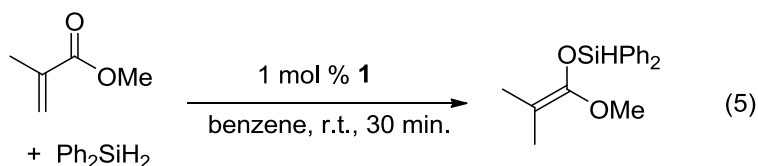


The ^1H NMR spectrum of the crude reaction mixture contained a broad signal at 0.74 ppm assigned to BMe_3 ³⁶ and singlet resonances at 0.98 and 3.38 ppm assigned to the To^{M} ancillary ligand. Two peaks were observed in the ^{11}B NMR spectrum at 86.5 and -18.3 ppm assigned to BMe_3 and To^{M} , respectively. Interestingly, the C_6F_5 group gave rise to five signals in

the ^{19}F NMR spectrum suggesting hindered rotation around the Mg–C bond (note that the phenyl group in the To^{M} ligand generally gives 3 signals). Solid $\text{To}^{\text{M}}\text{MgC}_6\text{F}_5$ was purified from the BMe_3 side product by washing with pentane.

The reaction of $\text{To}^{\text{M}}\text{MgMeB}(\text{C}_6\text{F}_5)_3$ and PhSiH_3 at r.t. in benzene- d_6 gives only starting materials after 30 min. Over ca. 24 h, $\text{To}^{\text{M}}\text{MgMeB}(\text{C}_6\text{F}_5)_3$ undergoes C_6F_5 transfer and PhSiH_3 remains unconsumed. Micromolar-scale reactions in methylene chloride- d_2 yield a mixture of $\text{To}^{\text{M}}\text{MgC}_6\text{F}_5$, BMe_3 , $\text{B}(\text{C}_6\text{F}_5)_3$, and PhSiH_3 after 2 h. On the basis of these observations, $\text{To}^{\text{M}}\text{MgMeB}(\text{C}_6\text{F}_5)_3$ is not an intermediate in the formation of $\text{To}^{\text{M}}\text{MgHB}(\text{C}_6\text{F}_5)_3$. In fact, the aryl group transfer may be a decomposition pathway for $\text{To}^{\text{M}}\text{MgHB}(\text{C}_6\text{F}_5)_3$ in catalytic reactions (see below). Therefore, the currently preferred pathway for the formation of $\text{To}^{\text{M}}\text{MgHB}(\text{C}_6\text{F}_5)_3$ involves methide abstraction by a transient borane-silane adduct (Scheme 1, Path C).

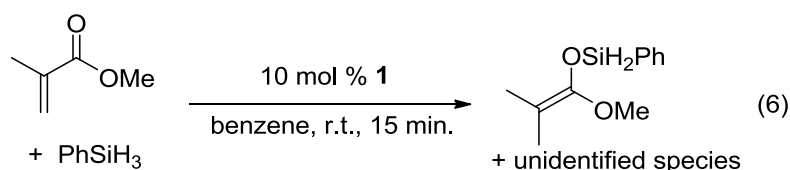
α,β -Unsaturated esters and silanes react in the presence of catalytic amounts of $\text{To}^{\text{M}}\text{MgHB}(\text{C}_6\text{F}_5)_3$ (**1**) through selective 1,4-hydrosilylation. For instance, the reaction of methylmethacrylate, Ph_2SiH_2 , and 1 mol % $\text{To}^{\text{M}}\text{MgHB}(\text{C}_6\text{F}_5)_3$ gives complete conversion of methyl methacrylate after 30 min. in benzene- d_6 , as determined by ^1H NMR spectroscopy (eq. 5).



The isolated silyl ketene acetal contained inequivalent methyl signals at 1.64 and 1.69 ppm in the ^1H NMR spectrum of the product ($(\text{Ph}_2\text{HSiO})(\text{MeO})\text{C}=\text{CMe}_2$), and a new singlet at 5.84 ppm was assigned to the SiH group. The $^{13}\text{C}\{^1\text{H}\}$ NMR spectrum contained a resonance at 150.93 ppm assigned to the acetal carbon, and a ^1H - ^{29}Si HMBC experiment revealed correlations

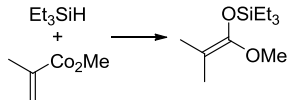
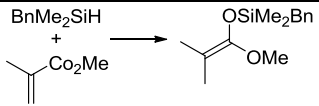
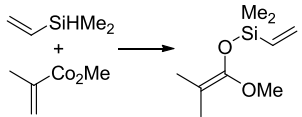
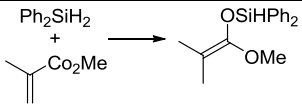
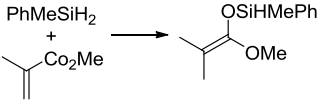
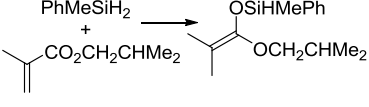
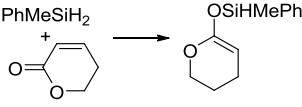
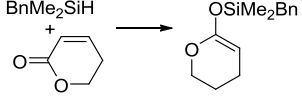
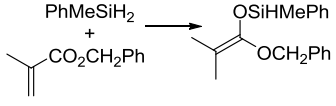
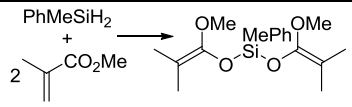
between the SiPh₂ groups in addition to the CMe₂ groups and the silicon-29 resonance at -14.5 ppm.

A range of silyl ketene acetals are prepared using **1** as the hydrosilylation catalyst (Table 1). Secondary and tertiary silanes effectively hydrosilylate methyl methacrylate, and the products are isolated in good yield. In addition, the cyclic α,β -unsaturated ester 5,6-dihydro-2H-pyran-2-one react with PhMeSiH₂ or BnMe₂SiH in the presence of **1**. Although, PhSiH₃ reacts rapidly with methyl methacrylate in the presence of 10 mol % To^MMgHB(C₆F₅)₃ to give the 1,4-hydrosilylation product, ((1-methoxy-2-methylpropenyl)oxy)phenylsilane, as well as unidentified byproducts (eq. 6). Purification of ((1-methoxy-2-methylpropenyl)oxy)phenylsilane from these impurities was not successful.



Free B(C₆F₅)₃ might be present in the reaction mixture as a result of its dissociation from **1**, so its action as a catalyst on silanes and α,β -unsaturated esters was probed. In the presence of 10 mol % B(C₆F₅)₃, methyl methacrylate reacts with phenylsilane instantaneously in benzene-*d*₆ to produce some of the unidentified peaks in the ¹H NMR spectrum for the reaction catalyzed by **1**; however, resonances for ((1-methoxy-2-methylpropenyl)oxy)phenylsilane were not observed. Furthermore, ¹H NMR spectra of mixtures of the esters and silanes studied in Table 1 with 10 mol % B(C₆F₅)₃ contained signals corresponding to several unidentified species as the major products likely resulting from ester cleavage,³⁷ and the signals assigned to the corresponding hydrosilylation products were minor (although the amounts varied between primary, secondary, and tertiary silanes). Thus, the catalytic hydrosilylation is not mediated by trace contamination of B(C₆F₅)₃. However, the presence of small amounts of B(C₆F₅)₃ likely produces the side products

Table 1. Hydrosilylation of α,β -unsaturated esters catalyzed by $\text{To}^{\text{M}}\text{MgHB}(\text{C}_6\text{F}_5)_3$

Reaction	catalyst loading (mol %)	Time (h)	% Yield (isolated)
	1	0.5	98
	1	0.5	99
	1	0.5	92
	1	0.5	96
	1	7 ^b	97
	2.5	8	41
	10	5	80
	1	0.5 ^c	83
	2.5	4	99
	5	12 ^d	32

^aReaction conditions: silane:acrylate = 1:1, benzene, r.t.; ^b60 °C; ^c35 °C; ^d80 °C.

observed in catalytic reactions of phenylsilane and methyl methacrylate mediated by **1**. These results also suggest that the transient silane-borane adducts postulated in $B(C_6F_5)_3$ -catalyzed carbonyl hydrosilylation are not central to the **1**-catalyzed hydrosilylation. In addition, $To^M MgHB(C_6F_5)_3$ reacts with neat methyl methacrylate to produce an insoluble polymer. This polymerization is observed as a competing reaction pathway with excess methyl methacrylate and with isobutyl methacrylate, and it accounts for the lower isolated yields when excess methacrylate is used.

A number of experiments further test the key features of the catalyst structure and the reaction pathway. First, a series of $To^M MgX$ compounds ($X = Me, C_6F_5, MeB(C_6F_5)_3, B(C_6F_5)_4$) were investigated as precatalysts for hydrosilylation of methyl methacrylate. A catalytic amount of the precursor $To^M MgMe$ reacts instantaneously with methyl methacrylate and $PhMeSiH_2$ in benzene- d_6 to give insoluble materials likely resulting from polymerization. Even though some of the silane is consumed in the reaction, neutral $To^M MgMe$ is not a viable hydrosilylation catalyst. 1H NMR spectra of a catalytic mixture of methyl methacrylate, $PhMeSiH_2$ and 10 mol % $To^M MgMeB(C_6F_5)_3$ shows only resonances assigned to methyl methacrylate and $PhMeSiH_2$, and signals associated with the hydrosilylation product were not detected. $To^M MgMeB(C_6F_5)_3$ is converted to $To^M MgC_6F_5$ under these conditions, and independent experiments show that $To^M MgC_6F_5$ is also not catalytically active. Ionic magnesium compounds were tested next. The reaction of $To^M MgMe$ and $[Ph_3C][B(C_6F_5)_4]$ in benzene- d_6 at room temperature gives $[To^M Mg][B(C_6F_5)_4]$ as a precipitate after 15 min. The reactants $PhMeSiH_2$ and methyl methacrylate are unchanged after 2 d at 80 °C in the presence of 10 mol % $[To^M Mg][B(C_6F_5)_4]$. From these experiments, we conclude that the $Mg\{\kappa^3-HB(C_6F_5)_3\}$ moiety is important for catalysis.

Under pseudo-first order conditions (using toluene- d_8 as solvent) with excess methylmethacrylate, the half-life for the disappearance of Ph_2SiH_2 is ~ 3 min. at 64°C and the silane reagent is completely consumed. However, the methacrylate polymerization side-reaction interferes with kinetic measurements under these conditions. In the presence of excess Ph_2SiH_2 with respect to the methacrylate, zero-order, first-order, and second-order kinetic plots of methyl methacrylate concentration vs. time are non-linear, and complete conversion is not reached. The decrease in catalytic rate is even more prominent in methylene-chloride- d_2 than in benzene- d_6 . In benzene- d_6 , the one-to-one addition of methyl methacrylate and PhMeSiH_2 is catalyzed by 10 mol% $\text{To}^{\text{M}}\text{MgHB}(\text{C}_6\text{F}_5)_3$ in less than 10 min. while equivalent reaction conditions in methylene chloride- d_2 give only 50% conversion after 24 h. Furthermore, the only To^{M} -containing ^1H NMR resonances observed in the catalytic reaction mixture (in methylene chloride- d_2) were those assigned to $\text{To}^{\text{M}}\text{MgC}_6\text{F}_5$. On the basis of faster conversion of $\text{To}^{\text{M}}\text{MgMeB}(\text{C}_6\text{F}_5)_3$ to $\text{To}^{\text{M}}\text{MgC}_6\text{F}_5$ in methylene chloride than in benzene, the lack of activity of $\text{To}^{\text{M}}\text{MgC}_6\text{F}_5$ as a hydrosilylation catalyst, and the lower catalytic activity in methylene chloride than in benzene, we suggest that catalyst deactivation occurs through a $[\text{Mg}]\text{-C-B}(\text{C}_6\text{F}_5)_3$ -containing species.

Conclusion

The silicon-carbon bond forming step involved in the synthesis of the catalyst $\text{To}^{\text{M}}\text{MgHB}(\text{C}_6\text{F}_5)_3$ may be related to the catalytic 1,4-hydrosilylation bond forming steps. For example, an adduct of the type $\text{To}^{\text{M}}\text{Mg}(\text{acrylate})^+$ or an enolate $\text{To}^{\text{M}}\text{MgOC}(\text{OMe})\text{CMe}_2$ might react with $\text{B}(\text{C}_6\text{F}_5)_3$ -activated silane to give the product. However, another, not yet identified, pathway might also be operative. Although $\text{To}^{\text{M}}\text{MgHB}(\text{C}_6\text{F}_5)_3$ reacts with methyl methacrylate, the resulting compound was not isolable. Our current efforts involve new catalysts that contain

the $[\text{HB}(\text{C}_6\text{F}_5)_3]^-$ motif that are more resistant to decomposition to facilitate kinetic studies and chiral ligands that may provide enantioselective hydrosilylations.

In this hydrosilylation reaction, a possible Mg–O bond-containing species, either as a catalytic intermediate or decomposition product, might have been assumed to inhibit the catalytic conversion based on the perceived bond strength. In fact $\text{To}^{\text{M}}\text{MgOR}$ species do not react with organosilanes, at least under the conditions we have explored.³⁸ In contrast to this expectation, the apparent catalyst decomposition involves aryl-group transfer to magnesium to give $\text{To}^{\text{M}}\text{MgC}_6\text{F}_5$. That is, in the presence of oxygenates, a magnesium catalyst is deactivated by magnesium-carbon bond formation rather than magnesium-oxygen bond formation. Moreover, the overall reaction of oxygenates (α,β -unsaturated esters) with oxophilic silicon substrates in the presence of an oxophilic magnesium catalytic center gives the first example of a magnesium-catalyzed hydrosilylation in which the $\text{Mg}\{\kappa^3\text{-HB}(\text{C}_6\text{F}_5)_3\}$ moiety appears to play a crucial role.

Experimental

General Procedures. All reactions were performed under a dry argon atmosphere using standard Schlenk techniques or under a nitrogen atmosphere in a glovebox, unless otherwise indicated. Benzene, toluene, pentane, diethyl ether, and tetrahydrofuran were dried and deoxygenated using an IT PureSolv system. THF- d_8 , methylene chloride- d_2 , and benzene- d_6 were heated to reflux over Na/K alloy and vacuum-transferred. $\text{To}^{\text{M}}\text{MgMe}$,³⁹ $\text{To}^{\text{M}}\text{ZnH}$,⁴⁰ $\text{B}(\text{C}_6\text{F}_5)_3$,⁴¹ and PhSiH_3 ⁴² were synthesized according to literature procedures. PhMeSiH_2 and BnMe_2SiH were synthesized according to the literature procedure for PhSiH_3 . Vinyl dimethylsilane, diphenylsilane, and triethylsilane were purchased from Gelest and purified by distillation under a dry argon atmosphere prior to use. Methylmethacrylate, benzyl

methacrylate, and isobutyl methacrylate were purchased from Alfa Aesar and degassed by three freeze-pump-thaw cycles prior to use. 5,6-Dihydro-2*H*-pyran-2-one was purchased from Acros and degassed by three freeze-pump-thaw cycles prior to use. ^1H , $^{13}\text{C}\{^1\text{H}\}$, and ^{11}B NMR spectra were collected on a Bruker AVII 600 spectrometer, a Bruker DRX-400 spectrometer, or a MR-400 spectrometer. ^{29}Si INEPT and ^1H - ^{29}Si HMBC spectra were collected on a Bruker AVII 600 spectrometer. ^{15}N chemical shifts were determined by ^1H - ^{15}N HMBC experiments on a Bruker AVII 600 spectrometer. ^{15}N chemical shifts were originally referenced to an external liquid NH_3 standard and recalculated to the CH_3NO_2 chemical shift scale by adding -381.9 ppm. Elemental analyses were performed using a Perkin-Elmer 2400 Series II CHN/S by the Iowa State Chemical Instrumentation Facility. X-ray diffraction data was collected on a Bruker APEX II diffractometer.

To^MMgHB(C₆F₅)₃ (1). A solution of To^MMgMe (0.134 g, 0.32 mmol) dissolved in benzene was added in a dropwise fashion into a benzene solution containing PhSiH₃ (0.069 g, 0.64 mmol) and B(C₆F₅)₃ (0.162 g, 0.32 mmol). A white precipitate formed as the reaction mixture stirred for 30 min. The precipitate settled after centrifugation, and the supernatant was decanted. The white solid was washed with pentane (3 × 5 mL) and dried under vacuum, providing analytically pure To^MMgHB(C₆F₅)₃ (0.286 g, 0.31 mmol, 97.6%). Once isolated, To^MMgHB(C₆F₅)₃ is soluble in benzene or toluene, and X-ray quality single crystals were grown from a concentrated toluene solution at -30 °C. ^1H NMR (600 MHz, benzene-*d*₆): δ 0.82 (s, 18 H, CNCMe₂CH₂O), 2.72 (br q, 1 H, MgHB(C₆F₅)₃), 3.30 (s, 6 H, CNCMe₂CH₂O), 7.38 (m, $^3J_{\text{HH}} = 7.2$ Hz, 1 H, *para*-C₆H₅), 7.56 (m, $^3J_{\text{HH}} = 7.6$ Hz, 2 H, *meta*-C₆H₅), 8.25 (d, $^3J_{\text{HH}} = 7.2$ Hz, 2 H, *ortho*-C₆H₅). $^{13}\text{C}\{^1\text{H}\}$ NMR (150 MHz, THF-*d*₈): δ 27.35 (CNCMe₂CH₂O, overlapping with THF-*d*₈), 66.13 (CNCMe₂CH₂O, overlapping with THF-*d*₈), 79.28 (CNCMe₂CH₂O), 130.24 (*para*-C₆H₅), 133.26

(*meta*-C₆H₅), 134.79 (C₆F₅), 135.74 (C₆F₅), 136.81 (C₆F₅), 137.49 (*ortho*-C₆H₅), 138.41 (C₆F₅), 142 (br, *ipso*-C₆H₅), 147.78 (C₆F₅), 149.35 (C₆F₅), 191 (CNCMe₂CH₂O). ¹¹B NMR (192 MHz, benzene-*d*₆): δ -18.2 (To^M), -21.1 (d, ¹J_{HB} = 69 Hz, MgHB(C₆F₅)₃). ¹⁹F NMR (544 MHz, benzene-*d*₆): δ -134.2 (*ortho*-C₆F₅), -156.5 (*para*-C₆F₅), -161.4 (*meta*-C₆F₅). ¹⁵N NMR (60 MHz, benzene-*d*₆): δ -162. IR (KBr, cm⁻¹): ν 2976 (s), 2937 (s), 2372 (w br, BH), 1642 (m), 1579 (s), 1511 (s), 1459 (s br), 1373 (m), 1271 (m), 1199 (m), 1180 (m), 1161 (m), 1087 (s), 965 (s br), 843 (w), 804 (w), 735 (w), 705 (w). Anal. Calcd. for C₃₉H₃₀B₂F₁₅MgN₃O₃: C, 50.94; H, 3.29; N, 4.57. Found C, 51.38; H, 3.41; N, 4.31. Mp: 166-167 °C.

To^MZnHB(C₆F₅)₃. To^MZnH (0.100 g, 0.22 mmol) and B(C₆F₅)₃ (0.114 g, 0.22 mmol) were dissolved in benzene (10 mL) and stirred for 10 min at ambient temperature. Evaporation of the solvent under reduced pressure and pentane washes (3 × 5 mL) produced analytically pure To^MZnHB(C₆F₅)₃ as a white solid (0.197 g, 0.20 mmol, 90.0%). X-ray quality single crystals were grown from a concentrated toluene solution of To^MZnHB(C₆F₅)₃ at -30°C. ¹H NMR (600 MHz, benzene-*d*₆): δ 0.68 (s, 18 H, CNCMe₂CH₂O), 2.73 (br, 1 H, ZnHB(C₆F₅)₃), 3.24 (s, 6 H, CNCMe₂CH₂O), 7.36 (m, ³J_{HH} = 7.2 Hz, 1 H, *para*-C₆H₅), 7.52 (m, ³J_{HH} = 7.2 Hz, 2 H, *meta*-C₆H₅), 8.16 (d, ³J_{HH} = 7.2 Hz, 2 H, *ortho*-C₆H₅). ¹³C{¹H} NMR (150 MHz, benzene-*d*₆): δ 26.32 (CNCMe₂CH₂O), 66.43 (CNCMe₂CH₂O), 81.12 (CNCMe₂CH₂O), 126.98 (*para*-C₆H₅), 127.52 (*meta*-C₆H₅), 136.15 (*ortho*-C₆H₅), 137.27 (C₆F₅), 138.94 (C₆F₅), 139 (br, *ipso*-C₆H₅), 139.92 (C₆F₅), 141.62 (C₆F₅), 147.98 (C₆F₅), 149.55 (C₆F₅), 192 (br, CNCMe₂CH₂O). ¹¹B NMR (192 MHz, benzene-*d*₆): δ -13.2 (br, ZnHB(C₆F₅)₃), -18.6 (To^M). ¹⁹F NMR (544 MHz, benzene-*d*₆): δ -163.0 (*meta*-C₆F₅), -156.9 (*para*-C₆F₅), -130.3 (*ortho*-C₆F₅). ¹⁵N NMR (60 MHz, benzene-*d*₆): δ -163.8. IR (KBr, cm⁻¹): ν 3082 (w), 3054 (w), 2978 (s), 2938 (m), 2906 (w), 2379 (w br), 1645 (m), 1567 (s), 1516 (s), 1467 (s), 1373 (m), 1281 (s), 1166 (s), 1102 (s), 968 (s), 896 (w), 844

(w), 790 (w), 763 (w), 733 (m), 705 (m), 662 (m), 648 (m), 554 (w). Anal. Calcd. for $C_{39}H_{30}B_2N_3O_3F_{15}Zn$: C, 48.76; H, 3.15; N, 4.37. Found: C, 48.77; H, 2.80; N, 4.08. Mp: 164-165 °C.

To^MMgMeB(C₆F₅)₃ (2). A pentane solution of B(C₆F₅)₃ (0.031 g, 0.059 mmol) was added to a concentrated solution of To^MMgMe (0.025 g, 0.059 mmol) in benzene. The reaction mixture was stirred for 15 min. and then allowed to stand for 30 min. as a white precipitate formed. The solvent was decanted, and the residue washed with pentane (3 × 5 mL) and then dried under vacuum to provide To^MMgMeB(C₆F₅)₃ (0.046 g, 0.049 mmol, 83.2%). When generated in situ, To^MMgMeB(C₆F₅)₃ is soluble in benzene-*d*₆ and CD₂Cl₂ and NMR spectra can be obtained, with the exception of ¹³C NMR spectral data due to the rate of conversion from To^MMgMeB(C₆F₅)₃ to To^MMgC₆F₅ being too fast. However, once solvent is removed and To^MMgMeB(C₆F₅)₃ isolated, it becomes insoluble in benzene and methylene chloride and only partially redissolves in THF-*d*₈. Though benzene, methylene chloride, and THF solvents were attempted, ¹³C NMR spectral data could not be obtained due to the low solubility of To^MMgMeB(C₆F₅)₃ and its spontaneous conversion to To^MMgC₆F₅. ¹H NMR (600 MHz, benzene-*d*₆): δ 0.79 (s, 18 H, CNCMe₂CH₂O), 1.27 (br s, 3 H, MgMeB(C₆F₅)₃), 3.23 (s, 6 H, CNCMe₂CH₂O), 7.35 (br, 1 H, *para*-C₆H₅), 7.51 (br, 2 H, *meta*-C₆H₅), 8.09 (br, 2 H, *ortho*-C₆H₅). ¹¹B NMR (192 MHz, benzene-*d*₆): δ -15.5 (MeB(C₆F₅)₃), -18.5 (To^M). ¹⁹F NMR (544 MHz, benzene-*d*₆): δ -134.8 (*ortho*-C₆F₅), -159.1 (*para*-C₆F₅), -163.4 (*meta*-C₆F₅). ¹⁵N NMR (60 MHz, benzene-*d*₆): δ -162.2. IR (KBr, cm⁻¹): ν 3037 (w), 2973 (s), 2935 (m), 1636 (m), 1541 (s), 1508 (s), 1458 (s), 1437 (s), 1374 (m), 1267 (m), 1202 (m), 1088 (s), 965 (s), 842 (w), 803 (w), 738 (w), 683 (w). Anal. Calcd. for C₄₀H₃₂B₂F₁₅MgN₃O₃: C, 51.46; H, 3.45; N, 4.50. Found C, 51.09; H, 3.20; N, 4.01. Mp: 205-207 °C (dec.).

To^MMgC₆F₅. B(C₆F₅)₃ (0.024 g, 0.047 mmol) and 1 equiv. of To^MMgMe (0.020 g, 0.047 mmol) were dissolved in methylene chloride, and the reaction mixture was stirred for 24 h, and then filtered. Solvent was removed under reduced pressure. The white solid was washed with pentane (3 × 5 mL) to afford To^MMgC₆F₅ (0.012 g, 0.021 mmol, 44.4%). ¹H NMR (600 MHz, benzene-*d*₆): δ 0.98 (s, 18 H, CNCMe₂CH₂O), 3.39 (s, 6 H, CNCMe₂CH₂O), 7.37 (m, ³J_{HH} = 7.2 Hz, 1 H, *para*-C₆H₅), 7.55 (m, ³J_{HH} = 7.6 Hz, 2 H, *meta*-C₆H₅), 8.25 (d, ³J_{HH} = 7.2 Hz, 2 H, *ortho*-C₆H₅). ¹³C{¹H} NMR (150 MHz, benzene-*d*₆): δ 28.08 (CNCMe₂CH₂O), 65.91 (CNCMe₂CH₂O), 80.81 (CNCMe₂CH₂O), *para*-C₆H₅ and *meta*-C₆H₅ overlapping with benzene-*d*₆, 136.41 (*ortho*-C₆H₅), C₆F₅ too low intensity to be observed, 148.29 (br, *ipso*-C₆H₅), 193.08 (br, CNCMe₂CH₂O). ¹¹B NMR (192 MHz, benzene-*d*₆): δ -18.3. ¹⁹F NMR (544 MHz, benzene-*d*₆): δ -110.5 (C₆F₅), -150.3 (C₆F₅), -155.8 (C₆F₅), -160.7 (C₆F₅), -162.9 (C₆F₅). ¹⁵N NMR (60 MHz, benzene-*d*₆): δ -157.7. IR (KBr, cm⁻¹): ν 2965 (s), 2926 (s), 2884 (m), 2853 (m), 1594 (s), 1510 (m), 1463 (s), 1366 (m), 1350 (w), 1268 (s), 1197 (m), 1152 (m), 1117 (w), 1086 (m), 967 (s), 892 (w), 839 (w), 810 (m), 746 (w), 703 (m). Anal. Calcd. for C₂₇H₂₉BF₅MgN₃O₃: C, 56.53; H, 5.10; N, 7.33. Found C, 57.01; H, 5.58; N, 6.89. Mp: 195-197 °C.

[To^MMg][B(C₆F₅)₄]. To^MMgMe (0.026 g, 0.062 mmol) and [Ph₃C][B(C₆F₅)₄] (0.057 g, 0.062 mmol) were dissolved in benzene (10 mL) and stirred for 30 min. to obtain a white precipitate, which was then isolated by decantation of the top liquid. Washing with benzene (3×5 mL) followed by drying under vacuum provided [To^MMg][B(C₆F₅)₄] (0.064 g, 0.059 mmol, 94.9%). Solution-phase characterization is given in THF-*d*₈ of the THF-*d*₈ adduct. ¹H NMR (600 MHz, THF-*d*₈): δ 1.28 (s, 18 H, CNCMe₂CH₂O), 3.90 (s, 6 H, CNCMe₂CH₂O), 7.01 (br, 1 H, *para*-C₆H₅), 7.07 (br, 2 H, *meta*-C₆H₅), 7.64 (br, 2 H, *ortho*-C₆H₅). ¹³C{¹H} NMR (150 MHz, THF-*d*₈): δ 28.61 (CNCMe₂CH₂O), 66.37 (CNCMe₂CH₂O), 80.49 (CNCMe₂CH₂O), 125.33 (*para*-

C₆H₅), 126.56 (*meta*-C₆H₅), 134.5 (br, *ipso*-C₆H₅), 136.00 (*ortho*-C₆H₅), 136.38 (C₆F₅), 138.02 (C₆F₅), 138.41 (C₆F₅), 140.02 (C₆F₅), 148.43 (C₆F₅), 150.07 (C₆F₅), 191 (br, CNCMe₂CH₂O). ¹¹B NMR (192 MHz, THF-*d*₈): δ -18.4, -20.2 (B(C₆F₅)₄). ¹⁹F NMR (544 MHz, THF-*d*₈): δ -134.6 (*ortho*-C₆F₅), -166.7 (*para*-C₆F₅), -170.3 (*meta*-C₆F₅). ¹⁵N NMR (THF-*d*₈, 60 MHz): δ -156. IR (KBr, cm⁻¹): ν 2981 (s), 1645 (m), 1559 (w), 1515 (s), 1464 (s), 1374 (w), 1277 (m), 1089 (s), 980 (s), 862 (s), 775 (m), 756 (m), 684 (m), 661 (m). Anal. Calcd. for C₄₅H₂₉B₂F₂₀MgN₃O₃: C, 49.79; H, 2.69; N, 3.87. Found C, 50.20; H, 2.49; N, 4.01. Mp: 86-88 °C.

(Et₃SiO)(MeO)C=CMe₂.⁴³ To^MMgHB(C₆F₅)₃ (0.011 g, 0.012 mmol), methyl methacrylate (0.117 g, 1.17 mmol), and Et₃SiH (0.136 g, 1.17 mmol) were stirred in C₆H₆ for 30 min. at r.t. Benzene was evaporated under reduced pressure to give a colorless gel. The product was extracted with pentane, and the extracts were evaporated to dryness under reduced pressure to afford a colorless liquid (0.249 g, 1.15 mmol, 98.0%). ¹H NMR (400 MHz, benzene-*d*₆): δ 0.707 (q, 6 H, ³J_{HH} = 12 Hz, SiCH₂CH₃), 1.03 (t, 9 H, ³J_{HH} = 12 Hz, SiCH₂CH₃), 1.69 (s, 3 H, (Et₃SiO)(MeO)C=CMe₂), 1.72 (s, 3 H, (Et₃SiO)(MeO)C=CMe₂), 3.35 (s, 3 H, OMe). ¹³C{¹H} NMR (150 MHz, benzene-*d*₆): δ 5.78 (SiCH₂CH₃), 7.25 (SiCH₂CH₃), 16.89 ((Et₃SiO)(MeO)C=CMe₂), 17.55 ((Et₃SiO)(MeO)C=CMe₂), 57.27 (OMe), 90.97 ((Et₃SiO)(MeO)C=CMe₂), 151.11 ((Et₃SiO)(MeO)C=CMe₂). ²⁹Si (119 MHz, benzene-*d*₆) δ 20.8. IR (KBr, cm⁻¹): ν 2957 (s), 2880 (s), 1736 (s), 1460 (m), 1414 (w), 1387 (w), 1329 (w), 1312 (w), 1259 (m), 1202 (s), 1177 (s), 1144 (s), 1099 (m), 1019 (m), 973 (w), 944 (w), 907 (w), 838 (s), 746 (s). Anal. Calcd. for C₁₁H₂₄O₂Si: C, 61.05; H, 11.18. Found C, 60.93; H, 8.73.

(BnMe₂SiO)(MeO)C=CMe₂. To^MMgHB(C₆F₅)₃ (0.011 g, 0.012 mmol), methyl methacrylate (0.117 g, 1.17 mmol), and BnMe₂SiH (0.176 g, 1.17 mmol) were stirred in C₆H₆ for 30 min. at

r.t. Evaporation of the volatile materials under reduced pressure afforded a colorless gel. The product was extracted with pentane, and the extracts were evaporated to dryness under reduced pressure to afford a colorless liquid (0.290 g, 1.16 mmol, 99.0%). ^1H NMR (600 MHz, benzene- d_6): δ 0.15 (s, 6 H, SiMe_2), 1.61 (s, 3 H, $(\text{BnMe}_2\text{SiO})(\text{MeO})\text{C}=\text{CMe}_2$), 1.71 (s, 3 H, $(\text{BnMe}_2\text{SiO})(\text{MeO})\text{C}=\text{CMe}_2$), 2.23 (s, 2H, PhCH_2Si), 3.29 (s, 3 H, OMe), 7.02 (m, 3 H, C_6H_5), 7.13 (m, 2 H, C_6H_5). $^{13}\text{C}\{^1\text{H}\}$ NMR (150 MHz, benzene- d_6): δ -1.44 (SiMe_2), 16.84 ($(\text{BnMe}_2\text{SiO})(\text{MeO})\text{C}=\text{CMe}_2$), 17.49 ($(\text{BnMe}_2\text{SiO})(\text{MeO})\text{C}=\text{CMe}_2$), 27.30 (PhCH_2Si), 57.01 (OMe), 91.41 ($(\text{BnMe}_2\text{SiO})(\text{MeO})\text{C}=\text{CMe}_2$), 125.14 (C_6H_5), 128.98 (C_6H_5), 129.20 (C_6H_5), 139.10 (*ipso*- C_6H_5), 150.64 ($(\text{BnMe}_2\text{SiO})(\text{MeO})\text{C}=\text{CMe}_2$). ^{29}Si (119 MHz, benzene- d_6) δ 15.7. IR (KBr, cm^{-1}): ν 3062 (w), 3027 (m), 2964 (s), 2919 (s), 2859 (s), 1706 (s), 1601 (m), 1494 (m), 1453 (m), 1410 (m), 1256 (s), 1203 (s), 1176 (s), 1058 (w), 1027 (s), 944 (s), 905 (w), 862 (s), 763 (s), 699 (s), 664 (w), 611 (w). Anal. Calcd. for $\text{C}_{14}\text{H}_{22}\text{O}_2\text{Si}$: C, 67.15; H, 8.86. Found C, 67.63; H, 8.73.

$(\text{H}_2\text{C}=\text{CH})\text{Me}_2\text{SiO}(\text{MeO})\text{C}=\text{CMe}_2$. $\text{To}^{\text{M}}\text{MgHB}(\text{C}_6\text{F}_5)_3$ (0.011 g, 0.012 mmol), methyl methacrylate (0.117 g, 1.17 mmol), and $(\text{CH}_2=\text{CH})\text{Me}_2\text{SiH}$ (0.101 g, 1.17 mmol) were stirred in benzene for 30 min. at r.t. The volatile materials were removed under reduced pressure, leaving behind a colorless gel. The product was extracted with pentane, and the extracts were evaporated to dryness under reduced pressure to afford a colorless liquid (0.201 g, 1.08 mmol, 92.1%). ^1H NMR (400 MHz, benzene- d_6): δ 0.26 (s, 6 H, Me_2Si), 1.67 (s, 3 H, $(\text{H}_2\text{C}=\text{CH})\text{Me}_2\text{SiO}(\text{MeO})\text{C}=\text{CMe}_2$), 1.73 (s, 3 H, $(\text{H}_2\text{C}=\text{CH})\text{Me}_2\text{SiO}(\text{MeO})\text{C}=\text{CMe}_2$), 3.34 (s, 3 H, OMe), 5.77 (d2, 1 H, $^3J_{\text{HH}} = 21$ Hz, $^2J_{\text{HH}} = 3.6$ Hz, $\text{H}_2\text{C}=\text{CHSi}$), 5.91 (d2, 1 H, $^3J_{\text{HH}} = 15$ Hz, $^2J_{\text{HH}} = 3.6$, $\text{H}_2\text{C}=\text{CHSi}$), 6.22 (d2, 1 H, $^3J_{\text{HH}} = 15$ Hz, $^2J_{\text{HH}} = 16$, $\text{H}_2\text{C}=\text{CHSi}$). $^{13}\text{C}\{^1\text{H}\}$ NMR (150 MHz, benzene- d_6): δ -1.20 (Me_2Si), 16.84 ($(\text{H}_2\text{C}=\text{CH})\text{Me}_2\text{SiO}(\text{MeO})\text{C}=\text{CMe}_2$), 17.57

$((\text{H}_2\text{C}=\text{CH})\text{Me}_2\text{SiO})(\text{MeO})\text{C}=\text{CMe}_2$, 56.90 (OMe), 91.01
 $((\text{H}_2\text{C}=\text{CH})\text{Me}_2\text{SiO})(\text{MeO})\text{C}=\text{CMe}_2$, 133.61 ($\text{H}_2\text{C}=\text{CHSi}$), 137.10 ($\text{H}_2\text{C}=\text{CHSi}$), 150.59
 $((\text{H}_2\text{C}=\text{CH})\text{Me}_2\text{SiO})(\text{MeO})\text{C}=\text{CMe}_2$. ^{29}Si (119 MHz, benzene- d_6) δ 17.5. IR (KBr, cm^{-1}): ν
 3055 (m), 2972 (s), 1716 (s), 1605 (w), 1567 (w), 1414 (m), 1266 (s), 1166 (s), 1029 (m), 955
 (m), 900 (w), 836 (s), 790 (s), 744 (w), 717 (w), 690 (m), 662 (m). Anal. Calcd. for $\text{C}_9\text{H}_{18}\text{O}_2\text{Si}$:
 C, 58.02; H, 9.74. Found C, 58.50; H, 9.62.

$(\text{Ph}_2\text{HSiO})(\text{MeO})\text{C}=\text{CMe}_2$. $\text{To}^{\text{M}}\text{MgHB}(\text{C}_6\text{F}_5)_3$ (0.011 g, 0.012 mmol), methyl methacrylate
 (0.117 g, 1.17 mmol), and Ph_2SiH_2 (0.216 g, 1.17 mmol) were stirred in C_6H_6 for 30 min. at r.t.
 Benzene was removed under reduced pressure, leaving behind a colorless gel. The product was
 extracted with pentane, and the extracts were evaporated to dryness under reduced pressure to
 afford a colorless liquid (0.331 g, 1.13 mmol, 96.3%). ^1H NMR (400 MHz, benzene- d_6): δ 1.64
 (s, 3 H, $(\text{Ph}_2\text{HSiO})(\text{MeO})\text{C}=\text{CMe}_2$), 1.69 (s, 3 H, $(\text{Ph}_2\text{HSiO})(\text{MeO})\text{C}=\text{CMe}_2$), 3.29 (s, 3 H,
 OMe), 5.84 (s, 1 H, SiH), 7.17 (m, 6 H, C_6H_5), 7.74 (m, 4 H, C_6H_5). $^{13}\text{C}\{^1\text{H}\}$ NMR (150 MHz,
 benzene- d_6): δ 16.79 ($(\text{Ph}_2\text{HSiO})(\text{MeO})\text{C}=\text{CMe}_2$), 17.42 ($(\text{Ph}_2\text{HSiO})(\text{MeO})\text{C}=\text{CMe}_2$), 57.92
 (OMe), 91.74 ($(\text{Ph}_2\text{HSiO})(\text{MeO})\text{C}=\text{CMe}_2$), 130.47 (C_6H_5), 131.12 (C_6H_5), 134.16 (*ipso*- C_6H_5),
 135.49 (C_6H_5), 136.39 (C_6H_5), 150.93 ($(\text{Ph}_2\text{HSiO})(\text{MeO})\text{C}=\text{CMe}_2$). ^{29}Si (119 MHz, benzene- d_6)
 δ -14.5 (d, $^1J_{\text{SiH}} = 201$ Hz). IR (KBr, cm^{-1}): ν 3094 (m), 2931 (s), 2158 (s), 1716 (s), 1661 (w),
 1598 (m), 1566 (w), 1548 (w), 1528 (w), 1437 (s), 1263 (m), 1169 (br s), 1029 (m), 949 (m), 858
 (s), 738 (s), 701 (s), 671 (w). Anal. Calcd. for $\text{C}_{17}\text{H}_{20}\text{O}_2\text{Si}$: C, 71.79; H, 7.09. Found C, 71.61; H,
 7.32.

3,4-dihydro-6-(phenylmethylsiloxy)-2H-pyran. $\text{To}^{\text{M}}\text{MgHB}(\text{C}_6\text{F}_5)_3$ (0.030 g, 0.033 mmol), 5,6-
 dihydro-2H-pyran-2-one (0.032 g, 0.33 mmol), and PhMeSiH_2 (0.042 g, 0.33 mmol) were stirred
 in benzene for 5 h at room temperature. Evaporation of the volatile materials provided a yellow

gel. The product was extracted with pentane, and the extracts were evaporated to dryness under reduced pressure to afford a pale yellow liquid (0.059 g, 0.26 mmol, 80.3%). ^1H NMR (600 MHz, benzene- d_6): δ 0.46 (d, 3 H, $^3J_{\text{HH}} = 3.0$ Hz, SiMe), 1.32 (pent, 2 H, $^3J_{\text{HH}} = 4.8$ Hz, $\text{OCH}_2\text{CH}_2\text{CH}_2\text{CH}=\text{C}-\text{OSiHMePh}$), 1.80 (m, 2 H, $\text{OCH}_2\text{CH}_2\text{CH}_2\text{CH}=\text{C}-\text{OSiHMePh}$), 3.68 (t, 2 H, $^3J_{\text{HH}} = 4.8$ Hz, $\text{OCH}_2\text{CH}_2\text{CH}_2\text{CH}=\text{C}-\text{OSiHMePh}$), 4.10 (t, 1 H, $^3J_{\text{HH}} = 3.6$ Hz, $\text{OCH}_2\text{CH}_2\text{CH}_2\text{CH}=\text{C}-\text{OSiHMePh}$), 5.46 (q, 1 H, $^3J_{\text{HH}} = 3.0$ Hz, SiH), 7.18 (m, 3 H, C_6H_5), 7.66 (m, 2 H, C_6H_5). $^{13}\text{C}\{^1\text{H}\}$ NMR (150 MHz, benzene- d_6): δ -1.91 (SiMe), 19.64 ($\text{OCH}_2\text{CH}_2\text{CH}_2\text{CH}=\text{C}-\text{OSiHMePh}$), 22.24 ($\text{OCH}_2\text{CH}_2\text{CH}_2\text{CH}=\text{C}-\text{OSiHMePh}$), 67.69 ($\text{OCH}_2\text{CH}_2\text{CH}_2\text{CH}=\text{C}-\text{OSiHMePh}$), 74.57 ($\text{OCH}_2\text{CH}_2\text{CH}_2\text{CH}=\text{C}-\text{OSiHMePh}$), 127.85 (C_6H_5), 130.08 (C_6H_5), 133.89 (C_6H_5), 138.21 (*ipso*- C_6H_5), 155.62 ($\text{OCH}_2\text{CH}_2\text{CH}_2\text{CH}=\text{C}-\text{OSiHMePh}$). ^{29}Si (119 MHz, benzene- d_6) δ -5.1 (d, $^1J_{\text{SiH}} = 218$ Hz). IR (KBr, cm^{-1}): ν 3070 (w), 3050 (w), 2957 (s), 2926 (s), 2854 (m), 2131 (s), 1738 (s), 1637 (w), 1592 (m), 1460 (m), 1429 (s), 1386 (w), 1255 (m), 1121 (s), 1079 (s), 879 (s), 846 (s), 796 (w), 725 (s), 700 (s). Anal. Calcd. for $\text{C}_{12}\text{H}_{16}\text{O}_2\text{Si}$: C, 65.41; H, 7.32. Found C, 65.73; H, 6.98.

3,4-dihydro-6-(benzyl dimethylsiloxy)-2H-pyran. $\text{To}^{\text{M}}\text{MgHB}(\text{C}_6\text{F}_5)_3$ (0.015 g, 0.015 mmol), 5,6-Dihydro-2H-pyran-2-one (0.160 g, 1.65 mmol), and BnMe_2SiH (0.245 g, 1.65 mmol) were stirred in C_6H_6 for 30 min. at 35 °C. Benzene was removed under reduced pressure, leaving behind a colorless gel. The product was extracted with pentane, and the extracts were evaporated to dryness under reduced pressure to afford a colorless liquid (0.335 g, 1.35 mmol, 82.9%). ^1H NMR (600 MHz, benzene- d_6): δ 0.18 (s, 6 H, SiMe_2), 1.39 (pent, 2 H, $^3J_{\text{HH}} = 4.8$ Hz, $\text{OCH}_2\text{CH}_2\text{CH}_2\text{CH}=\text{C}-\text{OSiMe}_2\text{Bn}$), 1.86 (m, 2 H, $\text{OCH}_2\text{CH}_2\text{CH}_2\text{CH}=\text{C}-\text{OSiMe}_2\text{Bn}$), 2.27 (s, 2 H, SiCH_2Ph), 3.72 (t, 2 H, $^3J_{\text{HH}} = 4.8$ Hz, $\text{OCH}_2\text{CH}_2\text{CH}_2\text{CH}=\text{C}-\text{OSiMe}_2\text{Bn}$), 4.02 (t, 1 H, $^3J_{\text{HH}} = 3.6$ Hz, $\text{OCH}_2\text{CH}_2\text{CH}_2\text{CH}=\text{C}-\text{OSiMe}_2\text{Bn}$), 7.01 (t, 1 H, $^3J_{\text{HH}} = 7.2$ Hz, C_6H_5), 7.06 (d, 2 H, $^3J_{\text{HH}} =$

7.2 Hz, C₆H₅), 7.14 (t, 2 H, ³J_{HH} = 7.2 Hz, C₆H₅). ¹³C{¹H} NMR (150 MHz, benzene-*d*₆): δ -1.31 (SiMe₂), 20.57 (OCH₂CH₂CH₂CH=C-OSiMe₂Bn), 23.04 (OCH₂CH₂CH₂CH=C-OSiMe₂Bn), 27.43 (PhCH₂Si), 67.53 (OCH₂CH₂CH₂CH=C-OSiMe₂Bn), 74.67 (OCH₂CH₂CH₂CH=C-OSiMe₂Bn), 125.10 (C₆H₅), 128.97 (C₆H₅), 129.23 (C₆H₅), 139.25 (*ipso*-C₆H₅), 155.50 (OCH₂CH₂CH₂CH=C-OSiMe₂Bn). ²⁹Si (119 MHz, benzene-*d*₆) δ 15.6. IR (KBr, cm⁻¹): ν 3081 (w), 3059 (w), 3025(w), 2957 (s), 1733 (s), 1600 (w), 1493 (m), 1452 (m), 1403 (m), 1253 (s), 1208 (s), 1157 (s), 1077 (s), 1057 (s), 907 (m), 838 (s), 762 (s), 700 (s), 619 (w). Anal. Calcd. for C₁₄H₂₀O₂Si: C, 67.70; H, 8.12. Found C, 67.77; H, 8.15.

(PhMeHSiO)(PhCH₂O)C=CMe₂. To^MMgHB(C₆F₅)₃ (0.027 g, 0.029 mmol), benzyl methacrylate (0.207 g, 1.17 mmol), and PhMeSiH₂ (0.149 g, 1.17 mmol) were stirred in C₆H₆ for 4 h at room temperature. The volatiles were evaporated under reduced pressure to give a colorless gel. The product was extracted with pentane, and the extracts were evaporated to dryness under reduced pressure to provide a colorless liquid (0.348 g, 1.16 mmol, 99.2%). ¹H NMR (600 MHz, benzene-*d*₆): δ 0.45 (d, 3 H, ³J_{HH} = 3.0 Hz, SiMe), 1.62 (s, 3 H, (PhMeHSiO)(PhCH₂O)C=CMe₂), 1.66 (s, 3 H, (PhMeHSiO)(PhCH₂O)C=CMe₂), 4.70 (s, 2 H, (PhMeHSiO)(PhCH₂O)C=CMe₂), 5.40 (q, 1 H, ³J_{HH} = 3.0 Hz, SiH), 7.08 (t, 1 H, ³J_{HH} = 7.2 Hz, OCH₂Ph), 7.13 (t, 2 H, ³J_{HH} = 7.2 Hz, OCH₂Ph), 7.17 (m, 3 H, SiPh), 7.25 (d, 2 H, ³J_{HH} = 7.2 Hz, OCH₂Ph), 7.66 (m, 2 H, SiPh). ¹³C{¹H} NMR (150 MHz, benzene-*d*₆): δ -2.37 (SiMe), 17.01 ((PhMeHSiO)(PhCH₂O)C=CMe₂), 17.44 ((PhMeHSiO)(PhCH₂O)C=CMe₂), 71.96 (OCH₂Ph), 92.83 ((PhMeHSiO)(PhCH₂O)C=CMe₂), 128.35 (OCH₂Ph), 128.66 (SiPh), 128.81 (OCH₂Ph), 128.84 (OCH₂Ph), 130.97 (SiPh), 134.61 (SiPh), 135.66 (*ipso*-SiPh), 149.22 ((PhMeHSiO)(PhCH₂O)C=CMe₂). ²⁹Si (119 MHz, benzene-*d*₆) δ -3.5 (d, ¹J_{SiH} = 216 Hz). IR (KBr, cm⁻¹): ν 3070 (m), 3032 (m), 2982 (m), 2915 (s), 2859 (m), 2146 (s), 1707 (s), 1591 (w),

1498 (w), 1455 (m), 1429 (m), 1384 (w), 1256 (s), 1161 (s), 1122 (s), 1008 (m), 964 (m), 866 (s), 734 (s), 698 (s). Anal. Calcd. for $C_{18}H_{22}O_2Si$: C, 72.44; H, 7.43. Found C, 71.98; H, 7.49.

(PhMeHSiO)(MeO)C=CMe₂. $To^MgHB(C_6F_5)_3$ (0.0428 g, 0.047 mmol), methyl methacrylate (0.467 g, 4.66 mmol), and PhMeSiH₂ (0.570 g, 4.66 mmol) were stirred in C₆H₆ for 7 h at 60 °C. Benzene was removed under reduced pressure to give a colorless gel. The product was extracted with pentane, and the extracts were evaporated to dryness under reduced pressure. Repeated Kugelrohr distillation (3×) under dynamic vacuum at 170 °C provided a colorless liquid (1.01 g, 4.54 mmol, 97.1%). ¹H NMR (600 MHz, benzene-*d*₆): δ 0.44 (d, 3 H, ³*J*_{HH} = 2.8 Hz, SiMe), 1.66 (s, 3 H, (PhMeHSiO)(MeO)C=CMe₂), 1.67 (s, 3 H, (PhMeHSiO)(MeO)C=CMe₂), 3.30 (s, 3 H, OMe), 5.36 (q, 1 H, ³*J*_{HH} = 2.8 Hz, SiH), 7.18 (m, 3 H, C₆H₅), 7.64 (m, 2 H, C₆H₅). ¹³C{¹H} NMR (150 MHz, benzene-*d*₆): δ -2.31 (SiMe), 16.78 ((PhMeHSiO)(MeO)C=CMe₂), 17.36 ((PhMeHSiO)(MeO)C=CMe₂), 57.41 (OMe), 91.31 ((PhMeHSiO)(MeO)C=CMe₂), 128.63 (C₆H₅), 130.92 (C₆H₅), 134.61 (C₆H₅), 135.73 (*ipso*-C₆H₅), 150.75 ((PhMeHSiO)(MeO)C=CMe₂). ²⁹Si (119 MHz, benzene-*d*₆) δ -3.8 (d, ¹*J*_{SiH} = 216 Hz). IR (KBr, cm⁻¹): ν 3062 (m), 2897 (s), 2809 (m), 2076 (s, ν_{SiH}), 1740 (s), 1589 (w), 1451 (m), 1369 (w), 1257 (s), 1178 (s), 863 (s), 802 (w), 775 (m), 741 (m), 705 (m). Anal. Calcd. for $C_{12}H_{18}O_2Si$: C, 64.82; H, 8.16. Found C, 64.85; H, 7.79.

(PhMeHSiO)(Me₂CHCH₂O)C=CMe₂. $To^MgHB(C_6F_5)_3$ (0.027 g, 0.029 mmol), isobutyl methacrylate (0.167 g, 1.17 mmol), and PhMeSiH₂ (0.149 g, 1.17 mmol) were stirred in C₆H₆ for 8 h at room temperature. The solvent was evaporated under reduced pressure, leaving behind a colorless gel. The product was extracted with pentane, and the extracts were evaporated to dryness under reduced pressure to provide a colorless liquid (0.126 g, 0.476 mmol, 40.5%). ¹H NMR (600 MHz, benzene-*d*₆): δ 0.46 (d, 3 H, ³*J*_{HH} = 3.0 Hz, SiMe), 0.85 (d, 3 H, ³*J*_{HH} = 6.6 Hz,

(PhMeHSiO)(Me₂CHCH₂O)C=CMe₂), 0.86 (d, 3 H, ³J_{HH} = 6.6 Hz, (PhMeHSiO)(Me₂CHCH₂O)C=CMe₂), 1.69 (s, 3 H, (PhMeHSiO)(Me₂CHCH₂O)C=CMe₂), 1.72 (s, 3 H, (PhMeHSiO)(Me₂CHCH₂O)C=CMe₂), 1.81 (m, 1 H, (PhMeHSiO)(Me₂CHCH₂O)C=CMe₂), 3.49 (d, 2 H, ³J_{HH} = 6.6 Hz, (PhMeHSiO)(Me₂CHCH₂O)C=CMe₂), 5.39 (q, 1 H, ³J_{HH} = 3.0 Hz, SiH), 7.18 (m, 3 H, C₆H₅), 7.66 (m, 2 H, C₆H₅). ¹³C{¹H} NMR (150 MHz, benzene-*d*₆): δ -2.26 (SiMe), 16.96 ((PhMeHSiO)(Me₂CHCH₂O)C=CMe₂), 17.50 ((PhMeHSiO)(Me₂CHCH₂O)C=CMe₂), 19.75 (OCH₂CHMe₂), 29.20 ((PhMeHSiO)(Me₂CHCH₂O)C=CMe₂), 76.78 ((PhMeHSiO)(Me₂CHCH₂O)C=CMe₂), 91.51 ((PhMeHSiO)(Me₂CHCH₂O)C=CMe₂), 128.62 (C₆H₅), 130.92 (C₆H₅), 134.62 (C₆H₅), 135.52 (*ipso*-C₆H₅), 149.96 ((PhMeHSiO)(Me₂CHCH₂O)C=CMe₂). ²⁹Si (119 MHz, benzene-*d*₆) δ -3.9 (d, ¹J_{SiH} = 222 Hz). IR (KBr, cm⁻¹): ν 2962 (s), 2926 (s), 2876 (s), 2141 (s), 1708 (s), 1470 (m), 1429 (m), 1393 (w), 1257 (s), 1166 (s), 1122 (s), 1024 (m), 969 (w), 868 (s), 732 (w), 700 (m), 611 (m). Anal. Calcd. for C₁₅H₂₄O₂Si: C, 68.13; H, 9.15. Found C, 68.06; H, 8.69.

PhMeSi(O(MeO)C=CMe₂)₂.⁴⁴ To^MMgHB(C₆F₅)₃ (0.05 g, 0.054 mmol), methyl methacrylate (0.226 g, 2.18 mmol), and PhMeSiH₂ (0.150 g, 1.09 mmol) were stirred in C₆H₆ for 12 h at 80 °C and isolated according to the procedure for **(1)**. Kugelrohr distillation under dynamic vacuum at 180 °C provided a colorless liquid (0.113 g, 0.351 mmol, 32.2%). ¹H NMR (600 MHz, benzene-*d*₆): δ 0.63 (s, 3 H, SiMe), 1.67 (s, 6 H, PhMeSi(O(MeO)C=CMe₂)₂), 1.69 (s, 6 H, PhMeSi(O(MeO)C=CMe₂)₂), 3.35 (s, 6 H, OMe), 7.19 (m, 3 H, C₆H₅), 7.83 (m, 2 H, C₆H₅). ¹³C{¹H} NMR (150 MHz, benzene-*d*₆): δ -3.15 (SiMe), 16.83 (PhMeSi(O(MeO)C=CMe₂)₂), 17.45 (PhMeSi(O(MeO)C=CMe₂)₂), 57.59 (OMe), 92.19 (PhMeSi(O(MeO)C=CMe₂)₂), 128.46 (C₆H₅), 131.04 (C₆H₅), 134.53 (C₆H₅), 134.72 (*ipso*-C₆H₅), 150.00

(PhMeSi(O(MeO)C=CMe₂)₂). ²⁹Si (119 MHz, benzene-*d*₆) δ -20.2. IR (KBr, cm⁻¹): ν 2966 (m), 2925 (s), 2859 (m), 1709 (s), 1593 (w), 1457 (m), 1384 (w), 1261 (s), 1205 (m), 1161 (s), 1125 (m), 1095 (w), 1027 (m), 949 (m), 873 (m), 855 (m), 794 (m), 737 (w), 700 (w). Anal. Calcd. for C₁₇H₂₆O₄Si: C, 63.32; H, 8.13. Found C, 62.85; H, 8.43.

References

- (1) (a) Marciniak, B. *Hydrosilylation : a comprehensive review on recent advances*; Springer: Berlin, 2009. (b) Marciniak, B. *Comprehensive handbook on hydrosilylation*; Pergamon Press: Oxford, 1992.
- (2) Dhillon, R. S. *Hydroboration and Organic Synthesis : 9-Borabicyclo [3.3.1] Nonane (9-BBN)*; Springer: Berlin, 2007.
- (3) (a) Denmark, S. E.; Regens, C. S. *Acc. Chem. Res.* **2008**, *41*, 1486. (b) Corbet, J.-P.; Mignani, G. *Chem. Rev.* **2006**, *106*, 2651. (c) Miyaura, N.; Suzuki, A. *Chem. Rev.* **1995**, *95*, 2457. (d) Jana, R.; Pathak, T. P.; Sigman, M. S. *Chem. Rev.* **2011**, *111*, 1417.
- (4) (a) Jones, G. R.; Landais, Y. *Tetrahedron* **1996**, *52*, 7599. (b) Fleming, I.; Henning, R.; Plaut, H. *J. Chem. Soc., Chem. Commun.* **1984**, 29. (c) Tamao, K.; Kakui, T.; Akita, M.; Iwahara, T.; Kanatani, R.; Yoshida, J.; Kumada, M. *Tetrahedron* **1983**, *39*, 983.
- (5) (a) Parks, D. J.; Blackwell, J. M.; Piers, W. E. *J. Org. Chem.* **2000**, *65*, 3090. (b) Parks, D. J.; Piers, W. E. *J. Am. Chem. Soc.* **1996**, *118*, 9440. (c) Rubin, M.; Schwier, T.; Gevorgyan, V. *J. Org. Chem.* **2002**, *67*, 1936. (d) Piers, W. E.; Marwitz, A. J. V.; Mercier, L. G. *Inorg. Chem.* **2011**, *50*, 12252.
- (6) Berkefeld, A.; Piers, W. E.; Parvez, M. *J. Am. Chem. Soc.* **2010**, *132*, 10660.
- (7) Koller, J.; Bergman, R. G. *Organometallics* **2012**, *31*, 2530.

- (8) (a) Ojima, I.; Kogure, T. *Organometallics* **1982**, *1*, 1390. (b) Ojima, I.; Nihonyanagi, M.; Kogure, T.; Kumagai, M.; Horiuchi, S.; Nakatsugawa, K.; Nagai, Y. *J. Organomet. Chem.* **1975**, *94*, 449. (c) Ojima, I.; Nihonyanagi, M.; Nagai, Y. *J. Chem. Soc., Chem. Commun.* **1972**, *0*, 938. (d) Johnson, C. R.; Raheja, R. K. *J. Org. Chem.* **1994**, *59*, 2287.
- (9) (a) Jurkauskas, V.; Sadighi, J. P.; Buchwald, S. L. *Org. Lett.* **2003**, *5*, 2417. (b) Huang, S.; Voigtritter, K. R.; Unger, J. B.; Lipshutz, B. H. *Synlett.* **2010**, *13*, 2041-2044. (c) Kim, H.; Yun, J. *Adv. Synth. Catal.* **2010**, *352*, 1881-1885. (d) Diez-Gonzalez, S.; Nolan, S. P. *Acc. Chem. Res.* **2008**, *41*, 349-358. (e) Diez-Gonzalez, S.; Nolan, S. P. *Transition Metal-Catalyzed Hydrosilylation of Carbonyl Compounds and Imines. A Review, Organic Preparations and Procedures International: The New Journal for Organic Synthesis*, **2007**, *39*, 523-559.
- (10) (a) Buch, F.; Harder, S. *Z. Naturforsch.* **2008**, *63b*, 169-177. (b) Buch, F.; Brettar, J.; Harder, S. *Angew. Chem. Int. Ed.* **2006**, *45*, 2741-2745. (c) Leich, V.; Spaniol, T. P.; Maron, L.; Okuda, J. *Chem. Commun.* **2014**, *50*, 2311-2314. (d) Barrett, A. G. M.; Crimmin, M. R.; Hill, M. S.; Procopiou, P. A. *Proc. R. Soc. A*, **2010**, *466*, 927-963.
- (11) Spielmann, J.; Harder, S. *Eur. J. Inorg. Chem.* **2008**, 1480-1486.
- (12) Hill, M. S.; Kociok-Kohn, G.; MacDougall, D. J.; Mahon, M. F.; Weetman, C. *Dalton Trans.* **2011**, *40*, 12500-12509.
- (13) (a) Das, S.; Möller, K.; Junge, K.; Beller, M. *Chem. Eur. J.* **2011**, *17*, 7414. (b) Junge, K.; Wendt, B.; Zhou, S.; Beller, M. *Eur. J. Org. Chem.* **2013**, *2013*, 2061. (c) Díez-González, S.; Scott, N. M.; Nolan, S. P. *Organometallics* **2006**, *25*, 2355.
- (14) Mukherjee, D.; Ellern, A.; Sadow, A. D. *Chem. Sci.* **2014**, *5*, 959.

- (15) (a) Berkefeld, A.; Piers, W. E.; Parvez, M.; Castro, L.; Maron, L.; Eisenstein, O. *J. Am. Chem. Soc.* **2012**, *134*, 10843. (b) Evans, W. J.; Forrestal, K. J.; Ansari, M. A.; Ziller, J. W. *J. Am. Chem. Soc.* **1998**, *120*, 2180. (c) Yan, K.; Schoendorff, G.; Upton, B. M.; Ellern, A.; Windus, T. L.; Sadow, A. D. *Organometallics* **2013**, *32*, 1300. (d) Yan, K.; Upton, B. M.; Ellern, A.; Sadow, A. D. *J. Am. Chem. Soc.* **2009**, *131*, 15110.
- (16) Anker, M. D.; Arrowsmith, M.; Bellham, P.; Hill, M. S.; Kociok-Kohn, G.; Liptrot, D. J.; Mahon, M. F.; Weetman, C. *Chem. Sci.* **2014**, *5*, 2826.
- (17) Dunne, J. F.; Neal, S. R.; Engelkemier, J.; Ellern, A.; Sadow, A. D. *J. Am. Chem. Soc.* **2011**, *133*, 16782.
- (18) Mukherjee, D.; Ellern, A.; Sadow, A. D. *Chem. Sci.* **2014**, *5*, 959.
- (19) Dunne, J. F.; Neal, S. R.; Engelkemier, J.; Ellern, A.; Sadow, A. D. *J. Am. Chem. Soc.* **2011**, *133*, 16782.
- (20) Cordero, B.; Gomez, V.; Platero-Prats, A. E.; Reves, M.; Echeverria, J.; Cremades, E.; Barragan, F.; Alvarez, S. *Dalton Trans.* **2008**, 2832.
- (21) Hedberg, K.; Schomaker, V. *J. Am. Chem. Soc.* **1951**, *73*, 1482.
- (22) Yang, X.; Stern, C. L.; Marks, T. J. *Angew. Chem. Int. Eng. Ed.* **1992**, *31*, 1375.
- (23) Anker, M. D.; Arrowsmith, M.; Bellham, P.; Hill, M. S.; Kociok-Kohn, G.; Liptrot, D. J.; Mahon, M. F.; Weetman, C. *Chem. Sci.* **2014**, *5*, 2826.
- (24) Evans, W. J.; Forrestal, K. J.; Ansari, M. A.; Ziller, J. W. *J. Am. Chem. Soc.* **1998**, *120*, 2180.
- (25) Yan, K.; Upton, B. M.; Ellern, A.; Sadow, A. D. *J. Am. Chem. Soc.* **2009**, *131*, 15110.
- (26) Anker, M. D.; Arrowsmith, M.; Bellham, P.; Hill, M. S.; Kociok-Kohn, G.; Liptrot, D. J.; Mahon, M. F.; Weetman, C. *Chem. Sci.* **2014**, *5*, 2826.

- (27) Berkefeld, A.; Piers, W. E.; Parvez, M.; Castro, L.; Maron, L.; Eisenstein, O. *J. Am. Chem. Soc.* **2012**, *134*, 10843.
- (28) Yang, X.; Stern, C. L.; Marks, T. J. *Angew. Chem. Int. Eng. Ed.* **1992**, *31*, 1375.
- (29) Mukherjee, D.; Ellern, A.; Sadow, A. D. *J. Am. Chem. Soc.* **2010**, *132*, 7582.
- (30) Mukherjee, D.; Ellern, A.; Sadow, A. D. *J. Am. Chem. Soc.* **2010**, *132*, 7582.
- (31) Parks, D. J.; Piers, W. E. *J. Am. Chem. Soc.* **1996**, *118*, 9440.
- (32) Houghton, A. Y.; Hurmalainen, J.; Mansikkamäki, A.; Piers, W. E.; Tuononen, H. M. *Nature Chemistry*, **2014**, *6*, 983-988.
- (33) Yang, X.; Stern, C. L.; Marks, T. J. *J. Am. Chem. Soc.* **1994**, *116*, 10015.
- (34) Yang, X.; Stern, C. L.; Marks, T. J. *Angew. Chem. Int. Eng. Ed.* **1992**, *31*, 1375.
- (35) (a) Wu, F.; Jordan, R. F. *Organometallics* **2005**, *24*, 2688. (b) Sadow, A. D.; Tilley, T. D. *Organometallics* **2003**, *22*, 3577.
- (36) (a) Krempner, C.; Köckerling, M.; Reinke, H.; Weichert, K. *Inorg. Chem.* **2006**, *45*, 3203.
(c) Walker, D. A.; Woodman, T. J.; Hughes, D. L.; Bochmann, M. *Organometallics* **2001**, *20*, 3772.
- (37) (a) Parks, D. J.; Blackwell, J. M.; Piers, W. E. *J. Org. Chem.* **2000**, *65*, 3090. (b) Parks, D. J.; Piers, W. E. *J. Am. Chem. Soc.* **1996**, *118*, 9440.
- (38) (a) Mukherjee, D.; Ellern, A.; Sadow, A. D. *Chem. Sci.* **2014**, *5*, 959. (b) Dunne, J. F.; Neal, S. R.; Engelkemier, J.; Ellern, A.; Sadow, A. D. *J. Am. Chem. Soc.* **2011**, *133*, 16782.
- (39) Dunne, J. F.; Fulton, D. B.; Ellern, A.; Sadow, A. D. *J. Am. Chem. Soc.* **2010**, *132*, 17680-17683.
- (40) Mukherjee, D.; Ellern, A.; Sadow, A. D. *J. Am. Chem. Soc.* **2010**, *132*, 7582-7583.

- (41) Wang, C.; Erker, G.; Kehr, G.; Wedeking, K.; Fröhlich, R. *Organometallics* **2005**, *24*, 4760-4773.
- (42) Sakurai, H.; Shoji, M.; Yajima, M.; Hosomk, A. *Synthesis*, **1984**, 598-600.
- (43) Hasegawa, A.; Naganawa, Y.; Fushimi, M.; Ishihara, K.; Yamamoto, H. *Org. Lett.* **2006**, *8*, 3175-3178.
- (44) Kita, Y.; Yasuda, H.; Sugiyama, Y.; Fukata, F.; Haruta, J.-I.; Tamura, Y. *Tetrahedron Lett.* **1983**, *24*, 1273-1276.

CHAPTER 6: MAGNESIUM-CATALYZED MILD REDUCTION OF TERTIARY AND SECONDARY AMIDES TO AMINES

Modified from a paper to be submitted to the *Journal of the American Chemical Society*

Nicole Lampland, Megan Hovey, Debabrata Mukherjee, Aaron D. Sadow*

Abstract

The first example of a catalytic hydroboration of amides for their deoxygenation to amines, employing an earth abundant magnesium-based catalyst, is reported. Tertiary and secondary amides are reduced to amines at room temperature in the presence of pinacolborane (HBpin) and catalytic amounts of $\text{To}^{\text{M}}\text{MgMe}$ ($\text{To}^{\text{M}} = \text{tris}(4,4\text{-dimethyl-2-oxazolinyl})\text{phenylborate}$). Catalyst initiation and speciation is complex in this system, as revealed by effects of concentration and order of substrate and HBpin addition in catalytic experiments. $\text{To}^{\text{M}}\text{MgH}_2\text{Bpin}$, a possible catalytically relevant species formed from $\text{To}^{\text{M}}\text{MgMe}$ and HBpin, reacts with *N,N*-dimethylbenzamide to give the catalytic product benzyldimethylamine in low yield. Instead, C–N and C–C bond cleavage pathways are observed to give Me_2NBpin and PhBpin, respectively. Alternatively, the reaction of $\text{To}^{\text{M}}\text{MgMe}$ and *N,N*-dimethylbenzamide slowly gives decomposition of $\text{To}^{\text{M}}\text{MgMe}$ over 24 h. Together, these data suggest that catalytic activation of $\text{To}^{\text{M}}\text{MgMe}$ requires both HBpin and amide, and $\text{To}^{\text{M}}\text{MgH}_2\text{Bpin}$ is not a catalytic intermediate. Thus, tertiary amides are selectively reduced to amines in good yield when catalytic amounts of $\text{To}^{\text{M}}\text{MgMe}$ are added to a mixture of amide and excess HBpin. In addition, secondary amides are reduced in the presence of 10 mol % $\text{To}^{\text{M}}\text{MgMe}$ and 4 equiv. of HBpin. Functional groups such as cyano, nitro and azo remain intact under the mild, room temperature reaction conditions.

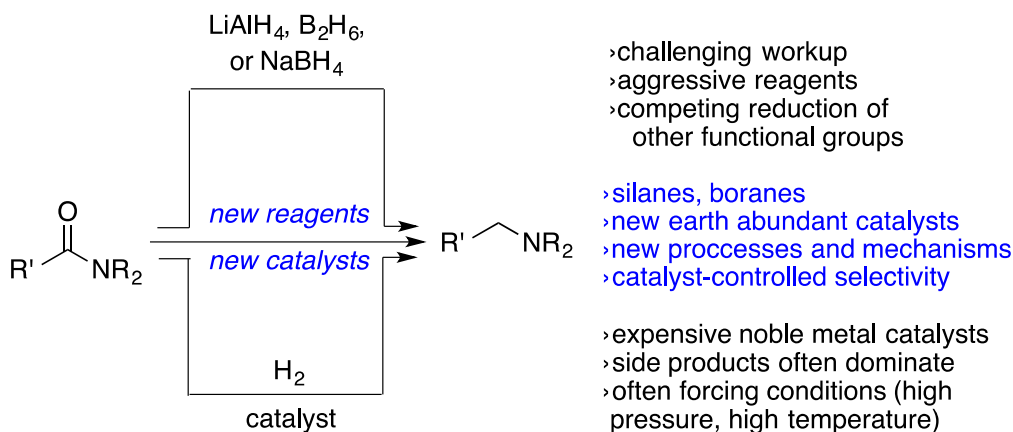
Introduction

The demand for efficient syntheses of amines is ever increasing due to the need to produce chemicals through sustainable processes and amines' continued importance in pharmaceutical, agrochemical, and materials chemistry applications.¹ Amides, which are naturally prevalent among biological molecules or are readily synthetically accessed, provide attractive starting materials for amine preparations through reductive transformations.² However, selective reduction of the amide functional group is challenging for thermodynamic and kinetic reasons, and often requires strongly reducing hydride reagents such as LiAlH_4 , NaBH_4 , or B_2H_6 that are also reactive towards many functional groups. Notably, these reagents contain both reducing hydrides and Lewis acid sites (Li, Na, B, or Al) to activate amides for reduction. An intermediate resulting from hydride attacking a Lewis acid-coordinated CO is similarly invoked for ester and amide reductions.³ Though this idea is accepted for stoichiometric reductions, minimal experimental evidence is available.⁴ Well-defined main group reductants, either as stoichiometric reagents or as part of catalytic systems, may also contribute experimental support for elementary steps in LiAlH_4 or NaBH_4 reductions.

A number of pathways have been reported for reductive interactions of metal compounds and amides, including deoxygenation to amines,⁵ deoxygenation and alkylation,⁶ dehydration to nitriles,⁷ and C-N bond cleavage to amines and aldehydes.⁸ While a range of late metal complexes have been reported to efficiently reduce amides through hydrosilylation⁹ and a few through hydrogenation,¹⁰ new catalytic processes are still needed to address the above challenges facing amide deoxygenations. In addition, few catalytic systems are able to effectively reduce primary, secondary, and tertiary amides,¹¹ and few catalysts are based on metal complexes other than non-oxophilic late metals.¹² Moreover, many catalysts require elevated temperatures for

effective operation. An exception is the $[\text{Ir}(\eta^2\text{-C}_8\text{H}_{14})_2\text{Cl}]_2/\text{Et}_2\text{SiH}_2$ system, which reduces secondary amides at room temperature.¹³ Other mild systems are applicable only for tertiary amides and employ main group metal catalysts.¹⁴

Scheme 1. Chemical routes for amide reduction.



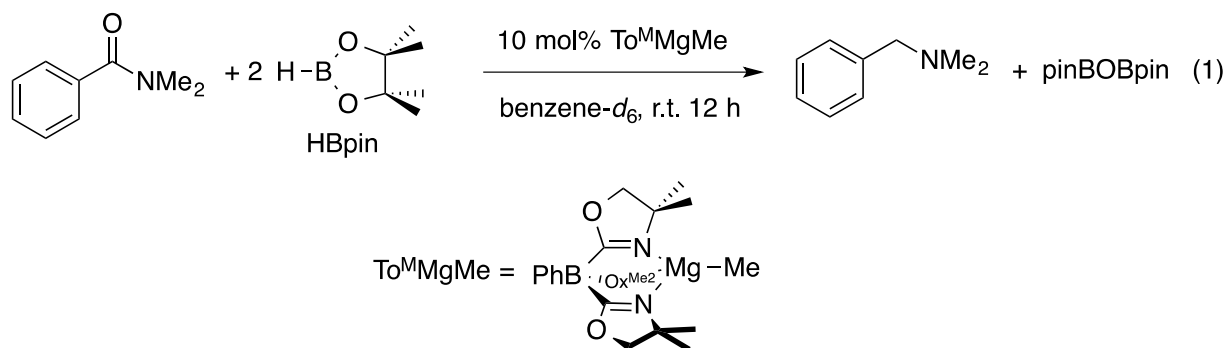
In contrast, the reduction of amides by catalytic hydroboration with HBpin is not reported. However, magnesium compounds have been shown to be good catalysts for the hydroboration of a number of carbonyl compounds and unsaturated substrates such as pyridine.¹⁵ Our group has recently found that $\text{To}^{\text{M}}\text{MgMe}$ (To^{M} = tris(4,4-dimethyl-2-oxazolanyl)phenylborate) catalytically reduces and cleaves esters with two equivalents of pinacolborane (HBpin) to give alkoxyboronic pinacol esters (ROBpin).¹⁶ Amides are slightly stabilized relative to esters, which can be shown by the ΔH_{rxn} for the metathesis reaction of methyl acetate and dimethylamine to *N,N*-dimethylacetamide and methanol, which is -7.5 kcal/mol.¹⁷

Thus, the feasibility and reaction pathway(s) of a magnesium-catalyzed amide reduction is of interest in relation to the ester reduction. In addition, the classic studies of Brown on

hydroboration and deoxygenation of amides with B_2H_6 reveal good selectivity, even with this highly reactive reagent.¹⁸ Herein we report the catalytic reduction of tertiary and secondary amides to amines using pinacolborane and the precatalyst $To^M MgMe$ under mild, room temperature conditions. The isolated magnesium dihydridopinacolborate adduct, $To^M MgH_2Bpin$, which is a precatalyst in the aforementioned ester cleavage, is not effective as a catalytic species in the reduction of amides. To the best of our knowledge, this report describes the first example of the catalytic hydroboration of amides. In addition, the intermediate species involved in amide and ester reductions appear to be inequivalently influenced by reaction conditions.

Results and Discussion

N,N-dimethylbenzamide reacts with 2 equiv. of pinacolborane (HBpin) upon addition of $To^M MgMe$ (10 mol %) to form benzyldimethylamine in 54% yield (eq. 1). Control experiments reveal that *N,N*-dimethylbenzamide and two equivalents of pinacolborane are unchanged after 24 hours at temperatures up to 120 °C in the absence of $To^M MgMe$.

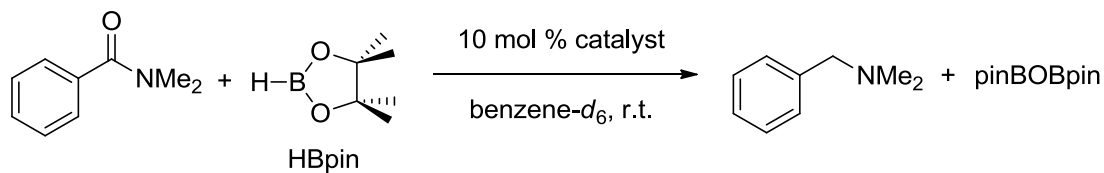


The $To^M MgMe$ -catalyzed amide deoxygenation reaction of equation 1 contrasts the hydroboration/reductive ester cleavage catalyzed by $To^M MgMe$, and instead follows the typically observed conversion of amides to amines in the presence of strong metal hydrides such as $LiAlH_4$ or $NaBH_4$.¹⁹ The by-product of the catalytic hydroboration/deoxygenation is pinBOBpin,

which is characterized by ^1H and ^{11}B NMR signals at 1.02 and 21.7 ppm, respectively (in benzene- d_6).²⁰

These catalytic experiments were initially performed by dissolving *N,N*-dimethylbenzamide and HBpin in benzene followed by addition of $\text{To}^{\text{M}}\text{MgMe}$. In contrast, benzyldimethylamine is not efficiently produced (18% yield) in experiments in which *N,N*-dimethylbenzamide is added to a solution of $\text{To}^{\text{M}}\text{MgMe}$ and HBpin. Instead, the magnesium compound and HBpin react instantaneously to give MeBpin and a black, intractable and catalytically inactive precipitate. Although this decomposition may be avoided (in the absence of amide) by adding $\text{To}^{\text{M}}\text{MgMe}$ to excess HBpin (>10 equiv.) to form $\text{To}^{\text{M}}\text{MgH}_2\text{Bpin}$, experiments in which *N,N*-dimethylbenzamide is added to a 20:1 mixture of HBpin: $\text{To}^{\text{M}}\text{MgMe}$ do not afford greater than ~20% benzyldimethylamine. In those experiments, the characteristic black precipitate is still observed. Furthermore, isolated $\text{To}^{\text{M}}\text{MgH}_2\text{Bpin}$ is less efficient as a catalyst precursor for amide reduction than $\text{To}^{\text{M}}\text{MgMe}$ (Table 1). Finally, the deoxygenation yield is poorer and C–N cleavage products are higher in reactions performed in methylene chloride. That solvent is effective for the formation of $\text{To}^{\text{M}}\text{MgH}_2\text{Bpin}$ as well as for the cleavage of esters. All of these observations contrast those of the $\text{To}^{\text{M}}\text{Mg}$ -catalyzed ester hydroboration,²¹ which is proposed to involve $\text{To}^{\text{M}}\text{Mg}\{\text{RO}(\text{H})\text{Bpin}\}$ as a catalytic intermediate formed from $\text{To}^{\text{M}}\text{MgH}_2\text{Bpin}$ and esters.

Other oxazoline-based magnesium compounds also show catalytic activity for hydroboration and deoxygenation of amides (Table 1), and the catalytic efficacy varies with substrate and ancillary oxazolinyborate-based ligand. The chiral C_3 -symmetric $\text{To}^{\text{P}}\text{MgMe}$ (To^{P} = tris(4*S*-isopropyl-2-oxazoliny)phenylborate) gives slightly greater conversion to benzyldimethylamine (67% NMR yield) than $\text{To}^{\text{M}}\text{MgMe}$ after 12 h, and 97% yield after 24 h.

Table 1. Deoxygenation of *N,N*-dimethylbenzamide with pinacolborane and catalyst

Catalyst	mol % cat.	HBpin equiv.	Time (h)	% Yield
 To ^P MgMe	10	2	12	67
	10	2	24	97
	10	4	24	78
 To ^M MgMe	10	2	12	54
	10	2	24	54
	10	4	12	94
	10	20	0.25	97
	5	20	0.5	97
	2	20	3	99
 To ^{MP} MgMe	10	2	26	46
	10	2	6	44
	10	2	12	44
 To ^M MgH ₂ Bpin	10	2	12	17
	10	4	24	30

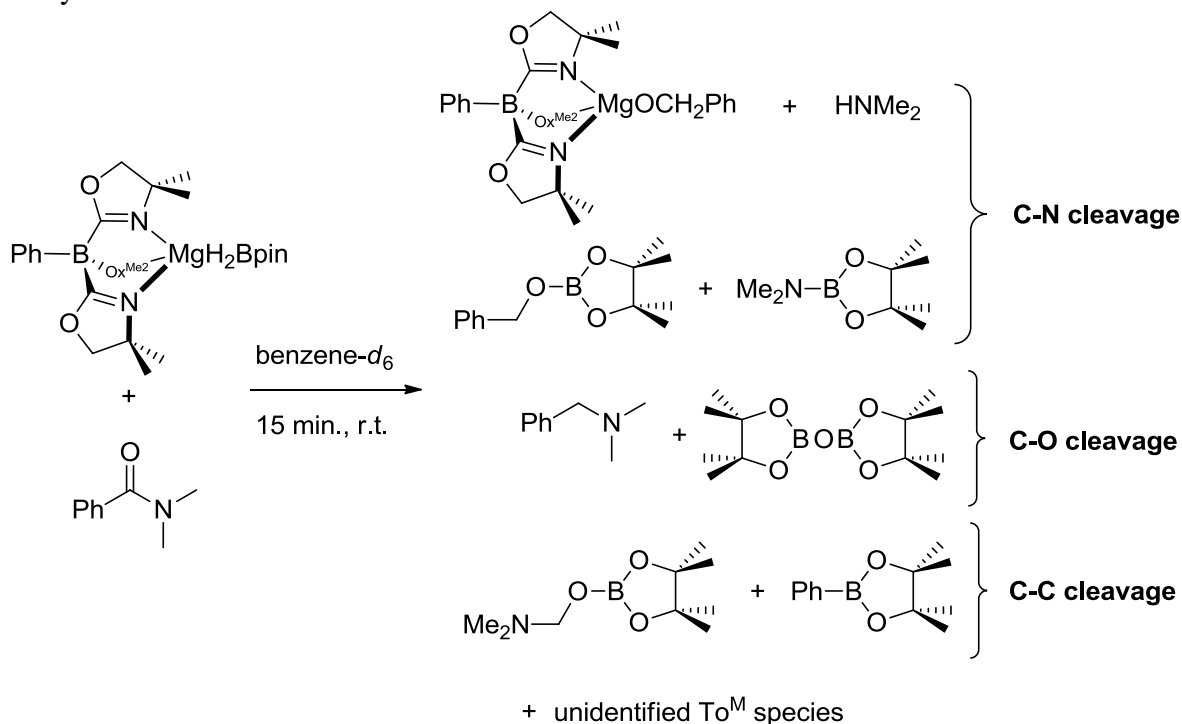
This product is obtained with 54% yield after 12 h when $\text{To}^{\text{M}}\text{MgMe}$ is the catalyst, and the same yield is measured after 24 h, indicating that the product does not decompose under the reaction conditions and the $\text{To}^{\text{P}}\text{Mg}$ -derived catalyst is longer-lived than the $\text{To}^{\text{M}}\text{Mg}$ -derived species. With $\text{To}^{\text{M}}\text{MgMe}$, yields are improved with even 4 equiv. of HBpin, whereas amine yield is decreased with greater concentration of HBpin when $\text{To}^{\text{P}}\text{MgMe}$ is the catalyst. The less efficient C_1 -symmetric $\text{To}^{\text{MP}}\text{MgMe}$ ($\text{To}^{\text{MP}} = \text{bis}(4,4\text{-dimethyl-2-oxazolinyl})(4S\text{-isopropyl-2-oxazolinyl})\text{phenylborate}$) requires >24 h for less than 50% yield, and amine yields are not improved with longer reaction times. Similarly, a bis(oxazolinyl)boratomagnesium methyl gives even lower yield with both short and long reaction times, implying that the catalyst quickly deactivates.

Although $\text{To}^{\text{P}}\text{MgMe}$ gives the highest yield in Table 1, most other substrates below in Table 2 are reduced in equal or higher yield with $\text{To}^{\text{M}}\text{MgMe}$ than with the C_3 -symmetric $\text{To}^{\text{P}}\text{MgMe}$ complex. In fact, for most tertiary and secondary amides, $\text{To}^{\text{M}}\text{MgMe}$ is a superior precatalyst in terms of reaction times, NMR yields, and selectivity. Moreover, 10, 5 or even 2 mol % $\text{To}^{\text{M}}\text{MgMe}$ as the catalyst provides benzyldimethylamine in >95% under optimized conditions with excess HBpin. There appears to be a trade-off between $\text{To}^{\text{M}}\text{MgMe}$ and HBpin loadings: high catalyst loading and low HBpin concentration give >90% yield of the amine while low catalyst loading requires a larger excess of HBpin.

The interaction of $\text{To}^{\text{M}}\text{MgH}_2\text{BPin}$ and amides could provide insight into pathways available during catalytic amide reduction and allow for further optimization. $\text{To}^{\text{M}}\text{MgH}_2\text{Bpin}$ and 1 equiv. of *N,N*-dimethylbenzamide give complete consumption of the amide and formation of benzyldimethylamine in 11% yield in a process that affords a mixture of species. In Scheme 2, pathways associated with C–O, C–N, and C–C cleavage are identified on the basis of the

assigned products. Two sets of new To^M -containing signals were observed. The major species was assigned to $To^M MgOCH_2Ph$ based on comparison to an authentic sample generated from $To^M MgMe$ and $HOCH_2Ph$. In addition, a signal at 2.15 ppm was assigned to $HNMe_2$ based on an identical chemical shift of an authentic dilute sample of dimethylamine in benzene- d_6 .

Scheme 2. Multiple pathways observed in reactions of $To^M MgH_2Bpin$ and *N,N*-dimethylbenzamide.



The starting material $To^M MgH_2Bpin$ and $To^M MgNMe_2$ are ruled out as the other To^M -containing species based on comparison with authentic samples. $PhCH_2OBpin$ and Me_2NBpin are formed; $PhCH_2OBpin$ was assigned on the basis of 1H and ^{11}B NMR spectroscopy and GC-MS (δ_H : 1.04, 4.96, 7.05, 7.10, 7.30; δ_B 22.7 and m/z 234.1),²² and Me_2NBpin was assigned on the basis of 1H and ^{11}B NMR spectroscopy (δ_H : 1.12, 2.64; δ_B 23.9).²³ A small signal in the GC-MS was assigned to $PhBpin$ based on its identical retention time as an authentic sample, its

parent ion peak of 204.1 m/z in the MS, and the overall similarity of daughter ion peaks in the MS. In addition, a signal in the GC-MS was assigned to $\text{Me}_2\text{NCH}_2\text{OBpin}$. Similarly, 2 equiv. of dimethylbenzamide rapidly gives benzyldimethylamine in 16% yield (vs. $\text{To}^{\text{M}}\text{MgH}_2\text{Bpin}$ as the limiting reagent) after 15 min, and no changes are observed after that point. In that experiment, *N,N*-dimethylbenzamide is partly consumed (37% *N,N*-dimethylbenzamide is unreacted) and several unidentified To^{M} -containing compounds are observed.

The dominance of the C–N bond cleavage pathway from the reaction of $\text{To}^{\text{M}}\text{MgH}_2\text{Bpin}$ contrasts the catalytic deoxygenation pathway observed with $\text{To}^{\text{M}}\text{MgMe}$ and excess HBpin. Amide deoxygenation requires two reducing equivalents, which could, in principle, be provided by $\text{To}^{\text{M}}\text{MgH}_2\text{Bpin}$. The experiments above, however, indicate that without excess HBpin, the second reducing equivalent in $\text{To}^{\text{M}}\text{MgH}_2\text{Bpin}$ goes to C–N bond cleavage. Based on this idea, the effect of excess HBpin on deoxygenation yields and reaction times was investigated. Neat HBpin results in nearly quantitative yields and fast reaction rates, and the optimal yield is obtained with excess pinacolborane (20 equiv., See Table 1) with a small volume of C_6D_6 for NMR experiments and enough C_6H_6 in scaled up reactions to dissolve the amide starting material. Moreover, the C–N cleavage products Me_2NBpin and $\text{PhCH}_2\text{OBpin}$ are not detected in these experiments with a high concentration of HBpin. Thus, the role of excess HBpin under catalytic conditions is not to give $\text{To}^{\text{M}}\text{MgH}_2\text{Bpin}$ in high yield because catalyst activation does not involve that compound as an intermediate. Instead, HBpin plays an important role in controlling selectivity toward deoxygenation vs. C–N cleavage.

An alternative pathway for catalyst activation might instead involve the interaction of $\text{To}^{\text{M}}\text{MgMe}$ and an amide. Interestingly, 1:1 or 1:2 mixtures of $\text{To}^{\text{M}}\text{MgMe}$ and *N,N*-dimethylbenzamide are unchanged after two hours at room temperature in benzene. After 24 h,

all $\text{To}^{\text{M}}\text{MgMe}$ signals disappeared, and multiple broad signals associated with unidentified To^{M} -containing species appeared. Neither $\text{H}[\text{To}^{\text{M}}]$ nor methane signals were detected, ruling out adventitious hydrolysis. However, ca. 95% of the initial *N,N*-dimethylbenzamide was unreacted. This process is much slower than the catalytic reaction and likely unrelated to amide deoxygenation. These observations also contrast the reaction of $\text{To}^{\text{M}}\text{MgMe}$ and EtOAc, which react instantaneously at room temperature to give acetone and $\text{To}^{\text{M}}\text{MgOEt}$.²⁴ The catalytic yields of benzyldimethylamine (51-54%), however, are similar when either 2 equiv. of HBpin are added to a mixture of $\text{To}^{\text{M}}\text{MgMe}$ and *N,N*-dimethylbenzamide or when catalyst is added to the mixture of HBpin and *N,N*-dimethylbenzamide. In total, these observations suggest that the formation of the active catalytic species requires all three reaction components ($\text{To}^{\text{M}}\text{MgMe}$, HBpin, and amide) and may involve an unusual dual substrate-catalyst initiation process.

Unfortunately, attempts to determine a quantitative catalytic rate law were hindered by precipitation that occurs during the reaction. Qualitatively, additional equivalents of HBpin (or increased HBpin concentration, with all other variables kept constant) results in faster disappearance of amide and faster appearance of the amine product. Higher catalyst concentration also provides faster conversions. Alternatively, a transient absorption at 330 nm, observed by in situ UV-vis spectroscopy, assigned to a reaction intermediate quickly increases in intensity in the early stages of the reaction and then slowly decays (Figure 1). This signal is attributed to a species that is formed from the combination of $\text{To}^{\text{M}}\text{MgMe}$, HBpin, and $\text{Ph}(\text{Me}_2\text{N})\text{C}=\text{O}$. Independent experiments indicate that bimolecular combinations ($\text{To}^{\text{M}}\text{MgMe}$ and HBpin or $\text{To}^{\text{M}}\text{MgMe}$ and $\text{Ph}(\text{Me}_2\text{N})\text{C}=\text{O}$) do not provide this absorbance, nor do the catalytic products produce this signal. To analyze the formation of the intermediate, we varied $[\text{To}^{\text{M}}\text{MgMe}]$, $[\text{HBpin}]$, and $[\textit{N,N}\text{-dimethylbenzamide}]$ and measured the slope of curves of

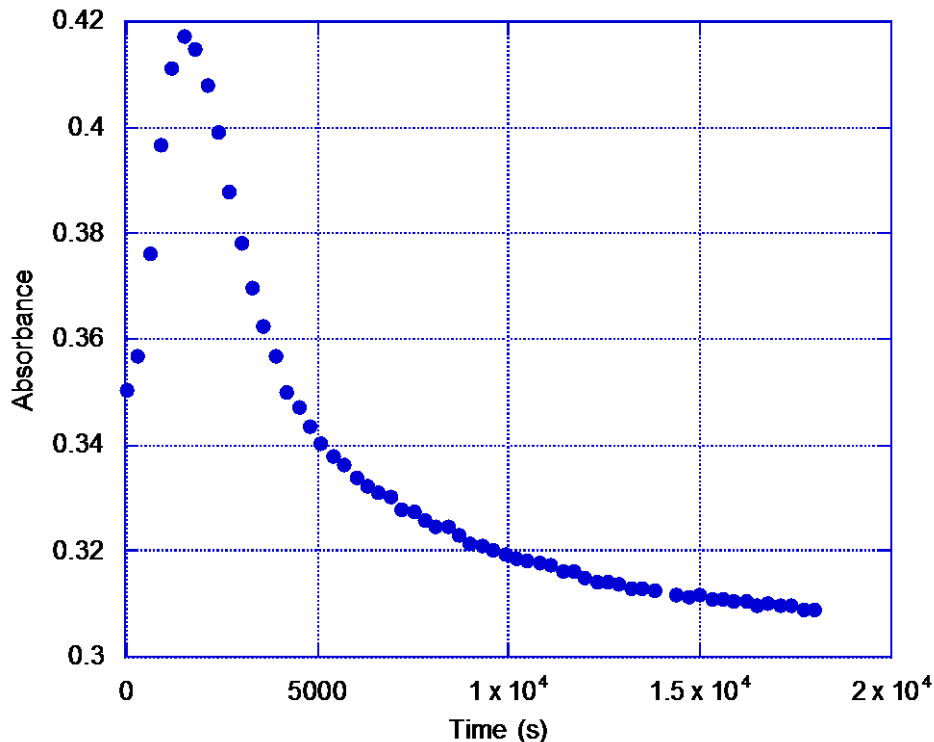


Figure 1. Plot of absorbance vs. time for the transient signal at 330 nm assigned to the catalytically active species.

absorbance at 330 nm vs. time for the initial portion of the reaction. Variation in the catalyst concentration from 3.95 mM to 7.91 mM provided a linear plot of initial rate ($d(\text{absorbance})/dt$) vs. $[\text{To}^{\text{M}}\text{MgMe}]$ ($k_{\text{obs}} \approx 0.02 \text{ s}^{-1}$; $[\text{HBpin}] = 0.791 \text{ M}$ and $[\text{Ph}(\text{Me}_2\text{N})\text{C}=\text{O}] = 0.040 \text{ M}$). Variation of $[\text{HBpin}]$ from 0.395 M to 1.79 M shows a generally increasing slope of $d(\text{absorbance})/dt$ with increasing $[\text{HBpin}]$, although the data is not sufficient for a quantitative linear least squares analysis. Interestingly, at low concentration of *N,N*-dimethylbenzamide, the initial rate shows little change at low concentration until 40 mM, but shows a sharp increase in rate above ~45 mM. These rate dependences parallel our general observations regarding effects of catalyst initiation on catalytic conversion. Based on these similarities, we suggest that the 330 nm signal

is due to a catalytically relevant species that contains $\text{To}^{\text{M}}\text{Mg}$, amide, and HBpin derived moieties.

This system gives reduction under mild conditions at room temperature with good yields (Table 2) and advantageously tolerates nitro and azo moieties that common stoichiometric reductants such as LiAlH_4 reduce. Aryl bromide is tolerated, and benzyl groups on the amide are not cleaved under reaction conditions. Notably, the conversion works with both aliphatic, aromatic, and formamide-based substrates. However, *N,N*-dimethyl acrylamide reacts instantaneously with $\text{To}^{\text{M}}\text{MgMe}$ and HBpin to give an unidentified precipitate.

Under catalytic hydroboration conditions, *N,N*-dibenzyl-4-cyanophenylamide gives the amide C–N cleavage product rather than the deoxygenated product (eq. 2); however, the cyano moiety is not reduced under the reaction conditions. Although the boronate-protected *p*-cyanobenzyl alcohol was not isolated, its NMR yield is equal to the NMR yield of dibenzylamine (89%), and dibenzylammonium chloride is isolated in 77% yield. The starting material contained $^{13}\text{C}\{^1\text{H}\}$ NMR signals at 114.1 and 118.5 ppm assigned to *ipso*- $\text{C}_6\text{H}_4\text{C}\equiv\text{N}$ and $\text{C}\equiv\text{N}$ signals, and similar resonances in pinBOCH₂C₆H₄CN were measured at 111.7 and 119.3 ppm.

Deoxygenation of the related electron-poor *para*-nitrophenyl amide is straightforward under the standard catalytic conditions.

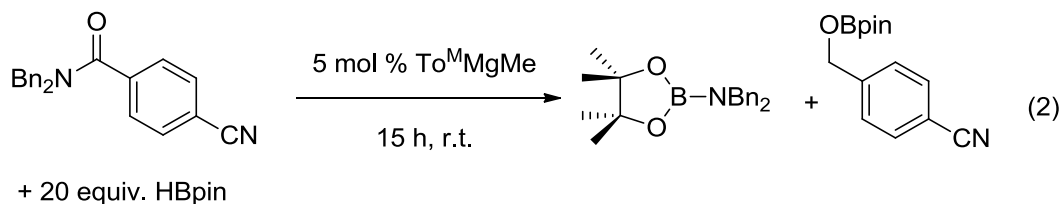
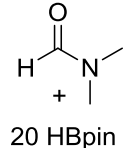
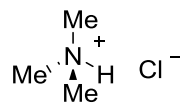
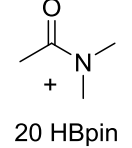
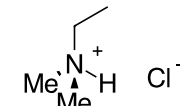
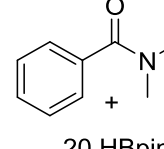
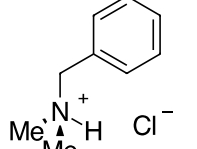
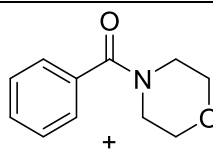
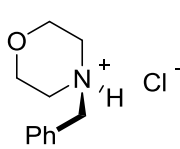
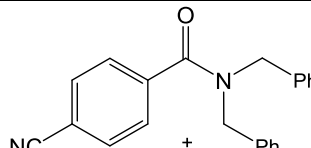
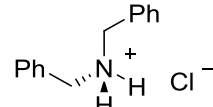
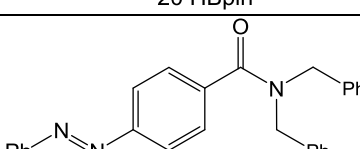
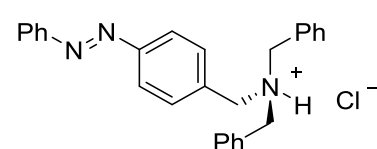
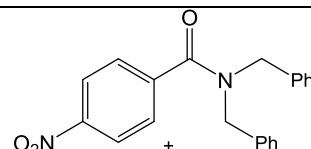
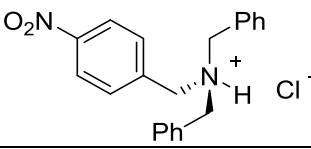
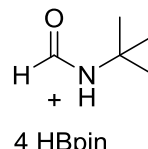
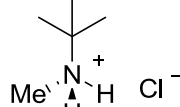
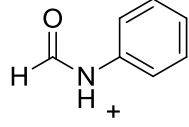
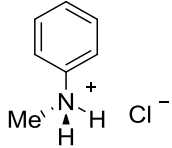
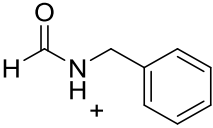
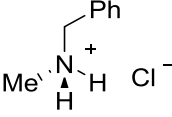
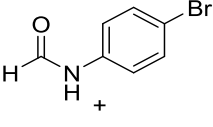
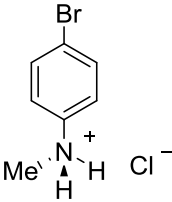


Table 2. Tertiary and secondary amides with $\text{To}^{\text{M}}\text{MgMe}$ catalyst and HBpin reductant

Reaction	Product	Cat. (mol%)	Time (h)	% Yield ^a
 20 HBpin	 Cl^-	2	0.1	77 (18)
 20 HBpin	 Cl^-	2	6	99 (91)
 20 HBpin	 Cl^-	2	3	99 (93)
 20 HBpin	 Cl^-	2	6	99 (92)
 20 HBpin	 Cl^-	5	15	89 (77)
 20 HBpin	 Cl^-	5	15	88 (79)
 20 HBpin	 Cl^-	5	15	83 (78)
 4 HBpin	 Cl^-	10	24	72 (71)

 4 HBpin	 Me ⁺ N ⁺ H Cl ⁻	10	48	99 (93)
 4 HBpin	 Me ⁺ N ⁺ H Cl ⁻	10	48	86 (85)
 4 HBpin	 Me ⁺ N ⁺ H Cl ⁻	10	48	71 (68)

^aNMR yield of amine and isolated yield of ammonium chloride salt in parenthesis.

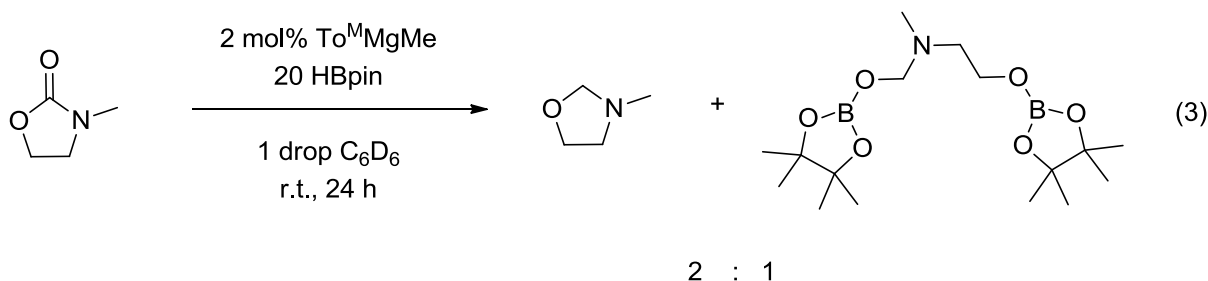
Secondary amides are also deoxygenated to secondary amines, although increased catalyst loading (Table 2) is required for high yield. Interestingly, the highest yields are obtained with 4 equiv. of HBpin with respect to the amide rather than the larger excess needed for tertiary amides. The fastest reactions and the highest yields are obtained with substrates containing small groups adjacent to the carbonyl, most notably the formamides. These observations, along with the significant variation of yield with a series of similar oxazoline-based ancillary ligands, suggest that sterics greatly affect the reaction. Significantly, formation of tertiary amines (e.g., PhNMe₂) via imine alkylation is not observed, which is a common pathway under hydrosilylation and hydrogenation conditions.²⁵

Previous studies of To^MMg-catalyzed ester reductive cleavage showed very fast conversions,²⁶ with reactions completing in less time than the above amide deoxygenation pathway. Our kinetic studies in that system implicated a catalyst-mediated reversible ester cleavage prior to hydroboration with To^MMg{RO(H)Bpin}. This mechanism is based on a half-order rate dependence on ester concentration and zero-order dependence on HBpin

concentration. Likely, the initial ester cleavage involves addition to the carbonyl. The present amide-reduction system shows some dependence on HBpin in terms of catalyst activation and qualitative effects on rates of product formation, but these catalytic amide hydroboration experiments have not proved amenable to quantitative kinetic studies. To further probe the catalytic additions, we turned to competition experiments between amides and esters.

In the competition reaction between an ester substrate and an amide substrate, the initial rates of consumption of phenyl formate and phenylformamide reactants were compared. Phenyl formate and phenylformamide, chosen for their similar steric and structural features, react with HBpin in the presence of 2.5 mol % $\text{To}^{\text{M}}\text{MgMe}$ to give the N-borylated phenylmethanamine and the boryl ether products MeOBpin and PhOBpin. Under the conditions of excess carbonyl vs. HBpin (formamide:formate:HBpin = 1:1:1) this competition experiment reveals that the rate of amide consumption is faster than the rate of ester consumption. The initial concentrations of phenylformamide and phenyl formate decrease by 0.14 M and 0.04 M, respectively, over the first 5 min. of the reaction. In contrast, when the concentration of HBpin is increased (formamide:formate:HBpin = 1:1:2 with all other variables held constant), the rate of amide consumption is slower than the rate of ester consumption. In this case, the initial concentrations of phenylformamide and phenyl formate decreased by 0.09 M and 0.13 M, respectively, over the first 5 min. of the reaction. With even higher amount of HBpin (formamide:formate:HBpin = 1:1:4), all of the ester substrate is consumed within 5 min., while ca. 50% phenylformamide is unreacted at that time. This contrasting behavior suggests that the magnesium catalyst structure changes with variations in HBpin concentration in the competition experiments. In addition, the species present with low HBpin concentration is more reactive toward amide, whereas at higher HBpin concentration, the catalytic species is more reactive toward esters.

An oxazolidinone substrate provides an alternative competition between ester cleavage and amide deoxygenation (eq. 3). This competition experiment compares product formation from either pathway, rather than initial consumption of ester or amide under conditions of low HBpin concentration needed in the above experiments.



Under conditions with a large excess of HBpin (20 equiv.), deoxygenation is favored 2:1 over ester cleavage as determined from the ratio of products in the ^{11}B NMR spectrum. Decreasing the amount of HBpin to 2 equiv. reduces the product ratio to 1.3:1, but amide deoxygenation is still favored. These reactions require 1 day for full conversion, which is similar to the rate of amide deoxygenation. The change in product ratio with lower [HBpin] in this case likely reflects the direct dependence of the amide deoxygenation reaction on the pinacolborane concentration observed in synthetic experiments.

Conclusion

This system is the first example of catalytic hydroboration for amide deoxygenation. $\text{To}^{\text{M}}\text{MgMe}$ generally outperforms the other tested oxazolinylborate-based magnesium complexes as an effective precatalyst for the hydroboration of amides, although the sensitivity of the reaction to conditions suggests that other catalysts based on oxophilic early metal centers should be explored in the future. Moreover, the results of this study clearly show that the pathway of amide reduction is tuned for C–O vs. C–N bond cleavage by HBpin concentration. Interestingly,

the C–N cleavage pathway occurs at low HBpin concentration, while the related ester reductive cleavage pathway is zero-order in HBpin. In contrast, amide deoxygenation shows a significant HBpin dependence. Overall, the magnesium catalyst activation and speciation for amide deoxygenation and ester cleavage appear to be inequivalent, and the interaction of HBpin with catalytic intermediates is distinct for the two transformations. Further work to clarify the pathway(s) for deoxygenation and C–N cleavage in amides is currently underway to clarify the identity of the reactive species.

Organosilanes are not effective reductants of amides in this oxazolinyborato magnesium system, nor are silanes effective in the related magnesium-catalyzed reductive cleavage of esters. Although silanes reduce amides to amines in many transition-metal-based catalytic systems, these catalysts are typically less oxophilic (e.g. iron group or later). In the present reduction employing a highly oxophilic magnesium center, the HBpin is likely important because of its ability to act as a hydride donor and as a Lewis acid. This principle may guide future developments of catalytic amide reductions to improve efficiency, yield, and selectivity for mild conversion methods.

Experimental

General Procedures. All reactions were performed under a dry argon atmosphere using standard Schlenk techniques or under a nitrogen atmosphere in a glovebox, unless otherwise indicated. Benzene, toluene, pentane, diethyl ether, and tetrahydrofuran were dried and deoxygenated using an IT PureSolv system. Benzene- d_6 was heated to reflux over Na/K alloy and vacuum-transferred. Chloroform- d_1 and water- d_2 were used as received. Tris(4*S*-isopropyl-2-oxazoliny)phenylborate (HTo^P),²⁷ PhB(Ox^{Me2})₂,²⁸ LiOx^{ipr},²⁹ To^MMgMe,³⁰ To^MMgH₂Bpin,³¹ 1-

benzoylmorpholine,³² *N,N*-dibenzyl-4-cyanobenzamide,³³ and *N,N*-dibenzyl-4-nitrobenzamide³⁴ were synthesized according to literature procedures. *N,N*-dimethylformamide, *N,N*-dimethylacetamide, *N,N*-dimethylbenzamide, *N*-phenylformamide, *N-tert*-butylformamide, *N*-(4-bromophenyl)formamide, and *N*-benzylformamide were purchased from Sigma Aldrich and used as received. Phenyl formate was purchased from Alfa Aesar and degassed by three freeze-pump-thaw cycles and stored over molecular sieves prior to use. 3-Methyl-2-oxazolidone was purchased from TCI America and used as received. ¹H, ¹³C{¹H}, and ¹¹B NMR spectra were collected on a Bruker AVII 600 spectrometer, a Bruker DRX-400 spectrometer, or a Varian MR-400 spectrometer. ¹⁵N chemical shifts were determined by ¹H-¹⁵N HMBC experiments on a Bruker AVII 600 spectrometer. ¹⁵N chemical shifts were originally referenced to an external liquid NH₃ standard and recalculated to the CH₃NO₂ chemical shift scale by adding -381.9 ppm. Elemental analyses were performed using a Perkin-Elmer 2400 Series II CHN/S by the Iowa State Chemical Instrumentation Facility. X-ray diffraction data was collected on a Bruker APEX II diffractometer.

To^PMgMe. Hydrogen tris(4*S*-isopropyl-2-oxazolinyl)phenylborate (HTo^P) (0.106 g, 0.23 mmol) and MgMe₂(O₂C₄H₈)₂ (0.074 g, 0.34 mmol) were stirred in benzene for 3 h. The solution was filtered, and the volatile components were evaporated under reduced pressure. The residue was washed with pentane (3 × 5 mL) and dried under vacuum to provided To^PMgMe (0.083 g, 0.18 mmol, 79.3%). ¹H NMR (600 MHz, benzene-*d*₆): δ -0.60 (s, 3 H, MgMe), 0.69 (m, 18 H, CNC(CHMe₂)HCH₂O), 1.67 (m, 3 H, CNC(CHMe₂)HCH₂O), 3.53 (m, 3 H, CNC(CHMe₂)HCH₂O), 3.62 (m, 6 H, CNC(CHMe₂)HCH₂O), 7.35 (t, ³J_{HH} = 7.2 Hz, 1 H, *para*-C₆H₅), 7.53 (t, ³J_{HH} = 7.2 Hz, 2 H, *meta*-C₆H₅), 8.25 (d, ³J_{HH} = 7.8 Hz, 2 H, *ortho*-C₆H₅). ¹³C{¹H} NMR (150 MHz, benzene-*d*₆): δ -16.23 (MgMe), 17.78 (CNCH(CHMe₂)CH₂O), 18.84

(CNCH(CHMe₂)CH₂O), 32.51 (CNCH(CHMe₂)CH₂O), 69.71 (CNCH(CHMe₂)CH₂O), 70.78 (CNCH(CHMe₂)CH₂O), 126.20 (*para*-C₆H₅), 127.22 (*meta*-C₆H₅), 136.46 (*ortho*-C₆H₅), 143 (br, *ipso*-C₆H₅), 194 (br, CNCH(CHMe₂)CH₂O). ¹¹B NMR (128 MHz, benzene-*d*₆): δ -18.0. IR (KBr, cm⁻¹): ν 2960 (s), 2921 (s), 2876 (s), 1588 (s, ν_{CN}), 1463 (m), 1369 (s), 1257 (s), 1195 (m), 1105 (s), 1070 (s), 1046 (m), 970 (m), 873 (s), 834 (w), 739 (m). Anal. Calcd. for C₂₅H₃₈BMgN₃O₃: C, 64.75; H, 8.26; N, 9.06. Found C, 64.33; H, 8.03 N, 8.69. Mp: 200-202 °C (dec).

Hydrogen bis(4,4-dimethyl-2-oxazolinyl)(4*S*-isopropyl-2-oxazolinyl)phenylborate (HTo^{MP}).

Bis(4,4-dimethyl-2-oxazolinyl)phenylborane (PhB(Ox^{Me2})₂) (0.412 g, 1.62 mmol) and 2-lithio-4*S*-isopropyl oxazolide (LiOx^{iPr}) (0.193 g, 1.62 mmol) were stirred in THF for 24 h. Evaporation of solvent under reduced pressure yielded a yellow oil. Et₃NHCl (0.176 g, 1.28 mmol) and methylene chloride were added to the residue. The mixture was stirred for 24 h and then passed through a neutral alumina column. The product was evaporated under reduced pressure to dryness, providing HTo^{MP} as a pale yellow oil (0.559 g, 1.41 mmol, 87.3%) of sufficient purity for synthetic purposes. ¹H NMR (600 MHz, benzene-*d*₆): δ 0.57 (d, 3 H, ³J_{HH} = 9.6 Hz, CNC(CHMe₂)HCH₂O), 0.74 (d, 3 H, ³J_{HH} = 9.6 Hz, CNC(CHMe₂)HCH₂O), 1.11 (s, 6 H, CNCMe₂CH₂O), 1.12 (s, 6 H, CNCMe₂CH₂O), 1.3 (br, 1 H, CNC(CHMe₂)HCH₂O), 3.3 (br, 1 H, CNC(CHMe₂)HCH₂O), 3.60 (m, 6 H, CH₂OCN), 7.21 (m, ³J_{HH} = 7.2 Hz, 1 H, *para*-C₆H₅), 7.41 (m, ³J_{HH} = 7.6 Hz, 2 H, *meta*-C₆H₅), 8.0 (br d, 2 H, *ortho*-C₆H₅), 13.2 (br, 1 H). ¹³C{¹H} NMR (150 MHz, benzene-*d*₆): δ 18.63 (CNC(CHMe₂)HCH₂O), 18.77 (CNC(CHMe₂)HCH₂O), 28.62 (CNCMe₂CH₂O), 28.73 (CNCMe₂CH₂O), 32.94 (CNC(CHMe₂)HCH₂O), 65.57 (CNCMe₂CH₂O), 65.77 (CNCMe₂CH₂O), 67.48 (CNC(CHMe₂)HCH₂O), 72.01 (CNC(CHMe₂)HCH₂O), 79.03 (CNCMe₂CH₂O), 79.10 (CNCMe₂CH₂O), 126.39 (*para*-C₆H₅),

127.94 (*meta*-C₆H₅), 134.77 (*ortho*-C₆H₅), 146 (br, *ipso*-C₆H₅), 185 (br, OCN), 192 (br, OCN). ¹¹B NMR (128 MHz, benzene-*d*₆): δ -17.8. ¹⁵N{¹H} NMR (benzene-*d*₆, 60.6 MHz): δ -149.5 (Ox^{Me2}). IR (KBr, cm⁻¹): ν 3070 (w), 2965 (s), 2928 (s), 2873 (m), 2295 (w), 1599 (s), 1462 (s), 1430 (s), 1363 (m), 1316 (m), 1260 (m), 1190 (m), 970 (s), 804 (w), 736 (m), 704 (s), 620 (w). Anal. Calcd. for C₂₂H₃₂BN₃O₃: C, 66.50; H, 8.12; N, 10.58. Found C, 66.01; H, 8.22; N, 10.06. Mp: 45-47 °C.

To^{MP}MgMe. HTo^{MP} (0.200 g, 0.50 mmol) and MgMe₂(O₂C₄H₈)₂ (0.173 g, 0.76 mmol) were stirred in benzene for 24 h. The reaction mixture was filtered, and solvent was removed under reduced pressure. The residue was washed with pentane (3 × 5 mL) and dried under vacuum giving To^{MP}MgMe (0.192 g, 0.44 mmol, 87.8%). ¹H NMR (600 MHz, benzene-*d*₆): δ -0.6 (br s, 3 H, MgMe), 0.64 (d, 3 H, ³J_{HH} = 7.2 Hz, CNCH(CHMe₂)CH₂O), 0.70 (d, 3 H, ³J_{HH} = 7.2 Hz, CNCH(CHMe₂)CH₂O), 1.01 (s, 3 H, CNCMe₂CH₂O), 1.02 (s, 3 H, CNCMe₂CH₂O), 1.07 (s, 3 H, CNCMe₂CH₂O), 1.08 (s, 3 H, CNCMe₂CH₂O), 1.5 (br m, 1 H, CNCH(CHMe₂)CH₂O), 3.43 (m, 6 H, CH₂O), 3.5 (br m, 1 H, CNCH(CHMe₂)CH₂O), 7.36 (m, ³J_{HH} = 7.2 Hz, 1 H, *para*-C₆H₅), 7.55 (m, ³J_{HH} = 7.6 Hz, 2 H, *meta*-C₆H₅), 8.31 (d, 2 H, *ortho*-C₆H₅). ¹³C{¹H} NMR (150 MHz, benzene-*d*₆): δ -17.2 (MgMe), 18.15 (CNCH(CHMe₂)CH₂O), 18.53 (CNCH(CHMe₂)CH₂O), 28.28 (CNCMe₂CH₂O), 28.48 (CNCMe₂CH₂O), 28.66 (CNCMe₂CH₂O), 32.60 (CNCH(CHMe₂)CH₂O), 65.61 (CNCMe₂CH₂O), 69.72 (CNCH(CHMe₂)CH₂O), 70.75 (CNCH(CHMe₂)CH₂O), 80.49 (CNCMe₂CH₂O), 126.23 (*para*-C₆H₅), 127.22 (*meta*-C₆H₅), 136.48 (*ortho*-C₆H₅), 137 (br, *ipso*-C₆H₅), 192 (br, OCN), 194 (br, OCN). ¹¹B NMR (128 MHz, benzene-*d*₆): δ -18.1. ¹⁵N{¹H} NMR (benzene-*d*₆, 60.6 MHz): δ -155.4 (CNCMe₂CH₂O). IR (KBr, cm⁻¹): ν 3046 (w), 2966 (s), 2929 (s), 2894 (s), 1589 (s), 1462 (m), 1369 (m), 1270 (m), 1196 (s), 1158 (m), 1025 (w), 963 (s), 839 (w), 740 (w), 704 (m). Anal. Calcd. for

$C_{23}H_{34}BMgN_3O_3$: C, 63.41; H, 7.87; N, 9.65. Found C, 63.66; H, 8.32; N, 10.06. Mp: 202-204 °C (dec).

PhMeB(Ox^{Me2})₂MgMe(THF)₂. PhB(Ox^{Me2})₂ (0.060 g, 0.24 mmol) and MgMe₂(O₂C₄H₈)₂ (0.077 g, 0.35 mmol) were stirred in a mixture of benzene and THF (50:1) for 24 h. The reaction mixture was then filtered, and solvent was removed under reduced pressure. The cream colored solid was washed with pentane (3 × 5 mL) and then dried under vacuum. Recrystallization from diethyl ether provided PhMeB(Ox^{Me2})₂MgMe(THF)₂ (0.074 g, 0.15 mmol, 63.8%). ¹H NMR (600 MHz, benzene-*d*₆): δ -0.8 (br s, 3 H, MgMe), 0.45 (br s, 3 H, BMe), 1.00 (s, 6 H, CNCMe₂CH₂O), 1.05 (s, 6 H, CNCMe₂CH₂O), 1.08 (br s, 8 H, THF), 3.3 (br s, 8 H, THF), 3.38 (d, 2 H, ³J_{HH} = 8.4 Hz, CNCMe₂CH₂O), 3.45 (d, 2 H, ³J_{HH} = 8.4 Hz, CNCMe₂CH₂O), 7.21 (t, 1 H, ³J_{HH} = 7.2 Hz, *para*-C₆H₅), 7.39 (t, 2 H, ³J_{HH} = 7.2 Hz, *meta*-C₆H₅), 7.80 (d, 2 H, ³J_{HH} = 7.2 Hz, *ortho*-C₆H₅). ¹³C{¹H} NMR (150 MHz, benzene-*d*₆): δ -14.9 (br, MgMe), 14.4 (br, BMe), 25.30 (THF), 28.66 (CNCMe₂CH₂O), 67.43 (CNCMe₂CH₂O), 69.43 (THF), 78.21 (CNCMe₂CH₂O), 125.31 (*para*-C₆H₅), 127.88 (*meta*-C₆H₅), 133.02 (*ortho*-C₆H₅), 155 (br, *ipso*-C₆H₅), 197 (br, CNCMe₂CH₂O). ¹¹B NMR (128 MHz, benzene-*d*₆): δ -17.0. ¹⁵N{¹H} NMR (benzene-*d*₆, 60.6 MHz): δ -170.2. IR (KBr, cm⁻¹): ν 2967 (s), 2927 (s), 2898 (s), 1570 (s), 1462 (m), 1369 (m), 1267 (m), 1194 (m), 1146 (m), 1003 (s), 970 (s), 879 (w), 831 (w), 709 (s), 517 (s). Anal. Calcd. for C₂₆H₄₃BMgN₂O₄: C, 64.69; H, 8.98; N, 5.80. Found C, 64.93; H, 8.72; N, 5.40. Mp: 104-106 °C.

N,N-dibenzyl-4-(phenyldiazenyl)benzamide. 4-(2-Phenyldiazenyl)-benzoyl chloride (0.50 g, 2.04 mmol) was added in one portion to a flask containing dibenzylamine (0.44 g, 2.24 mmol), triethylamine (0.26 g, 2.55 mmol) and 10 mL methylene chloride. The reaction mixture was stirred at r.t. for 1 h, and then 30 mL of methylene chloride was added to the reaction flask. The

solution was washed with 1 M HCl (3 × 50 mL), and the organic layer was filtered on a short silica gel column and then dried over sodium sulfate. The solution was filtered, and then solvent was removed under reduced pressure to give an orange solid (0.69 g, 1.70 mmol, 83.4%). ¹H NMR (benzene-*d*₆, 600 MHz): δ 4.2 (br s, 2 H, CH₂C₆H₅), 4.7 (br s, 2 H, CH₂C₆H₅), 6.9 (br, 2 H, CH₂C₆H₅), 7.10 (t, 3 H, ²J_{HH} = 7.2 Hz, -N=NC₆H₅), 7.14 (br, 6 H, CH₂C₆H₅), 7.18 overlapping with C₆D₆ (t, 2 H, ²J_{HH} = 7.8 Hz, -N=NC₆H₅), 7.25 (br, 2 H, CH₂C₆H₅), 7.51 (d, 2 H, ²J_{HH} = 8.4 Hz, C₆H₄-N=NC₆H₅), 7.83 (d, 2 H, ²J_{HH} = 8.4 Hz, C₆H₄-N=NC₆H₅), 7.97 (d, 2 H, ²J_{HH} = 7.2 Hz, -N=NC₆H₅). ¹³C{¹H} NMR (benzene-*d*₆, 150 MHz): δ 47.65 (N(CH₂C₆H₅)₂), 51.71 (N(CH₂C₆H₅)₂), 120.78 (aryl), 121.13 (aryl), 123.66 (aryl), 123.76 (aryl), 127.51 (aryl), 128.08 (aryl), 128.68 (aryl), 129.36 (aryl), 129.69 (aryl), 131.83 (aryl), 135.60 (aryl), 137.46 (aryl), 138.21 (aryl), 139.62 (aryl), 153.47 (aryl), 153.69 (aryl), 171.33 (C=O). ¹⁵N{¹H} NMR (benzene-*d*₆, 60 MHz, 25 °C): δ -272.4 (C₆H₄N=NC₆H₅), -266.1 (C₆H₄N=NC₆H₅). IR (KBr, cm⁻¹): ν 3059 (w), 3029 (w), 3008 (w), 2978 (w), 2925 (w), 2868 (w), 1630 (s), 1496 (m), 1451 (s), 1422 (s), 1363 (m), 1310 (m), 1287 (m), 1267 (m), 1246 (s), 1222 (w), 1205 (w), 1161 (m), 1145 (m), 1104 (w), 1077 (m), 1029 (w), 994 (s), 972 (w), 950 (w), 931 (w), 896 (w), 854 (s), 817 (w), 777 (s), 744 (s), 699 (s), 685 (s), 614 (w). HRMS Calcd. For [M+H]: 406.1919. Found: 406.1920. Anal. Calcd. for C₂₇H₂₃N₃O: C, 79.97; H, 5.72; N, 10.36. Found C, 79.60; H, 5.47; N, 10.28. Mp: 158-160 °C.

Catalytic deoxygenations:

Trimethylamine hydrochloride. A benzene solution (0.5 mL) of To^MMgMe (0.015 g, 0.035 mmol) was added dropwise to a solution containing *N,N*-dimethylformamide (0.130 g, 1.78 mmol), HBpin (4.54 g, 35.50 mmol), and 10 mL of benzene. The reaction mixture was stirred for 10 min., and then the solution was filtered through neutral alumina to remove the catalyst. 1 M

aqueous HCl was added to the filtered solution, and the mixture was stirred for 20 min. The aqueous layer was washed with methylene chloride, and then water was evaporated. The residue was recrystallized from EtOH, and then dried under reduced pressure to give a white solid (0.030 g, 0.31 mmol, 17.6%). The low yield is a result of the volatile nature of NMe₃, which is formed in higher yield in sealed NMR-scale experiments. The spectra of amine and ammonium chloride products match those of authentic samples. ¹H NMR (D₂O, 600 MHz): δ 2.87. ¹³C{¹H} NMR (D₂O, 100 MHz): δ 44.74. ¹⁵N{¹H} NMR (D₂O, 60 MHz): δ -352.1. HRMS (EI, m/z) Calcd. For C₃H₁₀N⁺: 60.0813. Found 60.0808.

Dimethylethylamine hydrochloride. A benzene solution (0.5 mL) of To^MMgMe (0.015 g, 0.035 mmol) was added dropwise to a solution containing *N,N*-dimethylacetamide (0.155 g, 1.78 mmol) and HBpin (4.54 g, 35.50 mmol). The reaction mixture was stirred for 6 h, and then the solution was filtered through neutral alumina to remove the catalyst. 1 M aqueous HCl was added to the filtrate, and the mixture was stirred for 20 min. The aqueous layer was washed with methylene chloride, and then water was evaporated. The residue was recrystallized from ethanol and then dried under reduced pressure to give a white solid in good yield (0.252 g, 2.30 mmol, 91.0%). The spectrum of the ammonium chloride product matched that of an authentic sample prepared from NMe₂Et and HCl. ¹H NMR (D₂O, 400 MHz): δ 1.34 (t, 3 H, ³J_{HH} = 7.2 Hz, NCH₂CH₃), 2.90 (s, 6 H, NMe₂), 3.23 (q, 2 H, ³J_{HH} = 7.2 Hz, NCH₂CH₃). ¹³C{¹H} NMR (D₂O, 100 MHz): δ 9.31 (NCH₂CH₃), 42.14 (NMe₂), 53.02 (NCH₂CH₃). ¹⁵N{¹H} NMR (D₂O, 60 MHz): δ -343.6. HRMS (EI, m/z) Calcd. For C₄H₁₂N⁺: 74.0969. Found: 74.0966.

Benzyl dimethylamine hydrochloride. A benzene solution (0.5 mL) of To^MMgMe (0.015 g, 0.035 mmol) was added dropwise to a solution containing *N,N*-dimethylbenzamide (0.265 g, 1.78 mmol), HBpin (4.54 g, 35.50 mmol) and enough benzene to dissolve *N,N*-

dimethylbenzamide (ca. 1 mL). The reaction mixture was stirred for 3 h, and then the solution was then filtered through alumina. Workup as above gives a white solid (0.283 g, 1.65 mmol, 92.6%). The spectrum of the NBnMe₂ was compared to literature values.³⁵ ¹H NMR (D₂O, 400 MHz): δ 2.82 (s, 6 H, NMe₂), 4.28 (s, 2 H, NCH₂C₆H₅), 7.49 (m, 5 H, NCH₂C₆H₅). ¹³C{¹H} NMR (D₂O, 150 MHz): δ 42.11 (NMe₂), 61.17 (NCH₂Ph), 129.34 (C₆H₅), 130.18 (*para* and *ipso*-C₆H₅), 130.80 (C₆H₅). HRMS (EI, m/z) Calcd. For C₉H₁₄N⁺: 136.1126. Found: 136.1120.

***N*-Benzylmorpholine hydrochloride.** A benzene solution (0.5 mL) of To^MMgMe (0.008 g, 0.019 mmol) was added dropwise to a solution containing 1-benzylmorpholine (0.181 g, 0.95 mmol), HBpin (2.43 g, 19.0 mmol), and sufficient benzene to dissolve 1-benzylmorpholine (ca. 1 mL). The reaction mixture was stirred for 6 h, and then the reaction was worked up as above to give the product as a white solid in good yield (0.186 g, 0.87 mmol, 92.1%). The spectrum of PhCH₂NC₄H₈O was compared to literature values.^{Error! Bookmark not defined.} ¹H NMR (D₂O, 400 MHz): δ 3.4 (br, 4 H, NCH₂CH₂O), 3.8–4.1 (br, 4 H, NCH₂CH₂O), 4.40 (s, 2 H, NCH₂C₆H₅), 7.55 (br, 5 H, NCH₂C₆H₅). ¹³C{¹H} NMR (D₂O, 150 MHz): δ 51.26 (NCH₂CH₂O), 60.87 (NCH₂Ph), 63.68 (NCH₂CH₂O), 127.92 (C₆H₅), 129.31 (C₆H₅), 130.35 (C₆H₅), 131.26 (C₆H₅). ¹⁵N{¹H} NMR (D₂O, 60 MHz): δ -333.0. HRMS (EI, m/z) Calcd. For C₁₁H₁₆NO⁺: 178.1232. Found: 178.1226.

***N,N*-Dibenzylamine hydrochloride.** A benzene solution (0.5 mL) of To^MMgMe (0.008 g, 0.019 mmol) was added dropwise to a solution containing *N,N*-dibenzyl-4-cyanobenzamide (0.123 g, 0.38 mmol), HBpin (0.97 g, 7.59 mmol), and enough benzene to dissolve *N,N*-dibenzyl-4-cyanobenzamide (ca. 5 mL). The reaction mixture was stirred for 15 h, and then the solution was filtered through neutral alumina to remove the catalyst. 1 M aqueous HCl was added to the filtered solution, and the mixture was stirred for 20 min. The aqueous layer was washed with

methylene chloride, and then water was evaporated. The residue was recrystallized from ethanol and then dried under reduced pressure to give a white solid of the ammonium chloride product (0.068 g, 0.29 mmol, 77.3%). The product was spectroscopically identical to an authentic sample prepared from HNBN_2 and HCl . ^1H NMR (D_2O , 400 MHz): δ 4.24 (s, 4 H, NCH_2), 7.47 (m, 10 H, C_6H_5). $^{13}\text{C}\{^1\text{H}\}$ NMR (D_2O , 150 MHz): δ 50.60 (NCH_2Ph), 129.28 (C_6H_5), 129.63 (C_6H_5), 129.82 (C_6H_5), 130.87 (C_6H_5). $^{15}\text{N}\{^1\text{H}\}$ NMR (D_2O , 60 MHz): δ -328.9. HRMS (EI, m/z) Calcd. For $\text{C}_{14}\text{H}_{16}\text{N}^+$: 198.1282. Found: 198.1276.

***N,N*-dibenzyl-4-(phenyldiazenyl)benzylamine hydrochloride.** A benzene solution (0.5 mL) of $\text{To}^{\text{M}}\text{MgMe}$ (0.008 g, 0.019 mmol) was added dropwise to a solution containing *N,N*-dibenzyl-4-(phenyldiazenyl)benzamide (0.154 g, 0.38 mmol), HBpin (0.97 g, 7.59 mmol), and enough benzene to dissolve *N,N*-dibenzyl-4-(phenyldiazenyl)benzamide (ca. 5 mL). The reaction mixture was stirred for 15 h, and then the solution was filtered through neutral alumina to remove the catalyst. 1 M aqueous HCl was added to the filtered solution, and the mixture was stirred for 20 min. An orange precipitate formed at the partition of the aqueous and organic layers. The solution was gravity filtered to collect the orange solid, which was then washed with pentane and dried under reduced pressure. Recrystallization from diethyl ether and methylene chloride (ca. 1:20) gave an orange solid (0.128 g, 0.30 mmol, 78.5%). ^1H NMR (CDCl_3 , 400 MHz): δ 4.2 (br s, 6 H, NCH_2), 7.46-7.97 (m, 14 H, C_6H_5 and C_6H_4), 13.1 (br s, 1 H, NH). $^{13}\text{C}\{^1\text{H}\}$ NMR (D_2O , 100 MHz): δ 55.94 (NCH_2Ph), 56.53 (NCH_2Ph), 123.19 (aryl), 123.62 (aryl), 128.84 (aryl), 129.28 (aryl), 129.51 (aryl), 130.12 (aryl), 131.56 (aryl), 131.68 (aryl), 131.69 (aryl), 132.41 (aryl), 152.58 (aryl), 153.32 (aryl). IR (KBr, cm^{-1}): ν 3401 (br m), 3042 (m), 2991 (w), 2955 (m), 2920 (m), 1583 (w), 1499 (m), 1452 (s), 1419 (m), 1372 (m), 1302 (w), 1217 (m), 1158 (w), 1018 (m), 927 (m), 861 (m), 833 (w), 753 (s), 698 (s), 563 (m). HRMS (EI,

m/z) Calcd. For $C_{27}H_{26}N_3^+$: 392.2127. Found: 392.2124.

***N,N*-dibenzyl-4-nitrobenzylamine hydrochloride.**³⁶ A benzene solution (0.5 mL) of $To^M MgMe$ (0.008 g, 0.019 mmol) was added dropwise to a solution containing *N,N*-dibenzyl-4-nitrobenzamide (0.131 g, 0.38 mmol), HBpin (0.97 g, 7.59 mmol), and enough benzene to dissolve *N,N*-dibenzyl-4-nitrobenzamide (ca. 5 mL). The reaction mixture was stirred for 15 h, and then the solution was filtered through neutral alumina to remove the catalyst. 1 M aqueous HCl was added to the filtered solution, and the mixture was stirred for 20 min. The product was extracted from the aqueous layer with methylene chloride, and the solvent was concentrated under reduced pressure. Pentane was added to the concentrated methylene chloride solution to precipitate a white solid. The solid was separated from the solution by centrifugation followed by decanting the solvent. Recrystallization from diethyl ether and methylene chloride (ca. 1:20) gave a pale yellow solid (0.109 g, 0.29 mmol, 78.4%). The spectrum of $[HNBn_2(p-C_6H_4NO_2)]Cl$ was identical to the literature report.^{Error! Bookmark not defined.} 1H NMR ($CDCl_3$, 600 MHz): δ 4.16 and 4.25 (br, 6 H, $NCH_2C_6H_4NO_2$ and $NCH_2C_6H_5$), 7.46 (br, 6 H, $NCH_2C_6H_5$), 7.63 (br, 4 H, $NCH_2C_6H_5$), 7.97 (br, 2 H, C_6H_4), 8.25 (br, 2 H, C_6H_4), 13.37 (br s, 1 H, NH). $^{13}C\{^1H\}$ NMR (D_2O , 150 MHz): δ 55.39 (NCH_2Ph), 57.13 (NCH_2Ph), 124.41 (aryl), 128.52 (aryl), 129.71 (aryl), 130.50 (aryl), 131.65 (aryl), 132.47 (aryl), 136.38 (aryl), 148.77 (aryl). IR (KBr, cm^{-1}): ν 3215 (s br), 3045 (w), 3006 (w), 1606 (w), 1519 (s, ν_{NO}), 1455 (s), 1347 (s, ν_{NO}), 1194 (s), 1110 (w), 1022 (w), 914 (w), 883 (m), 825 (m), 751 (m), 700 (m), 646 (m), 547 (m). HRMS (EI, m/z) Calcd. For $C_{21}H_{21}N_2O_2^+$: 333.1603. Found: 333.1599.

***tert*-Butylmethylamine hydrochloride.** A benzene solution (1 mL) of $To^M MgMe$ (0.029 g, 0.069 mmol) was added dropwise to a solution containing *N-tert*-butylformamide (0.070 g, 0.69 mmol), HBpin (0.35 g, 2.76 mmol), and enough benzene to dissolve *N-tert*-butylformamide (ca.

1 mL). The reaction mixture was stirred for 24 h, and then the solution was filtered through neutral alumina to remove the catalyst. 1 M aqueous HCl was added to the solution, and the mixture was stirred for 20 min. The aqueous layer was washed with methylene chloride, and then water was evaporated. The residue was recrystallized from ethanol and then dried under reduced pressure to give the product as a white solid (0.061 g, 0.49 mmol, 70.9%). The spectrum of $[\text{H}_2\text{NMe}^t\text{Bu}]\text{Cl}$ was identical to the literature report.³⁷ ^1H NMR (D_2O , 400 MHz): δ 1.37 (s, 9 H, NCMe_3), 2.65 (s, 3 H, NMe). $^{13}\text{C}\{^1\text{H}\}$ NMR (D_2O , 150 MHz): δ 24.47 (NCMe_3), 26.19 (NMe, assignment supported by a ^1H - ^{13}C HMQC experiment), 56.42 (NCMe_3). $^{15}\text{N}\{^1\text{H}\}$ NMR (D_2O , 60 MHz): δ -329.5. HRMS (EI, m/z) Calcd. For $\text{C}_5\text{H}_{14}\text{N}^+$: 88.1126. Found: 88.1123.

***N*-methyl-*N*-4-bromophenylamine hydrochloride.** A benzene solution (0.5 mL) of $\text{To}^{\text{M}}\text{MgMe}$ (0.017 g, 0.040 mmol) was added dropwise to a solution containing *N*-(4-bromophenyl)formamide (0.080 g, 0.40 mmol), HBpin (0.20 g, 1.60 mmol), and enough benzene to dissolve *N*-(4-bromophenyl)formamide (ca. 5 mL). The reaction mixture was stirred for 48 h, and then the solution was filtered through neutral alumina to remove the catalyst. Workup as for trimethylammonium chloride gave the product as a white solid (0.061 g, 0.27 mmol, 68.4%). The spectrum of $\text{HNMe}(p\text{-C}_6\text{H}_5\text{Br})$ was compared to literature values.³⁸ ^1H NMR (D_2O , 400 MHz): δ 2.85 (s, 3 H, NMe), 6.98 (d, 2 H, $^3J_{\text{HH}} = 8.0$ Hz, C_6H_4), 7.52 (d, 2 H, $^3J_{\text{HH}} = 8.0$ Hz, C_6H_4). $^{13}\text{C}\{^1\text{H}\}$ NMR (D_2O , 150 MHz): δ 36.48 (NMe), 122.57 ($\text{C}_6\text{H}_4\text{Br}$), 123.44 ($\text{C}_6\text{H}_4\text{Br}$), 133.34 ($\text{C}_6\text{H}_4\text{Br}$), 136.00 ($\text{C}_6\text{H}_4\text{Br}$). HRMS (EI, m/z) Calcd. For $\text{C}_7\text{H}_9\text{BrN}^+$: 185.9918. Found: 185.9910.

Methylbenzylamine hydrochloride. A benzene solution (0.5 mL) of $\text{To}^{\text{M}}\text{MgMe}$ (0.025 g, 0.059 mmol) was added dropwise to a solution containing *N*-benzylformamide (0.080 g, 0.59 mmol), HBpin (0.30 g, 2.37 mmol), and enough benzene to dissolve *N*-benzylformamide (ca. 5 mL). The reaction mixture was stirred for 48 h, and then the solution was filtered through alumina to

remove the catalyst. Workup as described above for trimethylammonium chloride gave the product as a white solid (0.079 g, 0.50 mmol, 84.9%). The NMR spectra matched those of an authentic sample prepared from HNMeBn and HCl. ^1H NMR (D_2O , 400 MHz): δ 2.75 (s, 3 H, NMe), 4.24 (s, 2 H, $\text{NCH}_2\text{C}_6\text{H}_5$), 7.53 (br s, 5 H, $\text{NCH}_2\text{C}_6\text{H}_5$). $^{13}\text{C}\{^1\text{H}\}$ NMR (D_2O , 150 MHz): δ 32.12 (NMe), 52.36 (NCH_2Ph), 129.29 (C_6H_5), 129.69 (C_6H_5), 129.76 (C_6H_5), 130.72 (C_6H_5). $^{15}\text{N}\{^1\text{H}\}$ NMR (D_2O , 60 MHz): δ -343.4. HRMS (EI, m/z) Calcd. For $\text{C}_8\text{H}_{12}\text{N}^+$: 122.0970. Found: 122.0966.

***N*-methylaniline hydrochloride.** A benzene solution (1 mL) of $\text{To}^{\text{M}}\text{MgMe}$ (0.024 g, 0.057 mmol) was added dropwise to a solution containing *N*-phenylformamide (0.070 g, 0.57 mmol), HBpin (0.30 g, 2.31 mmol), and enough benzene to dissolve *N*-phenylformamide (ca. 5 mL). The reaction mixture was stirred for 48 h, and then the solution was filtered through neutral alumina to remove the catalyst. 1 M aqueous HCl was added to the filtered solution, and the mixture was stirred for 20 min. The aqueous layer was washed with methylene chloride, and then water was evaporated. The residue was recrystallized from ethanol, and then dried under reduced pressure to give a white solid (0.077 g, 0.54 mmol, 92.8%). The NMR spectra matched those of the ammonium chloride prepared from an authentic sample of *N*-methylaniline allowed to react with HCl. ^1H NMR (D_2O , 600 MHz): δ 3.10 (s, 3 H, NMe), 7.49 (d, 2 H, $^3J_{\text{HH}} = 7.8$ Hz, *ortho*- C_6H_5), 7.55 (t, 1 H, $^3J_{\text{HH}} = 7.2$ Hz, *para*- C_6H_5) 7.60 (t, 2 H, $^3J_{\text{HH}} = 7.8$ Hz, *meta*- C_6H_5). $^{13}\text{C}\{^1\text{H}\}$ NMR (D_2O , 100 MHz): δ 36.65 (NMe), 121.62 (C_6H_5), 129.61 (C_6H_5), 130.33 (C_6H_5), 136.44 (C_6H_5). $^{15}\text{N}\{^1\text{H}\}$ NMR (D_2O , 60 MHz): δ -352.1. HRMS (EI, m/z) Calcd. For $\text{C}_7\text{H}_{10}\text{N}^+$: 108.0813. Found: 108.0806.

Procedure for the competition experiment between phenyl formate and *N*-phenylformamide. A solution with known concentration of phenyl formate (10.3 μL , 0.09

mmol, 0.3 M), *N*-phenylformamide (0.011 g, 0.09 mmol, 0.3 M), and HBpin (1 equiv: 13.8 μ L, 0.09 mmol; 2 equiv: 27.6 μ L, 0.19 mmol; 4 equiv: 55.2 μ L, 0.38 mmol) with a known concentration of $\text{Si}(\text{SiMe}_3)_4$ was prepared. An solution of known concentration of $\text{To}^{\text{M}}\text{MgMe}$ (0.0047 mmol, 0.016 M) and $\text{Si}(\text{SiMe}_3)_4$ was prepared, with equal volume as the substrate solution. The concentration of substrate and catalyst solutions were verified by integrating their independent ^1H NMR spectra. The two solution were mixed and the resulting reaction mixture was quickly placed in the NMR probe. The reactions were monitored by ^1H NMR spectroscopy using a Bruker DRX-400 spectrometer. Single scan spectra were acquired automatically at 1 min. time intervals at room temperature. The concentrations of phenyl formate and *N*-phenylformamide were determined by comparison of weighted integrals of appropriate resonances to the known concentration of the internal standard $\text{Si}(\text{SiMe}_3)_4$ after the first 5 min. of the reaction.

References

- (1) Lawrence, S. A., *Amines : synthesis, properties, and applications*. Cambridge University Press: New York, 2004; p. 371.
- (2) (a) Smith, A. M.; Whyman, R. *Chem. Rev.* **2014**, *114*, 5477-5510. (b) Dodds, D. L.; Cole-Hamilton, D. J., Catalytic Reduction of Amides Avoiding LiAlH_4 or B_2H_6 . In *Sustainable Catalysis: Challenges and Practices for the Pharmaceutical and Fine Chemical Industries*, Dunn, P. J.; Hii, K. K.; Krische, M. J.; Williams, M. T., Eds. Wiley: Hoboken NJ, 2013; p. 1-36.
- (3) Gaylord, N. G. *Reduction with Complex Metal Hydrides*. Interscience Publishers: New York, 1956; p 1046.

- (4) Smith, A. M.; Whyman, R. *Chem. Rev.* **2014**, *114*, 5477-5510.
- (5) (a) Igarashi, M.; Fuchikami, T. *Tetrahedron Lett.* **2001**, *42*, 1945-1947. (b) Cheng, C.; Brookhart, M. *J. Am. Chem. Soc.* **2012**, *134*, 11304-11307. (c) Park, S.; Brookhart, M. *J. Am. Chem. Soc.* **2011**, *134*, 640-653. (d) Das, S.; Addis, D.; Junge, K.; Beller, M. *Chem. Eur. J.* **2011**, *17*, 12186-12192. (e) Li, Y.; Molina de La Torre, J. A.; Grabow, K.; Bentrup, U.; Junge, K.; Zhou, S.; Brückner, A.; Beller, M. *Angew. Chem. Int. Ed.* **2013**, *52*, 11577-11580. (f) Reeves, J. T.; Tan, Z.; Marsini, M. A.; Han, Z. S.; Xu, Y.; Reeves, D. C.; Lee, H.; Lu, B. Z.; Senanayake, C. H. *Adv. Syn. Catal.* **2013**, *355*, 47-52.
- (6) (a) Stein, M.; Breit, B. *Angew. Chem. Int. Ed.* **2013**, *52*, 2231-2234. (b) Li, B.; Sortais, J.-B.; Darcel, C. *Chem. Commun.* **2013**, *49*, 3691-3693. (c) Hanada, S.; Ishida, T.; Motoyama, Y.; Nagashima, H. *J. Org. Chem.* **2007**, *72*, 7551-7559.
- (7) Zhou, S.; Junge, K.; Addis, D.; Das, S.; Beller, M. *Org. Lett.* **2009**, *11*, 2461-2464.
- (8) (a) Balaraman, E.; Gnanaprakasam, B.; Shimon, L. J. W.; Milstein, D. *J. Am. Chem. Soc.* **2010**, *132*, 16756-16758. (b) Barrios-Francisco, R.; Balaraman, E.; Diskin-Posner, Y.; Leitun, G.; Shimon, L. J. W.; Milstein, D. *Organometallics* **2013**, *32*, 2973-2982.
- (9) (a) Cheng, C.; Brookhart, M. *J. Am. Chem. Soc.* **2012**, *134*, 11304-11307. (b) Park, S.; Brookhart, M. *J. Am. Chem. Soc.* **2011**, *134*, 640-653. (c) Hanada, S.; Tsutsumi, E.; Motoyama, Y.; Nagashima, H. *J. Am. Chem. Soc.* **2009**, *131*, 15032-15040.
- (10) (a) Stein, M.; Breit, B. *Angew. Chem. Int. Ed.* **2013**, *52*, 2231-2234. (b) Balaraman, E.; Gnanaprakasam, B.; Shimon, L. J. W.; Milstein, D. *J. Am. Chem. Soc.* **2010**, *132*, 16756-16758. (c) Barrios-Francisco, R.; Balaraman, E.; Diskin-Posner, Y.; Leitun, G.; Shimon, L. J. W.; Milstein, D. *Organometallics* **2013**, *32*, 2973-2982.

- (11) Li, Y.; Molina de La Torre, J. A.; Grabow, K.; Bentrup, U.; Junge, K.; Zhou, S.; Brückner, A.; Beller, M. *Angew. Chem. Int. Ed.* **2013**, *52*, 11577-11580.
- (12) (a) Fernandes, A. C.; Romão, C. C. *J. Mol. Catal. A: Chem.* **2007**, *272*, 60-63. (b) Xie, W.; Zhao, M.; Cui, C. *Organometallics* **2013**, *32*, 7440-7444.
- (13) Cheng, C.; Brookhart, M. *J. Am. Chem. Soc.* **2012**, *134*, 11304-11307.
- (14) (a) Xie, W.; Zhao, M.; Cui, C. *Organometallics* **2013**, *32*, 7440-7444. (b) Das, S.; Addis, D.; Zhou, S.; Junge, K.; Beller, M. *J. Am. Chem. Soc.* **2010**, *132*, 1770-1771. (c) Sakai, N.; Fujii, K.; Konakahara, T. *Tetrahedron Lett.* **2008**, *49*, 6873-6875.
- (15) (a) Arrowsmith, M.; Hadlington, T. J.; Hill, M. S.; Kociok-Kohn, G. *Chem. Commun.* **2012**, *48*, 4567-4569. (b) Arrowsmith, M.; Hill, M. S.; Hadlington, T.; Kociok-Kohn, G.; Weetman, C. *Organometallics* **2011**, *30*, 5556-5559. (c) Anker, M. D.; Arrowsmith, M.; Bellham, P.; Hill, M. S.; Kociok-Kohn, G.; Liptrot, D. J.; Mahon, M. F.; Weetman, C. *Chem. Sci.* **2014**, *5*, 2826-2830.
- (16) Mukherjee, D.; Ellern, A.; Sadow, A. D. *Chem. Sci.* **2014**, *5*, 959-964.
- (17) Guthrie, J. P. *J. Am. Chem. Soc.* **1974**, *96*, 3608-3615.
- (18) (a) Brown, H. C.; Heim, P. *J. Am. Chem. Soc.* **1964**, *86*, 3566-3567. (b) Brown, H. C.; Heim, P. *J. Org. Chem.* **1973**, *38*, 912-916.
- (19) (a) Hajos, A. *Studies in Organic Chemistry 1: Complex Hydrides*; Elsevier: Budapest, 1979. (b) Seyden-Penne, J. *Reductions by the Alumino- and Boro-hydrides in Organic Synthesis*; VCH: New York, 1991. (c) Smith, M. B.; March, J. *March's Advanced Organic Chemistry: Reactions, Mechanisms and Structure*, 6th ed.; Wiley: New York, 2007.
- (20) Bontemps, S.; Sabo-Etienne, S. *Angew. Chem. Int. Ed.* **2013**, *52*, 10253-10255.
- (21) Mukherjee, D.; Ellern, A.; Sadow, A. D. *Chem. Sci.* **2014**, *5*, 959-964.

- (22) (a) Oshima, K.; Ohmura, T.; Suginome, M. *J. Am. Chem. Soc.* **2011**, *133*, 7324-7327. (b) Koren-Selfridge, L.; Londino, H. N.; Vellucci, J. K.; Simmons, B. J.; Casey, C. P.; Clark, T. *B. Organometallics* **2009**, *28*, 2085-2090.
- (23) Ohmura, T.; Masuda, K.; Suginome, M. *J. Am. Chem. Soc.* **2008**, *130*, 1526-1527.
- (24) Mukherjee, D.; Ellern, A.; Sadow, A. D. *Chem. Sci.* **2014**, *5*, 959-964.
- (25) Smith, A. M.; Whyman, R., *Chem. Rev.* **2014**, *114*, 5477-5510.
- (26) Mukherjee, D.; Ellern, A.; Sadow, A. D. *Chem. Sci.* **2014**, *5*, 959-964.
- (27) Wu, K.; Mukherjee, D.; Ellern, A.; Sadow, A. D.; Geiger, W. E. *New J. Chem.* **2011**, *35*, 2169-2178.
- (28) Dunne, J. F.; Manna, K.; Wiench J. W.; Ellern, A.; Pruski, M.; Sadow, A. D. *Dalton Trans.* **2010**, *39*, 641-653.
- (29) Baird, B.; Pawlikowski, A. V.; Su, J.; Wiench, J. W.; Pruski, M.; Sadow, A. D. *Inorg. Chem.* **2008**, *47*, 10208-10210.
- (30) Dunne, J. F.; Fulton, D. B.; Ellern, A.; Sadow, A. D. *J. Am. Chem. Soc.* **2010**, *132*, 17680-17683.
- (31) Mukherjee, D.; Ellern, A.; Sadow, A. D. *Chem. Sci.* **2014**, *5*, 959-964.
- (32) Zhou, S.; Junge, K.; Addis, D.; Das, S.; Beller, M. *Angew. Chem. Int. Ed.* **2009**, *48*, 9507-9510.
- (33) Blondiaux, E.; Cantat, T. *Chem. Commun.* **2014**, *50*, 9349-9352.
- (34) Blondiaux, E.; Cantat, T. *Chem. Commun.* **2014**, *50*, 9349-9352.
- (35) Reeves, J. T.; Tan, Z.; Marsini, M. A.; Han, Z. S.; Zu, Y.; Reeves, D. R.; Lee, H.; Lu, B. Z.; Senanayake, C. H. *Adv. Synth. Catal.* **2013**, *355*, 47-52.
- (36) Blondiaux, E.; Cantat, T. *Chem. Commun.* **2014**, *50*, 9349-9352.

(37) Gajda, T.; Koziara, A.; Zawadzki, S.; Zweirzak, A. *Synthesis* **1979**, 7, 549-552.

(38) Le, Z.-G.; Chen, Z.-C.; Hu, Y.; Zheng, Q.-G. *Synthesis* **2004**, 17, 2809-2812.

CHAPTER 7: CONCLUSION

General Conclusions

The need for utilizing main group metals in chemistry due to their many advantages (Lewis acidic, economical, and biocompatible) has been understood for decades. However, the fundamental study and incorporation of these elements in organometallic reactions and catalysis has lagged behind transition metals. The projects described in this thesis have probed new main group metal complexes, incorporating novel ligands, and explored reactive pathways that are common in transition metal chemistry, but relatively unexplored in main group metal chemistry.

The magnesium, calcium, and zinc disilyl complexes synthesized in this work incorporate multiple β -SiH functional groups via the new ligand $-\text{Si}(\text{SiHMe}_2)_3$. These compounds demonstrate interesting structural properties that contrast analogous alkyl complexes containing $-\text{C}(\text{SiHMe}_2)_3$. Notably, while the main group alkyl compounds contain non-classical, β -agostic-like interactions between the β -SiH and the metal center, the disilyl compounds show only evidence of classical, 2-center-2-electron bonding between the silyl ligand and the metal and only two-center Si-H bonds.

The absence of non-classical interactions and the long M-Si bonds may appear to favor the position of greatest nucleophilicity at the metal-bound silicon atoms rather than at the β -hydrogen atoms. However, in reactions with Lewis acids, both alkyl and silyl compounds exclusively afford β -hydrogen abstraction products over alkyl or silyl group abstraction products, revealing that the β -H atoms are sufficiently nucleophilic and sterics around the M-Si bonds may play a role in the selectivity. Moreover, though β -hydrogen elimination is rare for main group metals compared to transition metals, the incorporation of β -SiH groups has further demonstrated that β -hydrogen elimination is accessible and readily facilitated by Lewis acids.

In addition, incorporation of β -SiH sites in these main group metal compounds provides a diagnostic spectroscopic handle. The SiH moiety has a characteristic ν_{SiH} band in the 2100 cm^{-1} region of the IR spectrum and characteristic chemical shifts in the ^1H and ^{29}Si NMR spectra. This expands upon the accessible characterization methods for this class of compounds. Thus more in-depth studies and comparisons of the structural and behavioral properties among main group metal compounds and also similar transition metal compounds can be performed. The ability to compare highly studied transition metal systems with well-defined main group metal compounds will advance the fundamental knowledge of main group metals in organometallic chemistry and aid in understanding known transition metal processes.

For example, the magnesium precatalysts studied in this work reveal interesting conclusions for accessing known reactive pathways for transition metals that were previously unknown with magnesium. $\text{To}^{\text{M}}\text{MgHB}(\text{C}_6\text{F}_5)_3$ was found to give the first example of a magnesium-catalyzed hydrosilylation of esters, and $\text{To}^{\text{M}}\text{MgMe}$ effectively catalyzes the first example of a hydroboration of amides to amines. Notably, both systems incorporate a borane Lewis acid that works in tandem with the magnesium center. In the absence of the $\text{HB}(\text{C}_6\text{F}_5)_3$ moiety or the replacement of pinacolborane with silane, respectively, neither system gives catalytic activity under the reaction conditions tested.

These observations suggest the importance of a magnesium catalyst in the presence of oxygenate substrates working in combination with a borane that lends both nucleophilicity (hydride donor ability) and Lewis acidity (electrophilic boron center). This may have been hinted at by common stoichiometric reductions utilizing LiAlH_4 and NaBH_4 , which combine an electrophilic alkali metal cation with a nucleophilic hydride donor that is also presumed to

participate as a Lewis acid. Therefore, the main group metal systems in this work can also provide insights into the elementary steps in known stoichiometric processes.

Thus, the combination of a main group metal with a Lewis acid is a powerful motif, which can access stoichiometric and catalytic pathways, such as β -hydrogen elimination, hydrosilylation, and hydroboration, which are often considered rare in the context of main group metals. To further this chemistry, catalytic applications of the neutral and cationic main group metal silyl complexes requires additional exploration. Since the magnesium hydridoborate $\text{To}^{\text{M}}\text{MgHB}(\text{C}_6\text{F}_5)_3$ has shown catalytic reduction chemistry, the $\text{MSi}(\text{SiHMe}_2)_3\{\text{HB}(\text{C}_6\text{F}_5)_3\}\text{L}_n$ type complexes may also show promising catalytic activity. Magnesium catalysts with chiral ancillary ligands could also be developed to provide highly selective asymmetric reductions. In addition, since simple inorganic salts have been shown to promote Grignard reactivity, they may also enhance the reactivity of these homoleptic magnesium catalysts, and are worth exploring as they could also provide Lewis acidic and nucleophilic properties. This additional research into the fundamental knowledge of these main group metals will continue to open doors to green, economical, and facile organic and organometallic transformations.